ABSTRACT

RAJ, ANANT. Energy Transport in Low Dimensional Systems: Phonons and Beyond Phonon Descriptors (Under the direction of Dr. Jacob Eapen).

Thermal conduction in solid state electrical insulators has long been associated with the normal mode of the vibrating atoms known as phonons. In the quantum framework, phonons are treated as bosons, which can be described by the Boltzmann kinetic theory. While the concept of phonons is critical to explaining several thermal properties, recent developments are challenging the notion of phonons as the true carriers of heat. In an alternate framework, which is more fundamental, thermal conduction can be described by the linear response or equivalently, the Green-Kubo (GK) theory. The GK theory, however, does not lend itself naturally to identify the modes of vibrations in a crystalline state. In the past two decades, several attempts have been made to merge these two disparate theories though with limited success. The primary objective of this dissertation is to develop a theoretical framework that can accommodate the GK and phonon theories while maintaining mathematical and physical consistency.

Following a brief description of the phonon theory in Chapter 2, a mathematically consistent general solution to the phonon equation of motion is presented in Chapter 3. It is shown that the displacements necessarily should include a left moving and a right moving wave train to satisfy all the internal degrees of freedom. The identification of the amplitudes in +**q** and –**q** wave vector directions provides a fundamental breakthrough for describing the correct form of energy and heat current modes expressed in normal mode coordinates.

In Chapter 4, a numerically efficient method based on the ratio of normal mode coordinates of velocity to those of displacements is presented for determining the phonon dispersion curve. While the theory is known before, the method has never been employed for computing phonon dispersion using atomistic simulations. Case studies on a monoatomic chain, a diatomic chain, and graphene demonstrate that the ratio method outperforms in accuracy and speed over the conventional method of using a fast Fourier transform (FFT).

The most impactful results of the dissertation are presented in Chapters 5 and 6. First, the mathematical and physical consistency conditions for heat carrier modes are derived in Chapter 5. It is shown that a real microscopic heat flux in normal mode coordinates can be consistently defined, and the net phonon population can be expressed as a difference in amplitudes along $+\mathbf{q}$ and $-\mathbf{q}$ wave vector directions. It is further demonstrated that phonon-phonon cross-correlations, which emerge naturally, can play a dominant role in the thermal transport process, especially for low-dimension systems; the derivation also identifies a correction term for phonon self-correlations. Interestingly, the correction from energy correlations leads to phonon lifetimes that are noticeably lower than those estimated using the existing approaches.

For low dimensional systems, it is more appropriate to investigate the local heat current and energy fluctuations in appropriate normal coordinates than to probe an ill-defined thermal conductivity. In Chapter 6, the theoretical framework for analyzing local energy and heat current fluctuations in corresponding (energy/flux) normal coordinates is presented. These energy/current modes are then connected to the phonon normal modes that allows the exciting possibility of analyzing energy/heat modes in the more familiar framework of displacement (phonon) normal modes. First, the energy/current modes are derived exactly for a harmonic

one-dimensional monoatomic chain; the theoretical prediction is verified subsequently using atomistic simulations. The theoretical derivation reveals a rather intriguing denouement on the possible combinations of phonon modes. Even with harmonic interaction, pairs of phonon modes combine to produce energy/heat modes if and only if they satisfy the three-phonon scattering law. It is known that three-phonon processes are required for thermal dissipation, and the appearance of the three-phonon scattering condition, from the energy/current modes, indicates the distinct possibility of predicting the phonon interaction types directly from the pertinent microscopic variables (energy/current) – a long sought after goal in recent theoretical studies. The three-phonon synergy has the lowest order of interaction, and this condition arises naturally with the interference of energy/heat waves. It is anticipated that if anharmonicity and higher dimensionality are included, higher order processes will evolve naturally without the need to specify or postulate the nature of phonon interactions in thermal transport.

Energy Transport in Low Dimensional Systems: Phonons and Beyond Phonon Descriptors

by
Anant Raj

A dissertation submitted to the Graduate Faculty of
North Carolina State University
in partial fulfillment of the
requirements for the Degree of
Doctor of Philosophy

Nuclear Engineering

Raleigh, North Carolina

April 2017

APPROVED BY:

Dr. Jacob Eapen Chair, Advisory Committee	Dr. Korukonda Murty Advisory Committee
Dr. Jerzy Bernholc Advisory Committee	Dr. Keith Gubbins Advisory Committee

BIOGRAPHY

Anant Raj was born in Kanpur, Uttar Pradesh, India, as the youngest of the three children to Dr. Raj Kumar Srivastava and Anita Srivastava in 1987. He received his undergraduate degree in Mechanical Engineering from the Indian Institute of Technology, Kanpur in 2010. During his undergraduate studies, he started working on nuclear imaging under the guidance of Prof. Prabhat Munshi and later got an opportunity to pursue an internship at the Manchester University under the guidance of Prof. Philp J. Withers. Inspired by Prof. Munshi, he proceeded to pursue graduate studies in Nuclear Engineering from the North Carolina State University in Fall 2010. He received a Masters degree in Nuclear Engineering in 2013 and continued to pursue a PhD degree under the guidance of Prof. Jacob Eapen. During his graduate studies, he was introduced to the fascinating field of materials science and learned the intricacies of probing materials behavior using the tools of statistical mechanics and atomistic simulations. He got married to Prerna Prateek in 2013.

ACKNOWLEDGMENTS

Pursuing a PhD is like running a marathon rather than a sprint, which requires persistence and constant motivation over long periods of time. In the journey towards realizing my PhD degree, I had the pleasure of getting support and guidance from many people who I had encountered on the way. I am highly grateful to those who had an immeasurable impact during my journey and would like to thank a few people who played a key role in my academic life.

First, I would like to thank my research advisor, *Prof. Jacob Eapen*, who had been a source of great inspiration and constant motivation throughout my PhD program. I am greatly thankful to him for allowing me the liberty to pursue my interests and nourishing my creativity and free thinking. He helped me grow as a researcher and inculcated in me the enduring values of integrity and discipline.

Next, I would like to thank *Professors K.L. Murty*, *Jerzy Bernholc*, and *Keith Gubbins* for serving in my PhD committee. As distinguished experts in their fields, their advice was critical to the completion of my dissertation. Further, I would also like to thank *Prof. K.L. Murty* for helping me to develop a firm understanding of materials behavior, and *Prof. Jerzy Bernholc* for enabling me to develop a deep intuition for statistical mechanics from their lectures.

I would like to thank all my professors at NC State; it's been a great privilege to have attended their classes. In particular, I would like to thank *Prof. Ayman Hawari* for introducing me to a flavor of statistics I had never encountered before, and *Prof. Hany Abdel-Khalik* for enabling

me to develop an insight into linear algebra that would, for forever, be useful. I am also grateful to *Prof. Beth Overman* for nurturing my passion for teaching during the PTP program at NC State.

I have been fortunate to have shared my graduate office with some wonderful colleagues at NC State. *Walid* (Mohamed) and *Xiaojun* (Mei) who joined the research group before me were of immense help during the initial days of my PhD. *Ajay* (Annamareddy), and *Jin* (Wang) started their graduate studies with me at NC State. *Ajay* completed his Ph.D last year and has now joined the group as a postdoctoral associate; I have always had fruitful research discussions with him. *Jin* completed his masters at NC State and has completed his Ph.D studies from the University of Connecticut; I wish him all the luck. *Dillon* (Sanders) and *William* (Lowe) joined the group a few semesters after me. I have had a great time learning and discussing with them. *Yu* (Luo) and *Ahmed* (Darwish) are the latest members of the group, and I have high hopes for all of them. I have also had the opportunity of working with and learning from several postdoctoral associates. *Prithwish* (Nandi), *Brahmananda* (Chakraborty), *Ram* (Krishna), *Nilesh* (Kumar) – they have all been a source of great help and guidance. I am also grateful to the NE department staff, *Lisa* (Marshall), *Ganga* (Atukorala), *Robert* (Green) and *Chintan* (Kanani).

Graduate life without friends is unthinkable. I am deeply thankful to all my graduate school friends *Anup*, *Arpit*, *Ankita*, *Ajay*, *Sandhya*, *Sameer*, *Shrikant*, *Shilpa*, *Shubham*, *Dileep*, *Gaurav*, *Abhigna*, *Hina*, *Haritha*, *Arka*, *Shefali*, *Paridhi*, *Nilesh* and *Suman* for a memorable time in Raleigh and NC State.

I would also like to thank *Prof. Munshi*, who had been my mentor and a father figure to me during my undergraduate studies at IIT. He had inspired me to pursue graduate studies in nuclear engineering and had always been there for advice whenever I needed it. I am deeply indebted and would forever be grateful to him. I would like to thank all my professors at IIT; they had been a great source of inspiration and learning. I would also like to thank all my friends at IIT – I had learned a great deal from them, and would forever cherish the time I had spent with them.

Lastly, I would like to thank my family members. My father has been my role model and has inspired me to pursue a career in academia. He has given me the courage to face any hurdles in my path without fear. I hope to emulate his hard work, sincerity and work ethics. My mother – her unconditional love, affection, and encouragement gives me strength and hope to face any adversity. It's a small wonder on how she manages her 24/7 work schedule without a break! My mother-in-law has also been a great support over the last four years. My sisters, *Amrita* and *Ankita* – their unconditional love has been my prized possession all through my childhood. My brothers-in-law, *Amit*, *Saket*, and *Pranay*, who are a delight to be with, makes me feel more secure. My nieces, *Anannya*, *Aakarshita* and *Aradhya* and nephew *Adhyayan* give me a genuine reason to smile; I feel greatly blessed for having them in my family. Finally, I would like to thank my wife, *Prerna*. It's her love and patience that has kept me going for the last four years. It also gives me great strength and hope for a great future.

TABLE OF CONTENTS

LIST OF TABLES

LIST OF FIGURES

Chapter 1: INTRODUCTION

1.1 Motivation

Thermal management is important for optimizing the performance and design of electronic devices. With the recent advances in nanotechnology, there is a growing interest in studying the fundamental mechanisms of energy transport, both at micro and nanoscales [1-13]. The discovery of low dimensional materials such as graphene [14] and carbon nanotube (CNT) [15], which exhibit extraordinary electronic [16, 17], thermal [18-24] and mechanical [25-28] properties, has increased the prospects of them being used in advanced electronic devices [23, 29, 30]. In turn, this has heightened the necessity for investigating the key mechanisms of energy transport, not just at nanoscales, but also for systems with lower dimensionality [4, 31-40].

Designing experimental methods [41-43] for thermal characterization becomes more intricate at nanoscales; the complexity is further escalated for non-isotropic materials. Experimental characterization may also get affected by boundary and interface effects. Atomistic computational methods [6, 44-46] provide an alternate framework for probing the thermal transport mechanisms; they also have the additional capability of extracting atomic-level attributes, which is not always possible with experiments.

Heat conduction in solid state electrical insulators has long been associated with phonons – the normal modes of vibrating atoms of a system [47]; in the quantum framework, phonons are treated as bosons. The transport of phonons can be described by the Boltzmann kinetic theory, which assumes gas-like interactions among the phonons [48]. The phonon modes interact due to the anharmonicity in the interatomic potential, which lead to phonon-phonon scattering events. For example, a cubic term in the interatomic interaction leads to scattering events involving three-phonon modes (also referred to as three-phonon scattering) [48]. These scattering events can either conserve momentum as in the case of normal scattering (or *N*-process), or lead to a net change in the momentum post-scattering as in the case of Umklapp scattering (or the *U*-process) [48]. Of these, only the Umklapp scattering provides a net resistance to the flow of energy resulting in a finite thermal conductivity [48]. The phonon-phonon scattering events ensure that any fluctuations in the phonon population from the equilibrium expectation value as given by the Bose-Einstein distribution, decays in time, which relaxes the system back to the equilibrium state.

Methods based on Boltzmann transport equation (BTE) are widely used to assess the phonon transport mechanisms and thermal conductivity of materials. BTE methods [44, 49, 50] generally use the single mode relaxation time approximation (SMRA) to estimate the relaxation time for each phonon mode. Relaxation time along with phonon group velocities and specific heat is then used to estimate the thermal conductivity. The SMRA approach basically assumes that only a single phonon mode is excited while all other modes are in equilibrium. However, recent investigations [51] demonstrate that SMRA leads to inaccurate

predictions for low dimensional systems where cross phonon correlations are significant even at high temperatures. Thus for low dimensional systems, a complete solution to the BTE is required using more accurate models that are also more complex [47, 52].

In an alternate framework, which is more fundamental, thermal conduction can be described by the linear response or equivalently, the Green-Kubo (GK) theory [53, 54], which relates the thermal conductivity to the decay of correlations of heat current fluctuations at equilibrium. Equilibrium atomistic or molecular dynamics (MD) simulations – classical or *ab-initio* – can be advantageously employed to determine the correlation of the heat current fluctuations. However, this approach does not lend itself naturally to identify the phonon modes of vibrations.

Following the seminal work of Ladd and Moran [55], there have been several attempts in the last decade [44, 56-62] to merge the GK approach with the BTE to obtain individual phonon contributions to the energy transport from statistical mechanics first principles. The primary objective of this dissertation is to develop a theoretical framework that can accommodate the GK and phonon theories while maintaining mathematical and physical consistency that has not been apparent in the earlier attempts.

The energy transport in low-dimensional systems is quite different from that in bulk three-dimensional systems. The Fourier law of thermal conduction has been reported to break down for nanoscale and low dimensional systems [31, 33, 35, 63]. Further, the thermal conductivity no longer remains an intrinsic property but varies with the size of the system for low

dimensional systems. One of the widely studied one dimensional (1-D) systems is the 1-D FPU chain [64] that exhibits anomalous energy transport [31, 33, 65] with the thermal conductivity exhibiting a power law divergence with system size. More realistic systems such as hydrocarbon chains [56, 66] are also known to show a similar behavior. For two dimensional (2-D) systems such as graphene, the thermal conductivity increases logarithmically with size [67, 68]. This anomalous behavior is linked to hydrodynamic [40, 69, 70] and ballistic [71] energy transport rather than diffusive energy transport observed for bulk three dimensional (3-D) systems. The energy transport tends to the ballistic or hydrodynamic when the non-resistive normal scattering dominate over the resistive Umklapp scattering [40]. Under such circumstances, significant cross-correlations [56, 58] between different phonon modes emerge that manifest as collective phonon excitations [40, 72]. Thus for low dimensional systems, it is more appropriate to probe the local heat current and energy fluctuations in appropriate normal coordinates. The second objective of this dissertation, therefore, is to develop a theoretical framework for analyzing local energy and heat current fluctuations in the corresponding (energy/flux) normal coordinates and relating them to collective phonon excitations thereby raising the possibility of analyzing the energy and heat current normal modes in the framework of collective phonon excitations.

1.2 Outline of this Dissertation

Following a brief description of the phonon theory in Chapter 2, a mathematically consistent general solution to the phonon equation of motion is presented in Chapter 3. It is shown that the displacements necessarily should include a left moving and a right moving wave train to

satisfy all the internal degrees of freedom. The identification of the amplitudes in +**q** and –**q** wavevector directions provides a fundamental breakthrough for describing the correct form of heat current modes expressed in normal mode coordinates. In Chapter 4, a numerically efficient method based on the ratio of normal mode coordinates of velocity to those of displacements is presented for determining the phonon dispersion curve. While the theory is known before [73], the method has never been employed for computing phonon dispersion using atomistic simulations. Case studies on a monoatomic chain, a diatomic chain, and graphene demonstrate that the ratio method outperforms in accuracy and speed over the conventional method of using a fast Fourier transform (FFT) [38, 73-76] .

The most impactful results of the dissertation are presented in Chapters 5 and 6. First, the mathematical and physical consistency conditions for heat carrier modes are derived in Chapter 5. It is shown that a real microscopic heat flux in normal mode coordinates can be consistently defined, and the net phonon population can be expressed as a difference in amplitudes along +**q** and –**q** wavevector directions. It is further shown that phonon-phonon cross-correlations can play a dominant role in the thermal transport process, especially for low-dimension systems; the derivation also identifies a correction term for phonon self-correlations. Interestingly, the correction leads to phonon lifetimes from energy correlations that are significantly lower than those estimated using the existing approaches.

In Chapter 6, the theoretical framework for analyzing local energy and heat current fluctuations in corresponding (energy/flux) normal coordinates is presented. These energy/current modes are then connected to the phonon normal modes, which allows the exciting possibility of

analyzing energy/heat modes in the framework of more familiar displacement normal modes. First, the energy/current modes are derived exactly for a harmonic one-dimensional monoatomic chain; the theoretical prediction is verified later using atomistic simulations. The theoretical derivation reveals a rather intriguing denouement on the possible combinations of phonon modes. Even with harmonic interaction, pairs of phonon modes combine to produce energy/heat modes if and only if they satisfy the three-phonon scattering law. As described before, it is known that three-phonon processes are required for thermal dissipation. The appearance of the three-phonon scattering condition, from the energy/current modes, thus indicates the distinct possibility of predicting the phonon interaction types directly from the pertinent microscopic variables (energy/current) – a long sought after goal in recent theoretical studies.

Chapter 2: PHONON THEORY

Thermal conduction in solids is governed primarily by electrons and lattice vibrations. For metals, the thermal transport is usually dominated by electrons while for non-metals, the absence of free electrons leaves lattice vibrations as the only means of conduction of energy [77]. The discreetness of the lattice structure restricts the frequencies and the wavelengths by which the atoms in the lattice can vibrate, and the allowed vibrational modes are referred to as the *normal modes*. The quantum of excitation of any normal mode of vibration is called a *phonon*, which is analogous to a photon as a quantum of electromagnetic excitation. The basic concepts of phonons are now well-established and are elucidated in several solid state and thermal physics monographs such as by Ziman [78], Kittel [79], Peierls [48], Dove [73] and Lou [80], Srivastava [47], Chen [7] and Kaviany [52]. This chapter summarizes the key concepts of phonon dynamics and its relationship to thermal transport.

This chapter begins with the dynamics of a linear chain of atoms, which is best suited for developing the concept of normal or phonon modes. It is then followed by a general description of the phonon modes in a 3-D lattice, both in the classical and quantum framework. Finally, the last section delineates how thermal properties can be computed in the phonon formalism.

2.1 Linear chain of atoms

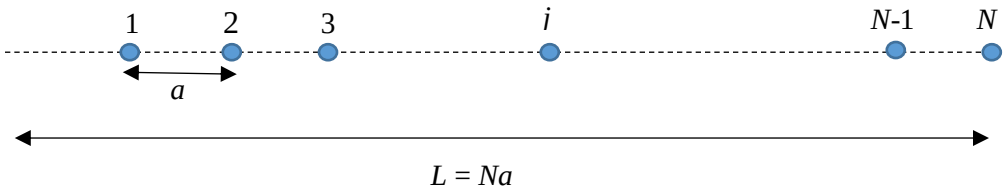

Figure 2.1: A linear chain of *N* atoms.

Consider a simple system of *N* atoms arranged in a linear chain as shown in *Figure 2.1*. The total length of the chain is *Na*, with *a* being the equilibrium separation between adjacent the atoms. The absolute position of the j^{th} atom at any instant is given by $x_j(t)$ while the displacement about its equilibrium position (ja) is given by $u_j(t)$ given by Eqn. (2.1). The atoms interact only with their immediate neighbors through a linear spring force with a spring constant *C* as given by Eqn. (2.2). Thus the linear chain comprises of *N* harmonic oscillators.

$$u_j(t) = x_j(t) - ja \tag{2.1}$$

$$F_{jk}(t) = -C\left(u_j(t) - u_k(t)\right) \tag{2.2}$$

The potential energy of interaction is given by Eqn. (2.3), and the net potential energy of the system and the net force on each atom are given by Eqns. (2.4) and (2.5):

$$U_{jk}(t) = \frac{1}{2}C\left(u_j(t) - u_k(t)\right)^2 \tag{2.3}$$

$$U(t) = \sum_{j>k} U_{jk}(t) \tag{2.4}$$

$$F_j(t) = C\left(u_{j-1}(t) - 2u_j(t) + u_{j+1}(t)\right) \tag{2.5}$$

The Newton's equation of motion for each atom is given by:

$$m\frac{\partial^2 u_j(t)}{\partial t^2} = C\left(u_{j-1}(t) - 2u_j(t) + u_{j+1}(t)\right) \tag{2.6}$$

A trial solution to the Eqn. (2.6) can be expressed as:

$$u_j(q,t) = \frac{A_q}{\sqrt{m}}\exp\left(i\left(qja - w_q t\right)\right) \tag{2.7}$$

The trial solution is that of a traveling wave with angular frequency w and wave vector q. The amplitude of the wave is equal to A_q, and the phase velocity is equal to w/q. The solution contains three constants – A, q, and w. The amplitude A is determined by the initial conditions while w is related to q *via* a dispersion relationship which will be discussed shortly. The boundary conditions restrict the allowed values for the wave vector. For a very long chain, each atom position will be nearly equivalent, and the boundaries will not have a significant effect. The customary approach for simulating an infinite system using a finite number of atoms is by joining the ends, which results in the Born-von Karman periodic boundary condition [81] – it essentially replicates the same system periodically as represented by Eqn. (2.8).

$$u_{j+N}(t) = u_j(t) \tag{2.8}$$

Substituting the solution from Eqn. (2.7) into Eqn. (2.8) gives:

$$\exp\left(i\left(qNa\right)\right) = 1 \tag{2.9}$$

Which restricts the wave vectors as given below:

$$q_r = r\frac{2\pi}{Na}; r = 0, \pm 1, \pm 2..... \tag{2.10}$$

Thus, only those wavelengths are allowed for which the total length of the system is an integral multiple of the wavelength. Every allowed wavelength is called the normal mode and it represents each independent mode of the system. The two longest wavelengths that are allowed in a 20-atom chain with a = 1 are shown in *Figure 2.2*. Though only certain discrete wavelengths are permitted, the variation in the wave vector space tends to continuous for a large chain ($N \rightarrow \infty$).

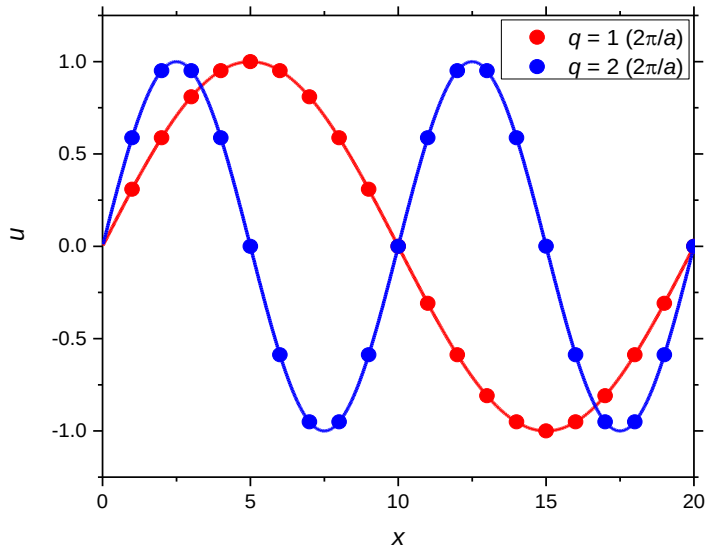

Figure 2.2: First two normal modes for a 20-atom chain with $a = 1$.

The atoms are only present at certain discrete locations, and thus the solution is physically meaningful only at these locations. The value of displacement at any point between these sites is irrelevant as it cannot be observed. Eqn. (2.11) shows that the displacements at these sites are identical for any two wave vectors that differ by an integral multiple of $2\pi/a$. As an example, *Figure 2.3* shows this equivalence for a 20-atom chain with $a = 1$, and for $q = 2\pi/a$, $q = 21\times(2\pi/a)$. Thus it is sufficient to consider only those wave vectors with a magnitude of $2\pi/a$ or less as represented by Eqn. (2.12). The positive and negative wave vectors represent waves moving in opposite directions.

$$u_j(q,t) = \frac{A_q}{\sqrt{m}}\exp\left(i\left(qja - w_q t\right)\right) = \frac{A_q}{\sqrt{m}}\exp\left(i\left(qja + 2nj\pi - w_q t\right)\right) = u_j\left(q + n\frac{2\pi}{a}, t\right); n \in \mathbb{Z} \qquad (2.11)$$

$$-\frac{\pi}{a} < q_r \le \frac{\pi}{a} \text{ or } -\frac{N}{2} < r \le \frac{N}{2} \qquad (2.12)$$

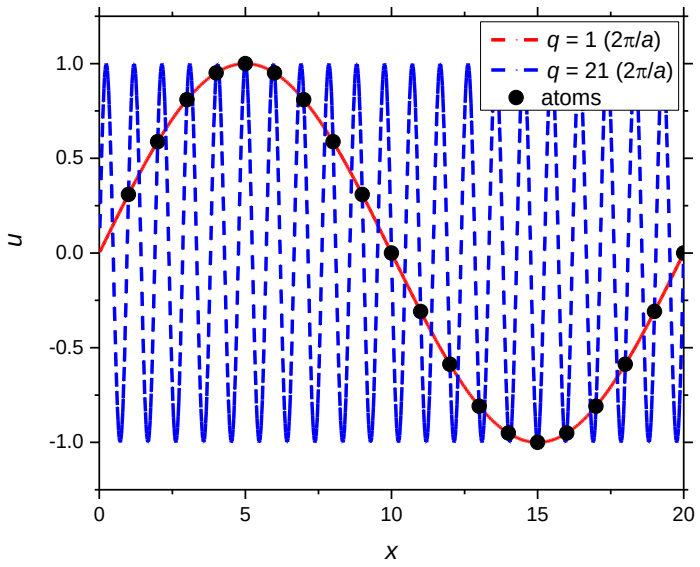

Figure 2.3: The equivalence of atomic displacements for two modes whose wave vectors differ by $2\pi/a$ for a 20-atom chain with $a = 1$.

The relationship between the wave vector and frequency, known as the dispersion relationship, can be obtained by plugging the solution from Eqn. (2.7) into Eqn. (2.6). *Figure 2.4* shows the dispersion curve for the linear chain as given by Eqn. (2.13). This sinusoidal variation of the dispersion curve is due to the discreteness of the lattice. The limits on the wave vector, as described before, appear from the atomic discreetness. The interval described by Eqn. (2.12) is called the first Brillouin zone and the wave vectors within the first Brillouin zone are sufficient to describe the linear chain system.

$$w_q = \sqrt{\frac{4C}{m}}\left|\sin\left(\frac{qa}{2}\right)\right| \tag{2.13}$$

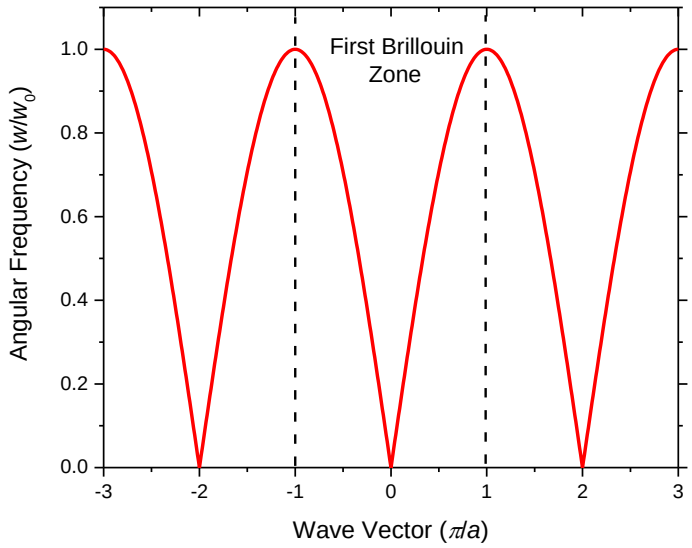

Figure 2.4: Dispersion curve for a 1-D linear chain. The angular frequency has been normalized to the peak value $w_0 = \sqrt{\frac{4C}{m}}$, and the wave vector has been normalized by π/a.

The general solution is a linear combination of all normal modes, and is given by Eqn. (2.14):

$$u_j(t) = \sum_{-\frac{\pi}{a} < q \le \frac{\pi}{a}} \frac{A_q}{\sqrt{m}} \exp\left(i\left(qja - w_q t\right)\right) \tag{2.14}$$

It can be observed from Eqn. (2.12) that an odd value of N will allow the following integer values: $r = 0, \pm1, \pm2, \ldots \pm(N\text{-}1)/2$; a total of N different values for r. Similarly, an even value of N will allow $r = 0, \pm1, \pm2, \ldots \pm N/2$. However, $r = N/2$ and $r = -N/2$ represent the same mode since they differ by $2\pi/a$. Thus both cases will result in N unique values of r.

The amplitude A_q is complex, and thus has a magnitude and a phase (in the exponential representation). Hence Eqn. (2.14) has a total of $2N$ constants to be determined. The initial

condition for the positions will only supply *N* equations. To completely determine the solution, another *N* equations are required; these are obtained from the initial conditions in the velocity. Thus it is essentially equivalent to making a transformation from 2*N* degrees of freedom for positions and velocities of the *N* atoms to a system of 2*N* degrees of freedom for the amplitudes and phases of the *N* normal modes of vibration of the atoms.

The total energy associated with each normal mode is related to the normal mode coordinate $Q(q,t)$ as given by Eqn. (2.15) and Eqn. (2.16):

$$Q(q,t) = \frac{1}{\sqrt{N}} \sum_j \sqrt{m} \exp\left(-i(qja)\right) u_j(t) \tag{2.15}$$

$$E(q,t) = \frac{1}{2}\left[\dot{Q}(q,t)\dot{Q}^*(q,t) + w_q{}^2 Q(q,t) Q^*(q,t)\right] \tag{2.16}$$

It can be shown [73] that the total energy (E) of the system is just the sum of individual contributions due to each normal mode (Eqn. (2.17)). However, in real space (**r**), the potential energy is coupled as shown in Eqn. (2.18):

$$E(t) = \sum_{-\frac{\pi}{a} < q \le \frac{\pi}{a}} \frac{1}{2}\left[\dot{Q}(q,t)\dot{Q}^*(q,t) + w_q{}^2 Q(q,t) Q^*(q,t)\right] = \sum_{-\frac{\pi}{a} < q \le \frac{\pi}{a}} E(q,t) \tag{2.17}$$

$$E(t) = \sum_{j=1}^{N} \frac{1}{2} m v_j{}^2(t) + \sum_{k<j} \frac{1}{2} C\left(u_j(t) - u_k(t)\right)^2 \tag{2.18}$$

In the classical theory, the amplitude of any normal mode is continuous and can take any arbitrary value. Thus a normal mode can have any arbitrary amount of energy associated with it. However, quantum theory puts constraints on the amount of energy each mode can possesses. The energy quanta associated with each normal mode is uniquely dependent on its frequency, and the quantum of excitation of a normal mode of vibration is referred to as the *phonon*.

For a perfect harmonic interaction, the individual normal modes do not interact with each other. Thus given the initial conditions, the amplitude of each normal mode gets fixed and does not change with time. This represents a system with an infinite thermal conductivity as it can sustain a finite and constant heat current without any temperature gradient. In real crystals, the the anharmonicity in the interatomic potential enables the normal modes to interact and thus impose a resistance to the flow of heat.

2.2 General three-dimensional lattice in classical framework

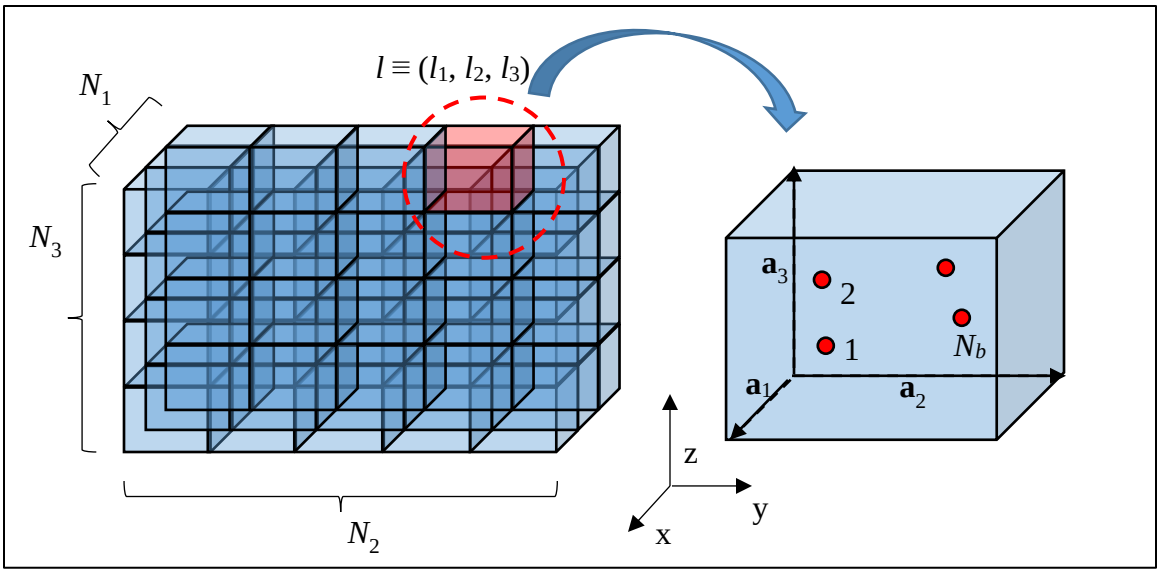

Figure 2.5: A general three-dimensional lattice with N_b atoms per unit cell.

Consider a general three-dimensional lattice with N_b atoms per unit cell as shown in *Figure 2.5*. The lattice vectors are given by $\mathbf{a}_1$, $\mathbf{a}_2$ and $\mathbf{a}_3$, and there are N_1, N_2 and N_3 unit cells along each of these vectors respectively, thus resulting in a total of $N_u = N_1N_2N_3$ unit cells and $N = N_uN_b$ atoms. The three lattice vectors need not be orthogonal to each other. Any unit cell can be referenced by three indices (l_1, l_2, l_3) or equivalently with just a single index l such that the two are related by Eqn. (2.19). The location of the origin of the l^{th} unit cell is denoted by $\mathbf{r}_l$ and is given by Eqn. (2.20). The equilibrium position of the j^{th} atom in a unit cell with respect to the origin of the unit cell is given by $\Delta\mathbf{r}_j$. The displacement of the j^{th} atom in the l^{th} unit cell from its equilibrium position is denoted by $\mathbf{u}(j,l,t)$ while its absolute position is denoted by $\mathbf{r}(j,l,t)$. The absolute and the relative positions are related by Eqn. (2.21).

$$(l_1, l_2, l_3) \equiv l, \text{ such that : } l = l_1 + (l_2 - 1) \times N_1 + (l_3 - 1) \times N_1 \times N_2 \tag{2.19}$$

$$\mathbf{r}_l = l_1 \mathbf{a}_1 + l_2 \mathbf{a}_2 + l_3 \mathbf{a}_3 \tag{2.20}$$

$$\mathbf{u}(j, l, t) = \mathbf{r}(j, l, t) - \mathbf{r}_l - \Delta \mathbf{r}_j \tag{2.21}$$

The state of the system at any instant is given by the relative displacements and velocities of each atom, and are denoted by the column vectors **u**(t) and **v**(*t*) as given in Eqn. (2.22). Thus there are a total of 6*N* degrees of freedom, with 3 degrees of freedom each for the displacement and velocity of every atom.

$$\mathbf{u}(t) = \begin{Bmatrix} \mathbf{u}(1,1,t) \\ \mathbf{u}(2,1,t) \\ \\ \mathbf{u}(N_b,1,t) \\ \mathbf{u}(1,2,t) \\ \\ \mathbf{u}(j,l,t) \\ \\ \mathbf{u}(N_b, N_u, t) \end{Bmatrix}, \mathbf{v}(t) = \begin{Bmatrix} \mathbf{v}(1,1,t) \\ \mathbf{v}(2,1,t) \\ \\ \mathbf{v}(N_b,1,t) \\ \mathbf{v}(1,2,t) \\ \\ \mathbf{v}(j,l,t) \\ \\ \mathbf{v}(N_b, N_u, t) \end{Bmatrix} \tag{2.22}$$

The potential energy of the system, which is a function of the displacements of each atom about the equilibrium position (Eqn. (2.23)), can be expanded using Taylor's expansion as shown in Eqn. (2.24).

$$U(t) = U(\mathbf{u}(t)) \tag{2.23}$$

$$U(t) = U_0 + \sum_{j,l,\alpha} \left. \frac{\partial\left(U\left(\mathbf{u}(t)\right)\right)}{\partial u_\alpha(j,l,t)} \right|_0 \times u_\alpha(j,l,t) + \frac{1}{2} \sum_{j',l',\beta} \sum_{j,l,\alpha} \left. \frac{\partial^2\left(U\left(\mathbf{u}(t)\right)\right)}{\partial u_\alpha(j,l,t)\partial u_\beta(j',l',t)} \right|_0 \times u_\alpha(j,l,t) u_\beta(j',l',t) + \text{....higher order terms} \tag{2.24}$$

The first term is a constant and is irrelevant to the dynamics and thus can be omitted. The second term goes to zero as a condition for equilibrium (see Eqn. (2.25)). The third term represents the forces experienced by the atoms.

$$\left. \frac{\partial\left(U\left(\mathbf{u}(t)\right)\right)}{\partial u_\alpha(j,l,t)} \right|_0 = 0 \tag{2.25}$$

The higher order terms can be neglected for small displacements about the equilibrium. Under the restrictive harmonic approximation, the potential energy can be approximated as in Eqn. (2.26):

$$U(t) \approx \frac{1}{2} \sum_{j',l',\beta} \sum_{j,l,\alpha} G_{j',l',\beta,j,l,\alpha} \times u_\alpha(j,l,t) u_\beta(j',l',t) \tag{2.26}$$

Above, *G* refers to the force constant and is defined by:

$$G_{j',l',\beta,j,l,\alpha} = \left. \frac{\partial^2\left(U\left(\mathbf{u}(t)\right)\right)}{\partial u_\alpha(j,l,t)\partial u_\beta(j',l',t)} \right|_0 \tag{2.27}$$

where α and β refer to the components of the vector along the coordinate axis. Thus $u_\alpha(j,l,t)$ denotes the displacement of the j^{th} atom of the l^{th} unit cell along the direction α at time t. The force on the j^{th} atom of the l^{th} unit cell is given by Eqn. (2.28):

$$F_\alpha\left(j,l,t\right)=m_j\frac{\partial^2\left(u_\alpha\left(j,l,t\right)\right)}{\partial t^2}=-\sum_{j',l',\beta}G_{j',l',\beta,j,l,\alpha}\times u_\beta\left(j',l',t\right) \tag{2.28}$$

The above equation admit traveling wave solutions of the form given by Eqn. (2.29):

$$u_\alpha^{\mathbf{q},p}\left(j,l,t\right)=\frac{1}{\sqrt{m_j}}A\left(\mathbf{q},p,t\right)e_{j,\alpha}\left(\mathbf{q},p\right)\exp\left(i\left(\mathbf{q}.\mathbf{r}_l-w\left(\mathbf{q},p\right)t\right)\right) \tag{2.29}$$

where $\mathbf{q}$ represents the wave vector while $w(\mathbf{q},p)$ represents the angular frequency. For every wave vector, there are $3N_b$ different possible frequencies each for a unique combination of the motion of the N_b basis atoms of the unit cell. The index p above refers to these modes and $e_{j,\alpha}(\mathbf{q},p)$ represents the unique combination for each mode. $A(\mathbf{q},p,t)$ gives the amplitude of the wave for the mode p.

The frequency and modes are obtained by substituting the solution from Eqn. (2.29) into Eqn. (2.28). This results in the dispersion relation given by Eqn. (2.30), where D denotes the dynamical matrix and is defined by Eqn. (2.31).

$$w^2\left(\mathbf{q},p\right)e_{j,\alpha}\left(\mathbf{q},p\right)=\sum_{j',\beta}D_{j,\alpha,j',\beta}\left(\mathbf{q}\right)e_{j',\beta}\left(\mathbf{q},p\right) \tag{2.30}$$

$$D_{j,\alpha,j',\beta}(\mathbf{q}) = \frac{1}{\sqrt{m_j m_{j'}}} \sum_{l,l'} G_{j',l',\beta,j,l,\alpha} \exp\left(i\left(\mathbf{q}.\left(\mathbf{r}_{l'} - \mathbf{r}_l\right)\right)\right) \tag{2.31}$$

The dispersion relation given in Eqn. (2.30) can be recast as:

$$\mathbf{D}(\mathbf{q})\mathbf{e}(\mathbf{q}, p) = w^2(\mathbf{q}, p)\mathbf{e}(\mathbf{q}, p) \tag{2.32}$$

Thus the dispersion relationship is simply an eigenvalue problem as represented by Eqn. (2.32) . The solution would thus give $3N_b$ eigenvalues and eigenvectors.

$$\mathbf{e}(\mathbf{q}, p) = \begin{Bmatrix} e_{1,x}(\mathbf{q}, p) \\ e_{1,y}(\mathbf{q}, p) \\ e_{1,z}(\mathbf{q}, p) \\ . \\ . \\ e_{N_b,x}(\mathbf{q}, p) \\ e_{N_b,y}(\mathbf{q}, p) \\ e_{N_b,z}(\mathbf{q}, p) \end{Bmatrix} \tag{2.33}$$

$$\mathbf{D}(\mathbf{q}) = \begin{pmatrix} D_{1,x,1,x}(\mathbf{q}) & D_{1,x,1,y}(\mathbf{q}) & D_{1,x,1,z}(\mathbf{q}) & . & . & D_{1,x,N_b,x}(\mathbf{q}) & D_{1,x,N_b,y}(\mathbf{q}) & D_{1,x,N_b,z}(\mathbf{q}) \\ D_{1,y,1,x}(\mathbf{q}) & D_{1,y,1,y}(\mathbf{q}) & D_{1,y,1,z}(\mathbf{q}) & . & . & D_{1,y,N_b,x}(\mathbf{q}) & D_{1,y,N_b,y}(\mathbf{q}) & D_{1,y,N_b,z}(\mathbf{q}) \\ D_{1,z,1,x}(\mathbf{q}) & D_{1,z,1,y}(\mathbf{q}) & D_{1,z,1,z}(\mathbf{q}) & . & . & D_{1,z,N_b,x}(\mathbf{q}) & D_{1,z,N_b,y}(\mathbf{q}) & D_{1,z,N_b,z}(\mathbf{q}) \\ . & . & . & . & . & . & . & . \\ . & . & . & . & . & . & . & . \\ D_{N_b,x,1,x}(\mathbf{q}) & D_{N_b,x,1,y}(\mathbf{q}) & D_{N_b,x,1,x}(\mathbf{q}) & . & . & D_{N_b,x,N_b,x}(\mathbf{q}) & D_{N_b,x,N_b,y}(\mathbf{q}) & D_{N_b,x,N_b,z}(\mathbf{q}) \\ D_{N_b,y,1,x}(\mathbf{q}) & D_{N_b,y,1,y}(\mathbf{q}) & D_{N_b,x,1,x}(\mathbf{q}) & . & . & D_{N_b,y,N_b,x}(\mathbf{q}) & D_{N_b,y,N_b,y}(\mathbf{q}) & D_{N_b,y,N_b,z}(\mathbf{q}) \\ D_{N_b,z,1,x}(\mathbf{q}) & D_{N_b,z,1,y}(\mathbf{q}) & D_{N_b,x,1,x}(\mathbf{q}) & . & . & D_{N_b,z,N_b,x}(\mathbf{q}) & D_{N_b,z,N_b,y}(\mathbf{q}) & D_{N_b,z,N_b,z}(\mathbf{q}) \end{pmatrix} \tag{2.34}$$

The format of the eigenvectors and the dynamical matrix is given in Eqn. (2.33) and Eqn. (2.34) respectively. Finally the dispersion relationship can be evaluated by solving the characteristic equation given by:

$$\left|D_{j,\alpha,j',\beta}(\mathbf{q}) - \delta_{\alpha\beta}\delta_{jj'}w^2(\mathbf{q},p)\right| = 0 \tag{2.35}$$

The eigenvalues denote the square of the frequency $w(\mathbf{q},p)$ while the eigenvectors give the mode of vibration $\mathbf{e}(\mathbf{q},p)$ for the wave vector $\mathbf{q}$ and mode p as discussed above. If the direction of vibration is parallel to the wave vector, then it is called a longitudinal mode while if it is perpendicular to the wave vector, then it is referred to as a transverse mode. However, for most cases, a clear distinction between the longitudinal and transverse modes is not possible unless the wave vector is directed along a high symmetry direction.

Eqn. (2.36) defines the reciprocal lattice vectors (**b**), and these are perpendicular to the lattice vectors (**a**) as shown in Eqn. (2.37).

$$\mathbf{b}_1 = \frac{2\pi(\mathbf{a}_2\times\mathbf{a}_3)}{\left|\mathbf{a}_1.(\mathbf{a}_2\times\mathbf{a}_3)\right|}, \mathbf{b}_2 = \frac{2\pi(\mathbf{a}_3\times\mathbf{a}_1)}{\left|\mathbf{a}_1.(\mathbf{a}_2\times\mathbf{a}_3)\right|}, \mathbf{b}_3 = \frac{2\pi(\mathbf{a}_1\times\mathbf{a}_2)}{\left|\mathbf{a}_1.(\mathbf{a}_2\times\mathbf{a}_3)\right|} \tag{2.36}$$

$$\mathbf{a}_i.\mathbf{b}_j = 2\pi\delta_{ij} \tag{2.37}$$

For the special case of $\mathbf{a}_1$, $\mathbf{a}_2$ and $\mathbf{a}_3$ being mutually perpendicular, the reciprocal vectors will be parallel to the regular lattice vectors. For the case with the added condition of $|\mathbf{a}_1| = |\mathbf{a}_2| =$

$|\mathbf{a}_3| = a$, apart from the condition for orthogonality, the reciprocal lattice vectors will be parallel to the regular lattice vectors with each having a magnitude of $b = 2\pi/a$.

Periodic boundary conditions (Eqn. (2.38)) impose restrictions on the wave vectors as below in Eqn.(2.39):

$$u_\alpha^{\mathbf{q},p}\left(j,l_1,l_2,l_3,t\right) = u_\alpha^{\mathbf{q},p}\left(j,l_1+N_1,l_2,l_3,t\right) = u_\alpha^{\mathbf{q},p}\left(j,l_1,l_2+N_2,l_3,t\right) = u_\alpha^{\mathbf{q},p}\left(j,l_1,l_2,l_3+N_3,t\right) \tag{2.38}$$

$$\exp\left(i\left(\mathbf{q}.\left(N_1\mathbf{a}_1\right)\right)\right) = \exp\left(i\left(\mathbf{q}.\left(N_2\mathbf{a}_2\right)\right)\right) = \exp\left(i\left(\mathbf{q}.\left(N_3\mathbf{a}_3\right)\right)\right) = 1 \tag{2.39}$$

The wave vector **q** is defined in the reciprocal lattice coordinates as given by Eqn. (2.40):

$$\mathbf{q} = q_1\mathbf{b}_1 + q_2\mathbf{b}_2 + q_3\mathbf{b}_3 \tag{2.40}$$

Defining the wave vector in the reciprocal gives a particular advantage when calculating its dot product with any vector in the regular lattice as seen in Eqn. (2.41). Thus, using the reciprocal lattice coordinates to represent **q** in the Eqn. (2.39) results in the allowed values for the wave vectors given by Eqn. (2.42).

$$\mathbf{q}.\mathbf{r}_l = \left(q_1\mathbf{b}_1 + q_2\mathbf{b}_2 + q_3\mathbf{b}_3\right).\left(l_1\mathbf{a}_1 + l_2\mathbf{a}_2 + l_3\mathbf{a}_3\right) = \left(q_1l_1 + q_2l_2 + q_3l_3\right)2\pi \tag{2.41}$$

$$q_1 = \frac{r_1}{N_1}; q_2 = \frac{r_2}{N_2}; q_3 = \frac{r_3}{N_3}; \forall r_1, r_2, r_3 \in \mathbb{Z} \tag{2.42}$$

The solution is physically meaningful only at discrete locations in the real space. Consider two wave vector **q** and **q**' that differ by a reciprocal lattice vector as given in Eqn. (2.43). The dot

products of these vectors with any real space vector are related by Eqn. (2.44). Thus, the displacement at any lattice position, due to any two wave vectors that differ by a reciprocal lattice vector are identical as shown in Eqn. (2.45). Hence a Brillouin zone can again be constructed, and only the vectors within the first Brillion zone need to be considered.

$$\mathbf{q} = q_1\mathbf{b}_1 + q_2\mathbf{b}_2 + q_3\mathbf{b}_3; \mathbf{q}' = \mathbf{q} + p_1\mathbf{b}_1 + p_2\mathbf{b}_2 + p_3\mathbf{b}_3; \forall p_1, p_2, p_3 \in \mathbb{Z} \tag{2.43}$$

$$\mathbf{q}'.\mathbf{r}_l = \mathbf{q}.\mathbf{r}_l + \left(p_1 l_1 + p_2 l_2 + p_3 l_3\right) 2\pi \tag{2.44}$$

$$\exp\left(i\left(\mathbf{q}.\mathbf{r}_l - w\left(\mathbf{q}, p\right)t\right)\right) = \exp\left(i\left(\mathbf{q}.\mathbf{r}_l + \left(p_1 l_1 + p_2 l_2 + p_3 l_3\right) 2\pi - w\left(\mathbf{q}, p\right)t\right)\right) \tag{2.45}$$

The wave propagates along the direction of the wave vector at the phase velocity defined by Eqn. (2.46):

$$\mathbf{v}_p\left(\mathbf{q}, p\right) = \frac{w\left(\mathbf{q}, p\right)}{|\mathbf{q}|}\frac{\mathbf{q}}{|\mathbf{q}|} \tag{2.46}$$

$$\mathbf{v}_g\left(\mathbf{q}, p\right) = \frac{\partial w\left(\mathbf{q}, p\right)}{\partial \mathbf{q}} = \frac{\partial w\left(\mathbf{q}, p\right)}{\partial q_x}\hat{i} + \frac{\partial w\left(\mathbf{q}, p\right)}{\partial q_y}\hat{j} + \frac{\partial w\left(\mathbf{q}, p\right)}{\partial q_z}\hat{k} \tag{2.47}$$

However, the energy transfer does not take place at the phase velocity but at the group velocity as defined by Eqn. (2.47). Note that the group velocity may or may not be parallel to the wave vector. Thus the propagation of energy may not be parallel to the direction of propagation of the wave.

2.3 Quantum framework

In the quantum framework, the positions and momenta are replaced by state vectors a shown in Eqn. (2.48) and follow the commutation relation given by Eqn. (2.49).

$$\left|\mathbf{u}\right\rangle \equiv \left|\mathbf{u}_{1,1}\mathbf{u}_{1,2}....\mathbf{u}_{N_u,N_b}\right\rangle ; \left|\mathbf{p}\right\rangle \equiv \left|\mathbf{p}_{1,1}\mathbf{p}_{1,2}....\mathbf{p}_{N_u,N_b}\right\rangle \tag{2.48}$$

$$\left[u_{l,r,\alpha}, p_{l',r',\beta}\right] = i\hbar\delta_{ll'}\delta_{rr'}\delta_{\alpha\beta} \tag{2.49}$$

The total energy is replaced by the Hamiltonian operator:

$$\hat{H} = \sum_{l,r,\alpha}\frac{1}{2m_l}\hat{p}_{l,r,\alpha}.\hat{p}_{l,r,\alpha} + \frac{1}{2}\sum_{l,r,\alpha}\sum_{l',r',\beta}\hat{u}_{l,r,\alpha}\hat{G}_{r,l,\alpha,r',l',\beta}\hat{u}_{l',r',\beta} \tag{2.50}$$

The problem now involves solving the Schrodinger's equation for the above Hamiltonian and obtaining the eigenvalues and the eigenvectors. Symmetry arguments can be used to obtain solutions similar to Eqn. (2.29) with the same dispersion relation and wave vectors; a detailed derivation can be found in Ziman [78].

The eigenvalues of the Hamiltonian operator denote the total energy associated with that mode, and the energy eigenvalue for the eigenmode with wave vector **q** and mode of vibration *p* is given by Eqn. (2.51):

$$E_{\mathbf{q},p} = \left(n_{\mathbf{q},p} + \frac{1}{2}\right)\hbar w(\mathbf{q}, p); n_{\mathbf{q},p} = 0,1,2.... \tag{2.51}$$

where $n_{\mathbf{q},p}$ is the occupation number of each mode. Thus the energy associated with any mode is now quantized. The lattice vibration, therefore, can be treated as a collection of particles similar to the electromagnetic wave being a collection of photons; as described before, this quantum of excitation for the lattice wave is called a phonon. However, it should be noted that unlike the photon, a phonon does not carry any real momentum. The wave vector of a lattice wave is similar to the momentum of a photon (both being equal to a constant divided by the wavelength), but the wave vector is not conserved in every phonon-phonon interaction [48, 78] as will be discussed in the next section.

The phonons follow the Bose-Einstein statistics, and the average occupation number of any mode is related to temperature as [77]:

$$\bar{n}_{\mathbf{q},p}(T) = \frac{1}{\exp\left(\frac{\hbar w(\mathbf{q},p)}{k_B T}\right) - 1} \tag{2.52}$$

The occupation number is related to the amplitude of the normal mode coordinates obtained using classical analysis, which is given by [73]:

$$\bar{n}_{\mathbf{q},p}(T) \approx \frac{1}{\hbar} w(\mathbf{q},p) \left\langle \left| Q(\mathbf{q},p,T) \right|^2 \right\rangle \tag{2.53}$$

$$\bar{E}_{\mathbf{q},p}(T) = \left(\bar{n}_{\mathbf{q},p}(T) + \frac{1}{2} \right) \hbar w(\mathbf{q},p) \approx k_B T; \forall T \gg 1 \tag{2.54}$$

Clearly, the average energy associated with any mode approaches the classical prediction of $k_B T$ at higher temperatures (see Eqn. (2.54)).

2.4 Thermal Properties

As the energy of the lattice is stored in the form of phonons, several of the thermal properties of a system can be explained using the phonon concept. This section will briefly describe how the specific heat, heat current, and the thermal conductivity can be expressed in the phonon framework. The average energy of the lattice due to any mode is given by:

$$\bar{E}(T) = \sum_{\mathbf{q},p} \bar{E}_{\mathbf{q},p}(T) = \sum_{\mathbf{q},p} \left(\frac{1}{\exp\left(\frac{\hbar w(\mathbf{q},p)}{k_B T} \right) - 1} + \frac{1}{2} \right) \hbar w(\mathbf{q},p) \tag{2.55}$$

Thus the molar specific heat is given by Eqns. (2.56) and (2.57); in the high-temperature limit, it tends to the classical value of $3R$, where R is the universal gas constant.

$$C_v(T) = \frac{N_A}{N} \sum_{\mathbf{q},p} \frac{\partial}{\partial T} \left(\frac{1}{\exp\left(\frac{\hbar w(\mathbf{q},p)}{k_B T} \right) - 1} + \frac{1}{2} \right) \hbar w(\mathbf{q},p) = \frac{N_A}{N} \sum_{\mathbf{q},p} C_v(\mathbf{q},p,T) \tag{2.56}$$

$$C_v(\mathbf{q},p,T) = \left(\frac{\hbar w(\mathbf{q},p)}{k_B T} \right)^2 \exp\left(\frac{\hbar w(\mathbf{q},p)}{k_B T} \right) \left(\exp\left(\frac{\hbar w(\mathbf{q},p)}{k_B T} \right) - 1 \right)^{-2} \tag{2.57}$$

The energy current due to a phonon mode is given by Eqn. (2.58). This is simply a product of the occupation number, the energy carried by each phonon and the velocity of transport.

$$\mathbf{J}(\mathbf{q}, p, t) = n_{\mathbf{q},p}(t)\hbar w(\mathbf{q}, p)\mathbf{v}_g(\mathbf{q}, p) \tag{2.58}$$

Note that the $\mathbf{v}_g$ for positive and negative wave vectors are in opposite directions while their average occupation numbers are the same. Thus the net heat current due to all modes is related to the difference in the phonon population as shown below:

$$\mathbf{J}(t) = \sum_{\mathbf{q},p} \delta n_{\mathbf{q},p}(t)\hbar w(\mathbf{q}, p)\mathbf{v}_g(\mathbf{q}, p) \tag{2.59}$$

Combining the positive and the negative modes:

$$\mathbf{J}(t) = \sum_{\mathbf{q}_+,p} \left(\delta n_{\mathbf{q},p}(t) - \delta n_{-\mathbf{q},p}(t)\right)\hbar w(\mathbf{q}, p)\mathbf{v}_g(\mathbf{q}, p) \tag{2.60}$$

Thus the net heat flow is due to the difference in the population between the positive and the negative modes – an important concept that will be highlighted later in this dissertation. At equilibrium, the average occupation number of both will be same, and thus there will be no net average energy flow. However, thermal fluctuations will cause the occupation number to deviate spontaneously, and thus there will be an instantaneous heat current due to the thermal fluctuations. The variance of the deviation of the population from the average value is related to the specific heat of the normal mode.

For an harmonic oscillator, the amplitudes of the normal modes are fixed by the initial conditions and do not change with time due to the lack of any interactions. Thus if the initial occupation number of the positive and negative modes are unequal, then there will be a constant finite heat current in the system. Since there is no resistance to the flow of energy, the system will exhibit an infinite thermal conductivity. Finite conductivity, therefore, requires interaction between the phonon modes. This interaction causes resistance to the flow of energy and is called phonon-phonon scattering, which is engendered by the higher order (anharmonic) interactions. As briefly described before, the cubic term in the interatomic potential induces interaction involving three-phonon modes; quartic term induces interactions involving four-phonon modes and so forth [48, 78]. In most cases, only the three-phonon interactions remain significant for thermal transport.

The theory of three-phonon interactions, as first described by Peierls [48], is outlined here without the detailed derivations. It involves interaction between two phonon modes to generate a third phonon mode. The phonon interaction is permitted only for the modes which satisfy the conditions given in Eqns. (2.61) and (2.62).

$$\mathbf{q}_1 + \mathbf{q}_2 = \mathbf{q}_3 + \mathbf{g} \tag{2.61}$$

$$w_1 + w_2 = w_3 \tag{2.62}$$

$$\mathbf{g} = i_1\mathbf{b}_1 + i_2\mathbf{b}_2 + i_3\mathbf{b}_3;\ \text{for } i_1, i_2, i_3 \in \mathbb{Z} \tag{2.63}$$

The first condition involving the wave vectors (in Eqn. (2.61)) is similar to a momentum conservation equation, though the phonon wave vectors are not always conserved. The vector **g** is any reciprocal lattice vector as given in Eqn. (2.63). For the special case where **g** equals zero, the net wave vector is conserved, and the interaction is called the normal scattering or the *N*-process. For the case when **g** is non-zero, the vector is not conserved and the interaction is called the Umklapp scattering or the *U*-process. *Figure 2.6* illustrates the two processes for a two-dimensional case. The second condition in Eqn. (2.62) is simply an energy conservation equation and is always valid.

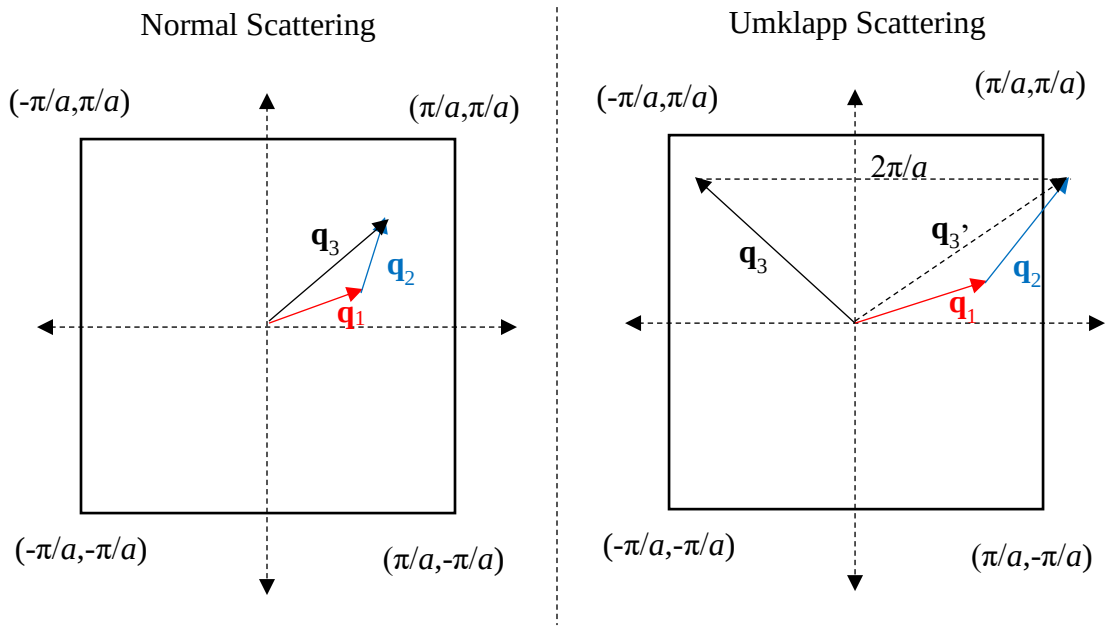

Figure 2.6: Two-dimensional representation of the Normal and Umklapp scattering process as described in [77].

Similarly, a phonon can split into two new phonons such that:

$$\mathbf{q}_1 = \mathbf{q}_2 + \mathbf{q}_3 + \mathbf{g} \tag{2.64}$$

$$w_1 = w_2 + w_3 \tag{2.65}$$

Thus a phonon once created, can scatter into different modes *via* three-phonon interactions (or higher order interactions) and hence has a finite lifetime or mean free path. This scattering by phonons generates a resistance to the flow of energy.

The phonon lifetimes can be evaluated through the Boltzmann transport equation (BTE). As described previously, it is customary to use a single mode relaxation time approximation (SMRA). The relaxation time can then be expressed as [77]:

$$\left(\frac{\partial n_{\mathbf{q},p}(t,T)}{\partial t}\right)_{scattering} \approx \frac{\left\langle n_{\mathbf{q},p}(T)\right\rangle - n_{\mathbf{q},p}(t,T)}{\tau(\mathbf{q},p,T)} \tag{2.66}$$

where τ is the lifetime of a phonon mode while the LHS represents the rate of phonon scattering. Thus the lifetime represents the average time taken by any fluctuation about the equilibrium expectation value to decay off. Using Eqn. (2.66) and SMRA, the thermal conductivity tensor can now be evaluated as [77]:

$$\kappa_{\alpha\beta}(T) = \frac{1}{V}\sum_{\mathbf{q},p} C_v(\mathbf{q},p,T) v_{g,\alpha}(\mathbf{q},p) v_{g,\beta}(\mathbf{q},p) \tau(\mathbf{q},p,T) \tag{2.67}$$

where α and β represent the components along the coordinate axes. For an isotropic material, the thermal conductivity can be treated as a scalar, which is given by:

$$\kappa(T) = \frac{1}{3V} \sum_{\mathbf{q},p,\alpha} C_v(\mathbf{q}, p, T) v_{g,\alpha}{}^2(\mathbf{q}, p) \tau(\mathbf{q}, p, T) \tag{2.68}$$

Note that the above equation is an approximation; more involved theoretical models for the solution of the BTE to assess the conductivity can be found elsewhere [7, 47, 52]. The methodology for analyzing phonon transport in the framework of statistical mechanics will be comprehensively described in the chapters that follow.

Chapter 3: REAL GENERAL SOLUTION TO THE PHONON EQUATION

3.1 Inconsistencies in the conventional approach

The equation of motion of an N-atom 3-D lattice with N_u unit-cells and N_b atoms per unit-cell, as discussed in Chapter 2, admits wave-like solutions. Eqn. (3.1) describes the force on the j^{th} atom of the l^{th} unit-cell along the direction α.

$$m_j \frac{\partial^2 \left(u_\alpha \left(j,l,t\right)\right)}{\partial t^2} = -\sum_{j',k',\beta} G_{j',l',\beta,j,l,\alpha} \times u_\beta \left(j',l',t\right) \tag{3.1}$$

Mathematically, the displacements (u) can be real or complex; for the former, there needs to be $6N_uN_b$ ($\equiv 6N$) initial conditions for a well-posed solution, while for latter, $12N$ initial conditions are required. For a physical system, the displacements (and other dynamical variables) are real at every instant of time. Hence in the conventional approach, the displacements are *assumed* to be real, and a form of solution, which is consistent with real displacements is assumed. A particular solution for real displacements of a mode of vibration with wave vector $\mathbf{q}$ and mode index p is shown in Eqn. (3.2) [73]:

$$u_\alpha^{\mathbf{q},p}\left(j,l,t\right) = \frac{1}{\sqrt{m_j}} A\left(\mathbf{q},p,t\right) e_{j,\alpha}\left(\mathbf{q},p\right) \exp\left(i\left(\mathbf{q}.\mathbf{r}_l - w\left(\mathbf{q},p\right)t\right)\right) \tag{3.2}$$

where A is a complex amplitude. In total, there are N_u different wave vectors with $3N_b$ different modes for each wave vector. A general solution is constructed using a linear combination of these modes as given below in Eqn. (3.3) [73]:

$$u_\alpha(j,l,t) = \sum_{\mathbf{q},p} \frac{1}{\sqrt{m_j}} A(\mathbf{q},p,t) e_{j,\alpha}(\mathbf{q},p) \exp\left(i\left(\mathbf{q}.\mathbf{r}_l - w(\mathbf{q},p)t\right)\right) \tag{3.3}$$

It is tacitly assumed that the displacements are real without a formal attestation. The general form shown in Eqn. (3.3) is sufficient, for example, to evaluate the phonon dispersion curves and the attendant properties. However, some deficiencies can be noted with this form. For example, the net phonon population for a given wave vector **q** cannot be represented by Eqn. (3.3); in turn, a real heat current is not expressible with this form. Mathematically, complex displacements are allowed by the governing equation which means there are $12N_bN_u$ required initial conditions. The solution in Eqn. (3.3) contains only $6N_bN_u$ degrees of freedom because the constant $A(\mathbf{q},p,t)$ allows only for $2\times3N_bN_u$ combinations for all **q** and p. Thus Eqn. (3.3) is mathematically incomplete. Clearly, the general solution requires additional terms to accommodate for all the degrees of freedom of the system. The next section describes the additional terms that can accommodate all the degrees of freedom.

3.2 Well-posed complete general solution

Substitution of the particular solution into the equation of motion results in the eigenvalue problem for the dynamical matrix as shown below:

$$\left|D_{j,\alpha,j',\beta}(\mathbf{q})-\delta_{\alpha\beta}\delta_{jj'}w^2(\mathbf{q},p)\right|=0 \tag{3.4}$$

Note that the eigenvalues of the dynamical matrix are equal to the square of the frequencies. Thus for any given wave vector, both positive and negative values of w, satisfy the equation of motion, and hence the complete solution should use both. Therefore, the complete solution can be constructed as:

$$u_\alpha(j,l,t)=\sum_{\mathbf{q},p}\frac{1}{\sqrt{m_j}}\begin{bmatrix}A^+(\mathbf{q},p,t)e_{j,\alpha}(\mathbf{q},p)\exp\left(i\left(\mathbf{q}.\mathbf{r}_l-w(\mathbf{q},p)t\right)\right)+\\ A^-(\mathbf{q},p,t)e_{j,\alpha}(\mathbf{q},p)\exp\left(i\left(\mathbf{q}.\mathbf{r}_l+w(\mathbf{q},p)t\right)\right)\end{bmatrix} \tag{3.5}$$

Note that two amplitude constants have now been introduced for the positive and negative branches of the solution. The addition of left and right propagating waves is a crucial piece of information missing earlier; it formalizes a real energy/heat current in terms of the difference between left and right moving phonon amplitudes (population). The solution now contains $12N_bN_u$ degrees of freedom and is appropriate to describe the system completely. Combining the terms with positive and negative **q** and neglecting the zeros wave vector (as it does not result in any motion), the solution can be written as:

$$u_\alpha(j,l,t)=\sum_{\mathbf{q}>0,p}\frac{1}{\sqrt{m_j}}\begin{bmatrix}A^+(\mathbf{q},p,t)e_{j,\alpha}(\mathbf{q},p)\exp\left(i\left(\mathbf{q}.\mathbf{r}_l-w(\mathbf{q},p)t\right)\right)+\\ A^-(\mathbf{q},p,t)e_{j,\alpha}(\mathbf{q},p)\exp\left(i\left(\mathbf{q}.\mathbf{r}_l+w(\mathbf{q},p)t\right)\right)+\\ A^+(-\mathbf{q},p,t)e_{j,\alpha}(-\mathbf{q},p)\exp\left(i\left(-\mathbf{q}.\mathbf{r}_l-w(\mathbf{q},p)t\right)\right)+\\ A^-(-\mathbf{q},p,t)e_{j,\alpha}(-\mathbf{q},p)\exp\left(i\left(-\mathbf{q}.\mathbf{r}_l+w(\mathbf{q},p)t\right)\right)\end{bmatrix} \tag{3.6}$$

Using the fact that the eigenmodes for positive and negative modes are conjugate to each other:

$$u_\alpha(j,l,t)=\sum_{\mathbf{q}>0,p}\frac{1}{\sqrt{m_j}}\begin{bmatrix}A^+(\mathbf{q},p,t)e_{j,\alpha}(\mathbf{q},p)\exp\left(i\left(\mathbf{q}.\mathbf{r}_l-w(\mathbf{q},p)t\right)\right)+\\ A^-(\mathbf{q},p,t)\left(e_{j,\alpha}(-\mathbf{q},p)\exp\left(i\left(-\mathbf{q}.\mathbf{r}_l-w(\mathbf{q},p)t\right)\right)\right)^*+\\ A^+(-\mathbf{q},p,t)e_{j,\alpha}(-\mathbf{q},p)\exp\left(i\left(-\mathbf{q}.\mathbf{r}_l-w(\mathbf{q},p)t\right)\right)+\\ A^-(-\mathbf{q},p,t)\left(e_{j,\alpha}(\mathbf{q},p)\exp\left(i\left(\mathbf{q}.\mathbf{r}_l-w(\mathbf{q},p)t\right)\right)\right)^*\end{bmatrix} \tag{3.7}$$

Clearly, a real solution at every instant of time requires that A is Hermitian, which is expressed as:

$$A^+(\mathbf{q},p,t)=\left(A^-(-\mathbf{q},p,t)\right)^* \tag{3.8}$$

$$A^-(\mathbf{q},p,t)=\left(A^+(-\mathbf{q},p,t)\right)^* \tag{3.9}$$

Thus a real solution with $6N_bN_u$ degrees of freedom is given by:

$$u_\alpha(j,l,t)=\sum_{\mathbf{q}>0,p}\frac{2}{\sqrt{m_j}}\mathrm{Re}\begin{bmatrix}A^+(\mathbf{q},p,t)e_{j,\alpha}(\mathbf{q},p)\exp\left(i\left(\mathbf{q}.\mathbf{r}_l-w(\mathbf{q},p)t\right)\right)+\\ A^+(-\mathbf{q},p,t)e_{j,\alpha}(-\mathbf{q},p)\exp\left(i\left(-\mathbf{q}.\mathbf{r}_l-w(\mathbf{q},p)t\right)\right)\end{bmatrix} \tag{3.10}$$

The amplitude $A^+(\mathbf{q},p,t)$ and eigenvector $e_{j,\alpha}(\mathbf{q},p)$ can be written as below:

$$A^+(\mathbf{q},p,t)=\left|A^+(\mathbf{q},p,t)\right|\exp\left(i\phi_+(\mathbf{q},p)\right) \tag{3.11}$$

$$e_{j,\alpha}(\mathbf{q},p)=\left|e_{j,\alpha}(\mathbf{q},p)\right|\exp\left(i\phi_{j,\alpha}(\mathbf{q},p)\right) \tag{3.12}$$

This gives:

$$u_\alpha(j,l,t) = \sum_{\mathbf{q}>0,p} \frac{2}{\sqrt{m_j}} \mathrm{Re}\left[\begin{array}{l} \left|A^+(\mathbf{q},p,t)e_{j,\alpha}(\mathbf{q},p)\right| \exp\left(i\left(\mathbf{q}.\mathbf{r}_l - w(\mathbf{q},p)t + \phi_+(\mathbf{q},p) + \phi_{j,\alpha}(\mathbf{q},p)\right)\right) + \\ \left|A^+(-\mathbf{q},p,t)e_{j,\alpha}(-\mathbf{q},p)\right| \exp\left(i\left(-\mathbf{q}.\mathbf{r}_l - w(-\mathbf{q},p)t + \phi_+(-\mathbf{q},p) + \phi_{j,\alpha}(-\mathbf{q},p)\right)\right) \end{array}\right] \quad (3.13)$$

Or equivalently:

$$u_\alpha(j,l,t) = \sum_{\mathbf{q},p} \frac{2}{\sqrt{m_j}} \left|A^+(\mathbf{q},p,t)e_{j,\alpha}(\mathbf{q},p)\right| \cos\left(\mathbf{q}.\mathbf{r}_l - w(\mathbf{q},p)t + \phi_+(\mathbf{q},p) + \phi_{j,\alpha}(\mathbf{q},p)\right) \quad (3.14)$$

The solution expressed by Eqn. (3.14) is now completely real and has $6N_bN_u$ degrees of freedom – $3N_bN_u$ for the wave amplitudes $|A^+(\mathbf{q},p,t)|$ and $3N_bN_u$ for the phases $\phi_+(\mathbf{q},p)$, and these are determined by the initial conditions. Note that $|e_{j,\alpha}(\mathbf{q},p)|$ and $\phi_{j,\alpha}(\mathbf{q},p)$ are fixed for a system and do not depend on the initial conditions. Since two atoms in a unit-cell are not at the same physical location, a wave traveling along any wave vector can have a phase difference at their respective locations – the term $\phi_{j,\alpha}(\mathbf{q},p)$ accommodates this phase difference.

3.3 Real cosine solution to the phonon equation

As demonstrated in the previous section, a cosine solution satisfies the equation of motion for the real displacements. This is compactly written as:

$$u_\alpha(j,l,t) = \sum_{\mathbf{q},p} \frac{1}{\sqrt{m_j}} \left|A(q,p,t)\right| \left|e_{j,\alpha}(\mathbf{q},p)\right| \cos\left(\mathbf{q}.\mathbf{r}_l - w(\mathbf{q},p)t + \phi(\mathbf{q},p) + \phi_{j,\alpha}(\mathbf{q},p)\right) \quad (3.15)$$

The above equation can further be simplified by restricting the initial phase between zero and π and merging the sign into the mode amplitude, *i.e.*, allowing it to acquire negative values:

$$u_\alpha(j,l,t) = \sum_{\mathbf{q},p} \frac{1}{\sqrt{m_j}} A(q,p,t) \left| e_{j,\alpha}(\mathbf{q},p) \right| \cos\left(\mathbf{q}.\mathbf{r}_l - w(\mathbf{q},p)t + \phi(\mathbf{q},p) + \phi_{j,\alpha}(\mathbf{q},p)\right) \tag{3.16}$$

$$0 \le \phi(\mathbf{q},p) \le \pi \tag{3.17}$$

$$A(q,p,t) \in \mathbb{R} \tag{3.18}$$

The values of $\mathbf{q}$, $w(\mathbf{q},p)$, $e_{j,\alpha}(\mathbf{q},p)$ and $\phi_{j,\alpha}(\mathbf{q},p)$ are fixed for any given system while $A(\mathbf{q},p,t)$ and $\phi(\mathbf{q},p)$ are determined from the initial conditions. For an anharmonic system, the modes can interact, and thus the mode amplitude $A(\mathbf{q},p,t)$ can vary with time. Restricting the phase $\phi(\mathbf{q},p)$ between zero and π, and allowing $A(\mathbf{q},p,t)$ to assume negative values, ensures that the phase remains independent of time. If only the modulus of the amplitude is taken, then there is a possibility for the phase to change by π once the mode decays to zero. A constant initial phase is also more suitable for ensemble averaging as will be demonstrated in the next section. Thus the form given in Eqn. (3.16) is most convenient and will be adopted in the analyses to follow.

3.4 Well-posed cosine solution for a linear chain

Consider a linear chain of N atoms with only nearest neighbor interaction as discussed previously in Chapter 2. As there is only one atom per unit-cell and only one dimension for motion, the subscripts for the vector components and bases have been omitted, and the vectors

simply are transformed into scalars. The equation of motion for the j^{th} atom and the potential energy due to interaction of atom j with atom k are given by:

$$F(j,t) = m\frac{\partial^2 u(j,t)}{\partial t^2} = C\left(u(j-1,t) - 2u(j,t) + u(j+1,t)\right) \tag{3.19}$$

$$U_{jk}(t) = \frac{1}{2}C\left(u(j,t) - u(k,t)\right)^2 \tag{3.20}$$

The cosine solution discussed in the previous section can be reduced as:

$$u(j,t) = \sum_q \frac{1}{\sqrt{m}} A(q)\cos\left(q.r_j - w(q)t + \phi(q)\right) \tag{3.21}$$

The allowed wave vectors and the corresponding frequencies are given by:

$$q = r\frac{2\pi}{Na}; r = 0, \pm 1, \pm 2..... \tag{3.22}$$

$$-\frac{\pi}{a} < q \le \frac{\pi}{a} \tag{3.23}$$

$$w(q) = \sqrt{\frac{4C}{m}}\left|\sin\left(\frac{qa}{2}\right)\right| \tag{3.24}$$

The phase and group velocities are given by Eqns. (3.25) and (3.26) respectively:

$$v_p(q) = \frac{w(q)}{q} = \frac{1}{q}\sqrt{\frac{4C}{m}}\left|\sin\left(\frac{qa}{2}\right)\right| \tag{3.25}$$

$$v_g(q) = \frac{\partial w(q)}{\partial q} = a\sqrt{\frac{C}{m}}\cos\left(\frac{qa}{2}\right)\frac{q}{|q|} \tag{3.26}$$

The total system potential energy is given by:

$$U(t) = \frac{1}{2}\sum_{j,k} U_{jk}(t) = \sum_{j,k}\frac{1}{4}C\left(u(j,t) - u(k,t)\right)^2 \tag{3.27}$$

Substituting the solution from Eqn. (3.21) into the above expression gives:

$$U(t) = \frac{1}{2}\sum_{j,k} U_{jk}(t) = \sum_{j,k}\frac{1}{4}C\left(\sum_q \frac{1}{\sqrt{m}}A(q)\begin{pmatrix}\cos\left(q.r_j - w(q)t + \phi(q)\right) - \\ \cos\left(q.r_k - w(q)t + \phi(q)\right)\end{pmatrix}\right)^2 \tag{3.28}$$

On simplification (see Appendix A), the following expression can be derived:

$$U(t) = \frac{N}{4}\sum_q A^2(q)w^2(q) + \frac{N}{4}\sum_q A(q)A(-q)w^2(q)\cos\left(-2w(q)t + \varphi(q) + \varphi(-q)\right) \tag{3.29}$$

Similarly, the kinetic energy of the system is given by:

$$K(t) = \sum_j \frac{1}{2}mv^2(j,t) = \sum_j \frac{1}{2}m\left(\sum_q\left[\frac{w(q)}{\sqrt{m}}A(q)\sin\left(q.r_j - w(q)t + \phi(q)\right)\right]\right)^2 \tag{3.30}$$

On simplification (see Appendix A):

$$K(t)=\frac{N}{4}\sum_{q}w^{2}(q)A^{2}(q)-\frac{N}{4}\sum_{q}w^{2}(q)A(q)A(-q)\cos\left(-2w(q)t+\varphi(q)+\varphi(-q)\right) \quad (3.31)$$

The total energy of the system is simply the sum of kinetic and potential energy, and is given by:

$$E(t)=K(t)+U(t)=\sum_{q}\frac{N}{2}w^{2}(q)A^{2}(q)=\sum_{q}E(q,t) \quad (3.32)$$

Thus the total energy associated with any mode is constant and keeps oscillating between the kinetic and potential energy; a detailed derivation of the above results can be found in Appendix A.

The average values of the kinetic and potential energies are both equal to half of the total energy. Since the system is purely classical, equipartition theorem is valid, and thus we have:

$$\langle K\rangle=\langle U\rangle=\frac{1}{2}\langle E\rangle=\frac{1}{2}k_{B}T \quad (3.33)$$

$$\frac{N}{2}w^{2}(q)\langle A^{2}(q)\rangle=k_{B}T \quad (3.34)$$

It may be noted that the past approach to estimate the energy associated with a normal mode uses the square of the normal mode coordinate as below (see for example [56]):

$$Q(q,t)=\frac{1}{\sqrt{N}}\sum_{j}\sqrt{m}\exp\left(-i(qja)\right)u_{j}(t) \quad (3.35)$$

$$Q(-q,t) = Q^*(q,t) \tag{3.36}$$

$$E(q,t) = \frac{1}{2}\left[\dot{Q}(q,t)\dot{Q}^*(q,t) + w_q{}^2 Q(q,t)Q^*(q,t)\right] = E(-q,t) \tag{3.37}$$

However, the above result is incorrect as it predicts the same amount of energy for both positive and negative q modes. The energy associated with the positive and negative modes does not need to be equal; in fact, a finite heat current results from a difference in the energy associated with the positive and the negative modes. If energy associated with positive and negative modes is equal, then it will only form stationary waves with no net transport of energy, which is unphysical. The normal mode coordinate result from the current work contains contributions from both positive and negative modes that will allow an instantaneous heat current in the system. While the conventional normal mode analysis gives an incorrect result for the *modal* energy (Eqn. (3.37)), it does give an accurate estimate of the *total* energy of the system (contributions from all modes) as shown below:

$$E(t) = \sum_q \frac{N}{2} w^2(q) A^2(q) = \sum_q \frac{1}{2}\left[\dot{Q}(q,t)\dot{Q}^*(q,t) + w_q{}^2 Q(q,t)Q^*(q,t)\right] \tag{3.38}$$

Another important quantity that can be modeled using normal modes is the velocity (v) autocorrelation function (VACF). VACF is defined as:

$$VACF(t) = \frac{\langle v(0)v(t)\rangle}{\langle v(0)v(0)\rangle} \tag{3.39}$$

For an *N*-particle system, this can be computed as:

$$VACF(t) = \frac{\frac{1}{N}\sum_j \langle v(j,0)v(j,t)\rangle}{\frac{1}{N}\sum_j \langle v(j,0)v(j,0)\rangle} \tag{3.40}$$

Expanding in terms of normal modes:

$$\sum_j \frac{\langle v(j,0)v(j,t)\rangle}{N} = \frac{1}{N}\sum_j \left\langle \sum_{qq'} \begin{bmatrix} \frac{w(q)}{\sqrt{m}} A(q)\sin\left(q.r_j + \phi(q)\right) \\ \frac{w(q')}{\sqrt{m}} A(q')\sin\left(q'.r_j - w(q')t + \phi(q')\right) \end{bmatrix} \right\rangle \tag{3.41}$$

It can be shown that (the details can be found in Appendix A):

$$\sum_j \langle v(j,0)v(j,t)\rangle = \sum_q \left\langle \frac{w^2(q)A^2(q)}{2m}\cos\left(w(q)t\right)\right\rangle \tag{3.42}$$

Using the relation for energy due to each mode (Eqn. (3.32)) and the equipartition theorem:

$$\sum_j \frac{\langle v(j,0)v(j,t)\rangle_T}{N} = \frac{k_B T}{mN}\sum_q \cos\left(w(q)t\right) \tag{3.43}$$

Substituting above relation back into Eqn. (3.40), gives VACF as:

$$VACF(t) = \frac{1}{N}\sum_{q}\cos\left(w(q)t\right) \tag{3.44}$$

Thus the Fourier transform of the VACF gives the density of states. It may be noted that for a system with anharmonicity, the mode amplitude correlation would decay leading to:

$$\sum_{j}\frac{\langle v(j,0)v(j,t)\rangle}{N} = \sum_{q}\left\langle \frac{w^2(q)A(q,0)A(q,t)}{2m}\cos\left(w(q)t\right)\right\rangle \tag{3.45}$$

Assuming an exponential decay for the correlation gives:

$$VACF(t) = \frac{1}{N}\sum_{q}\exp\left(-\frac{t}{\tau_q}\right)\cos\left(w(q)t\right) \tag{3.46}$$

Finally, the heat current for a two-body potential is defined as:

$$\mathbf{J}(t) = \frac{1}{V}\left[\sum_{j=1}^{N}E(j,t)\mathbf{v}(j,t) + \frac{1}{2}\sum_{j=1}^{N}\sum_{k=1,\neq j}^{N}\left[\mathbf{F}_{jk}(t).\mathbf{v}(j,t)\right]\mathbf{r}_{jk}\right] \tag{3.47}$$

For the linear chain considered here, this expression simplifies to:

$$J(t) = \frac{1}{V}\left[\sum_{j=1}^{N}E(j,t)v(j,t) + \frac{1}{2}\sum_{j=1}^{N}\sum_{k=1,\neq j}^{N}\left[F_{jk}(t).v(j,t)\right]x_{jk}(t)\right] \tag{3.48}$$

The first term, which is usually referred to as the kinetic heat current, does not lead to any significant energy transport for a non-diffusive system [82-84]. The second term, which is also

referred to as the potential heat current [82-84], is more significant. For the present work, this is more appropriately referred to as the virial heat current and is written as:

$$J_{vir}(t)=\frac{1}{2V}\left[\sum_{j=1}^{N}\left[\begin{matrix}\left(-C\left(u(j,t)-u(j-1,t)\right)v(j,t)\right)\left(u(j,t)-u(j-1,t)+a\right)\\ \left(-C\left(u(j,t)-u(j+1,t)\right)v_j(t)\right)\left(u(j,t)-u(j+1,t)-a\right)\end{matrix}\right]\right] \tag{3.49}$$

For small displacements about the equilibrium position, the virial heat current reduces to:

$$J_{vir}(t)\approx\frac{Ca}{2V}\left[\sum_{j=1}^{N}\left[\left(-\left(u(j,t)-u(j-1,t)\right)v(j,t)\right)+\left(\left(u(j,t)-u(j+1,t)\right)v(j,t)\right)\right]\right] \tag{3.50}$$

Substituting the general solution from Eqn. (3.21) into the above expression:

$$\begin{aligned}&J_{vir}(t)\approx\\ &\frac{-Ca}{2Vm}\left[\sum_{j=1}^{N}\sum_{q_1q_2}\begin{matrix}A(q_1,t)A(q_2,t)w(q_1)\sin\left(q_1ja-w(q_1)t+\varphi(q_1)\right)\times\\ \left(\cos\left(q_2(j+1)a-w(q_2)t+\varphi(q_2)\right)-\cos\left(q_2(j-1)a-w(q_2)t+\varphi(q_2)\right)\right)\end{matrix}\right]\end{aligned} \tag{3.51}$$

Simplifying:

$$J_{vir}(t)\approx\frac{Ca}{Vm}\sum_{q_1q_2}\left[\begin{matrix}A(q_1,t)A(q_2,t)w(q_1)\sin\left(\frac{q_2a}{2}\right)\cos\left(\frac{q_2a}{2}\right)\times\\ \sum_{j=1}^{N}\left[2\sin\left(q_1ja-w(q_1)t+\varphi(q_1)\right)\sin\left(q_2ja-w(q_2)t+\varphi(q_2)\right)\right]\end{matrix}\right] \tag{3.52}$$

Substituting the dispersion relation and the expression for group velocity from Eqns. (3.24) and (3.26) into the above expression:

$$J_{vir}(t) \approx \frac{1}{2V}\sum_{q_1 q_2}\left[\begin{array}{l} A(q_1,t)A(q_2,t)w(q_1)w(q_2)v_g(q_2)\times \\ \sum_{j=1}^{N}\left[\begin{array}{l}\cos\left((q_1-q_2)ja-\left(w(q_1)-w(q_2)\right)t+\varphi(q_1)-\varphi(q_2)\right)- \\ \cos\left((q_1+q_2)ja-\left(w(q_1)+w(q_2)\right)t+\varphi(q_1)+\varphi(q_2)\right)\end{array}\right]\end{array}\right] \tag{3.53}$$

The summation over all atoms would go to zero unless $q_1 = q_2$ or $q_1 = -q_2$. The virial heat current now can be expressed as:

$$J_{vir}(t) \approx \frac{N}{2V}\left[\begin{array}{l}\sum_q A^2(q,t)w^2(q)v_g(q)+ \\ \sum_q A(q,t)A(-q,t)w^2(q)v_g(q)\cos\left(2w(q)t-\varphi(q)-\varphi(-q)\right)\end{array}\right] \tag{3.54}$$

As the group velocities for the positive and negative modes are opposite to each other, the second term in the above summation would cancel off. Thus the virial heat current reduces to:

$$J_{vir}(t) \approx \frac{1}{V}\sum_q \frac{N}{2}A^2(q,t)w^2(q)v_g(q) \tag{3.55}$$

Substituting the expression for the energy due to each mode from Eqn. (3.32), the virial heat current can be written as:

$$J_{vir}(t) \approx \frac{1}{V}\sum_q E(q,t)v_g(q) \tag{3.56}$$

The above equation is identical to the quantum expression for heat current presented in Chapter 2.

3.5 Conclusion

In this chapter, the mathematical and physical consistency of the solution that is conventionally adopted for solving the phonon equation motion is discussed. It is shown that the general solution considered in the customary approach is mathematically insufficient. To cover all the degrees of freedom, two amplitude constants have been introduced for the positive and negative branches of the solution. The addition of left and right propagating waves is a crucial piece of information missing earlier, which formalizes a real energy current in terms of the difference between left and right moving phonon amplitude (population). A real cosine solution is then constructed that is appropriate to compute the properties of a 1-D chain without ambiguity.

Chapter 4: PHONON DISPERSION FROM RATIO OF CONJUGATE AMPLITUDES IN PHONON SPACE

4.1 Introduction

A key objective of any phonon analysis is to determine the phonon dispersion relationships. Experimentally, the dispersion can be probed using neutron scattering experiments or Raman spectroscopy techniques that involve interaction of phonons with other particles or waves [73]. Theoretically, it can be calculated by computing the dynamical matrix followed by evaluating its eigenvalues (Eqn. (2.35)). The dynamical matrix can be calculated very accurately, for example, by using *ab initio* simulations [85]. Recently, Kong [86] has developed a method to estimate the dynamical matrix directly from atomistic trajectories using a Green's function approach. In another approach, McGaughey *et al*. [61] has determined the phonon dispersion curve from atomistic simulations using the spectral energy density (SED).

The most popular method for estimating phonon dispersion from atomistic simulations [38, 73-76, 87, 88], perhaps, entails taking the Fourier transform of the correlation of the projection of the atomistic trajectories along the normal mode coordinates. The SED approach [61] uses the Fourier transform of the modal kinetic energies and is similar to this method. Dove [73] discusses two more approaches to determine phonon dispersion from atomistic trajectories.

The first one entails the use of equipartition theorem to determine the frequency using the relationship between normal mode amplitude, frequency, and energy. However, Dove cautions that this method may not be very accurate as the equipartition may fail during the simulations unless proper care in taken. It may be noted that Kong's approach [86] for computing the dynamical matrix also assumes equipartition of energy between the modes, and is very similar to Dove's first approach. The second method involves computing the ratio of the normal mode amplitudes for the velocity and displacement; this approach is valid even in the absence of modal energy equipartitioning. The approach is also computationally inexpensive when compared to the more popular method of using the Fourier transform of the normal mode amplitudes. While this approach is known [89-91], it has not been employed in any atomistic simulations for computing the phonon dispersion relationships. In this chapter, a formal proof for the method using the general solution developed previously is first presented, followed by a demonstration of the method for computing the phonon dispersion curves for three systems – (*i*) a monoatomic linear chain, (*ii*) a diatomic linear chain, and (*iii*) graphene.

4.2 Projection in Phonon Space

The state of a lattice system, defined by the displacement of atoms from the equilibrium position, and the velocities – denoted by vectors $\mathbf{u}(t)$ and $\mathbf{v}(t)$, respectively – is given by:

$$\mathbf{u}(t)=\begin{Bmatrix}\mathbf{u}(1,1,t)\\ \mathbf{u}(2,1,t)\\ \\ \mathbf{u}(N_b,1,t)\\ \mathbf{u}(1,2,t)\\ \\ \mathbf{u}(j,l,t)\\ \\ \mathbf{u}(N_b,N_u,t)\end{Bmatrix},\mathbf{v}(t)=\begin{Bmatrix}\mathbf{v}(1,1,t)\\ \mathbf{v}(2,1,t)\\ \\ \mathbf{v}(N_b,1,t)\\ \mathbf{v}(1,2,t)\\ \\ \mathbf{v}(j,l,t)\\ \\ \mathbf{v}(N_b,N_u,t)\end{Bmatrix} \tag{4.1}$$

These vectors can be split into smaller vectors, one each for the α component of every j^{th} basis atom, as:

$$\mathbf{u}_{\alpha,j}(t)=\begin{pmatrix}u_\alpha(j,1,t)\\ u_\alpha(j,2,t)\\ .\\ .\\ u_\alpha(j,N_u,t)\end{pmatrix};\mathbf{v}_{\alpha,j}(t)=\begin{pmatrix}v_\alpha(j,1,t)\\ v_\alpha(j,2,t)\\ .\\ .\\ v_\alpha(j,N_u,t)\end{pmatrix} \tag{4.2}$$

Define vector $\mathbf{B_q}$ for wave vector $\mathbf{q}$ as:

$$\mathbf{B}_\mathbf{q}=\frac{1}{\sqrt{N_u}}\begin{pmatrix}\exp\left(i\left(\mathbf{q}.\mathbf{r}_1\right)\right)\\ \exp\left(i\left(\mathbf{q}.\mathbf{r}_2\right)\right)\\ .\\ .\\ \exp\left(i\left(\mathbf{q}.\mathbf{r}_{N_u}\right)\right)\end{pmatrix} \tag{4.3}$$

Clearly, $\mathbf{B_q}$ satisfies:

$$\left(\mathbf{B_q}\right)^{\dagger}.\mathbf{B_{q'}} = \delta_{\mathbf{qq'}} \tag{4.4}$$

The projection of the α component of velocities and displacements of the j^{th} basis atom in the wave vector space for wave vector $\mathbf{q}$ is denoted by $\xi_{u,\alpha,j}(t)$ and $\xi_{v,\alpha,j}(t)$, respectively, and are given by:

$$\xi_{u,\alpha,j}\left(\mathbf{q},t\right) = \sqrt{m_j}\left(\mathbf{B_q}\right)^{\dagger}.\mathbf{u}_{\alpha,j}\left(t\right) = \sqrt{\frac{m_j}{N_u}}\begin{pmatrix} \exp\left(i\left(-\mathbf{q}.\mathbf{r}_1\right)\right) \\ \exp\left(i\left(-\mathbf{q}.\mathbf{r}_2\right)\right) \\ . \\ . \\ \exp\left(i\left(-\mathbf{q}.\mathbf{r}_{N_u}\right)\right) \end{pmatrix}^T \begin{pmatrix} u_\alpha\left(j,1,t\right) \\ u_\alpha\left(j,2,t\right) \\ . \\ . \\ u_\alpha\left(j,N_u,t\right) \end{pmatrix} \tag{4.5}$$

$$\xi_{v,\alpha,j}\left(\mathbf{q},t\right) = \sqrt{m_j}\left(\mathbf{B_q}\right)^{\dagger}.\mathbf{v}_{\alpha,j}\left(t\right) = \sqrt{\frac{m_j}{N_u}}\begin{pmatrix} \exp\left(i\left(-\mathbf{q}.\mathbf{r}_1\right)\right) \\ \exp\left(i\left(-\mathbf{q}.\mathbf{r}_2\right)\right) \\ . \\ . \\ \exp\left(i\left(-\mathbf{q}.\mathbf{r}_{N_u}\right)\right) \end{pmatrix}^T \begin{pmatrix} v_\alpha\left(j,1,t\right) \\ v_\alpha\left(j,2,t\right) \\ . \\ . \\ v_\alpha\left(j,N_u,t\right) \end{pmatrix} \tag{4.6}$$

The complete projection for the wave vector is denoted by $\boldsymbol{\xi}_u(\mathbf{q},t)$ and $\boldsymbol{\xi}_v(\mathbf{q},t)$:

$$\xi_u(\mathbf{q},t)=\begin{pmatrix}\xi_{u,x,1}(\mathbf{q},t)\\ \xi_{u,y,1}(\mathbf{q},t)\\ \xi_{u,z,1}(\mathbf{q},t)\\ \cdot\\ \cdot\\ \xi_{u,x,N_b}(\mathbf{q},t)\\ \xi_{u,y,N_b}(\mathbf{q},t)\\ \xi_{u,z,N_b}(\mathbf{q},t)\end{pmatrix};\xi_v(\mathbf{q},t)=\begin{pmatrix}\xi_{v,x,1}(\mathbf{q},t)\\ \xi_{v,y,1}(\mathbf{q},t)\\ \xi_{v,z,1}(\mathbf{q},t)\\ \cdot\\ \cdot\\ \xi_{v,x,N_b}(\mathbf{q},t)\\ \xi_{v,y,N_b}(\mathbf{q},t)\\ \xi_{v,z,N_b}(\mathbf{q},t)\end{pmatrix} \tag{4.7}$$

The components of the projections described above are not necessarily independent for an arbitrary system, as shown below, and thus do not constitute normal mode coordinates or the projection in phonon space.

$$\frac{\left\langle\left(\xi_{v,\alpha,j}(\mathbf{q})\right)^{*}\xi_{v,\alpha',j'}(\mathbf{q})\right\rangle}{\sqrt{\left\langle\left|\xi_{v,\alpha,j}(\mathbf{q})\right|^{2}\right\rangle\left\langle\left|\xi_{v,\alpha',j'}(\mathbf{q})\right|^{2}\right\rangle}}\neq\delta_{\alpha\alpha'}\delta_{jj'}\neq\frac{\left\langle\left(\xi_{u,\alpha,j}(\mathbf{q})\right)^{*}\xi_{u,\alpha',j'}(\mathbf{q})\right\rangle}{\sqrt{\left\langle\left|\xi_{u,\alpha,j}(\mathbf{q})\right|^{2}\right\rangle\left\langle\left|\xi_{u,\alpha',j'}\right|(\mathbf{q})^{2}\right\rangle}} \tag{4.8}$$

The next step is to find an appropriate projection, which is orthogonal. The eigenvector of the dynamical matrix for wave vector **q** and mode *p* is denoted by **e**(**q**,*p*) as shown in Eqn. (4.9). The eigenvectors follow the orthogonalization condition given by Eqns. (4.10) and (4.11).

$$\mathbf{e}(\mathbf{q}, p) = \begin{pmatrix} e_{1,x}(\mathbf{q}, p) \\ e_{1,y}(\mathbf{q}, p) \\ e_{1,z}(\mathbf{q}, p) \\ . \\ . \\ e_{N_b,x}(\mathbf{q}, p) \\ e_{N_b,y}(\mathbf{q}, p) \\ e_{N_b,z}(\mathbf{q}, p) \end{pmatrix} \tag{4.9}$$

$$\left(\mathbf{e}(\mathbf{q}, p)\right)^{\dagger} \mathbf{e}(\mathbf{q}, p') = \delta_{pp'} \tag{4.10}$$

$$\sum_{p} e_{j,\alpha}(-\mathbf{q}, p) e_{j',\alpha'}(\mathbf{q}, p) = \delta_{jj'}\delta_{\alpha\alpha'} \tag{4.11}$$

Now define the projection of displacement and velocity in phonon space is denoted by $\chi_u(\mathbf{q},p,t)$ and $\chi_v(\mathbf{q},p,t)$, respectively, as shown below.

$$\chi_u(\mathbf{q}, p, t) = \left(\mathbf{e}(\mathbf{q}, p)\right)^{\dagger} . \xi_u(\mathbf{q}, t) = \begin{pmatrix} e_{1,x}(-\mathbf{q}, p) \\ e_{1,y}(-\mathbf{q}, p) \\ e_{1,z}(-\mathbf{q}, p) \\ . \\ . \\ e_{N_b,x}(-\mathbf{q}, p) \\ e_{N_b,y}(-\mathbf{q}, p) \\ e_{N_b,z}(-\mathbf{q}, p) \end{pmatrix}^{T} \begin{pmatrix} \xi_{u,x,1}(\mathbf{q}, t) \\ \xi_{u,y,1}(\mathbf{q}, t) \\ \xi_{u,z,1}(\mathbf{q}, t) \\ . \\ . \\ \xi_{u,x,N_b}(\mathbf{q}, t) \\ \xi_{u,y,N_b}(\mathbf{q}, t) \\ \xi_{u,z,N_b}(\mathbf{q}, t) \end{pmatrix} \tag{4.12}$$

The complete phonon space projection for a wave vector $\mathbf{q}$ is defined by the vectors $\boldsymbol{\chi}_u(\mathbf{q},t)$ and $\boldsymbol{\chi}_v(\mathbf{q},t)$ for the displacement and velocity, respectively. These projections are given by:

$$\mathbf{e}(\mathbf{q}) = \begin{pmatrix} e_{1,x}(\mathbf{q},1) & e_{1,x}(\mathbf{q},2) & . & . & . & e_{1,x}(\mathbf{q},p) & . & e_{1,x}(\mathbf{q},3N_b) \\ e_{1,y}(\mathbf{q},1) & e_{1,y}(\mathbf{q},2) & . & . & . & e_{1,y}(\mathbf{q},p) & . & e_{1,y}(\mathbf{q},3N_b) \\ e_{1,z}(\mathbf{q},1) & e_{1,z}(\mathbf{q},2) & . & . & . & e_{1,z}(\mathbf{q},p) & . & e_{1,z}(\mathbf{q},3N_b) \\ . & . & . & . & . & . & . & . \\ . & . & . & . & . & . & . & . \\ e_{N_b,x}(\mathbf{q},1) & e_{N_b,x}(\mathbf{q},2) & . & . & . & e_{N_b,x}(\mathbf{q},p) & . & e_{N_b,x}(\mathbf{q},3N_b) \\ e_{N_b,y}(\mathbf{q},1) & e_{N_b,y}(\mathbf{q},2) & . & . & . & e_{N_b,y}(\mathbf{q},p) & . & e_{N_b,y}(\mathbf{q},3N_b) \\ e_{N_b,z}(\mathbf{q},1) & e_{N_b,z}(\mathbf{q},2) & . & . & . & e_{N_b,z}(\mathbf{q},p) & . & e_{N_b,z}(\mathbf{q},3N_b) \end{pmatrix} \tag{4.13}$$

$$\boldsymbol{\chi}_u(\mathbf{q},t) = \begin{pmatrix} \chi_u(\mathbf{q},1,t) \\ \chi_u(\mathbf{q},2,t) \\ . \\ . \\ . \\ \chi_u(\mathbf{q},p,t) \\ . \\ \chi_u(\mathbf{q},3N_b,t) \end{pmatrix}; \boldsymbol{\chi}_v(\mathbf{q},t) = \begin{pmatrix} \chi_v(\mathbf{q},1,t) \\ \chi_v(\mathbf{q},2,t) \\ . \\ . \\ . \\ \chi_v(\mathbf{q},p,t) \\ . \\ \chi_v(\mathbf{q},3N_b,t) \end{pmatrix} \tag{4.14}$$

$$\boldsymbol{\chi}_u(\mathbf{q},t) = \left(\mathbf{e}(\mathbf{q})\right)^{\dagger} . \boldsymbol{\xi}_u(\mathbf{q},t) \tag{4.15}$$

$$\boldsymbol{\chi}_v(\mathbf{q},t) = \left(\mathbf{e}(\mathbf{q})\right)^{\dagger} . \boldsymbol{\xi}_v(\mathbf{q},t) \tag{4.16}$$

The above projections in the phonon space are now independent of each other and thus follow the relation below:

$$\frac{\left\langle \left(\chi_v(\mathbf{q},p)\right)^* \chi_v(\mathbf{q},p') \right\rangle}{\sqrt{\left\langle \left|\chi_v(\mathbf{q},p)\right|^2 \right\rangle \left\langle \left|\chi_v(\mathbf{q},p')\right|^2 \right\rangle}} = \delta_{pp'} = \frac{\left\langle \left(\chi_u(\mathbf{q},p)\right)^* \chi_u(\mathbf{q},p') \right\rangle}{\sqrt{\left\langle \left|\chi_u(\mathbf{q},p)\right|^2 \right\rangle \left\langle \left|\chi_u(\mathbf{q},p')\right|^2 \right\rangle}} \tag{4.17}$$

Although the matrix **e**(**q**) is not known, it can be calculated following the approach discussed by Dove [73] (using the relation given by Eqn. (4.17)), as shown next:

$$\boldsymbol{\chi}_u(\mathbf{q},t).\left(\boldsymbol{\chi}_u(\mathbf{q},t)\right)^{\dagger} = \left(\left(\mathbf{e}(\mathbf{q})\right)^{\dagger}.\boldsymbol{\xi}_u(\mathbf{q},t)\right)\left(\left(\mathbf{e}(\mathbf{q})\right)^{\dagger}.\boldsymbol{\xi}_u(\mathbf{q},t)\right)^{\dagger} \tag{4.18}$$

$$\left\langle \boldsymbol{\chi}_u(\mathbf{q}).\left(\boldsymbol{\chi}_u(\mathbf{q})\right)^{\dagger}\right\rangle = \left(\mathbf{e}(\mathbf{q})\right)^{\dagger}\left\langle \boldsymbol{\xi}_u(\mathbf{q}).\left(\boldsymbol{\xi}_u(\mathbf{q})\right)^{\dagger}\right\rangle.\mathbf{e}(\mathbf{q}) \tag{4.19}$$

The matrix $\left\langle \boldsymbol{\chi}_u(\mathbf{q}).\left(\boldsymbol{\chi}_u(\mathbf{q})\right)^{\dagger}\right\rangle$ is diagonal, which follows from the relation given by Eqn. (4.17), while the matrix $\left\langle \boldsymbol{\xi}_u(\mathbf{q}).\left(\boldsymbol{\xi}_u(\mathbf{q})\right)^{\dagger}\right\rangle$ is Hermitian. Thus Eqn. (4.19) represents the diagonalization of a Hermitian matrix. Hence, **e**(**q**) is simply a matrix whose columns are the eigenvectors of the matrix $\left\langle \boldsymbol{\xi}_u(\mathbf{q}).\left(\boldsymbol{\xi}_u(\mathbf{q})\right)^{\dagger}\right\rangle$, which can be computed directly from an atomitsic simulation. The eigenvectors then can be estimated and used to obtain the projections in the phonon space through Eqns. (4.15) and (4.16). Also, note that the matrix **e**(**q**) that diagonalizes matrix $\left\langle \boldsymbol{\xi}_u(\mathbf{q}).\left(\boldsymbol{\xi}_u(\mathbf{q})\right)^{\dagger}\right\rangle$ is unique. The next two sections will demonstrate that the eigenvectors of the dynamical matrix does indeed diagonalizes it thus impling that the eigenvectors of $\left\langle \boldsymbol{\xi}_u(\mathbf{q}).\left(\boldsymbol{\xi}_u(\mathbf{q})\right)^{\dagger}\right\rangle$ and the dynamical matrix are one and the same.

4.3 Phonon space projections due to the general solution

Consider the general solution for the displacement along direction α for the j^{th} atom of the l^{th} unit cell:

$$\mathbf{u}_{\alpha,j}(\mathbf{q},p,t)=\frac{1}{\sqrt{m_j}}A(q,p,t)\left|e_{j,\alpha}(\mathbf{q},p)\right|\begin{pmatrix}\cos\left(\mathbf{q}.\mathbf{r}_1-w(\mathbf{q},p)t+\phi(\mathbf{q},p)+\phi_{j,\alpha}(\mathbf{q},p)\right)\\ \cos\left(\mathbf{q}.\mathbf{r}_2-w(\mathbf{q},p)t+\phi(\mathbf{q},p)+\phi_{j,\alpha}(\mathbf{q},p)\right)\\ .\\ .\\ \cos\left(\mathbf{q}.\mathbf{r}_{N_u}-w(\mathbf{q},p)t+\phi(\mathbf{q},p)+\phi_{j,\alpha}(\mathbf{q},p)\right)\end{pmatrix} \quad (4.20)$$

As discussed in Chapter 3, this solution is equivalent to the solution given by **Eqn. (3.5),** with the complex exponential replaced by a real cosine term since the actual displacements of the atoms are real. The complex exponential solution contains 6*N* constants, *i.e*. the real and imaginary parts of the amplitudes $A(\mathbf{q},p,t)$ for 3*N* independent modes. Similarly, the real cosine solution also contains 6*N* independent constants, 3*N* for the values of the real amplitudes $A(\mathbf{q},p,t)$ and 3*N* for the initial phases $\varphi(\mathbf{q},p)$. The total displacement can thus be written as:

$$\mathbf{u}_{\alpha,j}(t)=\sum_{\mathbf{q},p}\mathbf{u}_{\alpha,j}(\mathbf{q},p,t)=$$

$$\sum_{\mathbf{q},p}\frac{1}{\sqrt{m_j}}A(q,p,t)\left|e_{j,\alpha}(\mathbf{q},p)\right|\begin{pmatrix}\cos\left(\mathbf{q}.\mathbf{r}_1-w(\mathbf{q},p)t+\phi(\mathbf{q},p)+\phi_{j,\alpha}(\mathbf{q},p)\right)\\ \cos\left(\mathbf{q}.\mathbf{r}_2-w(\mathbf{q},p)t+\phi(\mathbf{q},p)+\phi_{j,\alpha}(\mathbf{q},p)\right)\\ .\\ .\\ \cos\left(\mathbf{q}.\mathbf{r}_{N_u}-w(\mathbf{q},p)t+\phi(\mathbf{q},p)+\phi_{j,\alpha}(\mathbf{q},p)\right)\end{pmatrix} \quad (4.21)$$

Note that the velocities are given by the derivative of the displacements. For harmonic interactions $A(\mathbf{q},p,t)$ remains constant, and thus the rate of change is zero. For an anharmonic interactions, the rate of change is not zero, but the decay is small compared to the contribution from the vibrating cosine term, and thus can be neglected. Thus the velocities are given by:

$$\mathbf{v}_{\alpha,j}(t)=\sum_{\mathbf{q},p}\frac{1}{\sqrt{m_j}}w(\mathbf{q},p)A(q,p,t)\left|e_{j,\alpha}(\mathbf{q},p)\right|\begin{pmatrix}\sin\left(\mathbf{q}.\mathbf{r}_1-w(\mathbf{q},p)t+\phi(\mathbf{q},p)+\phi_{j,\alpha}(\mathbf{q},p)\right)\\ \sin\left(\mathbf{q}.\mathbf{r}_2-w(\mathbf{q},p)t+\phi(\mathbf{q},p)+\phi_{j,\alpha}(\mathbf{q},p)\right)\\ .\\ .\\ \sin\left(\mathbf{q}.\mathbf{r}_{N_u}-w(\mathbf{q},p)t+\phi(\mathbf{q},p)+\phi_{j,\alpha}(\mathbf{q},p)\right)\end{pmatrix} \quad (4.22)$$

Evaluation the projection along the wave vector:

$$\xi_{u,\alpha,j}(\mathbf{q},t)=$$
$$\sum_{\mathbf{q}',p}\frac{A(\mathbf{q}',p,t)\left|e_{j,\alpha}(\mathbf{q}',p)\right|}{\sqrt{N_u}}\begin{pmatrix}\exp\left(i\left(-\mathbf{q}.\mathbf{r}_1\right)\right)\\ \exp\left(i\left(-\mathbf{q}.\mathbf{r}_2\right)\right)\\ .\\ .\\ \exp\left(i\left(-\mathbf{q}.\mathbf{r}_{N_u}\right)\right)\end{pmatrix}^T\begin{pmatrix}\cos\left(\mathbf{q}'.\mathbf{r}_1-w(\mathbf{q}',p)t+\phi(\mathbf{q}',p)+\phi_{j,\alpha}(\mathbf{q}',p)\right)\\ \cos\left(\mathbf{q}'.\mathbf{r}_2-w(\mathbf{q}',p)t+\phi(\mathbf{q}',p)+\phi_{j,\alpha}(\mathbf{q}',p)\right)\\ .\\ .\\ \cos\left(\mathbf{q}'.\mathbf{r}_{N_u}-w(\mathbf{q}',p)t+\phi(\mathbf{q}',p)+\phi_{j,\alpha}(\mathbf{q}',p)\right)\end{pmatrix} \quad (4.23)$$

Expanding as a summation:

$$\xi_{u,\alpha,j}(\mathbf{q},t)=$$
$$\sum_{\mathbf{q}',p}\frac{A(\mathbf{q}',p,t)\left|e_{j,\alpha}(\mathbf{q}',p)\right|}{\sqrt{N_u}}\sum_j\cos\left(\mathbf{q}'.\mathbf{r}_j-w(\mathbf{q}',p)t+\phi(\mathbf{q}',p)+\phi_{j,\alpha}(\mathbf{q}',p)\right)\exp\left(i\left(-\mathbf{q}.\mathbf{r}_j\right)\right) \quad (4.24)$$

Expanding the exponential gives:

$$\xi_{u,\alpha,j}(\mathbf{q},t) = \sum_{\mathbf{q}',p} \frac{A(\mathbf{q}',p,t)\left|e_{j,\alpha}(\mathbf{q}',p)\right|}{\sqrt{N_u}} \sum_j \begin{bmatrix} \cos(-\mathbf{q}.\mathbf{r}_j)\cos(\mathbf{q}'.\mathbf{r}_j - w(\mathbf{q}',p)t + \phi(\mathbf{q}',p) + \phi_{j,\alpha}(\mathbf{q}',p)) + \\ i\sin(-\mathbf{q}.\mathbf{r}_j)\cos(\mathbf{q}'.\mathbf{r}_j - w(\mathbf{q}',p)t + \phi(\mathbf{q}',p) + \phi_{j,\alpha}(\mathbf{q}',p)) \end{bmatrix} \quad (4.25)$$

Simplifying:

$$\xi_{u,\alpha,j}(\mathbf{q},t) = \sum_{\mathbf{q}',p} \frac{A(\mathbf{q}',p,t)\left|e_{j,\alpha}(\mathbf{q}',p)\right|}{2\sqrt{N_u}} \sum_j \begin{bmatrix} \cos((\mathbf{q}'-\mathbf{q}).\mathbf{r}_j - w(\mathbf{q}',p)t + \phi(\mathbf{q}',p) + \phi_{j,\alpha}(\mathbf{q}',p)) \\ +\cos((\mathbf{q}'+\mathbf{q}).\mathbf{r}_j - w(\mathbf{q}',p)t + \phi(\mathbf{q}',p) + \phi_{j,\alpha}(\mathbf{q}',p)) \\ +i\sin((\mathbf{q}'-\mathbf{q}).\mathbf{r}_j - w(\mathbf{q}',p)t + \phi(\mathbf{q}',p) + \phi_{j,\alpha}(\mathbf{q}',p)) \\ -i\sin((\mathbf{q}'+\mathbf{q}).\mathbf{r}_j - w(\mathbf{q}',p)t + \phi(\mathbf{q}',p) + \phi_{j,\alpha}(\mathbf{q}',p)) \end{bmatrix} \quad (4.26)$$

The summation over *j* goes to zero unless **q** = **q**' or **q** = **-q**':

$$\xi_{u,\alpha,j}(\mathbf{q},t) = \sum_p \begin{bmatrix} \frac{A(\mathbf{q},p,t)\left|e_{j,\alpha}(\mathbf{q},p)\right|\sqrt{N_u}}{2} \begin{bmatrix} \cos(-w(\mathbf{q},p)t + \phi(\mathbf{q},p) + \phi_{j,\alpha}(\mathbf{q},p)) \\ +i\sin(-w(\mathbf{q},p)t + \phi(\mathbf{q},p) + \phi_{j,\alpha}(\mathbf{q},p)) \end{bmatrix} + \\ \frac{A(-\mathbf{q},p,t)\left|e_{j,\alpha}(-\mathbf{q},p)\right|\sqrt{N_u}}{2} \begin{bmatrix} +\cos(-w(\mathbf{q},p)t + \phi(-\mathbf{q},p) + \phi_{j,\alpha}(-\mathbf{q},p)) \\ -i\sin(-w(\mathbf{q},p)t + \phi(-\mathbf{q},p) + \phi_{j,\alpha}(-\mathbf{q},p)) \end{bmatrix} \end{bmatrix} \quad (4.27)$$

Expanding the sine and the cosine terms to separate $\varphi_{j\alpha}(\mathbf{q},p)$:

$$\xi_{u,\alpha,j}(\mathbf{q},t)=\sum_{p}\left[\begin{array}{l}\dfrac{A(\mathbf{q},p,t)\left|e_{j,\alpha}(\mathbf{q},p)\right|\sqrt{N_u}}{2}\left[\begin{array}{l}\cos\left(-w(\mathbf{q},p)t+\phi(\mathbf{q},p)\right)\cos\left(\phi_{j,\alpha}(\mathbf{q},p)\right)\\-\sin\left(-w(\mathbf{q},p)t+\phi(\mathbf{q},p)\right)\sin\left(\phi_{j,\alpha}(\mathbf{q},p)\right)\\+i\sin\left(-w(\mathbf{q},p)t+\phi(\mathbf{q},p)\right)\cos\left(\phi_{j,\alpha}(\mathbf{q},p)\right)\\+i\cos\left(-w(\mathbf{q},p)t+\phi(\mathbf{q},p)\right)\sin\left(\phi_{j,\alpha}(\mathbf{q},p)\right)\end{array}\right]+\\\dfrac{A(-\mathbf{q},p,t)\left|e_{j,\alpha}(-\mathbf{q},p)\right|\sqrt{N_u}}{2}\left[\begin{array}{l}\cos\left(-w(\mathbf{q},p)t+\phi(-\mathbf{q},p)\right)\cos\left(\phi_{j,\alpha}(\mathbf{q},p)\right)\\+\sin\left(-w(\mathbf{q},p)t+\phi(-\mathbf{q},p)\right)\sin\left(\phi_{j,\alpha}(\mathbf{q},p)\right)\\-i\sin\left(-w(\mathbf{q},p)t+\phi(-\mathbf{q},p)\right)\cos\left(\phi_{j,\alpha}(\mathbf{q},p)\right)\\+i\cos\left(-w(\mathbf{q},p)t+\phi(-\mathbf{q},p)\right)\sin\left(\phi_{j,\alpha}(\mathbf{q},p)\right)\end{array}\right]\end{array}\right] \tag{4.28}$$

Combining the terms:

$$\xi_{u,\alpha,j}(\mathbf{q},t)=\\\sum_{p}\left[\begin{array}{l}\dfrac{A(\mathbf{q},p,t)\left|e_{j,\alpha}(\mathbf{q},p)\right|\sqrt{N_u}}{2}\left[\begin{array}{l}\cos\left(-w(\mathbf{q},p)t+\phi(\mathbf{q},p)\right)\exp\left(i\phi_{j,\alpha}(\mathbf{q},p)\right)\\+i\sin\left(-w(\mathbf{q},p)t+\phi(\mathbf{q},p)\right)\exp\left(i\phi_{j,\alpha}(\mathbf{q},p)\right)\end{array}\right]+\\\dfrac{A(-\mathbf{q},p,t)\left|e_{j,\alpha}(\mathbf{q},p)\right|\sqrt{N_u}}{2}\left[\begin{array}{l}\cos\left(-w(\mathbf{q},p)t+\phi(-\mathbf{q},p)\right)\exp\left(i\phi_{j,\alpha}(\mathbf{q},p)\right)\\-i\sin\left(-w(\mathbf{q},p)t+\phi(-\mathbf{q},p)\right)\exp\left(i\phi_{j,\alpha}(\mathbf{q},p)\right)\end{array}\right]\end{array}\right] \tag{4.29}$$

Merging the phase and magnitude of $e_{j\alpha}(\mathbf{q},p)$:

$$\xi_{u,\alpha,j}(\mathbf{q},t)=\sum_{p}\left[\begin{array}{l}\dfrac{A(\mathbf{q},p,t)e_{j,\alpha}(\mathbf{q},p)\sqrt{N_u}}{2}\left[\begin{array}{l}\cos\left(-w(\mathbf{q},p)t+\phi(\mathbf{q},p)\right)\\+i\sin\left(-w(\mathbf{q},p)t+\phi(\mathbf{q},p)\right)\end{array}\right]+\\\dfrac{A(-\mathbf{q},p,t)e_{j,\alpha}(\mathbf{q},p)\sqrt{N_u}}{2}\left[\begin{array}{l}\cos\left(-w(\mathbf{q},p)t+\phi(-\mathbf{q},p)\right)\\-i\sin\left(-w(\mathbf{q},p)t+\phi(-\mathbf{q},p)\right)\end{array}\right]\end{array}\right] \tag{4.30}$$

The normal mode coordinate is obtained by:

$$\chi_u(\mathbf{q},p,t)=\sum_{j,\alpha} e_{j,\alpha}(-\mathbf{q},p)\,\xi_{u,\alpha,j}(\mathbf{q},t) \tag{4.31}$$

Substituting the relation from Eqn. (4.30) into Eqn. (4.31):

$$\chi_u(\mathbf{q},p,t)= \sum_{j,\alpha} e_{j,\alpha}(-\mathbf{q},p)\sum_{p'}\begin{bmatrix} \dfrac{A(\mathbf{q},p',t)e_{j,\alpha}(\mathbf{q},p')\sqrt{N_u}}{2}\begin{bmatrix}\cos\left(-w(\mathbf{q},p')t+\phi(\mathbf{q},p')\right)\\ +i\sin\left(-w(\mathbf{q},p')t+\phi(\mathbf{q},p')\right)\end{bmatrix}+ \\ \dfrac{A(-\mathbf{q},p',t)e_{j,\alpha}(\mathbf{q},p')\sqrt{N_u}}{2}\begin{bmatrix}+\cos\left(-w(\mathbf{q},p')t+\phi(-\mathbf{q},p')\right)\\ -i\sin\left(-w(\mathbf{q},p')t+\phi(-\mathbf{q},p')\right)\end{bmatrix} \end{bmatrix} \tag{4.32}$$

Simplifying:

$$\chi_u(\mathbf{q},p,t)= \sum_{p'}\begin{bmatrix} \dfrac{\sqrt{N_u}A(\mathbf{q},p',t)}{2}\begin{bmatrix}\cos\left(-w(\mathbf{q},p')t+\phi(\mathbf{q},p')\right)\\ +i\sin\left(-w(\mathbf{q},p')t+\phi(\mathbf{q},p')\right)\end{bmatrix}\sum_{j,\alpha}\left(e_{j,\alpha}(\mathbf{q},p)\right)^{*}.e_{j,\alpha}(\mathbf{q},p')+ \\ \dfrac{\sqrt{N_u}A(-\mathbf{q},p',t)}{2}\begin{bmatrix}+\cos\left(-w(\mathbf{q},p')t+\phi(-\mathbf{q},p')\right)\\ -i\sin\left(-w(\mathbf{q},p')t+\phi(-\mathbf{q},p')\right)\end{bmatrix}\sum_{j,\alpha}\left(e_{j,\alpha}(\mathbf{q},p)\right)^{*}.e_{j,\alpha}(\mathbf{q},p') \end{bmatrix} \tag{4.33}$$

Thus the normal mode coordinate for displacement is given by:

$$\chi_u(\mathbf{q},p,t)= \begin{bmatrix} \dfrac{\sqrt{N_u}A(\mathbf{q},p,t)}{2}\begin{bmatrix}\cos\left(-w(\mathbf{q},p)t+\phi(\mathbf{q},p)\right)\\ +i\sin\left(-w(\mathbf{q},p)t+\phi(\mathbf{q},p)\right)\end{bmatrix}+ \\ \dfrac{\sqrt{N_u}A(-\mathbf{q},p,t)}{2}\begin{bmatrix}+\cos\left(-w(\mathbf{q},p)t+\phi(-\mathbf{q},p)\right)\\ -i\sin\left(-w(\mathbf{q},p)t+\phi(-\mathbf{q},p)\right)\end{bmatrix} \end{bmatrix} \tag{4.34}$$

Similarly, the normal mode projection for velocities is calculated as below:

$$\xi_{v,\alpha,j}(\mathbf{q},t)=\sum_{\mathbf{q}',p}\left(\begin{array}{l}\dfrac{w(\mathbf{q}',p)A(\mathbf{q}',p,t)\left|e_{j,\alpha}(\mathbf{q}',p)\right|}{\sqrt{N_u}}\times \\ \begin{pmatrix}\exp\left(i\left(-\mathbf{q}.\mathbf{r}_1\right)\right)\\ \exp\left(i\left(-\mathbf{q}.\mathbf{r}_2\right)\right)\\ .\\ .\\ \exp\left(i\left(-\mathbf{q}.\mathbf{r}_{N_u}\right)\right)\end{pmatrix}^T\begin{pmatrix}\sin\left(\mathbf{q}'.\mathbf{r}_1-w(\mathbf{q}',p)t+\phi(\mathbf{q}',p)+\phi_{j,\alpha}(\mathbf{q}',p)\right)\\ \sin\left(\mathbf{q}'.\mathbf{r}_2-w(\mathbf{q}',p)t+\phi(\mathbf{q}',p)+\phi_{j,\alpha}(\mathbf{q}',p)\right)\\ .\\ .\\ \sin\left(\mathbf{q}'.\mathbf{r}_{N_u}-w(\mathbf{q}',p)t+\phi(\mathbf{q}',p)+\phi_{j,\alpha}(\mathbf{q}',p)\right)\end{pmatrix}\end{array}\right) \tag{4.35}$$

Expanding as a summation:

$$\xi_{v,\alpha,j}(\mathbf{q},t)=\sum_{\mathbf{q}',p}\left(\begin{array}{l}\dfrac{w(\mathbf{q}',p)A(\mathbf{q}',p,t)\left|e_{j,\alpha}(\mathbf{q}',p)\right|}{\sqrt{N_u}}\times \\ \sum_j\sin\left(\mathbf{q}'.\mathbf{r}_j-w(\mathbf{q}',p)t+\phi(\mathbf{q}',p)+\phi_{j,\alpha}(\mathbf{q}',p)\right)\exp\left(i\left(-\mathbf{q}.\mathbf{r}_j\right)\right)\end{array}\right) \tag{4.36}$$

Expanding the exponential:

$$\xi_{v,\alpha,j}(\mathbf{q},t)=\sum_{\mathbf{q}',p}\left(\begin{array}{l}\dfrac{w(\mathbf{q}',p)A(\mathbf{q}',p,t)\left|e_{j,\alpha}(\mathbf{q}',p)\right|}{\sqrt{N_u}}\times \\ \sum_j\left[\begin{array}{l}\cos\left(-\mathbf{q}.\mathbf{r}_j\right)\sin\left(\mathbf{q}'.\mathbf{r}_j-w(\mathbf{q}',p)t+\phi(\mathbf{q}',p)+\phi_{j,\alpha}(\mathbf{q}',p)\right)+\\ i\sin\left(-\mathbf{q}.\mathbf{r}_j\right)\sin\left(\mathbf{q}'.\mathbf{r}_j-w(\mathbf{q}',p)t+\phi(\mathbf{q}',p)+\phi_{j,\alpha}(\mathbf{q}',p)\right)\end{array}\right]\end{array}\right) \tag{4.37}$$

Simplifying:

$$\xi_{v,\alpha,j}(\mathbf{q},t)=\sum_{\mathbf{q}',p}\left(\begin{array}{l}\dfrac{w(\mathbf{q}',p)\,A(\mathbf{q}',p,t)\left|e_{j,\alpha}(\mathbf{q}',p)\right|}{2\sqrt{N_u}}\times \\ \sum_{j}\left[\begin{array}{l}\sin\left((\mathbf{q}'-\mathbf{q}).\mathbf{r}_j-w(\mathbf{q}',p)t+\phi(\mathbf{q}',p)+\phi_{j,\alpha}(\mathbf{q}',p)\right) \\ +\sin\left((\mathbf{q}'+\mathbf{q}).\mathbf{r}_j-w(\mathbf{q}',p)t+\phi(\mathbf{q}',p)+\phi_{j,\alpha}(\mathbf{q}',p)\right) \\ -i\cos\left((\mathbf{q}'-\mathbf{q}).\mathbf{r}_j-w(\mathbf{q}',p)t+\phi(\mathbf{q}',p)+\phi_{j,\alpha}(\mathbf{q}',p)\right) \\ +i\cos\left((\mathbf{q}'+\mathbf{q}).\mathbf{r}_j-w(\mathbf{q}',p)t+\phi(\mathbf{q}',p)+\phi_{j,\alpha}(\mathbf{q}',p)\right)\end{array}\right]\end{array}\right) \tag{4.38}$$

The summation over j goes to zero unless $\mathbf{q} = \mathbf{q}'$ or $\mathbf{q} = -\mathbf{q}'$:

$$\xi_{v,\alpha,j}(\mathbf{q},t)= \\ \sum_{p}\left[\begin{array}{l}\dfrac{\sqrt{N_u}\,w(\mathbf{q},p)\,A(\mathbf{q},p,t)\left|e_{j,\alpha}(\mathbf{q},p)\right|}{2}\left[\begin{array}{l}\sin\left(-w(\mathbf{q},p)t+\phi(\mathbf{q},p)+\phi_{j,\alpha}(\mathbf{q},p)\right) \\ -i\cos\left(-w(\mathbf{q},p)t+\phi(\mathbf{q},p)+\phi_{j,\alpha}(\mathbf{q},p)\right)\end{array}\right]+ \\ \dfrac{\sqrt{N_u}\,w(-\mathbf{q},p)\,A(-\mathbf{q},p,t)\left|e_{j,\alpha}(-\mathbf{q},p)\right|}{2}\left[\begin{array}{l}\sin\left(-w(-\mathbf{q},p)t+\phi(-\mathbf{q},p)+\phi_{j,\alpha}(-\mathbf{q},p)\right) \\ +i\cos\left(-w(-\mathbf{q},p)t+\phi(-\mathbf{q},p)+\phi_{j,\alpha}(-\mathbf{q},p)\right)\end{array}\right]\end{array}\right] \tag{4.39}$$

Expanding the sine and the cosine term to separate $\varphi_{j\alpha}(\mathbf{q},p)$:

$$\xi_{v,\alpha,j}(\mathbf{q},t) =$$

$$\sum_{p}\left[\begin{array}{l}\dfrac{\sqrt{N_u}\,w(\mathbf{q},p)\,A(\mathbf{q},p,t)\left|e_{j,\alpha}(\mathbf{q},p)\right|}{2}\left[\begin{array}{l}\sin\left(-w(\mathbf{q},p)t+\phi(\mathbf{q},p)\right)\cos\left(\phi_{j,\alpha}(\mathbf{q},p)\right)\\ +\cos\left(-w(\mathbf{q},p)t+\phi(\mathbf{q},p)\right)\sin\left(\phi_{j,\alpha}(\mathbf{q},p)\right)\\ -i\cos\left(-w(\mathbf{q},p)t+\phi(\mathbf{q},p)\right)\cos\left(\phi_{j,\alpha}(\mathbf{q},p)\right)\\ +i\sin\left(-w(\mathbf{q},p)t+\phi(\mathbf{q},p)\right)\sin\left(\phi_{j,\alpha}(\mathbf{q},p)\right)\end{array}\right]+\\ \dfrac{\sqrt{N_u}\,w(-\mathbf{q},p)\,A(-\mathbf{q},p,t)\left|e_{j,\alpha}(\mathbf{q},p)\right|}{2}\left[\begin{array}{l}\sin\left(-w(\mathbf{q},p)t+\phi(-\mathbf{q},p)\right)\cos\left(\phi_{j,\alpha}(\mathbf{q},p)\right)\\ -\cos\left(-w(\mathbf{q},p)t+\phi(-\mathbf{q},p)\right)\sin\left(\phi_{j,\alpha}(\mathbf{q},p)\right)\\ +i\cos\left(-w(\mathbf{q},p)t+\phi(-\mathbf{q},p)\right)\cos\left(\phi_{j,\alpha}(\mathbf{q},p)\right)\\ +i\sin\left(-w(\mathbf{q},p)t+\phi(-\mathbf{q},p)\right)\sin\left(\phi_{j,\alpha}(\mathbf{q},p)\right)\end{array}\right]\end{array}\right] \tag{4.40}$$

Combining the terms:

$$\xi_{v,\alpha,j}(\mathbf{q},t) =$$

$$\sum_{p}\left[\begin{array}{l}\dfrac{\sqrt{N_u}\,w(\mathbf{q},p)\,A(\mathbf{q},p,t)\left|e_{j,\alpha}(\mathbf{q},p)\right|}{2}\left[\begin{array}{l}\sin\left(-w(\mathbf{q},p)t+\phi(\mathbf{q},p)\right)\exp\left(i\phi_{j,\alpha}(\mathbf{q},p)\right)\\ -i\cos\left(-w(\mathbf{q},p)t+\phi(\mathbf{q},p)\right)\exp\left(i\phi_{j,\alpha}(\mathbf{q},p)\right)\end{array}\right]+\\ \dfrac{\sqrt{N_u}\,w(\mathbf{q},p)\,A(-\mathbf{q},p,t)\left|e_{j,\alpha}(\mathbf{q},p)\right|}{2}\left[\begin{array}{l}\sin\left(-w(\mathbf{q},p)t+\phi(-\mathbf{q},p)\right)\exp\left(i\phi_{j,\alpha}(\mathbf{q},p)\right)\\ +i\cos\left(-w(\mathbf{q},p)t+\phi(-\mathbf{q},p)\right)\exp\left(i\phi_{j,\alpha}(\mathbf{q},p)\right)\end{array}\right]\end{array}\right] \tag{4.41}$$

Merging the phase and magnitude of $e_{j\alpha}(\mathbf{q},p)$:

$$\xi_{v,\alpha,j}(\mathbf{q},t) = \sum_{p}\left[\begin{array}{l}\dfrac{\sqrt{N_u}\,w(\mathbf{q},p)\,A(\mathbf{q},p,t)\,e_{j,\alpha}(\mathbf{q},p)}{2}\left[\begin{array}{l}\sin\left(-w(\mathbf{q},p)t+\phi(\mathbf{q},p)\right)\\ -i\cos\left(-w(\mathbf{q},p)t+\phi(\mathbf{q},p)\right)\end{array}\right]+\\ \dfrac{\sqrt{N_u}\,w(\mathbf{q},p)\,A(-\mathbf{q},p,t)\,e_{j,\alpha}(\mathbf{q},p)}{2}\left[\begin{array}{l}\sin\left(-w(\mathbf{q},p)t+\phi(-\mathbf{q},p)\right)\\ +i\cos\left(-w(\mathbf{q},p)t+\phi(-\mathbf{q},p)\right)\end{array}\right]\end{array}\right] \tag{4.42}$$

The normal mode coordinate now can be obtained by:

$$\chi_v(\mathbf{q},p,t)=\sum_{j,\alpha}e_{j,\alpha}(-\mathbf{q},p)\,\xi_{v,\alpha,j}(\mathbf{q},t) \tag{4.43}$$

Substituting the relation from Eqn. (4.42) into Eqn. (4.43):

$$\chi_v(\mathbf{q},p,t)=\sum_{j,\alpha}e_{j,\alpha}(-\mathbf{q},p)\sum_{p'}\left[\begin{array}{l}\left(\begin{array}{l}\frac{\sqrt{N_u}\,w(\mathbf{q},p')\,A(\mathbf{q},p',t)\,e_{j,\alpha}(\mathbf{q},p')}{2}\times\\ \left[\begin{array}{l}\sin\left(-w(\mathbf{q},p')t+\phi(\mathbf{q},p')\right)\\ -i\cos\left(-w(\mathbf{q},p')t+\phi(\mathbf{q},p')\right)\end{array}\right]\end{array}\right)+\\ \left(\begin{array}{l}\frac{\sqrt{N_u}\,w(\mathbf{q},p')\,A(-\mathbf{q},p',t)\,e_{j,\alpha}(\mathbf{q},p')}{2}\times\\ \left[\begin{array}{l}\sin\left(-w(\mathbf{q},p')t+\phi(-\mathbf{q},p')\right)\\ +i\cos\left(-w(\mathbf{q},p')t+\phi(-\mathbf{q},p')\right)\end{array}\right]\end{array}\right)\end{array}\right] \tag{4.44}$$

Simplifying:

$$\chi_v(\mathbf{q},p,t)=\sum_{p'}\left[\begin{array}{l}\left(\begin{array}{l}\frac{\sqrt{N_u}\,w(\mathbf{q},p')\,A(\mathbf{q},p',t)}{2}\times\\ \left[\begin{array}{l}\sin\left(-w(\mathbf{q},p')t+\phi(\mathbf{q},p')\right)\\ -i\cos\left(-w(\mathbf{q},p')t+\phi(\mathbf{q},p')\right)\end{array}\right]\end{array}\right)\sum_{j,\alpha}\left(e_{j,\alpha}(\mathbf{q},p)\right)^{*}.e_{j,\alpha}(\mathbf{q},p')+\\ \left(\begin{array}{l}\frac{\sqrt{N_u}\,w(\mathbf{q},p')\,A(-\mathbf{q},p',t)}{2}\times\\ \left[\begin{array}{l}\sin\left(-w(\mathbf{q},p')t+\phi(-\mathbf{q},p')\right)\\ +i\cos\left(-w(\mathbf{q},p')t+\phi(-\mathbf{q},p')\right)\end{array}\right]\end{array}\right)\sum_{j,\alpha}\left(e_{j,\alpha}(\mathbf{q},p)\right)^{*}.e_{j,\alpha}(\mathbf{q},p')\end{array}\right] \tag{4.45}$$

Thus the normal mode coordinate for displacement is related to the individual mode amplitude as:

$$\chi_v(\mathbf{q},p,t)=\begin{bmatrix}\left(\frac{\sqrt{N_u}w(\mathbf{q},p)A(\mathbf{q},p,t)}{2}\begin{bmatrix}\sin\left(-w(\mathbf{q},p)t+\phi(\mathbf{q},p)\right)\\-i\cos\left(-w(\mathbf{q},p)t+\phi(\mathbf{q},p)\right)\end{bmatrix}\right)+\\\left(\frac{\sqrt{N_u}w(\mathbf{q},p)A(-\mathbf{q},p,t)}{2}\begin{bmatrix}\sin\left(-w(\mathbf{q},p)t+\phi(-\mathbf{q},p)\right)\\+i\cos\left(-w(\mathbf{q},p)t+\phi(-\mathbf{q},p)\right)\end{bmatrix}\right)\end{bmatrix} \tag{4.46}$$

Summarizing, the normal mode coordinates are given by:

$$\chi_u(\mathbf{q},p,t)=\frac{\sqrt{N_u}}{2}\begin{bmatrix}A(\mathbf{q},p,t)\exp\left(i\left(-w(\mathbf{q},p)t+\phi(\mathbf{q},p)\right)\right)+\\A(-\mathbf{q},p,t)\exp\left(-i\left(-w(\mathbf{q},p)t+\phi(-\mathbf{q},p)\right)\right)\end{bmatrix}=\left(\chi_u(-\mathbf{q},p,t)\right)^* \tag{4.47}$$

$$\chi_v(\mathbf{q},p,t)=$$
$$\frac{\sqrt{N_u}w(\mathbf{q},p)}{2}\begin{bmatrix}\left(A(\mathbf{q},p,t)\exp\left(i\left(-w(\mathbf{q},p)t+\phi(\mathbf{q},p)-\frac{\pi}{2}\right)\right)\right)+\\\left(A(-\mathbf{q},p,t)\exp\left(-i\left(-w(\mathbf{q},p)t+\phi(-\mathbf{q},p)-\frac{\pi}{2}\right)\right)\right)\end{bmatrix}=\left(\chi_v(-\mathbf{q},p,t)\right)^* \tag{4.48}$$

Note that in the above equations, the normal mode coordinate for any wave vector contains contributions from waves moving in both positive and negative directions.

4.4 Correlations of the phonon space projections

As discussed in the previous subsections, the normal mode coordinates are orthogonal *i.e.*, the cross-correlation between distinct modes is zero. The orthogonality will be verified next. Starting with the normal mode displacement correlation:

$$\left\langle \left(\chi_u(\mathbf{q},p,t)\right)^* . \chi_u(\mathbf{q},p',t) \right\rangle = \frac{N_u}{4} \left\langle \begin{bmatrix} A(\mathbf{q},p,t)\exp\left(-i\left(-w(\mathbf{q},p)t+\phi(\mathbf{q},p)\right)\right)+ \\ A(-\mathbf{q},p,t)\exp\left(i\left(-w(\mathbf{q},p)t+\phi(-\mathbf{q},p)\right)\right) \end{bmatrix} \begin{bmatrix} A(\mathbf{q},p',t)\exp\left(i\left(-w(\mathbf{q},p')t+\phi(\mathbf{q},p')\right)\right)+ \\ A(-\mathbf{q},p',t)\exp\left(-i\left(-w(\mathbf{q},p')t+\phi(-\mathbf{q},p')\right)\right) \end{bmatrix} \right\rangle \quad (4.49)$$

Dropping the time term by substituting $t = 0$:

$$\left\langle \left(\chi_u(\mathbf{q},p,0)\right)^* . \chi_u(\mathbf{q},p',0) \right\rangle = \frac{N_u}{4} \left\langle \begin{bmatrix} A(\mathbf{q},p,0)\exp\left(-i\left(\phi(\mathbf{q},p)\right)\right)+ \\ A(-\mathbf{q},p,0)\exp\left(i\left(\phi(-\mathbf{q},p)\right)\right) \end{bmatrix} \begin{bmatrix} A(\mathbf{q},p',0)\exp\left(i\left(\phi(\mathbf{q},p')\right)\right)+ \\ A(-\mathbf{q},p',0)\exp\left(-i\left(\phi(-\mathbf{q},p')\right)\right) \end{bmatrix} \right\rangle \quad (4.50)$$

Expanding the product:

$$\left\langle \left(\chi_u(\mathbf{q},p,0)\right)^* . \chi_u(\mathbf{q},p',0)\right\rangle =$$
$$\frac{N_u}{4}\begin{bmatrix} \left\langle A(\mathbf{q},p,0)A(\mathbf{q},p',0)\exp\left(i\left(\phi(\mathbf{q},p')-\phi(\mathbf{q},p)\right)\right)\right\rangle \\ +\left\langle A(\mathbf{q},p,0)A(-\mathbf{q},p',0)\exp\left(-i\left(\phi(-\mathbf{q},p')+\phi(\mathbf{q},p)\right)\right)\right\rangle \\ +\left\langle A(-\mathbf{q},p,0)A(\mathbf{q},p',0)\exp\left(i\left(\phi(\mathbf{q},p')+\phi(-\mathbf{q},p)\right)\right)\right\rangle \\ +\left\langle A(-\mathbf{q},p,0)A(-\mathbf{q},p',0)\exp\left(-i\left(\phi(-\mathbf{q},p')-\phi(-\mathbf{q},p)\right)\right)\right\rangle \end{bmatrix} \tag{4.51}$$

The phase angles for positive and negative wave vectors are independent of each other. Thus the ensemble average for the exponential of the sum of these phases goes to zero:

$$\left\langle \left(\chi_u(\mathbf{q},p,0)\right)^* . \chi_u(\mathbf{q},p',0)\right\rangle =$$
$$\frac{N_u}{4}\begin{bmatrix} \left\langle A(\mathbf{q},p,0)A(\mathbf{q},p',0)\exp\left(i\left(\phi(\mathbf{q},p')-\phi(\mathbf{q},p)\right)\right)\right\rangle \\ +\left\langle A(-\mathbf{q},p,0)A(-\mathbf{q},p',0)\exp\left(-i\left(\phi(-\mathbf{q},p')-\phi(-\mathbf{q},p)\right)\right)\right\rangle \end{bmatrix} \tag{4.52}$$

Clearly, if $p \neq p$', then the phase angels will not cancel, and thus the ensemble average goes to zero. Thus the correlation can be expressed as:

$$\left\langle \left(\chi_u(\mathbf{q},p,0)\right)^* . \chi_u(\mathbf{q},p',0)\right\rangle = \frac{N_u}{4}\left[\left\langle A(\mathbf{q},p,0)^2\right\rangle + \left\langle A(-\mathbf{q},p,0)^2\right\rangle\right]\delta_{pp'} \tag{4.53}$$

Similarly:

$$\left\langle \left(\chi_v(\mathbf{q},p,0)\right)^* . \chi_v(\mathbf{q},p',0)\right\rangle = \frac{w^2(\mathbf{q},p)N_u}{4}\left[\left\langle A(\mathbf{q},p,0)^2\right\rangle + \left\langle A(-\mathbf{q},p,0)^2\right\rangle\right]\delta_{pp'} \tag{4.54}$$

Thus, using the eigenvectors of the dynamical matrix for **e**(**q**) does indeed diagonalize the correlation $\left\langle \xi_u(\mathbf{q}).\left(\xi_u(\mathbf{q})\right)^{\dagger} \right\rangle$. Dividing Eqn. (4.54) by Eqn. (4.53), it can now be shown that:

$$w^2(\mathbf{q}, p) = \frac{\left\langle \left(\chi_v(\mathbf{q}, p, 0)\right)^* . \chi_v(\mathbf{q}, p, 0) \right\rangle}{\left\langle \left(\chi_u(\mathbf{q}, p, 0)\right)^* . \chi_u(\mathbf{q}, p, 0) \right\rangle} \tag{4.55}$$

Thus the square of the frequency is the ratio of the correlation for velocity projection and displacement projection in the phonon space as shown in Eqn. (4.55); this relationship provides a tractable method for computing the dispersion relation using atomistic trajectories.

In the Fourier transform method, time correlation of the velocity normal modes is used; which is defined as:

$$\left\langle \left(\chi_v(\mathbf{q}, p, 0)\right)^* . \chi_v(\mathbf{q}, p, t) \right\rangle = \frac{N_u}{4} \left\langle \begin{bmatrix} A(\mathbf{q}, p, 0)\exp\left(-i\left(\phi(\mathbf{q}, p)\right)\right) + \\ A(-\mathbf{q}, p, 0)\exp\left(i\left(\phi(-\mathbf{q}, p)\right)\right) \end{bmatrix} \begin{bmatrix} A(\mathbf{q}, p, t)\exp\left(i\left(-w(\mathbf{q}, p)t + \phi(\mathbf{q}, p)\right)\right) + \\ A(-\mathbf{q}, p, t)\exp\left(-i\left(-w(\mathbf{q}, p)t + \phi(-\mathbf{q}, p)\right)\right) \end{bmatrix} \right\rangle \tag{4.56}$$

The phase angle for the cross terms in the product above (i.e., terms containing both $A(\mathbf{q})$ and $A(-\mathbf{q})$) will not cancel off, thus giving zero ensemble average. Hence:

$$\left\langle \left(\chi_v(\mathbf{q},p,0)\right)^* . \chi_v(\mathbf{q},p,t)\right\rangle =$$
$$\frac{w^2(\mathbf{q},p)N_u}{4}\left[\begin{array}{l}\left\langle A(\mathbf{q},p,0)A(\mathbf{q},p,t)\exp\left(i\left(-w(\mathbf{q},p)t\right)\right)\right\rangle \\ +\left\langle A(-\mathbf{q},p,0)A(-\mathbf{q},p,t)\exp\left(-i\left(-w(\mathbf{q},p)t\right)\right)\right\rangle\end{array}\right] \quad (4.57)$$

The exponentials are independent of the ensemble average and only depend on time:

$$\left\langle \left(\chi_v(\mathbf{q},p,0)\right)^* . \chi_v(\mathbf{q},p,t)\right\rangle =$$
$$\frac{w^2(\mathbf{q},p)N_u}{4}\left[\begin{array}{l}\left\langle A(\mathbf{q},p,0)A(\mathbf{q},p,t)\right\rangle\exp\left(i\left(-w(\mathbf{q},p)t\right)\right) \\ +\left\langle A(-\mathbf{q},p,0)A(-\mathbf{q},p,t)\right\rangle\exp\left(-i\left(-w(\mathbf{q},p)t\right)\right)\end{array}\right] \quad (4.58)$$

The ensemble average for the amplitude correlations of positive and negative wave vectors is same due to symmetry:

$$\left\langle \left(\chi_v(\mathbf{q},p,0)\right)^* . \chi_v(\mathbf{q},p,t)\right\rangle =$$
$$\frac{w^2(\mathbf{q},p)N_u}{4}\left[\begin{array}{l}\left\langle A(\mathbf{q},p,0)A(\mathbf{q},p,t)\right\rangle\exp\left(i\left(-w(\mathbf{q},p)t\right)\right) \\ +\left\langle A(\mathbf{q},p,0)A(\mathbf{q},p,t)\right\rangle\exp\left(-i\left(-w(\mathbf{q},p)t\right)\right)\end{array}\right] \quad (4.59)$$

Simplifying:

$$\left\langle \left(\chi_v(\mathbf{q},p,0)\right)^* . \chi_v(\mathbf{q},p,t)\right\rangle = \frac{w^2(\mathbf{q},p)N_u}{2}\left\langle A(\mathbf{q},p,0)A(\mathbf{q},p,t)\right\rangle\cos\left(w(\mathbf{q},p)t\right) \quad (4.60)$$

Thus the time correlation of the projection of velocities in phonon space is given by Eqn. (4.60) . Clearly, the Fourier transform of this correlation can be used to obtain the peak frequency for any wave vector (and hence, the dispersion relation).

4.5 Results

Based on the theoretical formulations described in the previous section, phonon dispersion relationships are calculated using two methods as shown below:

- Ratio Method:

$$w_{Ratio}(\mathbf{q}, p) = \sqrt{\frac{\left\langle \left(\chi_v(\mathbf{q}, p, 0)\right)^* . \chi_v(\mathbf{q}, p, 0) \right\rangle}{\left\langle \left(\chi_u(\mathbf{q}, p, 0)\right)^* . \chi_u(\mathbf{q}, p, 0) \right\rangle}} \tag{4.61}$$

- FFT Method:

$$\chi_v(\mathbf{q}, p, w) = \int_{-\infty}^{\infty} \left\langle \left(\chi_v(\mathbf{q}, p, 0)\right)^* . \chi_v(\mathbf{q}, p, t) \right\rangle \exp(-iwt)\, dt \tag{4.62}$$

$$w_{FFT}(\mathbf{q}, p) = peak\left(\chi_v(\mathbf{q}, p, w)\right) \tag{4.63}$$

The FFT method, which is well-established, will be used to assess the fidelity of the ratio method. For the FFT method, the dispersion is obtained by extracting the frequency corresponding to the peak value of the Fourier transform of the time correlation of the velocity normal mode as shown in Eqn. (4.62). Though both methods require calculation of the velocity normal mode correlations, the ratio method uses the value of the correlation only time t = 0

while the FFT method requires the correlation over a long period of time for resolving the low frequencies from the Fourier transform. Thus the ratio method will computationally be less expensive – a definite advantage over the FFT method. It is further shown that in this section that the ratio method is also more accurate than the FFT method. Three systems that are considered for the benchmark tests are:

- Monoatomic Linear Chain
- Diatomic Linear Chain
- Graphene

4.5.1 Monoatomic Linear Chain

Consider a linear monoatomic chain of *N* atoms as described in Chapter 2. The atoms interact with each other with a harmonic potential given by:

$$U_{jk}^{Harmonic}(t) = \frac{1}{2} C \left(u_j(t) - u_k(t) \right)^2 \tag{4.64}$$

The spring constant is chosen to simulate the harmonic approximation of a Lennard-Jones (LJ) interaction [92]; this is done to enable comparison with the actual LJ potential (see next equation) to study effects of anharmonicity at a later stage.

$$U_{jk}^{LJ}(t) = 4\varepsilon \left[\left(\frac{\sigma}{u_j(t) - u_k(t)} \right)^{12} - \left(\frac{\sigma}{u_j(t) - u_k(t)} \right)^{6} \right] \tag{4.65}$$

The harmonic approximation of the above LJ potential gives:

$$C = \frac{36\varepsilon\sqrt[3]{4}}{\sigma^2}; a = 2^{\frac{1}{6}}\sigma \tag{4.66}$$

The cutoff for the interaction is set up such that only the immediate neighbors interact. As shown previously, the theoretical expression for the dispersion relation is given by:

$$w_q = \sqrt{\frac{4C}{m}}\left|\sin\left(\frac{qa}{2}\right)\right| \tag{4.67}$$

where q is the wave vector, w is the angular frequency and m is the mass of each atom. LJ parameters for Argon are used in order to convert the results into SI units [92]. It is observed that using any form of rescaling for controlling the temperature or pressure affects the equipartition of energy between the modes. Thus the system is run under a NVE ensemble for long enough time after the initial NVT equilibration to redistribute the energy between the modes, before sampling of data for computing the correlations commences.

Figure 4.1 shows the Fourier transform of the velocity normal mode coordinate as given in Eqn. (4.62), for a monoatomic chain of 100 atoms at 0.5 K. The peak frequency values form a dark red strip, which corresponds to the phonon dispersion curve. The peak values are extracted from the Fourier transform using the peak extraction algorithms in MATLAB. The dispersions using both FFT and the ratio method are shown in *Figure 4.2* along with the theoretical prediction given by Eqn. (4.67). It can be seen that the dispersion obtained from both the

methods overlap with the theoretical prediction. The errors in the prediction from the two methods are shown in *Figure 4.3* – clearly, the ratio method gives a much smaller error as compared to the FFT method. The overall root mean square (RMS) error due to the ratio method is about 0.0020 THz while that due to the FFT method is 0.0277 THz, almost an order of magnitude higher. Thus the ratio method is not only computationally less expensive but is also about ten times more accurate than the FFT method for the harmonic 1-D chain.

The same dispersion curve for a 1000 atom chain at 0.5 K is shown in *Figure 4.4*. For a larger system size, the resolution of the wave vector space gets finer. Thus the change in frequency between successive wave vectors is minuscule. The FFT method is not able to resolve this fine difference and thus produces a curve with steps rather than a smooth dispersion as shown by the ratio method. The FFT method thus needs a larger correlation time to resolve the frequencies more accurately.

Figure 4.5 shows a comparison of the dispersion for LJ potential and its harmonic approximation calculated using the ratio method. The curves overlap almost exactly for the low temperature of 0.5 K because the interaction is nearly harmonic with the LJ interaction. *Figure 4.6* shows a comparison of the LJ dispersion curve at 0.5 and 5 K. While the curves overlap, there is a subtle change in the dispersion behavior near the zone boundary for the higher temperature. This reduction arises from the anharmonicity, but the effect is still quite small because of the relatively low thermal amplitudes at 5 K.

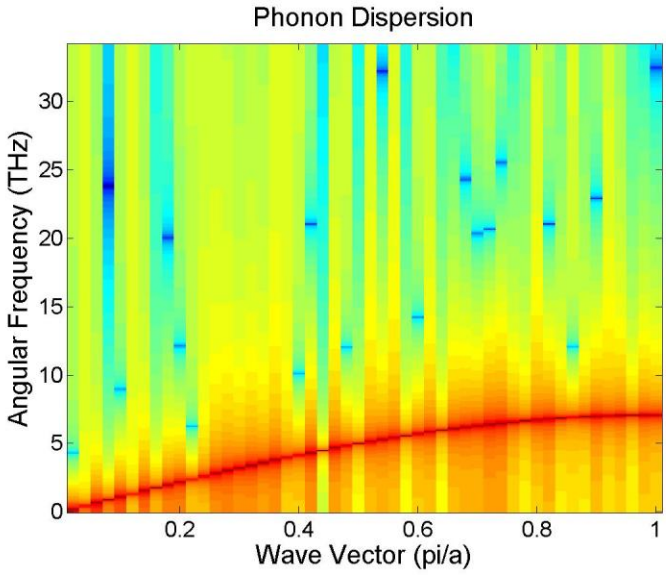

Figure 4.1: Fourier transform of the time correlation of the velocity normal coordinate as described in Eqn. (4.62). The peak frequencies give the phonon dispersion, observed as the dark red curve in the figure.

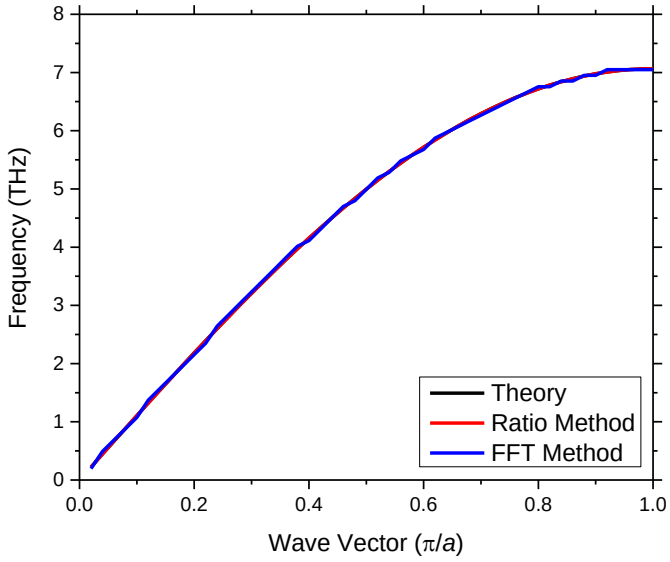

Figure 4.2: Phonon dispersion of a harmonic 1-D chain of 100 atoms at 0.5 K.

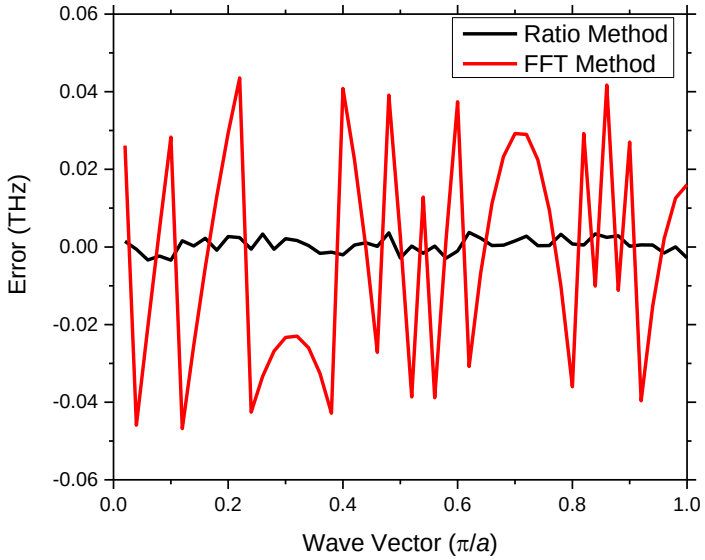

Figure 4.3: Error in the dispersion predicted by the ratio and the FFT method for a 100 atom harmonic 1-D chain at 5 K.

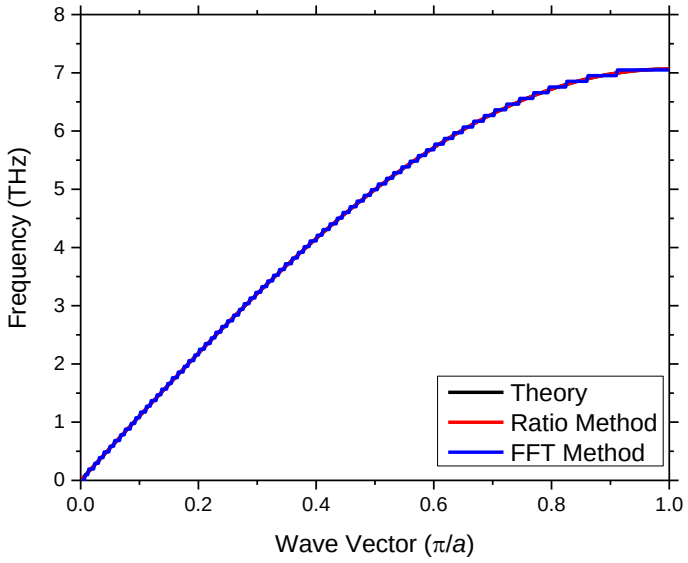

Figure 4.4: Phonon dispersion of a harmonic 1-D chain of 1000 atoms at 0.5 K.

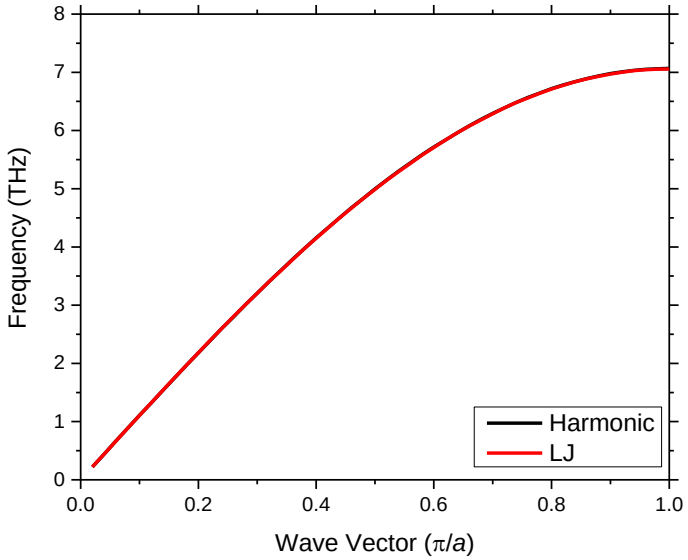

Figure 4.5: Phonon dispersion curves of a 1-D chain of 100 atoms at 0.5 K with harmonic and LJ potentials.

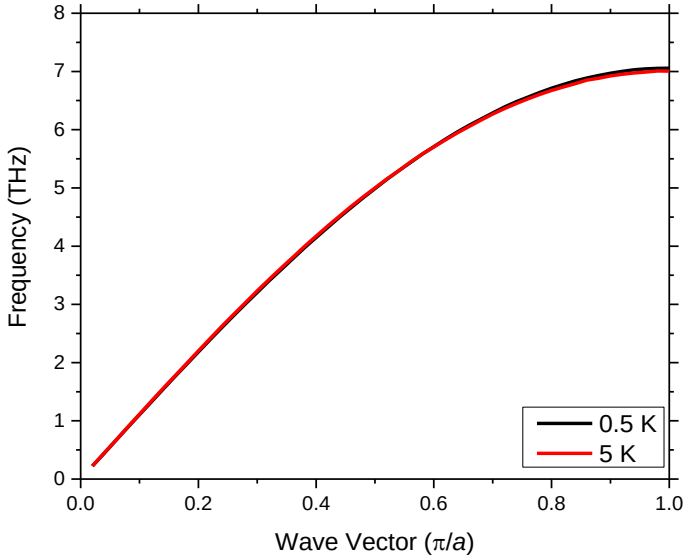

Figure 4.6: Phonon dispersion of a 1D chain of 100 atoms with LJ interaction at 0.5 K and 5 K.

4.5.2 Diatomic Linear Chain

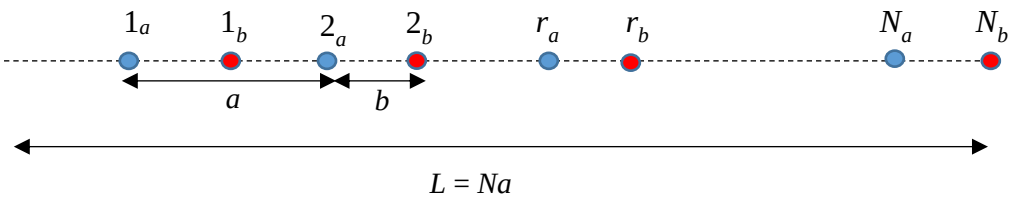

Figure 4.7: Diatomic linear chain with 2*N* atoms.

Next, consider the diatomic chain as shown in *Figure 4.7*. The potential of interaction is exactly the same as in the case of the monoatomic chain; however, the masses of adjacent atoms are different. The interatomic spacings are defined as:

$$a = 2b \text{ and } b = 2^{\frac{1}{6}}\sigma \tag{4.68}$$

The theoretical expression for the dispersion relation for the diatomic chain is given by:

$$w_r = \sqrt{\frac{(m_a + m_b)C}{m_a m_b} \pm \frac{C\sqrt{(m_a + m_b)^2 - 4m_a m_b \sin^2\left(\frac{q_r a}{2}\right)}}{m_a m_b}} \tag{4.69}$$

For the diatomic chain, two phonon branches are observed in the dispersion relation. The branch with the negative sign (in Eqn. (4.69)) corresponds to adjacent atoms moving in the same phase and is called the acoustic mode, while the branch with the positive sign corresponds to the adjacent atoms moving out of phase, which is referred to as the optical mode.

The dispersion curves for a mass ratio of 1.0 and 2.0 at 0.5 K with harmonic interactions are shown in *Figure 4.8* and *Figure 4.9*, respectively (the chain with a mass ratio of 1.0 is identical to a monoatomic chain). Also note that the value of *a* for the diatomic case is twice that of the monoatomic case. For a mass ratio of 2.0, the optical and the acoustic branches separate and a bandgap is created. For both the cases, the curves calculated using the ratio method and the FFT method overlap almost exactly with the theoretical prediction given by Eqn. (4.69). The root mean square error from the two methods is presented in *Table 4.1*. Although both methods are quite accurate, the ratio method outperforms the FFT method judging by the RMS errors.

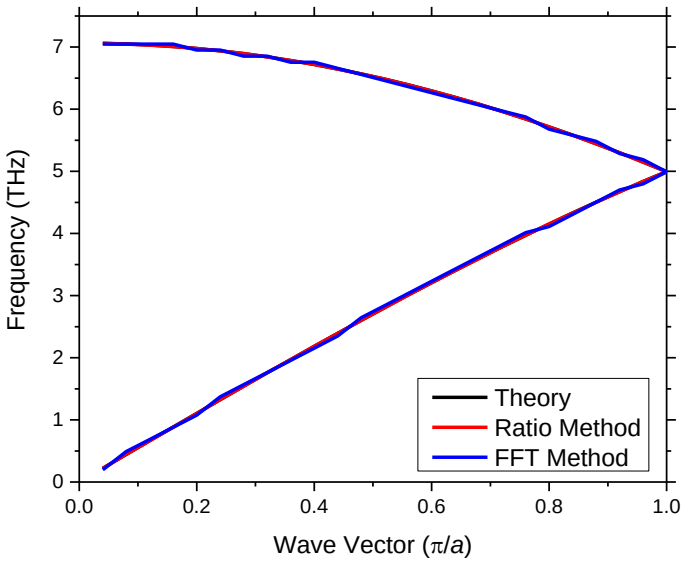

Figure 4.8: Phonon dispersion of the diatomic chain with 100 atoms at 0.5 K with a mass ratio of 1.0.

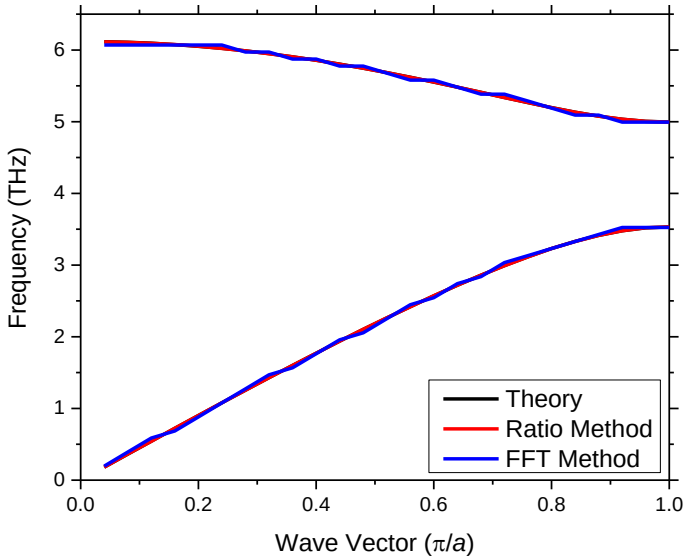

Figure 4.9: Phonon dispersion of the diatomic chain with 100 atoms at 0.5 K with a mass ratio of 2.0.

Table 4.1: Root mean square error in the calculation of the dispersion curves by the ratio and the FFT methods.

Number of atoms	Chain type and phonon branch			RMS Error (THz)	
				Ratio Method	FFT Method
100	Monoatomic			0.0020	0.0277
1000	Monoatomic			0.0020	0.0279
100	Diatomic	$m_A/m_B = 1.0$	Acoustic	0.0013	0.0300
			Optical	0.0014	0.0249
100	Diatomic	$m_A/m_B = 2.0$	Acoustic	0.0012	0.0266
			Optical	0.0011	0.0283

4.5.3 Graphene

This section focuses on a two-dimensional graphene system with a realistic interatomic potential. Although the equilibrium structure of graphene is two-dimensional, the atoms are free to move in three dimensions, and thus the system is essentially three dimensional, and

each atom possesses six degrees of freedom (three each for position and momenta). The structure of graphene [93] along with the details of the unit-cell and the reciprocal lattice is shown in *Figure 4.10*. The graphene unit-cell consists of a two-atom basis and is shown as dashed rhombi with lattice vectors $\mathbf{a}_1$ and $\mathbf{a}_2$. Each atom is represented as a blue circle while the origin of each unit-cell is shown as a red circle. The two lattice vectors are at an angle 120˚ from each other, and the system is so aligned such that $\mathbf{a}_1$ points along the positive *x*-axis and both $\mathbf{a}_1$ and $\mathbf{a}_2$ lie along the *xy*-plane. Thus the basal plane is along the *xy*-plane.

The lattice vectors are related to the C-C bond length *a* as given below:

$$\mathbf{a}_1 = \sqrt{3}a\hat{i} \tag{4.70}$$

$$\mathbf{a}_2 = \sqrt{3}a\left[-\frac{1}{2}\hat{i} + \frac{\sqrt{3}}{2}\hat{j}\right] \tag{4.71}$$

$$\mathbf{a}_3 = c\hat{k} \tag{4.72}$$

$$|\mathbf{a}_1| = |\mathbf{a}_2| = \sqrt{3}a \tag{4.73}$$

Although the structure is two-dimensional, a third lattice vector is defined for the sake of completeness and for defining the reciprocal lattice vectors $\mathbf{b}_1$ and $\mathbf{b}_2$ (see Eqns (4.74) to (4.77)). The magnitude of the third lattice vector is simply taken to be equal to the inter-layer separation for graphite.

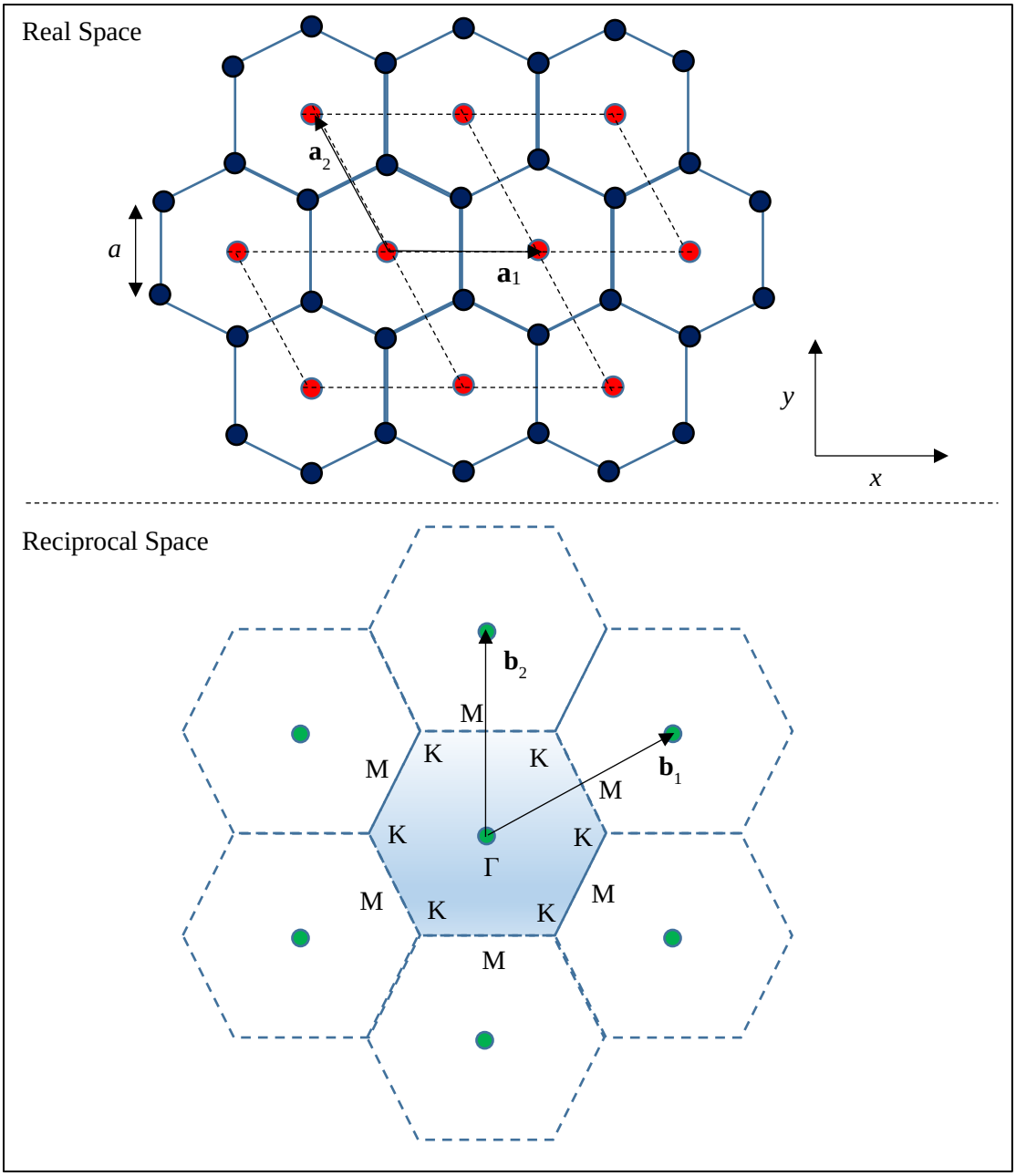

Figure 4.10: Real space (top) and the reciprocal space (bottom) for graphene. For the real space, the blue circles represent atoms while the red circles represent the lattice sites. The lattice vectors are given by $\mathbf{a}_1$ and $\mathbf{a}_2$ while the C-C bond length is given by a. The x-axis is along the zigzag direction while the y-axis is along the armchair direction. The dashed rhombi constitute individual unit-cells with a two atom basis. For the reciprocal lattice, the green circles represent the reciprocal lattice sites. The reciprocal lattice vectors are given $\mathbf{b}_1$ and $\mathbf{b}_2$. Γ represents the zone center while M and K represent the high symmetry directions.

$$\mathbf{b}_1 = \frac{2\pi(\mathbf{a}_2 \times \mathbf{a}_3)}{|\mathbf{a}_1.(\mathbf{a}_2 \times \mathbf{a}_3)|}, \mathbf{b}_2 = \frac{2\pi(\mathbf{a}_3 \times \mathbf{a}_1)}{|\mathbf{a}_1.(\mathbf{a}_2 \times \mathbf{a}_3)|}, \mathbf{b}_3 = \frac{2\pi(\mathbf{a}_1 \times \mathbf{a}_2)}{|\mathbf{a}_1.(\mathbf{a}_2 \times \mathbf{a}_3)|} \tag{4.74}$$

$$\mathbf{b}_1 = \frac{2\pi}{a}\left(\frac{2}{3}\right)\left[\frac{\sqrt{3}}{2}\hat{i} + \frac{1}{2}\hat{j}\right] \tag{4.75}$$

$$\mathbf{b}_2 = \frac{2\pi}{a}\left(\frac{2}{3}\right)\hat{j} \tag{4.76}$$

$$|\mathbf{b}_1| = |\mathbf{b}_2| = \frac{4\pi}{3a} \tag{4.77}$$

The reciprocal lattice vectors $\mathbf{b}_1$ and $\mathbf{b}_2$ are at an angle of 60˚ to each other with $\mathbf{b}_2$ pointing along the *y*-axis in the present configuration. The reciprocal lattice points are represented by green circles, and the shaded hexagon forms the first Brillouin zone. The high symmetry points are marked as *M* and *K*.

It should be noted that the relation between the lattice parameter and bond length given in Eqn.(4.73) is valid only at 0K when the atoms do not move, and the structure is exactly two dimensional. At finite temperatures, the atoms start to vibrate, and the graphene sheet shrinks to accommodate for the vibrations perpendicular to the basal plane. This causes the lattice parameter for graphene to decrease with temperature initially [94].

For the present work, atomistic simulations are performed at 30 K (to compare with theoretical dispersion curves which are valid strictly at 0 K) and 300 K (to study the behavior at room temperature) thus spanning one order of magnitude in the temperature range. The system is initially equilibrated in a NPT ensemble with zero pressure using Berendson [95] thermostat

and barostat, and then run under a NVE ensemble for long enough time to redistribute the energy between the modes. The simulation consists of 60 unit cells along both unit vectors *i.e.*, a total of 7,200 atoms. Tersoff [96] potential with parameters optimized [97] for phonon dispersion of graphene is used for describing the interatomic interactions. Recently, Emmanuel *et al*. [98] have used the FFT method to study the phonon dispersion of graphene with several interatomic potentials and have reported the Tersoff potential with the optimized parameters (used in the present work) to be the most suitable and accurate. A similar observation has also been made by Zou *et al*. [24] using both the SED method [61] and the Green's function approach by Kong [86]. The dispersion is calculated only along the high symmetry directions with Γ-M branch pointing along the *y*-axis and the Γ-K branch pointing along the *x*-axis. Periodic boundary conditions are used along the lattice vector directions but not along the *x* and *y* directions.

The dispersion curves computed using the FFT method and the ratio method at 30 K are shown in *Figure 4.11* and *Figure 4.12*, respectively. The Longitudinal Acoustic (LA) branch is shown in black, Transverse Acoustic (TA) branch in red, Flexural Acoustic (ZA) branch in blue, Longitudinal Optical (LO) branch in green, Transverse Optical (TO) branch in brown and the Flexural Optical (ZO) branch in magenta. Lindsay and Broido [97] has theoretically calculated the dispersion curves for the optimized Tersoff parameters; the reference data extracted from their work has been added as black dots in the dispersion curves. Both the ratio method and the FFT method depict a good match to the reference data, but the ratio method appears to be more accurate visually, especially for the LO and TO branches. The dispersion computed by

the two methods is compared in *Figure 4.13*; all the branches overlap apart from the TO and LO branch; clearly, the FFT method overestimates these branches. Quantitatively, the root mean square error in the dispersion computed using the two methods as compared to the reference data is given in *Table 4.2*. The Ratio method outperforms the FFT method for all the branches, with the difference in the error for LO and TO branches being the most prominent. However, the difference in the error magnitudes for graphene is not as huge as it is for the linear chain. It should be noted that for graphene, an exact expression for the dispersion relation is not available.

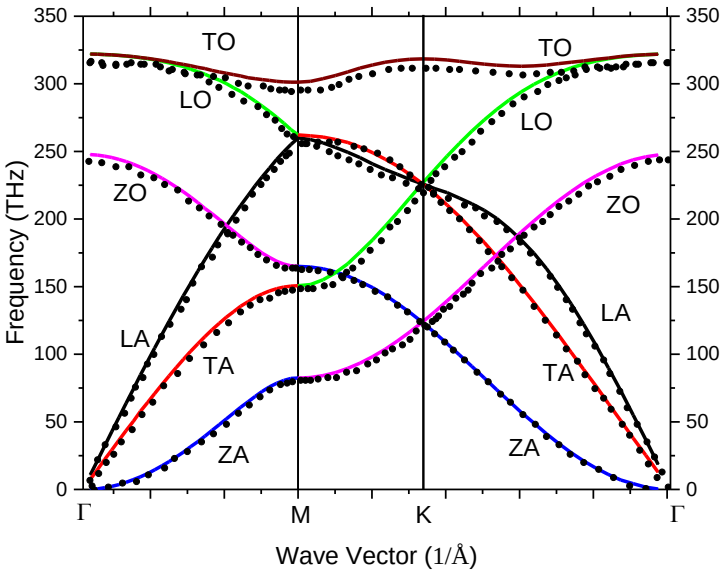

Figure 4.11: Dispersion curve for graphene along high symmetry directions computed using the FFT of velocity normal mode correlation in time. The color coding is as follows; Longitudinal Acoustic (LA) branch: black, Transverse Acoustic (TA) branch: red, Flexural Acoustic (ZA) branch: blue, Longitudinal Optical (LO) branch: green, Transverse Optical (TO) branch: brown and Flexural Optical (ZO) branch: magenta. The reference data from Lindsay and Broido [97] with Tersoff potential used in the present study is shown as black circles.

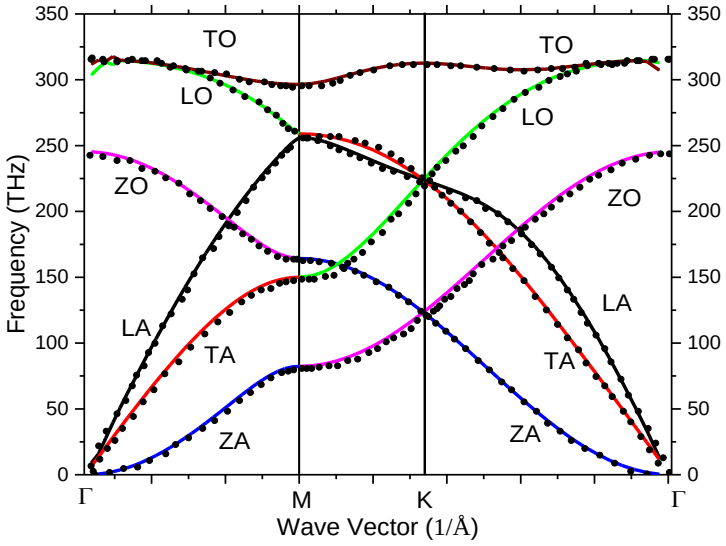

Figure 4.12: Dispersion curve for graphene along high symmetry directions computed using the ratio of conjugate variables in phonon space. The color coding is as follows; Longitudinal Acoustic (LA) branch: black, Transverse Acoustic (TA) branch: red, Flexural Acoustic (ZA) branch: blue, Longitudinal Optical (LO) branch: green, Transverse Optical (TO) branch: brown and Flexural Optical (ZO) branch: magenta. The reference data from Lindsay and Broido [97] with Tersoff potential used in the present study is shown as black circles.

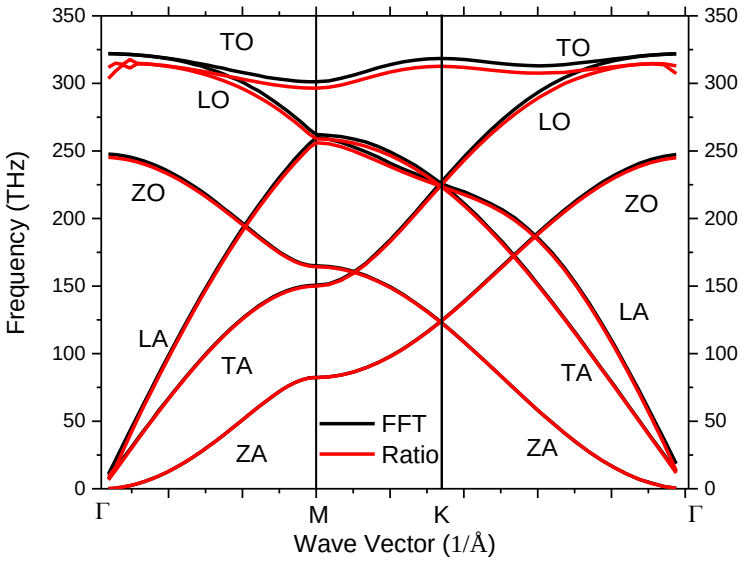

Figure 4.13: Comparison of the dispersion curve for graphene along high symmetry directions computed using the FFT of velocity normal mode correlation in time (black) and computed using the ratio of conjugate variables in phonon space (red).

Table 4.2: The root mean square error in the computation of the dispersion relation using the ratio and the FFT method for each phonon branch of graphene.

Wave Vector Direction	Branch	RMS Error (THz)	
		Ratio Method	FFT Method
Γ-M	LA	2.9481	4.4833
	TA	3.9885	4.5790
	ZA	2.2801	2.2940
	LO	2.8518	5.1305
	TO	1.4168	5.6841
	ZO	2.2299	3.7898
Γ-K	LA	1.9294	3.4513
	TA	1.9817	2.6383
	ZA	1.1602	1.3854
	LO	3.5168	6.1068
	TO	1.9112	6.5438
	ZO	3.5476	4.4409

Figure 4.14 and *Figure 4.15* show the comparison of the dispersion curves at 30 K and 300 K using the FFT method and the ratio method, respectively. A small dip in the LO and TO branches with increasing temperature has been reported before [98]. It is interesting to note that the ratio method is able to capture this small dip more prominently than with the FFT approach.

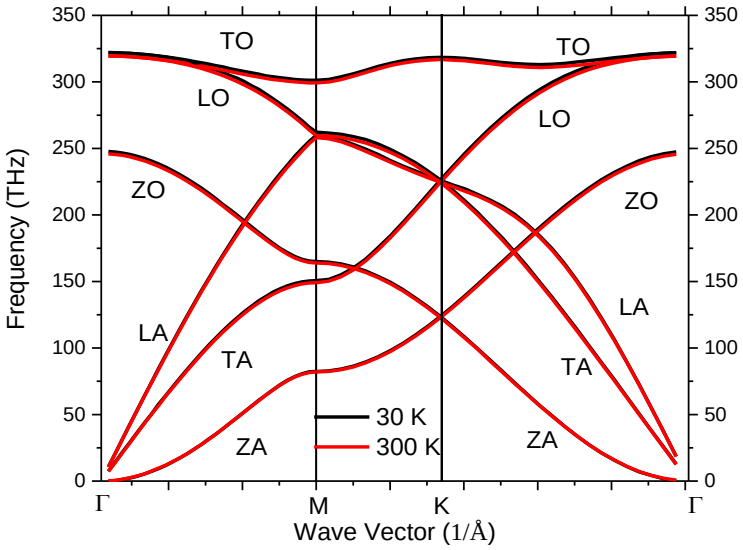

Figure 4.14: Comparison of the dispersion curve for graphene along high symmetry directions computed using the FFT of velocity normal mode correlation at 30 K (black) and 300 K (red).

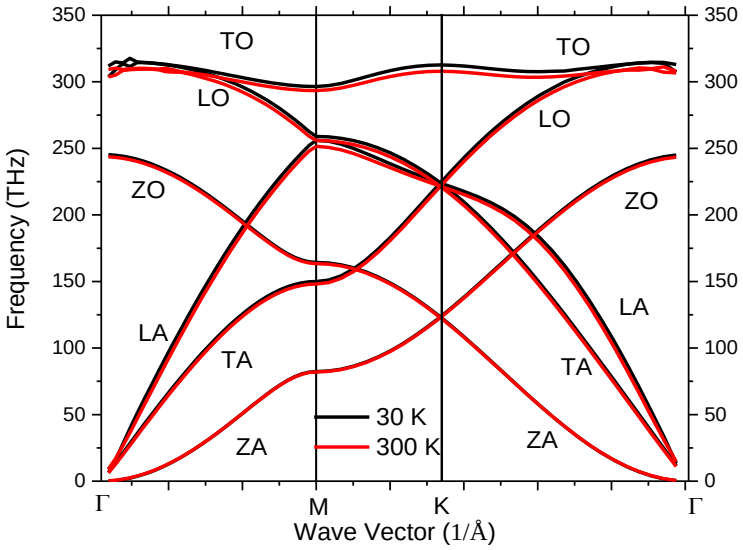

Figure 4.15: Comparison of the dispersion curve for graphene along high symmetry directions computed using the ratio of conjugate variables in phonon space at 30 K (black) and 300 K (red).

4.6 Conclusion

Expressions for the phonon space projections in terms of the amplitudes of the real cosine solution is presented this chapter. These expressions are used to obtain an analytical form for the time correlation functions of the phonon space projections. The ratio of the time correlation functions of the phonon space projections for velocity to that of displacement is shown to be equal to the square of the mode frequency – a result that is also previously known. Atomistic simulations are then performed to obtain the phonon dispersion curves using this expression (referred to as the ratio method) for three benchmark cases: a linear monoatomic chain, a linear diatomic chain, and graphene. For all the three cases, the ratio method is observed to be demonstrably superior in computational speed relative to the popular Fourier transform method; it also outperforms in accuracy by a fair margin.

Chapter 5: MATHEMATICAL AND PHYSICAL CONSISTENCY FOR HEAT CARRIER MODES

5.1 Introduction

A promising and efficient technique for obtaining the phonon dispersion relationship using atomistic trajectories is described in the previous chapter. Once the dispersion relationship is known, further analysis can be conducted to investigate the interaction between the phonon modes that underpin the thermodynamic and thermo-mechanical properties. It is briefly described in Chapter 2 that the anharmonicity of the interacting potential is responsible for the phonon-phonon interactions; for example, the cubic term in the potential leads to three-phonon interactions, quartic term leads to four-phonon interactions and so forth. In the quantum picture, these interactions are called phonon-phonon scattering. Three-phonon scattering involving three-phonon modes is usually the most dominant. Thus, a traveling phonon carrying energy can scatter into different phonon modes, which causes resistance to the flow of energy, which is known as thermal resistance. Thus, a knowledge of the phonon scattering processes and the lifetimes of the phonon modes are essential for understanding the thermal conduction behavior of a crystalline system.

In their seminal work, Ladd and Moran [55] developed a methodology to estimate phonon relaxation times using the decay of the energy associated with individual phonon modes (since the mode energy is proportional to the phonon population). McGaughey and Kaviany [59, 60]

modified this approach and used a two-step decay model for the heat flux autocorrelation function (HACF) [53, 54] to separate the thermal conductivity contributions from the short-range and long-range phonons; this method was extended by Alexander *et al*. [99] for decomposing the phonon thermal conductivity of a monoatomic lattice. In recent years, a similar approach has been reported in several investigations [44, 56, 62, 100].

In the work of Zushi *et al*. [36] phonon lifetimes were computed directly from the decay of the phonon normal mode coordinates; however, this appears to be incorrect because the phonon population is proportional to the square of the magnitude of the correlation. An alternate method was proposed by Thomas and McGaughey et al. [61] using the spectral energy density (SED) – this approach has since been employed in other investigations [101, 102]. Volz *et al*. [4, 103-105] developed a method for obtaining the spectral heat current from non-equilibrium systems and used it to obtain spectral thermal conductivity across interfaces using non-equilibrium atomistic simulations. . A review of the different methods employed for spectral decomposition of thermal conductivity can be found in the review article by Feng and Ruan [106].

Gill and Lewis [20, 57, 58] recently developed an approach starting from statistical mechanics *first principles*, namely, the Green-Kubo formalism [53, 54] involving time correlations of the heat currents, to separate the contributions from the positive and the negative phonon modes. Critically, this approach relies on defining an imaginary heat current due to each phonon mode, with only the *sum* of the contributions from the positive and negative modes being real and physically meaningful. More importantly, this work does not crucially identify the mechanistic

basis of heat flow *i.e.*, the modal heat flow arises from the *difference* between the phonon modes traveling along the positive and negative wave vectors.

The work presented in this chapter employs the *mathematically consistent* real cosine solution described in Chapter 3 to obtain the phonon population associated with individual modes. The phonon population is then used to obtain the individual mode heat currents – an important step that has been missing in prior investigations. While the expression for the *total* heat current due to the sum of the contributions from the positive and negative modes derived in the present approach agrees with that proposed by Gill and Lewis [20, 57, 58], the current approach provides an important expression for the individual amplitudes of the waves traveling along **q** and –**q** directions that is critically needed to define a *real* heat current. Thus, the current work identifies that the heat current in the phonon normal mode formalism is mathematically and physically real and not an imaginary quantity which cannot be observed [20, 57, 58]. Three significant findings from this study are: (*i*) the phonon lifetimes from energy correlations are significantly lower than those estimated using the existing approaches, and (*ii*) phonon-phonon cross-correlations can play a dominant role in thermal transport process, especially for low-dimension systems, (*iii*) thermal conductivity can be partitioned among two phonon modes – self and cross; while the phonon contributions from self and cross terms have been reported before [58], a correction term arising from the difference in the heat fluxes moving in +**q** and –**q** directions is a new finding from this dissertation.

5.2 Theoretical formulation

5.2.1 Extracting individual mode amplitudes

Recalling from the previous chapters, the net displacement, and velocity due the individual modes from the general solution is given by:

$$\mathbf{u}_{\alpha,j}(t)=\sum_{\mathbf{q},p}\mathbf{u}_{\alpha,j}(\mathbf{q},p,t)=$$

$$\sum_{\mathbf{q},p}\frac{1}{\sqrt{m_j}}A(q,p,t)\left|e_{j,\alpha}(\mathbf{q},p)\right|\begin{pmatrix}\cos\left(\mathbf{q}.\mathbf{r}_1-w(\mathbf{q},p)t+\phi(\mathbf{q},p)+\phi_{j,\alpha}(\mathbf{q},p)\right)\\ \cos\left(\mathbf{q}.\mathbf{r}_2-w(\mathbf{q},p)t+\phi(\mathbf{q},p)+\phi_{j,\alpha}(\mathbf{q},p)\right)\\ .\\ .\\ \cos\left(\mathbf{q}.\mathbf{r}_{N_u}-w(\mathbf{q},p)t+\phi(\mathbf{q},p)+\phi_{j,\alpha}(\mathbf{q},p)\right)\end{pmatrix} \tag{5.1}$$

$$\mathbf{v}_{\alpha,j}(t)=\sum_{\mathbf{q},p}\mathbf{v}_{\alpha,j}(\mathbf{q},p,t)=$$

$$\sum_{\mathbf{q},p}\frac{1}{\sqrt{m_j}}w(\mathbf{q},p)A(q,p,t)\left|e_{j,\alpha}(\mathbf{q},p)\right|\begin{pmatrix}\sin\left(\mathbf{q}.\mathbf{r}_1-w(\mathbf{q},p)t+\phi(\mathbf{q},p)+\phi_{j,\alpha}(\mathbf{q},p)\right)\\ \sin\left(\mathbf{q}.\mathbf{r}_2-w(\mathbf{q},p)t+\phi(\mathbf{q},p)+\phi_{j,\alpha}(\mathbf{q},p)\right)\\ .\\ .\\ \sin\left(\mathbf{q}.\mathbf{r}_{N_u}-w(\mathbf{q},p)t+\phi(\mathbf{q},p)+\phi_{j,\alpha}(\mathbf{q},p)\right)\end{pmatrix} \tag{5.2}$$

The corresponding normal mode coordinates are given by:

$$\chi_u(\mathbf{q},p,t)=\frac{\sqrt{N_u}}{2}\begin{bmatrix}A(\mathbf{q},p,t)\exp\left(i\left(-w(\mathbf{q},p)t+\phi(\mathbf{q},p)\right)\right)+\\ A(-\mathbf{q},p,t)\exp\left(-i\left(-w(\mathbf{q},p)t+\phi(-\mathbf{q},p)\right)\right)\end{bmatrix}=\left(\chi_u(-\mathbf{q},p,t)\right)^* \tag{5.3}$$

$$\chi_v(\mathbf{q},p,t) = \frac{\sqrt{N_u}w(\mathbf{q},p)}{2}\left[\begin{array}{l}\left(A(\mathbf{q},p,t)\exp\left(i\left(-w(\mathbf{q},p)t+\phi(\mathbf{q},p)-\frac{\pi}{2}\right)\right)\right)+\\ \left(A(-\mathbf{q},p,t)\exp\left(-i\left(-w(\mathbf{q},p)t+\phi(-\mathbf{q},p)-\frac{\pi}{2}\right)\right)\right)\end{array}\right] = \left(\chi_v(-\mathbf{q},p,t)\right)^* \quad (5.4)$$

Eqns. (5.3) and (5.4) can be simplified to obtain the individual normal mode amplitudes as:

$$A(\mathbf{q},p,t) = \frac{1}{\sqrt{N_u}}\left(\chi_u(\mathbf{q},p,t)+\frac{i}{w(\mathbf{q},p)}\chi_v(\mathbf{q},p,t)\right)\exp\left(-i\left(-w(\mathbf{q},p)t+\phi(\mathbf{q},p)\right)\right) \quad (5.5)$$

$$A(-\mathbf{q},p,t) = \frac{1}{\sqrt{N_u}}\left(\chi_u(\mathbf{q},p,t)-\frac{i}{w(\mathbf{q},p)}\chi_v(\mathbf{q},p,t)\right)\exp\left(i\left(-w(\mathbf{q},p)t+\phi(-\mathbf{q},p)\right)\right) \quad (5.6)$$

Eliminating the unknown phase angles $\varphi(\mathbf{q},p)$ and $\varphi(-\mathbf{q},p)$ to obtain the square of the amplitudes:

$$A^2(\mathbf{q},p,t) = \frac{1}{N_u}\left[\begin{array}{l}\left(\chi_u(\mathbf{q},p,t)+\frac{i}{w(\mathbf{q},p)}\chi_v(\mathbf{q},p,t)\right)\times\\ \left(\left(\chi_u(\mathbf{q},p,t)\right)^*-\frac{i}{w(\mathbf{q},p)}\left(\chi_v(\mathbf{q},p,t)\right)^*\right)\end{array}\right] \quad (5.7)$$

$$A^2(-\mathbf{q},p,t) = \frac{1}{N_u}\left[\begin{array}{l}\left(\chi_u(\mathbf{q},p,t)-\frac{i}{w(\mathbf{q},p)}\chi_v(\mathbf{q},p,t)\right)\times\\ \left(\left(\chi_u(\mathbf{q},p,t)\right)^*+\frac{i}{w(\mathbf{q},p)}\left(\chi_v(\mathbf{q},p,t)\right)^*\right)\end{array}\right] \quad (5.8)$$

Thus the individual mode amplitudes can be extracted from the normal mode coordinates for displacements and velocities. The next section will connect the individual modes amplitudes to the mode population and energy.

5.2.2 Individual mode population and energy

The total energy of the system can be described in terms of normal mode coordinates as given below in Eqn. (5.9). A proof for this relationship can be found elsewhere [73].

$$E(t)=\sum_{\mathbf{q},p}\frac{1}{2}\left[w^2(\mathbf{q},p)\chi_u(\mathbf{q},p,t)\chi_u^*(\mathbf{q},p,t)+\chi_v(\mathbf{q},p,t)\chi_v^*(\mathbf{q},p,t)\right] \tag{5.9}$$

Based on the above relation, one approach is to define the energy associated with each individual mode as [56]:

$$E_{old}(\mathbf{q},p,t)=\frac{1}{2}\left[w^2(\mathbf{q},p)\chi_u(\mathbf{q},p,t)\chi_u^*(\mathbf{q},p,t)+\chi_v(\mathbf{q},p,t)\chi_v^*(\mathbf{q},p,t)\right] \tag{5.10}$$

The above relation implies that the energy associated with positive and negative wave vectors is the same, which is physically inconsistent. The total energy associated with an individual mode for a monoatomic linear chain was shown to be given by:

$$E(q,t)=\frac{N}{2}w^2(q)A^2(q) \tag{5.11}$$

A detailed derivation of the above relation is given in Appendix A. Generalizing the above relation for a three-dimensional lattice (the subscript *'pw'* denotes present work)

$$E_{pw}\left(\mathbf{q}, p, t\right) = \frac{N_u}{2} w^2\left(\mathbf{q}, p\right) A^2\left(\mathbf{q}, p, t\right) \tag{5.12}$$

On substituting the expressions for the normal mode coordinates in terms of the individual mode amplitudes (Eqns. (5.3) and (5.4)) into Eqn. (5.10), it can be shown that:

$$E_{old}\left(\mathbf{q}, p, t\right) = \frac{N_u w^2\left(\mathbf{q}, p\right)}{4}\left(A^2\left(\mathbf{q}, p, t\right) + A^2\left(-\mathbf{q}, p, t\right)\right) \tag{5.13}$$

This leads to the following expression:

$$E_{old}\left(\mathbf{q}, p, t\right) = \frac{1}{2}\left[E_{pw}\left(\mathbf{q}, p, t\right) + E_{pw}\left(-\mathbf{q}, p, t\right)\right] \tag{5.14}$$

Thus the existing expression for energy (denoted with the subscript *old*) associated with a mode is actually the average of the contributions from the positive and negative wave vectors. It may be noted here that the sum of the energy due to all modes *i.e.*, is the total system energy is same from both the existing approach and the present work.

$$E\left(t\right) = \sum_{\mathbf{q}, p} E_{old}\left(\mathbf{q}, p, t\right) = \sum_{\mathbf{q}, p} E_{pw}\left(\mathbf{q}, p, t\right) \tag{5.15}$$

Phonon population from both the approaches can now be obtained from the associated mode energy. They are given as:

$$n_{pw}(\mathbf{q}, p) \approx \frac{N_u}{2\hbar} w(\mathbf{q}, p) A^2(\mathbf{q}, p, t) \tag{5.16}$$

$$n_{old}(\mathbf{q}, p) \approx \frac{N_u}{4\hbar} w(\mathbf{q}, p)\left[A^2(\mathbf{q}, p, t) + A^2(-\mathbf{q}, p, t)\right] \tag{5.17}$$

$$n_{old}(\mathbf{q}, p) = \frac{n_{pw}(\mathbf{q}, p) + n_{pw}(-\mathbf{q}, p)}{2} \tag{5.18}$$

Thus the existing expression for phonon population is simply the arithmetic average of the left and right moving phonon population. Unlike in the present (*pw*) approach, there is no mechanism to extract the difference between the phonon populations within the existing (*old*) framework. And finally, the energy quantization can be written as:

$$E_{pw}(\mathbf{q}, p, t) = \left(n_{pw}(\mathbf{q}, p) + \frac{1}{2}\right)\hbar w(\mathbf{q}, p) \tag{5.19}$$

5.2.3 Heat current and conductivity

As discussed in Chapter 2, the heat current is related the phonon population as:

$$\mathbf{J}(\mathbf{q}, p, t) = \frac{1}{V} n_{\mathbf{q},p}(t) \hbar w(\mathbf{q}, p) \mathbf{v}_g(\mathbf{q}, p) \tag{5.20}$$

Substituting the expression for phonon population from Eqn. (5.16) into Eqn. (5.20) gives the modal heat current; it is expressed as:

$$\mathbf{J}(\mathbf{q}, p, t) = \frac{N_u}{2V} w^2(\mathbf{q}, p) A^2(\mathbf{q}, p, t) \mathbf{v}_g(\mathbf{q}, p) \tag{5.21}$$

Note that the *exact* expression for heat current from individual modes for a monoatomic linear chain that is presented in Chapter 3 has the form given in Eqn. (5.21). The total heat current of the system is given by:

$$\mathbf{J}(t) = \sum_{\mathbf{q}, p} \mathbf{J}(\mathbf{q}, p, t) = \sum_{\mathbf{q}, p} \frac{N_u}{2V} w^2(\mathbf{q}, p) A^2(\mathbf{q}, p, t) \mathbf{v}_g(\mathbf{q}, p) \tag{5.22}$$

Combining the terms from positive and negative wave vectors, the *total* heat current due to the *net* contributions from the positive and negative modes can be expressed as:

$$\mathbf{J}(t) = \sum_{\mathbf{q}^+, p} \frac{N_u}{2V} w^2(\mathbf{q}, p) \left[A^2(\mathbf{q}, p, t) - A^2(-\mathbf{q}, p, t) \right] \mathbf{v}_g(\mathbf{q}, p) \tag{5.23}$$

Note that the net heat current is expressed as the difference between contributions from the left and right moving phonon modes. In a previous work, Gill and Lewis [20] have defined an imaginary (non-oscillating) modal component of the heat current; it is given by:

$$\mathbf{J}_{GL}(\mathbf{q}, p, t) = \frac{i}{V} w(\mathbf{q}, p) \chi_v(\mathbf{q}, p, t) \chi_u^*(\mathbf{q}, p, t) \mathbf{v}_g(\mathbf{q}, p) \tag{5.24}$$

The *total* heat current from Gill and Lewis is then given by:

$$\mathbf{J}_{GL}(t) = \sum_{\mathbf{q},p} \mathbf{J}_{GL}(\mathbf{q},p,t) = \sum_{\mathbf{q},p} \frac{i}{V} w(\mathbf{q},p)\chi_v(\mathbf{q},p,t)\chi_u^*(\mathbf{q},p,t)\mathbf{v}_g(\mathbf{q},p) \tag{5.25}$$

Combining the positive and negative wave vectors, the *total* heat current due to the *net* contribution from the positive and negative modes can be expressed as:

$$\mathbf{J}_{GL}(t) = \sum_{\mathbf{q}^+,p} \frac{i}{V} w(\mathbf{q},p)\left[\chi_v(\mathbf{q},p,t)\chi_u(-\mathbf{q},p,t) - \chi_v(-\mathbf{q},p,t)\chi_u(\mathbf{q},p,t)\right]\mathbf{v}_g(\mathbf{q},p) \tag{5.26}$$

Substituting the expression for normal mode coordinate from Eqns. (5.3) and (5.4) into Eqn. (5.26) gives the following expression:

$$\mathbf{J}_{GL}(t) = \sum_{\mathbf{q}^+,p} \frac{N_u}{2V} w^2(\mathbf{q},p)\left[A^2(\mathbf{q},p,t) - A^2(-\mathbf{q},p,t)\right]\mathbf{v}_g(\mathbf{q},p) \tag{5.27}$$

Thus the modal heat current expression defined by Gill and Lewis is complex and does not a hold a real physical meaning, whereas, the modal heat current defined in the present work (Eqn. (5.21)) is real and physically consistent. Note that the sum of current due to the positive and negative modes from the current work and Gill and Lewis are mathematically equivalent.

Coming back to the total heat current given in Eqn. (5.23), this expression can be written in terms of modal energy as:

$$\mathbf{J}(t) = \sum_{\mathbf{q}^+, p} \left[E(\mathbf{q}, p, t) - E(-\mathbf{q}, p, t) \right] \mathbf{v}_g(\mathbf{q}, p) \tag{5.28}$$

Define the difference in energy between positive and negative modes as:

$$E_{Diff}(\mathbf{q}, p, t) = E(\mathbf{q}, p, t) - E(-\mathbf{q}, p, t) = \delta E(\mathbf{q}, p, t) - \delta E(-\mathbf{q}, p, t) \tag{5.29}$$

Thus the total heat current depends on the difference in the energy content between the positive and the negative mode:

$$\mathbf{J}(t) = \sum_{\mathbf{q}^+, p} E_{Diff}(\mathbf{q}, p, t) \mathbf{v}_g(\mathbf{q}, p) \tag{5.30}$$

The conductivity is related to the heat current correlation as [53, 54] :

$$\kappa_{\alpha\beta}^{GK} = \frac{V}{k_B T^2} \lim_{t \to \infty} \int_0^t \left\langle J_\alpha(0) J_\beta(t) \right\rangle dt \tag{5.31}$$

Substituting the expression for heat current from Eqn. (5.30) to Eqn. (5.31) results in:

$$\kappa_{\alpha\beta}^{GK} = \frac{1}{V k_B T^2} \sum_{\mathbf{q}^+, p} \sum_{\mathbf{q}'^+, p'} \left[v_{g,\alpha}(\mathbf{q}, p) v_{g,\alpha}(\mathbf{q}', p') \int_0^t \left\langle E_{Diff}(\mathbf{q}, p, 0) E_{Diff}(\mathbf{q}', p', t) \right\rangle dt \right] \tag{5.32}$$

Thus, the conductivity depends on the correlation of the difference in energy content between positive and negative modes. Substituting back the expression for $E_{Diff}(\mathbf{q}, p, t)$ in terms of excess energy $\delta E(\mathbf{q}, p, t)$:

$$\kappa_{\alpha\beta}^{GK} = \frac{1}{Vk_B T^2} \sum_{\mathbf{q}^+, p} \sum_{\mathbf{q}^{+'}, p'} \left[\begin{array}{l} v_{g,\alpha}(\mathbf{q}, p) v_{g,\alpha}(\mathbf{q}', p') \\ \int_0^t \left\langle \left[\delta E(\mathbf{q}, p, 0) - \delta E(-\mathbf{q}, p, 0) \right] \left[\delta E(\mathbf{q}, p, t) - \delta E(-\mathbf{q}, p, t) \right] \right\rangle dt \end{array} \right] \quad (5.33)$$

Simplifying:

$$\kappa_{\alpha\beta}^{GK} = \frac{2}{Vk_B T^2} \sum_{\mathbf{q}^+, p} \sum_{\mathbf{q}^{+'}, p'} \left[\begin{array}{l} v_{g,\alpha}(\mathbf{q}, p) v_{g,\alpha}(\mathbf{q}', p') \\ \int_0^t \left[\left\langle \delta E(\mathbf{q}, p, 0) \delta E(\mathbf{q}', p, t) \right\rangle - \left\langle \delta E(\mathbf{q}, p, 0) \delta E(-\mathbf{q}', p, t) \right\rangle \right] dt \end{array} \right] \quad (5.34)$$

Thus it can be shown that the total thermal conductivity is composed of two major contributions – self and cross:

$$\kappa_{\alpha\beta}^{GK} = \kappa_{\alpha\beta}^{GK,Self} + \kappa_{\alpha\beta}^{GK,Cross} \quad (5.35)$$

where:

$$\kappa_{\alpha\beta}^{GK,Self} = \frac{2}{Vk_B T^2} \sum_{\mathbf{q}^+, p} \left[\begin{array}{l} v_{g,\alpha}(\mathbf{q}, p) v_{g,\beta}(\mathbf{q}, p) \\ \int_0^t \left[\left\langle \delta E(\mathbf{q}, p, 0) \delta E(\mathbf{q}, p, t) \right\rangle - \left\langle \delta E(\mathbf{q}, p, 0) \delta E(-\mathbf{q}, p, t) \right\rangle \right] dt \end{array} \right] \quad (5.36)$$

$$\kappa_{\alpha\beta}^{GK,Cross} = \frac{2}{Vk_B T^2} \sum_{(\mathbf{q}^+,p)\neq(\mathbf{q}'^+,p')} \left[\begin{array}{l} v_{g,\alpha}(\mathbf{q},p) v_{g,\beta}(\mathbf{q}',p') \\ \int_0^t \left[\left\langle \delta E(\mathbf{q},p,0) \delta E(\mathbf{q}',p,t) \right\rangle - \left\langle \delta E(\mathbf{q},p,0) \delta E(-\mathbf{q}',p,t) \right\rangle \right] dt \end{array} \right] \tag{5.37}$$

If the cross correlations between modes is assumed to be zero, then the net conductivity can be approximated as:

$$\kappa_{\alpha\beta}^{GK} = \frac{1}{V} \sum_{\mathbf{q},p} \left[\begin{array}{l} \frac{\left\langle \delta E^2(\mathbf{q},p) \right\rangle}{k_B T^2} v_{g,\alpha}(\mathbf{q},p) v_{g,\beta}(\mathbf{q},p) \\ \int_0^t \left[\frac{\left\langle \delta E(\mathbf{q},p,0) \delta E(\mathbf{q},p,t) \right\rangle}{\left\langle \delta E^2(\mathbf{q},p) \right\rangle} \right] dt \end{array} \right] \tag{5.38}$$

The specific heat of a normal mode is related to the energy fluctuations as:

$$C_v(\mathbf{q},p) = \frac{\left\langle \delta E^2(\mathbf{q},p) \right\rangle}{k_B T^2} \tag{5.39}$$

Since it is customary to define the phonon mode lifetime as [56]:

$$\tau(\mathbf{q},p) = \int_0^t \left[\frac{\left\langle \delta E(\mathbf{q},p,0) \delta E(\mathbf{q},p,t) \right\rangle}{\left\langle \delta E^2(\mathbf{q},p) \right\rangle} \right] dt \tag{5.40}$$

The thermal conductivity can be expressed in the familiar form as:

$$\kappa_{\alpha\beta}^{GK} = \frac{1}{V}\sum_{\mathbf{q},p} C_v(\mathbf{q},p) v_{g,\alpha}(\mathbf{q},p) v_{g,\beta}(\mathbf{q},p) \tau(\mathbf{q},p) \tag{5.41}$$

The above expression is identical to the expression obtained from BTE with the single mode relaxation time (SMRT) approximation. However, this expression is only an approximation because it neglects the cross term from the conductivity given in Eqn. (5.37). Gill and Lewis [20, 57, 58] have demonstrated that the cross term can make a significant contribution to the thermal conductivity, in particular for low dimensional systems.

Interestingly, the self-term defined in Eqn. (5.41), neglects the correlation $\langle \delta E(\mathbf{q},p,0)\delta E(-\mathbf{q},p,t)\rangle$ from Eqn. (5.36),. Thus the self-term can be further split as a difference between the BTE term and a correction due to the correlation between the positive and negative modes at finite time. Thus the self-term can be rewritten as:

$$\kappa_{\alpha\beta}^{GK,Self} = \kappa_{\alpha\beta}^{GK,BTE} - \kappa_{\alpha\beta}^{GK,correction} \tag{5.42}$$

$$\kappa_{\alpha\beta}^{GK,BTE} = \frac{1}{V}\sum_{\mathbf{q},p} C_v(\mathbf{q},p) v_{g,\alpha}(\mathbf{q},p) v_{g,\beta}(\mathbf{q},p) \tau(\mathbf{q},p) \tag{5.43}$$

$$\kappa_{\alpha\beta}^{GK,correction} = \frac{2}{Vk_BT^2}\sum_{\mathbf{q}^+,p}\left[v_{g,\alpha}(\mathbf{q},p) v_{g,\beta}(\mathbf{q},p) \int_0^t \left[\langle \delta E(\mathbf{q},p,0)\delta E(-\mathbf{q},p,t)\rangle\right] dt \right] \tag{5.44}$$

Now the components of thermal conductivity can be written as:

$$\kappa_{\alpha\beta}^{GK} = \kappa_{\alpha\beta}^{GK,Self} + \kappa_{\alpha\beta}^{GK,Cross} = \kappa_{\alpha\beta}^{GK,BTE} - \kappa_{\alpha\beta}^{GK,correction} + \kappa_{\alpha\beta}^{GK,Cross} \tag{5.45}$$

5.3 Results

Atomistic simulations are performed on graphene using the same system configuration and equilibration procedure that was described in Section 4.5.3 before. The simulation consists of 60 unit cells along both unit vectors contributing to a total of 7200 atoms. The heat current for the thermal conductivity calculation using the GK analysis is described by Eqn. (5.46) – a detailed proof for the equation can be found in Appendix B.

$$\mathbf{J} = \sum_{i=1}^{N} \varepsilon_i \mathbf{v}_i + \sum_{i=1}^{N} \sum_{j=1;\, j\neq i}^{N} \left[\frac{\mathbf{r}_{ij}}{2} \left[\left(\mathbf{F}_{ij}^{ij} + \mathbf{F}_{ij}^{ji} \right) . \mathbf{v}_i \right] + \sum_{k=1;k\neq i,\, j}^{N} \left\{ \frac{\mathbf{r}_{ik}}{2} \left[\mathbf{F}_{ij}^{ik} . \mathbf{v}_i \right] + \frac{\mathbf{r}_{ij} + \mathbf{r}_{ik}}{2} \left[\mathbf{F}_{ij}^{jk} . \mathbf{v}_i \right] \right\} \right] \qquad (5.46)$$

5.3.1 Modal Energy distribution

Figure 5.1 shows the distribution of the energy associated with the individual LA phonon modes in graphene with wave vectors along the Γ-M branch; as evident the distribution shows an exponential behavior. The slope of the linear region of the individual curves is shown in *Figure 5.2*. Clearly, the slope for all phonon modes is close to -1.0; similar results are observed for all phonon branches for both Γ-M and Γ-K directions, and at both 30 K and 300 K. Thus the probability that a mode with wave vector **q** and branch *p* contains energy *E* is proportional to exponential of $-E/k_BT$, which is exactly equal to the classical prediction for the probability of finding a system in a state with energy *E* in the canonical ensemble (see Eqn. (5.47) below).

$$P_{\mathbf{q},p}(E) = \frac{\exp\left(-\frac{E}{k_B T}\right)}{\int_0^\infty \exp\left(-\frac{E}{k_B T}\right) dE} \tag{5.47}$$

The simulations thus demonstrate that equipartition of energy holds good for each phonon mode. The expectation value of the energy associated with a mode, as given by Eqn. (5.48), is simply $k_B T$.

$$\left\langle E(\mathbf{q}, p) \right\rangle = \int_0^\infty E \times P_{\mathbf{q},p}(E)\, dE = \frac{\int_0^\infty E \exp\left(-\frac{E}{k_B T}\right) dE}{\int_0^\infty \exp\left(-\frac{E}{k_B T}\right) dE} = k_B T \tag{5.48}$$

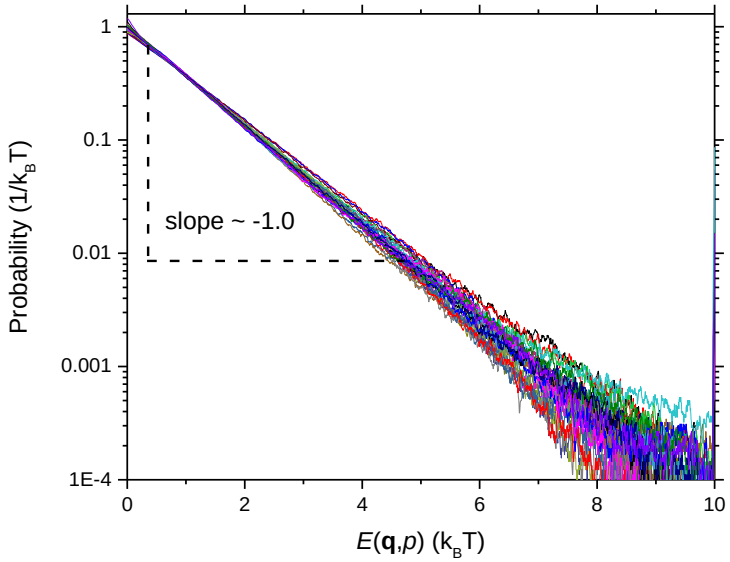

Figure 5.1: Probability distribution of the energy associated with the individual modes for the LA branch of graphene with wave vectors along the Γ-M direction at 300 K.

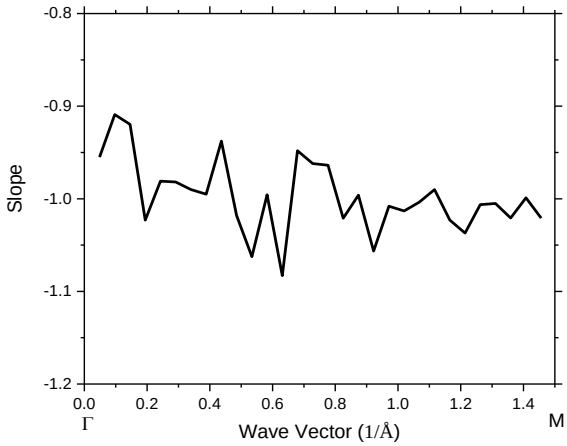

Figure 5.2: Slope of the linear region of the probability distribution shown in Figure 5.1 for different phonon modes.

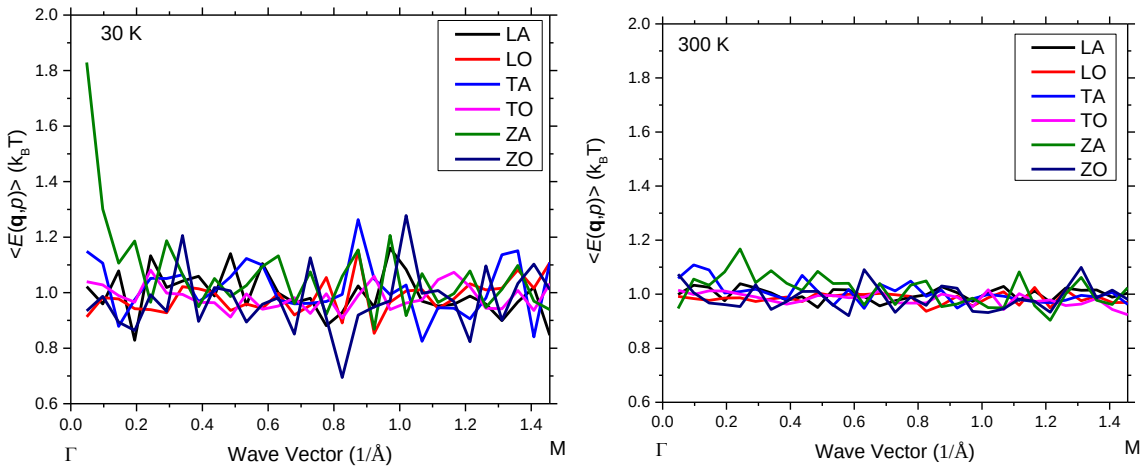

Figure 5.3: Average energy content of each mode for graphene in units of (k_BT) with wave vectors along the Γ-M direction at 30 K (left) and 300 K (right).

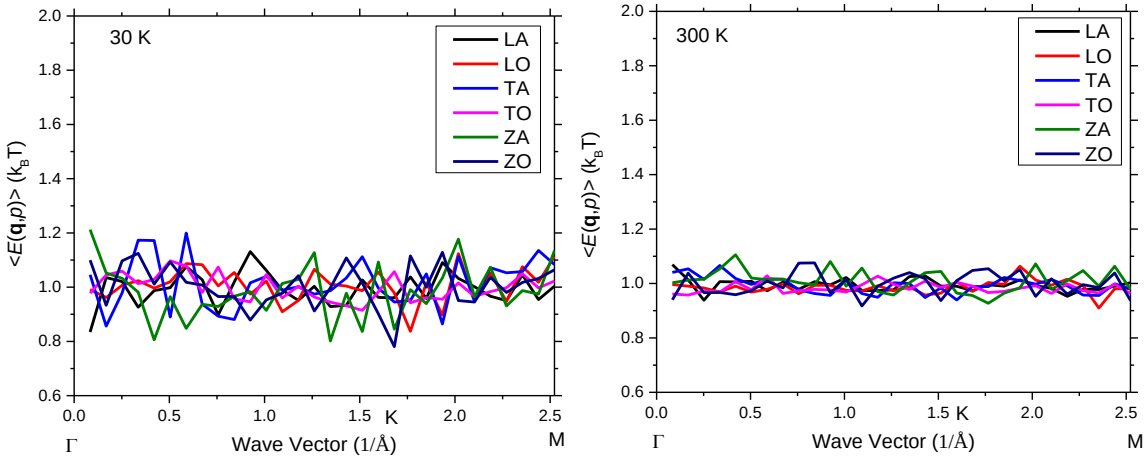

Figure 5.4: Average energy content of each mode for graphene in units of (k_BT) with wave vectors along the Γ-K direction at 30 K (left) and 300 K (right).

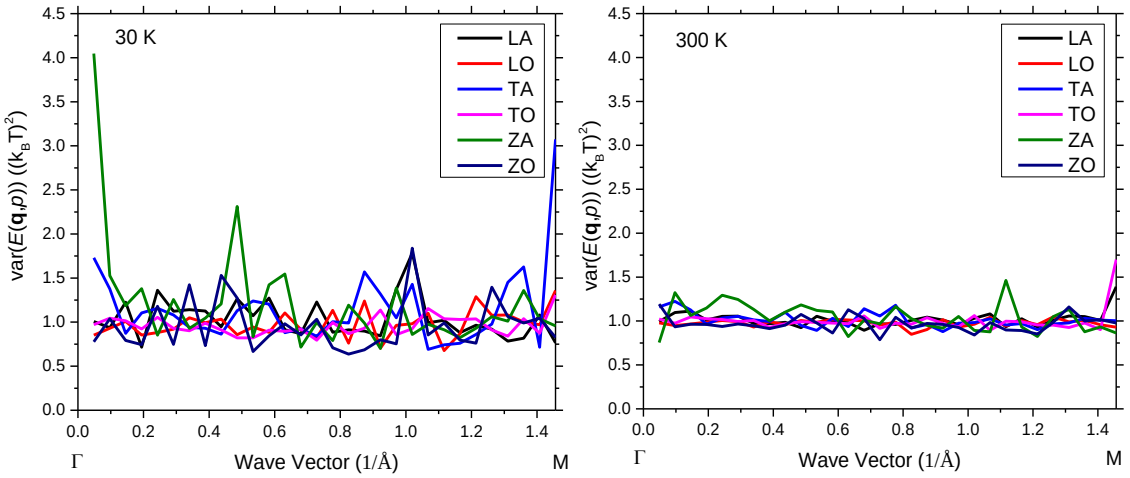

Figure 5.5: Variance of the energy of each mode for graphene in units of $(k_BT)^2$ with wave vectors along the Γ-M direction at 30 K (left) and 300 K (right).

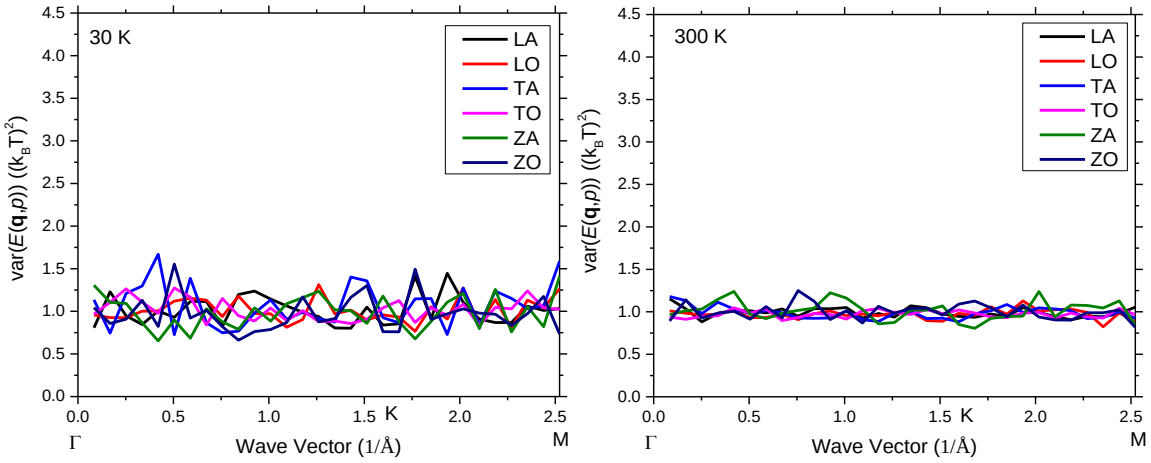

Figure 5.6: Variance of the energy of each mode for graphene in units of $(k_BT)^2$ with wave vectors along the Γ-*K* direction at 30 K (left) and 300 K (right).

Figure 5.3 shows the average energy content in the units of k_BT for all modes with wave vectors along the Γ-M direction for graphene at 30 K (left panel) and 300 K (right panel); *Figure 5.4* show the same curve for wave vectors along the Γ-K direction. Except the long wavelength ZA modes along the Γ-M direction at 30 K, all other modes show excellent agreement with the expected theoretical value of k_BT as given in Eqn. (5.48). The curves are smoother at 300 K relative to 30 K because at higher temperatures, there is greater interaction between the phonon modes. A lower deviation from the expected value, therefore, is observed at higher temperatures.

The variance of the energy content of a mode is of greater significance than the expectation value of the energy, since the specific heat of the mode is proportional to it. The variance in the energy associated with each phonon mode is given by:

$$\left\langle \left(\delta E\left(\mathbf{q}, p\right)\right)^2 \right\rangle = \int_0^\infty \left(E - k_B T\right)^2 \times P_{\mathbf{q},p}\left(E\right) dE = \frac{\int_0^\infty \left(E - k_B T\right)^2 \exp\left(-\frac{E}{k_B T}\right) dE}{\int_0^\infty \exp\left(-\frac{E}{k_B T}\right) dE} = \left(k_B T\right)^2 \qquad (5.49)$$

The theoretical expectation value for the variance of energy is $(k_B T)^2$ as given by Eqn. (5.49). *Figure 5.5* shows the variance of the modal energy content in the units of $(k_B T)^2$ for all modes with wave vectors along the Γ-M direction with graphene at 30 *K* (left panel) and 300 K (right panel); *Figure 5.6* shows the same curve for wave vectors along the Γ-K direction. As before, except for the long wavelength ZA modes along the Γ-M direction at 30 K, all other modes show a good agreement with the theoretical prediction. Further, the theoretical prediction implies that the specific heat for each mode is constant at all temperatures, which is true in the classical limit (see Eqn. (5.50)).

$$C_v\left(\mathbf{q}, p\right) = \frac{\left\langle \left(\delta E\left(\mathbf{q}, p\right)\right)^2 \right\rangle}{k_B T^2} = k_B \qquad (5.50)$$

Thus, the atomistic simulations confirm that the specific heat is largely independent of the phonon modes (see *Figure 5.5* and *Figure 5.6*). A key consequence of this result is that the thermal conductivity as predicted by Eqn. (5.41) is solely dependent on the group velocity and the lifetime of the modes; mode-dependent specific heat does not appear in the classical limit.

Another interesting observation is that there is a self-term correction for the modal thermal conductivity, which is given by:

$$\kappa_{\alpha\beta}^{GK,Self} = \frac{2}{Vk_BT^2}\sum_{\mathbf{q}^+,p}\left[\begin{array}{l} v_{g,\alpha}(\mathbf{q},p)v_{g,\beta}(\mathbf{q},p) \\ \int_0^t \left[\left\langle \delta E(\mathbf{q},p,0)\delta E(\mathbf{q},p,t)\right\rangle - \left\langle \delta E(\mathbf{q},p,0)\delta E(-\mathbf{q},p,t)\right\rangle\right]dt \end{array}\right] \tag{5.51}$$

Thus the self-term of the conductivity does not directly depends on the correlation of the energy content of the mode, but on the difference of the energy content between the positive and the negative modes. Note that the initial correlation is given by:

$$\left\langle \left(\delta E(\mathbf{q},p,0)\right)^2\right\rangle - \left\langle \delta E(\mathbf{q},p,0)\delta E(-\mathbf{q},p,0)\right\rangle = \frac{1}{2}\mathrm{var}\left(E_{Diff}(\mathbf{q},p,0)\right) \tag{5.52}$$

Figure 5.7 shows the variance of the energy difference between the positive and the negative mode in the units of $(k_BT)^2$ for all modes with wave vectors along the Γ-M direction for graphene at 30 K (left panel) and 300 K (right panel); *Figure 5.8* shows the same for the Γ-K direction. An expectation value of nearly $2(k_BT)^2$ is observed for all modes except for the long wavelength ZA modes along the Γ-M direction at 30 K. Due to their weak interactions with other modes, it is not surprising that the low-temperature ZA modes are not fully thermalized.

As seen from Eqn. (5.52), a value of $2(k_BT)^2$ for $\mathrm{var}\left(E_{Diff}(\mathbf{q},p)\right)$ suggests that the initial correlation between the excess energy content of the positive and negative modes, *i.e.*, $\left\langle \delta E(\mathbf{q},p,0)\delta E(-\mathbf{q},p,t)\right\rangle$ will go to zero. This is quite intuitive since the excess energy associated with the positive mode has no physical reason to stay correlated to that of the negative mode.

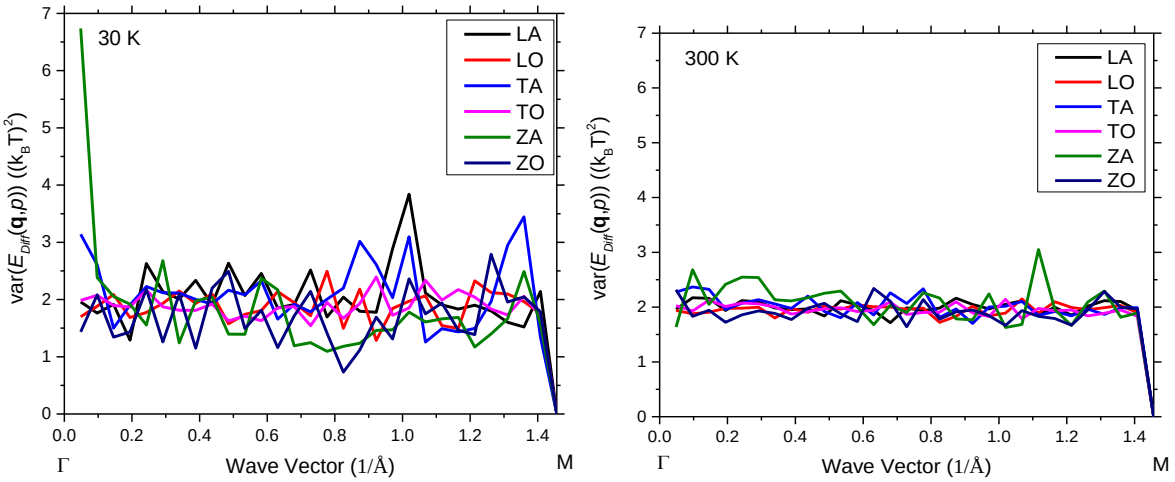

Figure 5.7: Variance of the energy difference between positive and negative modes for graphene in units of $(k_BT)^2$ with wave vectors along the Γ-M direction at 30 K (left) and 300 K (right).

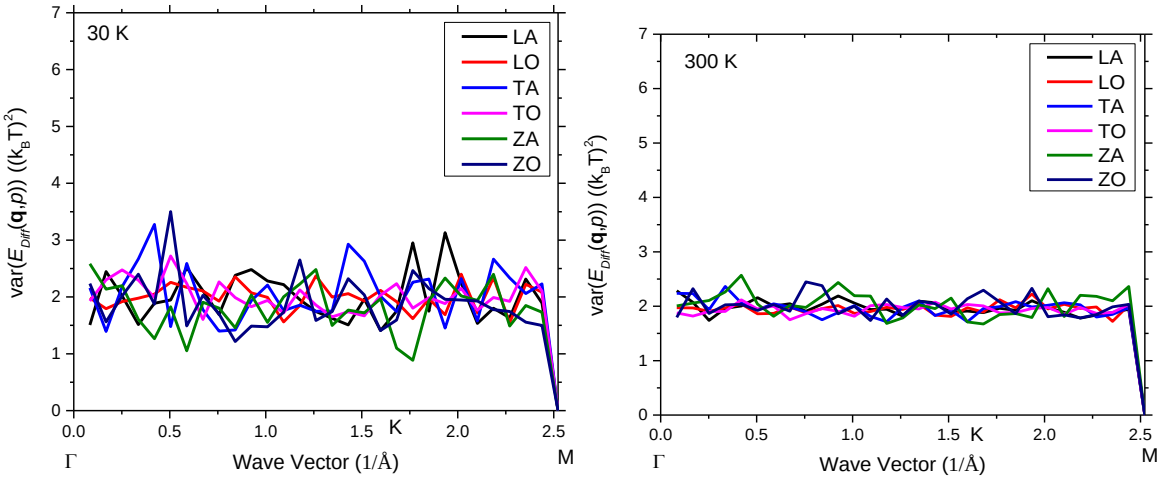

Figure 5.8: Variance of the energy difference between positive and negative modes for graphene in units of $(k_BT)^2$ with wave vectors along the Γ-K direction at 30 K (left) and 300 K (right).

However, as time proceeds, the excess energy along the positive mode will eventually flow along the negative mode, *i.e.*, the positive and negative modes will communicate at finite times.

Even though the initial correlation is zero, the correlation at finite time, therefore, is expected to be non-zero – a prediction that is also confirmed by the simulations. *Figure 5.9* shows the evolution of each term from Eqn. (5.53) normalized to $(k_BT)^2$ for one of the ZA modes along the Γ-M direction for graphene at 300 K. The correlation $<\delta E(\mathbf{q},p,0)\delta E(-\mathbf{q},p,t)>$ (blue curve) starts at zero, but slowly builds up with time before decaying off. As mentioned before, the excess energy in the positive mode will eventually flow into the negative mode. Thus if only the first term in the RHS of Eqn. (5.53) (red curve) is used for estimating the mode lifetime as in Eqn. (5.40), an overestimation is likely.

$$\frac{\left\langle E_{Diff}\left(\mathbf{q},p,0\right)E_{Diff}\left(\mathbf{q},p,t\right)\right\rangle}{2}=\left\langle \delta E\left(\mathbf{q},p,0\right)\delta E\left(\mathbf{q},p,t\right)\right\rangle-\left\langle \delta E\left(\mathbf{q},p,0\right)\delta E\left(-\mathbf{q},p,t\right)\right\rangle \qquad (5.53)$$

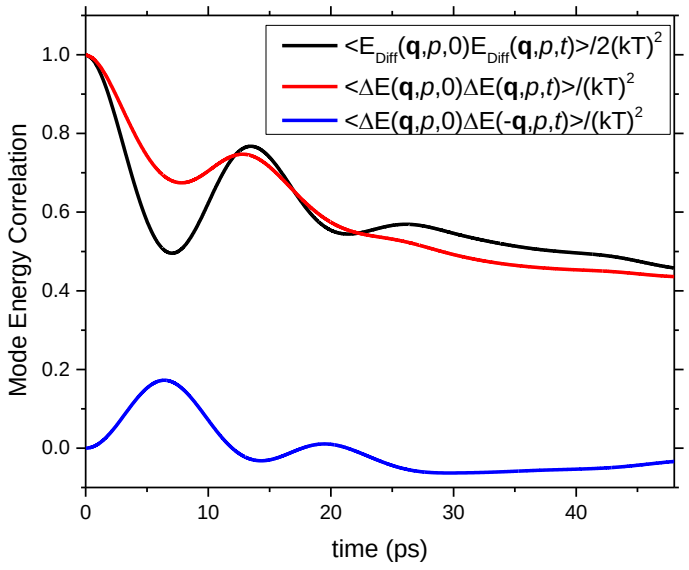

Figure 5.9: Evolution of the excess energy correlations for one of the ZA modes along the Γ-M direction for graphene at 300 K.

As discussed earlier, the self-term of the conductivity can be estimated by computing the mode lifetime. The existing approach to estimating the lifetime is given by [56]:

$$\tau_{Old}(\mathbf{q}, p) = \int_0^t \left[\frac{\left\langle \delta E_{old}(\mathbf{q}, p, 0) \delta E_{old}(\mathbf{q}, p, t) \right\rangle}{\left\langle \delta E_{old}{}^2(\mathbf{q}, p, 0) \right\rangle} \right] dt \tag{5.54}$$

However, the existing expression for mode energy, as shown below, contains contributions from both positive and negative modes as previously demonstrated:

$$E_{Old}(\mathbf{q}, p, t) = \frac{1}{2}\left[E_{pw}(\mathbf{q}, p, t) + E_{pw}(-\mathbf{q}, p, t) \right] \tag{5.55}$$

Substituting Eqn. (5.55) back into Eqn. (5.54) gives the lifetime as:

$$\tau_{Old}(\mathbf{q}, p) = \int_0^t \left[\frac{\left\langle \delta E_{pw}(\mathbf{q}, p, 0) \delta E_{pw}(\mathbf{q}, p, t) \right\rangle + \left\langle \delta E_{pw}(\mathbf{q}, p, 0) \delta E_{pw}(-\mathbf{q}, p, t) \right\rangle}{\left\langle \left(\delta E_{pw}(\mathbf{q}, p, 0) \right)^2 \right\rangle} \right] dt \tag{5.56}$$

However, the correct expression for the mode lifetime is given by:

$$\tau(\mathbf{q}, p) = \int_0^t \left[\frac{\left\langle \delta E_{pw}(\mathbf{q}, p, 0) \delta E_{pw}(\mathbf{q}, p, t) \right\rangle - \left\langle \delta E_{pw}(\mathbf{q}, p, 0) \delta E_{pw}(-\mathbf{q}, p, t) \right\rangle}{\left\langle \left(\delta E_{pw}(\mathbf{q}, p, 0) \right)^2 \right\rangle} \right] dt \tag{5.57}$$

Thus, the existing approach (denoted by the subscript *old*) will overestimate the mode lifetime by twice the area of the blue curve shown in *Figure 5.9*.

5.3.2 Modal phonon lifetimes for graphene

In this section, the modal lifetimes for graphene, simulated using the optimized Tersoff interatomic potential [97], is presented (see details in Section 4.5.3). The basal plane conductivity at 300 K is evaluated to be approximately 2500 W/mK using the GK formalism [53, 54] with the heat current autocorrelation (HACF) converging in ~200 ps. The simulated thermal conductivity typically depends on the interatomic potential, the size of the simulation cell, and the choice of the heat current expression; reported values fall in the range of 300 – 20000 Wm/K [20, 107-113]. Experimental studies also span a broad range from 600 – 5300 W/mK [22, 23, 114-116].

In the current work, the correlation $\left\langle E_{Diff}\left(\mathbf{q}, p, 0\right) E_{Diff}\left(-\mathbf{q}, p, t\right)\right\rangle$ has been computed only up to ~50 ps due to the somewhat high computational cost. The phonon lifetimes at 300 K reported in previous investigations [24, 102, 107] exceed 50 ps for the low-frequency modes, especially for the flexural phonons. Further, the HACF takes ~200 ps to converge for the present configuration. Thus the truncation of the above correlation at 50 ps is expected to underestimate the phonon lifetimes. The focus of the simulations, however, is not to compute the exact phonon lifetimes, but to demonstrate the existence of finite lifetime correction terms discussed in the previous section.

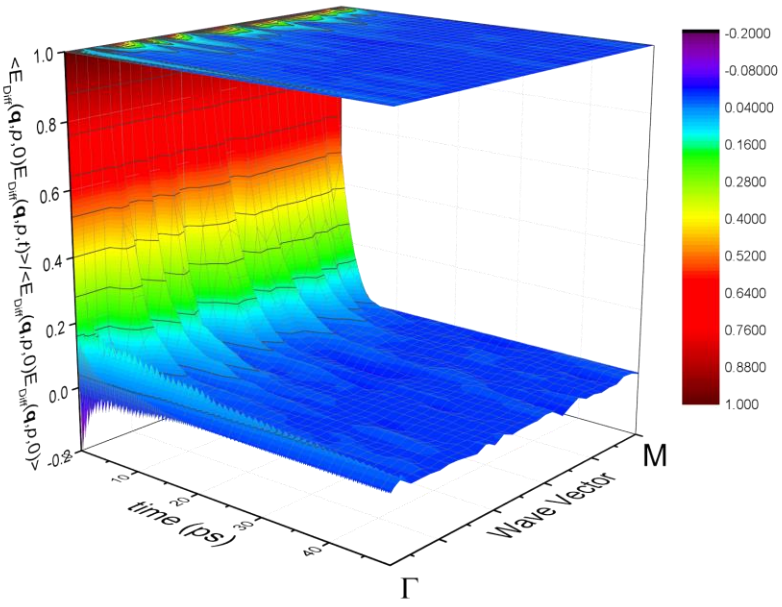

Figure 5.10: Evolution of the correlation for the difference in the energy content between the positive and negative modes for the LA branch with wave vectors along the Γ-M direction for graphene at 300 K.

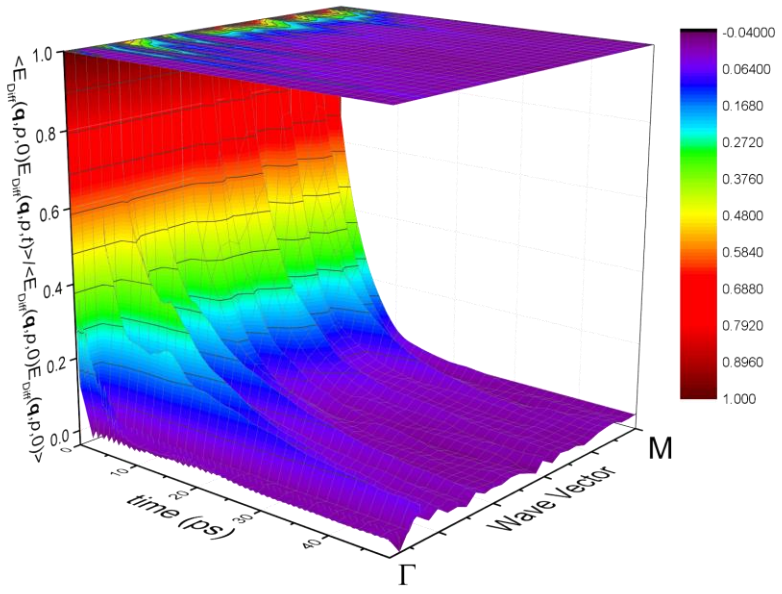

Figure 5.11: Evolution of the correlation for the difference in the energy content between the positive and negative modes for the TA branch with wave vectors along the Γ-M direction for graphene at 300 K.

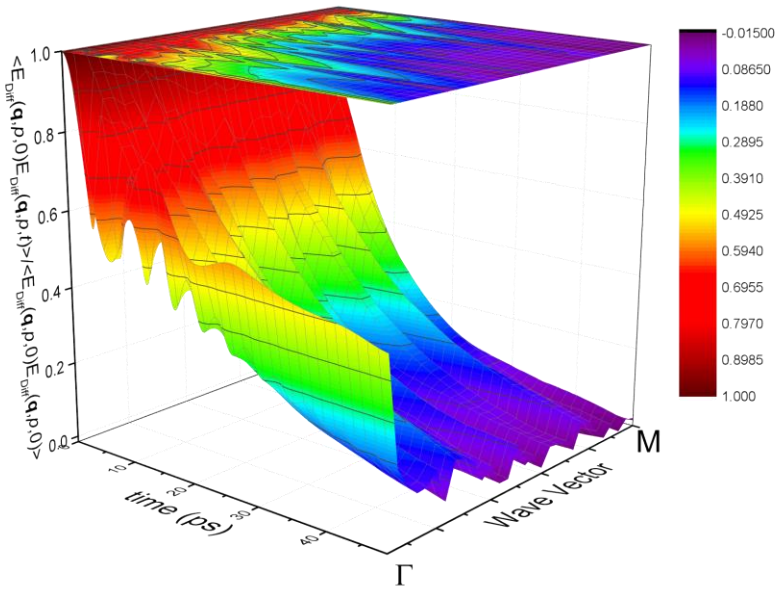

Figure 5.12: Evolution of the correlation for the difference in the energy content between the positive and negative modes for the ZA branch with wave vectors along the Γ-M direction for graphene at 300 K.

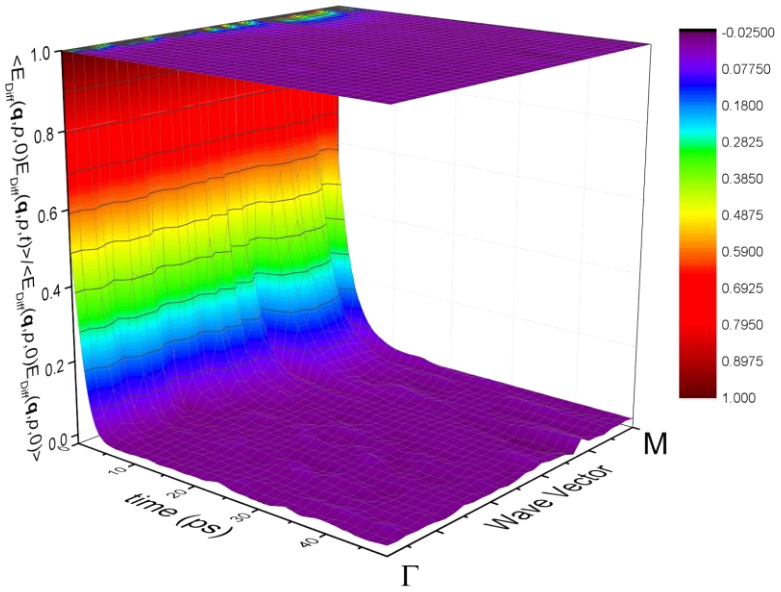

Figure 5.13: Evolution of the correlation for the difference in the energy content between the positive and negative modes for the LO branch with wave vectors along the Γ-M direction for graphene at 300 K.

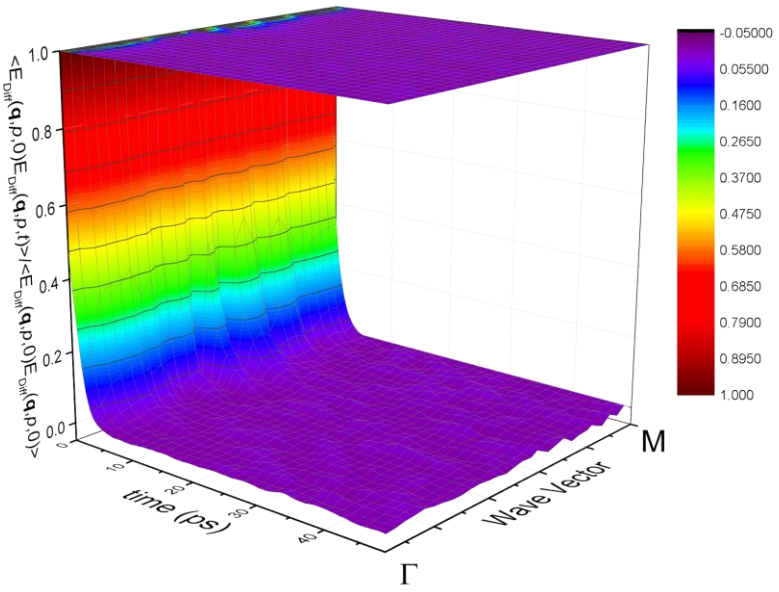

Figure 5.14: Evolution of the correlation for the difference in the energy content between the positive and negative modes for the TO branch with wave vectors along the Γ-M direction for graphene at 300 K.

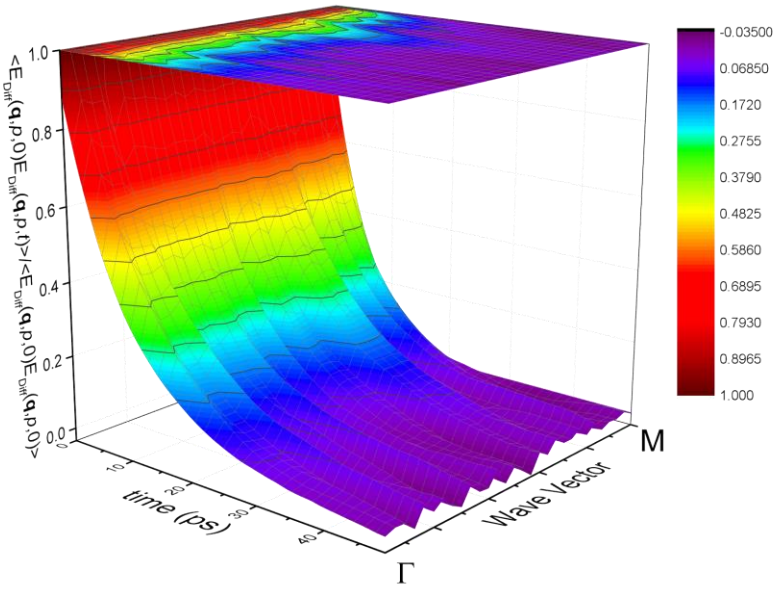

Figure 5.15: Evolution of the correlation for the difference in the energy content between the positive and negative modes for the ZO branch with wave vectors along the Γ-M direction for graphene at 300 K.

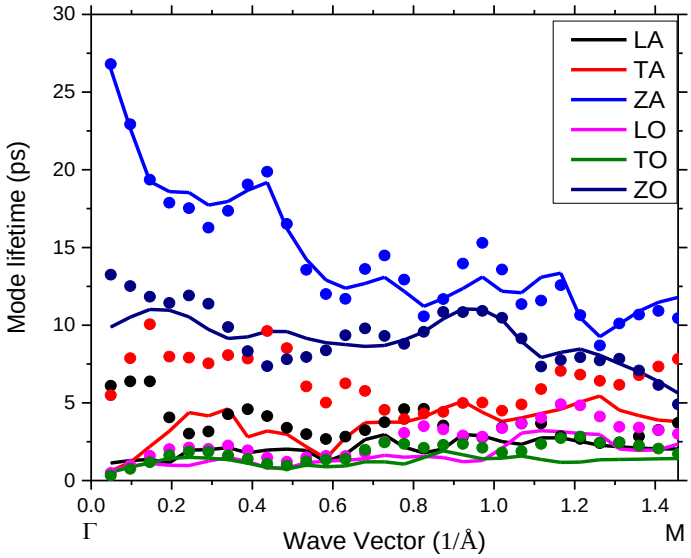

Figure 5.16: Phonon lifetimes estimated from the decay of the energy difference correlation for modes with wave vector along the Γ-M direction at 300 K. The solid lines have been computed using the current approach while the dots have been computed using the existing approach. The difference between the magnitudes between the current and existing approaches is appreciable (except for the flexural phonons, for which the correlations have not converged).

Figure 5.10 to *Figure 5.15* show the evolution of the correlation for the difference of energy between the positive and the negative branches for the LA, TA, ZA, LO, TO and ZO branches, respectively, with the wave vectors aligned along the Γ-M direction. All the longitudinal and transverse modes seem to have decayed within 50 ps while both ZA and ZO branches show a slower decay, especially for the long wavelength ZA modes. Thus for the flexural modes, the correlation needs to be evaluated for a longer time range to capture the complete decay process. For this reason, the present calculations will underestimate the lifetimes of the flexural phonons.

The phonon lifetimes computed for the aforementioned curves using Eqn. (5.57) with the limit of the integral set to ~50 ps are shown in *Figure 5.16*. The lifetimes calculated using the existing approach, given by Eqn. (5.56), have been overlaid in the figure as circles with the corresponding color. Clearly, the existing approach overestimates the lifetimes of the LA and TA modes as predicted in the previous section. The ZA modes are also likely to be overestimated if the integral is computed for a longer time. Note that higher lifetimes for the flexural mode have been reported in past work [24, 102, 107, 117].

5.4 Conclusion

Using the expression for phonon space projection in terms of the real cosine general solution, the individual mode amplitudes of the waves moving along the +**q** and -**q** directions are extracted. The mode amplitudes are then used to construct the individual mode energies; it is demonstrated that the existing approach (prior to this work) for calculating the mode energies actually computes the arithmetic mean of the energies of the waves traversing along the +**q** and -**q** directions. Thus the existing approach is unable to resolve the *difference* in the energies of the left and right moving waves that is critical for computing the net heat current and conductivity.

Using the current approach, a physically consistent expression for the modal heat current is derived. It is then employed to resolve the total thermal conductivity into self and a cross contributions –a result, which is previously known. The self-contribution is further partitioned into a BTE term (previously known) and a correction term (predicted from this work).

Atomistic simulations on graphene demonstrate that the correction term is significant for the LA and TA phonon branches; thus the existing approach overestimates the phonon lifetimes for these branches due to correlation between +**q** and –**q** modes. As observed in past investigations [20, 40, 56-58, 72] the cross-correlations between the phonon modes are significant for low dimensional systems. Interestingly, collective phonon excitations emerge from such cross-correlations. In the next chapter of this dissertation, the local heat current and energy fluctuations are probed through the normal modes of vibrations for these variables, which are then used to evaluate collective phonon excitations.

Chapter 6: BEYOND PHONON DESCRIPTORS

6.1 Introduction

Gill and Lewis [20, 57, 58] previously have shown that the cross-correlations, or equivalently, the collective phonon excitations are important, particularly for low dimensional systems; other investigators [40, 56, 72] have also arrived at a similar conclusion. The analysis in Chapter 5 has probed the origin of self and non-zero cross-correlations from well-posed statistical mechanical first principles. Further, the Fourier's law of thermal conduction itself breaks down in low dimensional systems [31, 33, 35, 63], which makes the GK formalism inapplicable. Thus, several low-dimensional systems have reported anomalous behavior in thermal transport [31, 33, 56, 65]. For low dimensional systems, it is more appropriate to examine the local energy and heat current fluctuations in appropriate normal coordinates. These correlations (energy/current modes) can also be connected to the phonon normal modes, which allows the exciting possibility of analyzing energy/heat modes in the framework of the more familiar phonon (displacement) normal modes.

In this chapter, the behavior of local energy and heat current fluctuations is analyzed by extracting the normal modes of oscillation of these variables. First, these energy/current modes are derived exactly for a harmonic 1-D chain; the theoretical prediction is then verified using atomistic simulations. The theoretical analysis reveals a rather intriguing outcome on the possible combinations of energy/heat normal modes. Even with harmonic interactions, energy

and heat modes combine if and only if they satisfy the three-phonon scattering law. It is known that three-phonon processes are required for thermal dissipation, and the appearance of the three-phonon scattering condition from the theoretical derivation indicates the plausibility of predicting the phonon interaction types directly from the phase space variables. The three-phonon scattering event has the lowest order of interaction, and the condition arises naturally in the buildup of energy/heat waves. If anharmonicity and higher dimensionality are included, higher order processes will evolve naturally in the classical framework without the need to specify or postulate the nature of phonon interactions in thermal transport.

A recent investigation [51] has proposed collective excitation of multiple phonon modes, denominated as *relaxons*, to be the actual heat carriers. The nature of the energy and heat current normal modes analyzed in the current work has certain similarities, but are restricted to multiple pair interactions within the harmonic approximation. First, an exact derivation of the energy and heat modes is presented for a 1-D harmonic chain.

6.2 Theoretical formulation

Consider a monoatomic linear chain of N atoms interacting through a harmonic potential as described in Chapter 2. Similar to the velocities and displacements, the total energy and heat current of the system are defined as:

$$\mathbf{J}(t)=\begin{pmatrix} J(1,t) \\ J(2,t) \\ . \\ . \\ J(N,t) \end{pmatrix}, \mathbf{E}(t)=\begin{pmatrix} E(1,t) \\ E(2,t) \\ . \\ . \\ E(N,t) \end{pmatrix} \tag{6.1}$$

where $J(l,t)$ and $E(l,t)$ denote the heat current and total energy of the l^{th} atom, respectively. These are defined by:

$$E(l,t)=\frac{1}{2}mv^2(l,t)+\frac{1}{2}\sum_{k\neq l}U_{lk}(t) \tag{6.2}$$

$$J(l,t)=E(l,t)v(l,t)+\frac{1}{2}\sum_{k\neq l}\left(F_{lk}(t)v(l,t)\right)r_{lk}(t) \tag{6.3}$$

The force acting on atom l from an atom k is given by:

$$F_{lk}(t)=-\frac{\partial U_{lk}(t)}{\partial r_{lk}(t)} \tag{6.4}$$

The displacement and velocity for the phonons, from the general solution, are given by:

$$u(l,t)=\sum_q \frac{1}{\sqrt{m}}A(q)\cos\left(q.r_l-w(q)t+\phi(q)\right) \tag{6.5}$$

$$v(l,t)=\sum_q \frac{1}{\sqrt{m}}w(q)A(q)\sin\left(q.r_l-w(q)t+\phi(q)\right) \tag{6.6}$$

$$q = r\frac{2\pi}{Na}; r = 0, \pm 1, \pm 2..... \tag{6.7}$$

Substituting the general solution into the energy expression (for a harmonic interaction) gives (see Appendix A for details):

$$E(l,t) = \sum_{q_1,q_2} E^{q_1,q_2}(l,t) \tag{6.8}$$

$$E^{q_1,q_2}(l,t) = \left[\begin{array}{l} \frac{1}{4} w(q_1) w(q_2) A(q_1) A(q_2) \\ \left(\cos\left((q_1 - q_2)la - \left(w(q_1) - w(q_2)\right)t + \left(\varphi(q_1) - \varphi(q_2)\right)\right)\right) \\ \times\left(1 + \frac{q_1}{|q_1|}\frac{q_2}{|q_2|}\cos\left((q_1 - q_2)\frac{a}{2}\right)\right) - \\ \cos\left((q_1 + q_2)la - \left(w(q_1) + w(q_2)\right)t + \left(\varphi(q_1) + \varphi(q_2)\right)\right) \\ \times\left(1 + \frac{q_1}{|q_1|}\frac{q_2}{|q_2|}\cos\left((q_1 + q_2)\frac{a}{2}\right)\right) \end{array}\right] \tag{6.9}$$

As discussed before, for a non-diffusive system, only the virial part *i.e.*, the second term from Eqn. (6.3), makes a significant contribution to the energy transport. The virial part of heat current can be approximated as (see Appendix A for details):

$$J_{vir}(l,t) = \sum_{q_1,q_2} J_{vir}^{q_1,q_2}(l,t) \tag{6.10}$$

$$J_{vir}^{q_1,q_2}(l,t) = \left[\begin{array}{l} \frac{1}{2V} A(q_1) A(q_2) w(q_1) w(q_2) v_g(q_2) \\ \left[\cos\left((q_1 - q_2)la - \left(w(q_1) - w(q_2)\right)t + \varphi(q_1) - \varphi(q_2)\right)\right. \\ \left.-\cos\left((q_1 + q_2)la - \left(w(q_1) + w(q_2)\right)t + \varphi(q_1) + \varphi(q_2)\right)\right] \end{array}\right] \tag{6.11}$$

Thus, both energy and heat current are expected to form traveling waves at finite wave vectors. Further, these waves are formed due to the *interference* between normal mode pairs. In order to extract the wave amplitudes, the normal mode coordinates for energy and heat current with a wave vector q are defined similarly to those for phonons. These are given by:

$$\chi_E(q,t) = \left(\mathbf{B}_q\right)^T .\mathbf{E}(t) = \sqrt{\frac{1}{N}} \begin{pmatrix} \exp\left(i\left(q.r_1\right)\right) \\ \exp\left(i\left(q.r_2\right)\right) \\ . \\ . \\ \exp\left(i\left(q.r_N\right)\right) \end{pmatrix}^T \begin{pmatrix} E(1,t) \\ E(2,t) \\ . \\ . \\ E(N,t) \end{pmatrix} \tag{6.12}$$

$$\chi_J(q,t) = \left(\mathbf{B}_q\right)^T .\mathbf{J}(t) = \sqrt{\frac{1}{N}} \begin{pmatrix} \exp\left(i\left(q.r_1\right)\right) \\ \exp\left(i\left(q.r_2\right)\right) \\ . \\ . \\ \exp\left(i\left(q.r_N\right)\right) \end{pmatrix}^T \begin{pmatrix} J(1,t) \\ J(2,t) \\ . \\ . \\ J(N,t) \end{pmatrix} \tag{6.13}$$

where vector $\mathbf{B}_q$ is defined as:

$$\mathbf{B}_q = \frac{1}{\sqrt{N}} \begin{pmatrix} \exp\left(i\left(q.r_1\right)\right) \\ \exp\left(i\left(q.r_2\right)\right) \\ . \\ . \\ \exp\left(i\left(q.r_N\right)\right) \end{pmatrix} \tag{6.14}$$

The time correlation for energy and heat current normal modes is defined as:

$$E_{corr}^{NM}(q,t)=\left\langle \chi_E(q,0)\chi_E(-q,t)\right\rangle \tag{6.15}$$

$$J_{corr}^{NM}(q,t)=\left\langle \chi_J(q,0)\chi_J(-q,t)\right\rangle \tag{6.16}$$

The relationship of the above normal modes to energy/heat space-time correlations will be described in the next section.

6.3 Energy and heat current space-time correlations and normal modes

Define energy and heat current at a point in space as:

$$E(r,t)=\sum_{l=1}^{N}E(l,t)\delta(r-r_l) \tag{6.17}$$

$$J(r,t)=\sum_{l=1}^{N}J(l,t)\delta(r-r_l) \tag{6.18}$$

The fluctuations of energy and heat current in space/time can be formally quantified using the space-time correlation functions given by:

$$G_E(r,t)=\left\langle E(0,0)E(r,t)\right\rangle \tag{6.19}$$

$$G_J(r,t)=\left\langle J(0,0)J(r,t)\right\rangle \tag{6.20}$$

These correaltion functions represent the probability of heat and energy fluctuations traveling to a point *r* in time *t*. In the reciprocal space, the above correlations are defined as:

$$G_E(q,t) = \int \langle E(0,0)E(r,t)\rangle \exp(-iq.r)\,dr \tag{6.21}$$

$$G_J(q,t) = \int \langle J(0,0)J(r,t)\rangle \exp(-iq.r)\,dr \tag{6.22}$$

Substituting Eqn. (6.17) into Eqn. (6.19), it can be shown that:

$$G_E(r,t) = \frac{1}{N}\left\langle \sum_{j_1=1}^{N}\sum_{j_2=1}^{N} E(j_2,0)E(j_2,t)\delta\left(r + r_{j_1} - r_{j_2}\right)\right\rangle \tag{6.23}$$

Now substituting Eqn. (6.23) into Eqn. (6.21):

$$G_E(q,t) = \int \frac{1}{N}\left\langle \sum_{j_1=1}^{N}\sum_{j_2=1}^{N} E(0,0)E(j_2,t)\delta\left(r + r_{j_1} - r_{j_2}\right)\right\rangle \exp(-iq.r)\,dr \tag{6.24}$$

Evaluating the integral for the delta function:

$$G_E(q,t) = \sum_{j_1=1}^{N}\sum_{j_2=1}^{N} \langle E(j_1,0)E(j_2,t)\rangle \exp\left(-iq.\left(r_{j_2} - r_{j_1}\right)\right) \tag{6.25}$$

Combining the terms:

$$G_E(q,t) = \left\langle \sum_{j_1=1}^{N} E(j_1,0) \exp\left(iq.r_{j_1}\right) \sum_{j_2=1}^{N} E(j_2,t) \exp\left(-iq.r_{j_2}\right) \right\rangle \tag{6.26}$$

which gives:

$$G_E(q,t) = \left\langle \chi_E(q,0)\, \chi_E(-q,t) \right\rangle = E_{corr}^{NM}(q,t) \tag{6.27}$$

where NM indicates *normal modes*. Similarly, it can be shown that:

$$G_J(q,t) = \left\langle \chi_J(q,0)\, \chi_J(-q,t) \right\rangle = J_{corr}^{NM}(q,t) \tag{6.28}$$

Thus the correlation of the normal modes of energy/heat current is directly related to the space-time correlations of energy/heat current fluctuations.

6.4 Normal mode projections

The amplitudes of the energy and heat current waves can be extracted by projecting the spatial variation onto the normal mode space. This section elaborates how the normal mode projections are related to the pair contributions from individual phonon modes.

6.4.1 Energy normal modes

Substituting the expression for energy from Eqn. (6.8) into Eqn. (6.12), the normal mode projection can be expressed as:

$$\chi_E(q,t)=\sum_{q_1}\sum_{q_2}\sum_{j}\left(\begin{array}{l}\frac{1}{4\sqrt{N}}w(q_1)w(q_2)A(q_1)A(q_2)\left(\cos(qja)+i\sin(qja)\right)\times \\ \left(\begin{array}{l}\cos\left((q_1-q_2)\,ja-\left(w(q_1)-w(q_2)\right)t+\left(\varphi(q_1)-\varphi(q_2)\right)\right) \\ \times\left(1+\frac{q_1}{|q_1|}\frac{q_2}{|q_2|}\cos\left((q_1-q_2)\frac{a}{2}\right)\right)- \\ \cos\left((q_1+q_2)\,ja-\left(w(q_1)+w(q_2)\right)t+\left(\varphi(q_1)+\varphi(q_2)\right)\right) \\ \times\left(1+\frac{q_1}{|q_1|}\frac{q_2}{|q_2|}\cos\left((q_1+q_2)\frac{a}{2}\right)\right)\end{array}\right)\end{array}\right) \tag{6.29}$$

Expanding the cosine to separate the angles:

$$\chi_E(q,t)=\sum_{q_1}\sum_{q_2}\sum_{j}\left(\begin{array}{l}\frac{1}{4\sqrt{N}}w(q_1)w(q_2)A(q_1)A(q_2)\left(\cos(qja)+i\sin(qja)\right)\times \\ \left(\begin{array}{l}\left(\begin{array}{l}\cos\left((q_1-q_2)\,ja\right)\cos\left(\left(w(q_1)-w(q_2)\right)t-\varphi(q_1)+\varphi(q_2)\right)+ \\ \sin\left((q_1-q_2)\,ja\right)\sin\left(\left(w(q_1)-w(q_2)\right)t-\varphi(q_1)+\varphi(q_2)\right)\end{array}\right) \\ \times\left(1+\frac{q_1}{|q_1|}\frac{q_2}{|q_2|}\cos\left((q_1-q_2)\frac{a}{2}\right)\right)- \\ \left(\begin{array}{l}\cos\left((q_1+q_2)\,ja\right)\cos\left(\left(w(q_1)+w(q_2)\right)t-\varphi(q_1)-\varphi(q_2)\right)+ \\ \sin\left((q_1+q_2)\,ja\right)\sin\left(\left(w(q_1)+w(q_2)\right)t-\varphi(q_1)-\varphi(q_2)\right)\end{array}\right) \\ \times\left(1+\frac{q_1}{|q_1|}\frac{q_2}{|q_2|}\cos\left((q_1+q_2)\frac{a}{2}\right)\right)\end{array}\right)\end{array}\right) \tag{6.30}$$

Multiplying and expanding:

$$\chi_E(q,t)=\sum_{q_1}\sum_{q_2}\sum_{j}\frac{1}{4\sqrt{N}}w(q_1)w(q_2)A(q_1)A(q_2)\times\left(\begin{array}{l}\left(\begin{array}{l}\left(\cos\left(\left(q+q_1-q_2\right)ja\right)+\cos\left(\left(q-q_1+q_2\right)ja\right)\right)\\ \times\cos\left(\left(w(q_1)-w(q_2)\right)t-\varphi(q_1)+\varphi(q_2)\right)+\\ i\left(\cos\left(\left(q-q_1+q_2\right)ja\right)-\cos\left(\left(q+q_1-q_2\right)ja\right)\right)\\ \times\sin\left(\left(w(q_1)-w(q_2)\right)t-\varphi(q_1)+\varphi(q_2)\right)\end{array}\right)\\ \times\left(1+\frac{q_1}{|q_1|}\frac{q_2}{|q_2|}\cos\left(\left(q_1-q_2\right)\frac{a}{2}\right)\right)-\\ \left(\begin{array}{l}\left(\cos\left(\left(q+q_1+q_2\right)ja\right)+\cos\left(\left(q-q_1-q_2\right)ja\right)\right)\\ \times\cos\left(\left(w(q_1)+w(q_2)\right)t-\varphi(q_1)-\varphi(q_2)\right)+\\ i\left(\cos\left(\left(q-q_1-q_2\right)ja\right)-\cos\left(\left(q+q_1+q_2\right)ja\right)\right)\\ \times\sin\left(\left(w(q_1)+w(q_2)\right)t-\varphi(q_1)-\varphi(q_2)\right)\end{array}\right)\\ \times\left(1+\frac{q_1}{|q_1|}\frac{q_2}{|q_2|}\cos\left(\left(q_1+q_2\right)\frac{a}{2}\right)\right)\end{array}\right) \tag{6.31}$$

Consider just first Brillion zone:

$$-\frac{\pi}{a}<q\le\frac{\pi}{a} \tag{6.32}$$

$$-3\frac{\pi}{a}<q\pm q_1\pm q_2\le 3\frac{\pi}{a} \tag{6.33}$$

The projection for positive and negative wave vectors are simply conjugate of each other. Thus consider only positive wave vectors:

$$-2\frac{\pi}{a}<q\pm q_1\pm q_2\le 3\frac{\pi}{a} \tag{6.34}$$

It is interesting to note that non-zero values for the normal mode projection are obtained only for:

$$q \pm q_1 \pm q_2 = 0, \frac{2\pi}{a} \tag{6.35}$$

Solutions to the previous equation (for $q = 0.3\pi/a$) are shown in *Figure 6.1*. Note that only the line segments that are bounded by the dashed inner black box represent a possible solution. Clearly, there are eight branches of the solution. Now define:

$$L(q_1, q_2) = \frac{1}{4}\sqrt{N} m w(q_1) w(q_2) A(q_1) A(q_2) \tag{6.36}$$

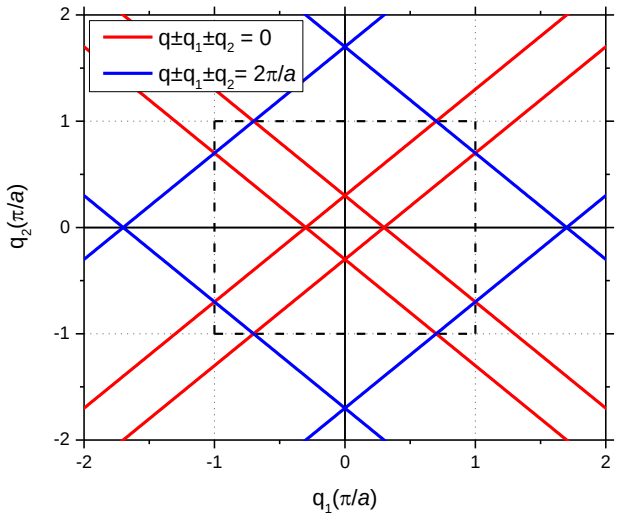

Figure 6.1: Solutions to Eqn. (6.35) for $q = 0.3\pi/a$.

Thus Eqn. (6.31) can be expanded as:

$$\chi_E(q,t)=\left[\begin{array}{l}
\left(\begin{array}{l}
\sum_{q_1}\left(-\frac{\pi}{a}<q_1<\frac{\pi}{a}-q;q_2=q_1+q\right):\left(1+\frac{q_1}{|q_1|}\frac{q_2}{|q_2|}\cos\left((q_1-q_2)\frac{a}{2}\right)\right)\\
\times L(q_1,q_2)\left(\exp\left(-i\left(\left(w(q_1)-w(q_2)\right)t-\varphi(q_1)+\varphi(q_2)\right)\right)\right)\\
\sum_{q_1}\left(-\frac{\pi}{a}+q<q_1<\frac{\pi}{a};q_2=q_1-q\right):\left(1+\frac{q_1}{|q_1|}\frac{q_2}{|q_2|}\cos\left((q_1-q_2)\frac{a}{2}\right)\right)\\
\times L(q_1,q_2)\left(\exp\left(i\left(\left(w(q_1)-w(q_2)\right)t-\varphi(q_1)+\varphi(q_2)\right)\right)\right)
\end{array}\right)\\
\left(\begin{array}{l}
\sum_{q_1}\left(-\frac{\pi}{a}<q_1<\frac{\pi}{a}-q;q_2=-q_1-q\right):\left(1+\frac{q_1}{|q_1|}\frac{q_2}{|q_2|}\cos\left((q_1+q_2)\frac{a}{2}\right)\right)\\
\times L(q_1,q_2)\left(-\exp\left(-i\left(\left(w(q_1)+w(q_2)\right)t-\varphi(q_1)-\varphi(q_2)\right)\right)\right)\\
\sum_{q_1}\left(-\frac{\pi}{a}+q<q_1<\frac{\pi}{a};q_2=-q_1+q\right):\left(1+\frac{q_1}{|q_1|}\frac{q_2}{|q_2|}\cos\left((q_1+q_2)\frac{a}{2}\right)\right)\\
\times L(q_1,q_2)\left(-\exp\left(i\left(\left(w(q_1)+w(q_2)\right)t-\varphi(q_1)-\varphi(q_2)\right)\right)\right)
\end{array}\right)\\
\left(\begin{array}{l}
\sum_{q_1}\left(\frac{\pi}{a}-q<q_1<\frac{\pi}{a};q_2=q_1+q-\frac{2\pi}{a}\right):\left(1+\frac{q_1}{|q_1|}\frac{q_2}{|q_2|}\cos\left((q_1-q_2)\frac{a}{2}\right)\right)\\
\times L(q_1,q_2)\left(\exp\left(-i\left(\left(w(q_1)-w(q_2)\right)t-\varphi(q_1)+\varphi(q_2)\right)\right)\right)\\
\sum_{q_1}\left(-\frac{\pi}{a}<q_1<-\frac{\pi}{a}+q;q_2=\frac{2\pi}{a}+q_1-q\right):\left(1+\frac{q_1}{|q_1|}\frac{q_2}{|q_2|}\cos\left((q_1-q_2)\frac{a}{2}\right)\right)\\
\times L(q_1,q_2)\left(\exp\left(i\left(\left(w(q_1)-w(q_2)\right)t-\varphi(q_1)+\varphi(q_2)\right)\right)\right)
\end{array}\right)\\
\left(\begin{array}{l}
\sum_{q_1}\left(\frac{\pi}{a}-q<q_1<\frac{\pi}{a};q_2=\frac{2\pi}{a}-q_1-q\right):\left(1+\frac{q_1}{|q_1|}\frac{q_2}{|q_2|}\cos\left((q_1+q_2)\frac{a}{2}\right)\right)\\
\times L(q_1,q_2)\left(-\exp\left(-i\left(\left(w(q_1)+w(q_2)\right)t-\varphi(q_1)-\varphi(q_2)\right)\right)\right)\\
\sum_{q_1}\left(-\frac{\pi}{a}<q_1<-\frac{\pi}{a}+q;q_2=-q_1+q-\frac{2\pi}{a}\right):\left(1+\frac{q_1}{|q_1|}\frac{q_2}{|q_2|}\cos\left((q_1+q_2)\frac{a}{2}\right)\right)\\
\times L(q_1,q_2)\left(-\exp\left(i\left(\left(w(q_1)+w(q_2)\right)t-\varphi(q_1)-\varphi(q_2)\right)\right)\right)
\end{array}\right)
\end{array}\right] \tag{6.37}$$

Rearranging terms:

$$\chi_E(q,t)=\left[\begin{array}{l}\left(\begin{array}{l}\sum_{q_1}\left(-\frac{\pi}{a}<q_1<\frac{\pi}{a}-q;q_2=q_1+q\right):\left(1+\frac{q_1}{|q_1|}\frac{q_2}{|q_2|}\cos\left((q_1-q_2)\frac{a}{2}\right)\right)\\ \times L(q_1,q_2)\left(\exp\left(-i\left(\left(w(q_1)-w(q_2)\right)t-\varphi(q_1)+\varphi(q_2)\right)\right)\right)\\ \sum_{q_1}\left(\frac{\pi}{a}-q<q_1<\frac{\pi}{a};q_2=q_1+q-\frac{2\pi}{a}\right):\left(1+\frac{q_1}{|q_1|}\frac{q_2}{|q_2|}\cos\left((q_1-q_2)\frac{a}{2}\right)\right)\\ \times L(q_1,q_2)\left(\exp\left(-i\left(\left(w(q_1)-w(q_2)\right)t-\varphi(q_1)+\varphi(q_2)\right)\right)\right)\\ \sum_{q_1}\left(-\frac{\pi}{a}<q_1<-\frac{\pi}{a}+q;q_2=\frac{2\pi}{a}+q_1-q\right):\left(1+\frac{q_1}{|q_1|}\frac{q_2}{|q_2|}\cos\left((q_1-q_2)\frac{a}{2}\right)\right)\\ \times L(q_1,q_2)\left(\exp\left(i\left(\left(w(q_1)-w(q_2)\right)t-\varphi(q_1)+\varphi(q_2)\right)\right)\right)\\ \sum_{q_1}\left(-\frac{\pi}{a}+q<q_1<\frac{\pi}{a};q_2=q_1-q\right):\left(1+\frac{q_1}{|q_1|}\frac{q_2}{|q_2|}\cos\left((q_1-q_2)\frac{a}{2}\right)\right)\\ \times L(q_1,q_2)\left(\exp\left(i\left(\left(w(q_1)-w(q_2)\right)t-\varphi(q_1)+\varphi(q_2)\right)\right)\right)\end{array}\right)\\ \left(\begin{array}{l}\sum_{q_1}\left(-\frac{\pi}{a}<q_1<\frac{\pi}{a}-q;q_2=-q_1-q\right):\left(1+\frac{q_1}{|q_1|}\frac{q_2}{|q_2|}\cos\left((q_1+q_2)\frac{a}{2}\right)\right)\\ \times L(q_1,q_2)\left(-\exp\left(-i\left(\left(w(q_1)+w(q_2)\right)t-\varphi(q_1)-\varphi(q_2)\right)\right)\right)\\ \sum_{q_1}\left(\frac{\pi}{a}-q<q_1<\frac{\pi}{a};q_2=\frac{2\pi}{a}-q_1-q\right):\left(1+\frac{q_1}{|q_1|}\frac{q_2}{|q_2|}\cos\left((q_1+q_2)\frac{a}{2}\right)\right)\\ \times L(q_1,q_2)\left(-\exp\left(-i\left(\left(w(q_1)+w(q_2)\right)t-\varphi(q_1)-\varphi(q_2)\right)\right)\right)\\ \sum_{q_1}\left(-\frac{\pi}{a}<q_1<-\frac{\pi}{a}+q;q_2=-q_1+q-\frac{2\pi}{a}\right):\left(1+\frac{q_1}{|q_1|}\frac{q_2}{|q_2|}\cos\left((q_1+q_2)\frac{a}{2}\right)\right)\\ \times L(q_1,q_2)\left(-\exp\left(i\left(\left(w(q_1)+w(q_2)\right)t-\varphi(q_1)-\varphi(q_2)\right)\right)\right)\\ \sum_{q_1}\left(-\frac{\pi}{a}+q<q_1<\frac{\pi}{a};q_2=-q_1+q\right):\left(1+\frac{q_1}{|q_1|}\frac{q_2}{|q_2|}\cos\left((q_1+q_2)\frac{a}{2}\right)\right)\\ \times L(q_1,q_2)\left(-\exp\left(i\left(\left(w(q_1)+w(q_2)\right)t-\varphi(q_1)-\varphi(q_2)\right)\right)\right)\end{array}\right)\end{array}\right] \tag{6.38}$$

Substituting the relation between q_1 and q_2:

$$\chi_E(q,t)=\left[\begin{array}{l}\left(\begin{array}{l}\sum_{q_1}\left(-\frac{\pi}{a}<q_1<\frac{\pi}{a}-q;q_2=q_1+q\right):\left(1+\frac{q_1}{|q_1|}\frac{q_2}{|q_2|}\cos\left(\frac{qa}{2}\right)\right)\\ \times L(q_1,q_2)\left(\exp\left(-i\left(\left(w(q_1)-w(q_2)\right)t-\varphi(q_1)+\varphi(q_2)\right)\right)\right)\\ \sum_{q_1}\left(\frac{\pi}{a}-q<q_1<\frac{\pi}{a};q_2=q_1+q-\frac{2\pi}{a}\right):\left(1+\frac{q_1}{|q_1|}\frac{q_2}{|q_2|}\cos\left(\frac{qa}{2}+\pi\right)\right)\\ \times L(q_1,q_2)\left(\exp\left(-i\left(\left(w(q_1)-w(q_2)\right)t-\varphi(q_1)+\varphi(q_2)\right)\right)\right)\\ \sum_{q_1}\left(-\frac{\pi}{a}<q_1<-\frac{\pi}{a}+q;q_2=\frac{2\pi}{a}+q_1-q\right):\left(1+\frac{q_1}{|q_1|}\frac{q_2}{|q_2|}\cos\left(\frac{qa}{2}-\pi\right)\right)\\ \times L(q_1,q_2)\left(\exp\left(i\left(\left(w(q_1)-w(q_2)\right)t-\varphi(q_1)+\varphi(q_2)\right)\right)\right)\\ \sum_{q_1}\left(-\frac{\pi}{a}+q<q_1<\frac{\pi}{a};q_2=q_1-q\right):\left(1+\frac{q_1}{|q_1|}\frac{q_2}{|q_2|}\cos\left(\frac{qa}{2}\right)\right)\\ \times L(q_1,q_2)\left(\exp\left(i\left(\left(w(q_1)-w(q_2)\right)t-\varphi(q_1)+\varphi(q_2)\right)\right)\right)\end{array}\right)\\ \left(\begin{array}{l}\sum_{q_1}\left(-\frac{\pi}{a}<q_1<\frac{\pi}{a}-q;q_2=-q_1-q\right):\left(1+\frac{q_1}{|q_1|}\frac{q_2}{|q_2|}\cos\left(\frac{qa}{2}\right)\right)\\ \times L(q_1,q_2)\left(-\exp\left(-i\left(\left(w(q_1)+w(q_2)\right)t-\varphi(q_1)-\varphi(q_2)\right)\right)\right)\\ \sum_{q_1}\left(\frac{\pi}{a}-q<q_1<\frac{\pi}{a};q_2=\frac{2\pi}{a}-q_1-q\right):\left(1+\frac{q_1}{|q_1|}\frac{q_2}{|q_2|}\cos\left(\frac{qa}{2}-\pi\right)\right)\\ \times L(q_1,q_2)\left(-\exp\left(-i\left(\left(w(q_1)+w(q_2)\right)t-\varphi(q_1)-\varphi(q_2)\right)\right)\right)\\ \sum_{q_1}\left(-\frac{\pi}{a}<q_1<-\frac{\pi}{a}+q;q_2=-q_1+q-\frac{2\pi}{a}\right):\left(1+\frac{q_1}{|q_1|}\frac{q_2}{|q_2|}\cos\left(\frac{qa}{2}+\pi\right)\right)\\ \times L(q_1,q_2)\left(-\exp\left(i\left(\left(w(q_1)+w(q_2)\right)t-\varphi(q_1)-\varphi(q_2)\right)\right)\right)\\ \sum_{q_1}\left(-\frac{\pi}{a}+q<q_1<\frac{\pi}{a};q_2=-q_1+q\right):\left(1+\frac{q_1}{|q_1|}\frac{q_2}{|q_2|}\cos\left(\frac{qa}{2}\right)\right)\\ \times L(q_1,q_2)\left(-\exp\left(i\left(\left(w(q_1)+w(q_2)\right)t-\varphi(q_1)-\varphi(q_2)\right)\right)\right)\end{array}\right)\end{array}\right] \tag{6.39}$$

Using equivalence of wave vectors separated by a reciprocal lattice vector and simplifying:

$$\chi_E(q,t)=\left[\begin{array}{l}\left(\begin{array}{l}\sum_{q_1}\left(-\frac{\pi}{a}<q_1<\frac{\pi}{a}-q;q_2=q_1+q\right):\left(1+\frac{q_1}{|q_1|}\frac{q_2}{|q_2|}\cos\left(\frac{qa}{2}\right)\right)\\ \times L(q_1,q_2)\left(\exp\left(-i\left(\left(w(q_1)-w(q_2)\right)t-\varphi(q_1)+\varphi(q_2)\right)\right)\right)\\ \sum_{q_1}\left(\frac{\pi}{a}-q<q_1<\frac{\pi}{a};q_2=q_1+q\right):\left(1+\frac{q_1}{|q_1|}\frac{q_2}{|q_2|}\cos\left(\frac{qa}{2}\right)\right)\\ \times L(q_1,q_2)\left(\exp\left(-i\left(\left(w(q_1)-w(q_2)\right)t-\varphi(q_1)+\varphi(q_2)\right)\right)\right)\\ \sum_{q_1}\left(-\frac{\pi}{a}<q_1<-\frac{\pi}{a}+q;q_2=q_1-q\right):\left(1+\frac{q_1}{|q_1|}\frac{q_2}{|q_2|}\cos\left(\frac{qa}{2}\right)\right)\\ \times L(q_1,q_2)\left(\exp\left(i\left(\left(w(q_1)-w(q_2)\right)t-\varphi(q_1)+\varphi(q_2)\right)\right)\right)\\ \sum_{q_1}\left(-\frac{\pi}{a}+q<q_1<\frac{\pi}{a};q_2=q_1-q\right):\left(1+\frac{q_1}{|q_1|}\frac{q_2}{|q_2|}\cos\left(\frac{qa}{2}\right)\right)\\ \times L(q_1,q_2)\left(\exp\left(i\left(\left(w(q_1)-w(q_2)\right)t-\varphi(q_1)+\varphi(q_2)\right)\right)\right)\end{array}\right)\\ \left(\begin{array}{l}\sum_{q_1}\left(-\frac{\pi}{a}<q_1<\frac{\pi}{a}-q;q_2=-q_1-q\right):\left(1+\frac{q_1}{|q_1|}\frac{q_2}{|q_2|}\cos\left(\frac{qa}{2}\right)\right)\\ \times L(q_1,q_2)\left(-\exp\left(-i\left(\left(w(q_1)+w(q_2)\right)t-\varphi(q_1)-\varphi(q_2)\right)\right)\right)\\ \sum_{q_1}\left(\frac{\pi}{a}-q<q_1<\frac{\pi}{a};q_2=-q_1-q\right):\left(1+\frac{q_1}{|q_1|}\frac{q_2}{|q_2|}\cos\left(\frac{qa}{2}\right)\right)\\ \times L(q_1,q_2)\left(-\exp\left(-i\left(\left(w(q_1)+w(q_2)\right)t-\varphi(q_1)-\varphi(q_2)\right)\right)\right)\\ \sum_{q_1}\left(-\frac{\pi}{a}<q_1<-\frac{\pi}{a}+q;q_2=-q_1+q\right):\left(1+\frac{q_1}{|q_1|}\frac{q_2}{|q_2|}\cos\left(\frac{qa}{2}\right)\right)\\ \times L(q_1,q_2)\left(-\exp\left(i\left(\left(w(q_1)+w(q_2)\right)t-\varphi(q_1)-\varphi(q_2)\right)\right)\right)\\ \sum_{q_1}\left(-\frac{\pi}{a}+q<q_1<\frac{\pi}{a};q_2=-q_1+q\right):\left(1+\frac{q_1}{|q_1|}\frac{q_2}{|q_2|}\cos\left(\frac{qa}{2}\right)\right)\\ \times L(q_1,q_2)\left(-\exp\left(i\left(\left(w(q_1)+w(q_2)\right)t-\varphi(q_1)-\varphi(q_2)\right)\right)\right)\end{array}\right)\end{array}\right] \tag{6.40}$$

Merging the common terms:

$$\chi_E(q,t)=\left[\begin{array}{l}\sum_{q_1}\left(-\frac{\pi}{a}<q_1<\frac{\pi}{a};q_2=q_1+q\right):\left(1+\frac{q_1}{|q_1|}\frac{q_2}{|q_2|}\cos\left(\frac{qa}{2}\right)\right)\\ \times L(q_1,q_2)\left(\exp\left(-i\left(\left(w(q_1)-w(q_2)\right)t-\varphi(q_1)+\varphi(q_2)\right)\right)\right)\\ +\sum_{q_1}\left(-\frac{\pi}{a}<q_1<\frac{\pi}{a};q_2=q_1-q\right):\left(1+\frac{q_1}{|q_1|}\frac{q_2}{|q_2|}\cos\left(\frac{qa}{2}\right)\right)\\ \times L(q_1,q_2)\left(\exp\left(i\left(\left(w(q_1)-w(q_2)\right)t-\varphi(q_1)+\varphi(q_2)\right)\right)\right)\\ +\sum_{q_1}\left(-\frac{\pi}{a}<q_1<\frac{\pi}{a};q_2=-q_1-q\right):\left(1+\frac{q_1}{|q_1|}\frac{q_2}{|q_2|}\cos\left(\frac{qa}{2}\right)\right)\\ \times L(q_1,q_2)\left(-\exp\left(-i\left(\left(w(q_1)+w(q_2)\right)t-\varphi(q_1)-\varphi(q_2)\right)\right)\right)\\ +\sum_{q_1}\left(-\frac{\pi}{a}<q_1<\frac{\pi}{a};q_2=-q_1+q\right):\left(1+\frac{q_1}{|q_1|}\frac{q_2}{|q_2|}\cos\left(\frac{qa}{2}\right)\right)\\ \times L(q_1,q_2)\left(-\exp\left(i\left(\left(w(q_1)+w(q_2)\right)t-\varphi(q_1)-\varphi(q_2)\right)\right)\right)\end{array}\right] \tag{6.41}$$

The energy normal mode projection can now be expressed as:

$$F(q,q_1,q_2)=\frac{1}{4}\sqrt{N}w(q_1)w(q_2)A(q_1)A(q_2)\left(1+\frac{q_1}{|q_1|}\frac{q_2}{|q_2|}\cos\left(\frac{qa}{2}\right)\right) \tag{6.42}$$

$$\chi_E(q,t)=\sum_{-\frac{\pi}{a}<q_1<\frac{\pi}{a}}\left[\begin{array}{l}\left[(q_{2A}=q_1+q);(q_{2B}=q_1-q);(q_{2C}=-q_1-q);(q_{2D}=-q_1+q):\right]\\ F(q,q_1,q_{2A})\exp\left(-i\left(\left(w(q_1)-w(q_{2A})\right)t-\varphi(q_1)+\varphi(q_{2A})\right)\right)\\ +F(q,q_1,q_{2B})\exp\left(i\left(\left(w(q_1)-w(q_{2B})\right)t-\varphi(q_1)+\varphi(q_{2B})\right)\right)\\ -F(q,q_1,q_{2C})\exp\left(-i\left(\left(w(q_1)+w(q_{2C})\right)t-\varphi(q_1)-\varphi(q_{2C})\right)\right)\\ -F(q,q_1,q_{2D})\exp\left(i\left(\left(w(q_1)+w(q_{2D})\right)t-\varphi(q_1)-\varphi(q_{2D})\right)\right)\end{array}\right] \tag{6.43}$$

6.4.2 Heat current normal modes

Similarly, the heat current normal modes can be evaluated. Substituting the expression for virial part of heat current from Eqn. (6.11) into Eqn. (6.13) to obtain the normal mode projection:

$$\chi_{J_{vir}}(q,t)=\sum_{q_1}\sum_{q_2}\sum_{j}\left(\begin{array}{l}\frac{1}{2V\sqrt{N}}A(q_1)A(q_2)w(q_1)w(q_2)v_g(q_2)\\ \left[\begin{array}{l}\left(\begin{array}{l}\cos\left((q_1-q_2)\,ja-\left(w(q_1)-w(q_2)\right)t+\varphi(q_1)-\varphi(q_2)\right)-\\ \cos\left((q_1+q_2)\,ja-\left(w(q_1)+w(q_2)\right)t+\varphi(q_1)+\varphi(q_2)\right)\end{array}\right)\\ \times\left(\cos(qja)+i\sin(qja)\right)\end{array}\right]\end{array}\right) \tag{6.44}$$

Expanding the cosine to separate the angles:

$$\chi_{J_{vir}}(q,t)=\sum_{q_1}\sum_{q_2}\sum_{j}\left(\begin{array}{l}\frac{1}{2V\sqrt{N}}A(q_1)A(q_2)w(q_1)w(q_2)v_g(q_2)\\ \left[\begin{array}{l}\left(\begin{array}{l}\cos\left((q_1-q_2)\,ja\right)\cos\left(\left(w(q_1)-w(q_2)\right)t-\varphi(q_1)+\varphi(q_2)\right)\\ +\sin\left(\left(q_1-q_{2r_2}\right)ja\right)\sin\left(\left(w(q_1)-w(q_2)\right)t-\varphi(q_1)+\varphi(q_2)\right)\\ -\cos\left((q_1+q_2)\,ja\right)\cos\left(\left(w(q_1)+w(q_2)\right)t-\varphi(q_1)-\varphi(q_2)\right)\\ -\sin\left((q_1+q_2)\,ja\right)\sin\left(\left(w(q_1)+w(q_2)\right)t-\varphi(q_1)-\varphi(q_2)\right)\end{array}\right)\\ \times\left(\cos(qja)+i\sin(qja)\right)\end{array}\right]\end{array}\right) \tag{6.45}$$

Multiplying and expanding:

$$\chi_{J_{vir}}(q,t) =$$

$$\sum_{q_1}\sum_{q_2}\sum_{j}\left[\begin{array}{l}\frac{1}{2V\sqrt{N}}A(q_1)A(q_2)w(q_1)w(q_2)v_g(q_2)\\ \left(\begin{array}{l}\cos\left((q_1-q_2)\,ja\right)\cos(qja)\cos\left(\left(w(q_1)-w(q_2)\right)t-\varphi(q_1)+\varphi(q_2)\right)+\\ i\cos\left((q_1-q_2)\,ja\right)\sin(qja)\cos\left(\left(w(q_1)-w(q_2)\right)t-\varphi(q_1)+\varphi(q_2)\right)+\\ \sin\left((q_1-q_2)\,ja\right)\cos(qja)\sin\left(\left(w(q_1)-w(q_2)\right)t-\varphi(q_1)+\varphi(q_2)\right)+\\ i\sin\left((q_1-q_2)\,ja\right)\sin(qja)\sin\left(\left(w(q_1)-w(q_2)\right)t-\varphi(q_1)+\varphi(q_2)\right)-\\ \cos\left((q_1+q_2)\,ja\right)\cos(qja)\cos\left(\left(w(q_1)+w(q_2)\right)t-\varphi(q_1)-\varphi(q_2)\right)-\\ i\cos\left((q_1+q_2)\,ja\right)\sin(qja)\cos\left(\left(w(q_1)+w(q_2)\right)t-\varphi(q_1)-\varphi(q_2)\right)-\\ \sin\left((q_1+q_2)\,ja\right)\cos(qja)\sin\left(\left(w(q_1)+w(q_2)\right)t-\varphi(q_1)-\varphi(q_2)\right)-\\ i\sin\left((q_1+q_2)\,ja\right)\sin(qja)\sin\left(\left(w(q_1)+w(q_2)\right)t-\varphi(q_1)-\varphi(q_2)\right)\end{array}\right)\end{array}\right] \quad (6.46)$$

Combining the terms:

$$\chi_{J_{vir}}(q,t)=\sum_{q_1}\sum_{q_2}\sum_{j}\left[\begin{array}{l}\frac{1}{4V\sqrt{N}}A(q_1)A(q_2)w(q_1)w(q_2)v_g(q_2)\\ \left(\left(\cos\left((q+q_1-q_2)\,ja\right)+\cos\left((q-q_1+q_2)\,ja\right)\right)\right.\\ \times\cos\left(\left(w(q_1)-w(q_2)\right)t-\varphi(q_1)+\varphi(q_2)\right)+\\ i\left(\sin\left((q+q_1-q_2)\,ja\right)+\sin\left((q-q_1+q_2)\,ja\right)\right)\\ \times\cos\left(\left(w(q_1)-w(q_2)\right)t-\varphi(q_1)+\varphi(q_2)\right)+\\ \left(\sin\left((q+q_1-q_2)\,ja\right)-\sin\left((q-q_1+q_2)\,ja\right)\right)\\ \times\sin\left(\left(w(q_1)-w(q_2)\right)t-\varphi(q_1)+\varphi(q_2)\right)+\\ i\left(\cos\left((q-q_1+q_2)\,ja\right)-\cos\left((q+q_1-q_2)\,ja\right)\right)\\ \times\sin\left(\left(w(q_1)-w(q_2)\right)t-\varphi(q_1)+\varphi(q_2)\right)-\\ \left(\cos\left((q+q_1+q_2)\,ja\right)+\cos\left((q-q_1-q_2)\,ja\right)\right)\\ \times\cos\left(\left(w(q_1)+w(q_2)\right)t-\varphi(q_1)-\varphi(q_2)\right)-\\ i\left(\sin\left((q+q_1+q_2)\,ja\right)+\sin\left((q-q_1-q_2)\,ja\right)\right)\\ \times\cos\left(\left(w(q_1)+w(q_2)\right)t-\varphi(q_1)-\varphi(q_2)\right)-\\ \left(\sin\left((q+q_1+q_2)\,ja\right)-\sin\left((q-q_1-q_2)\,ja\right)\right)\\ \times\sin\left(\left(w(q_1)+w(q_2)\right)t-\varphi(q_1)-\varphi(q_2)\right)-\\ i\left(\cos\left((q-q_1-q_2)\,ja\right)-\cos\left((q+q_1+q_2)\,ja\right)\right)\\ \left.\times\sin\left(\left(w(q_1)+w(q_2)\right)t-\varphi(q_1)-\varphi(q_2)\right)\right)\end{array}\right] \tag{6.47}$$

Simplifying:

$$\chi_{J_{vir}}(q,t)=\sum_{q_1}\sum_{q_2}\sum_{j}\left[\begin{array}{l}\frac{1}{4V\sqrt{N}}A(q_1)A(q_2)w(q_1)w(q_2)v_g(q_2)\\ \left(\begin{array}{l}\left(\cos\left((q+q_1-q_2)\,ja\right)+\cos\left((q-q_1+q_2)\,ja\right)\right)\\ \times\cos\left(\left(w(q_1)-w(q_2)\right)t-\varphi(q_1)+\varphi(q_2)\right)+\\ i\left(\cos\left((q-q_1+q_2)\,ja\right)-\cos\left((q+q_1-q_2)\,ja\right)\right)\\ \times\sin\left(\left(w(q_1)-w(q_2)\right)t-\varphi(q_1)+\varphi(q_2)\right)-\\ \left(\cos\left((q+q_1+q_2)\,ja\right)+\cos\left((q-q_1-q_2)\,ja\right)\right)\\ \times\cos\left(\left(w(q_1)+w(q_2)\right)t-\varphi(q_1)-\varphi(q_2)\right)-\\ i\left(\cos\left((q-q_1-q_2)\,ja\right)-\cos\left((q+q_1+q_2)\,ja\right)\right)\\ \times\sin\left(\left(w(q_1)+w(q_2)\right)t-\varphi(q_1)-\varphi(q_2)\right)\end{array}\right)\end{array}\right] \tag{6.48}$$

Consider just first Brillion zone:

$$-\frac{\pi}{a}<q\le\frac{\pi}{a} \tag{6.49}$$

$$-3\frac{\pi}{a}<q\pm q_1\pm q_1\le 3\frac{\pi}{a} \tag{6.50}$$

Again, consider only positive q, which leads to non-zero contribution only for wave vectors satisfying:

$$q\pm q_1\pm q_2=0,\frac{2\pi}{a} \tag{6.51}$$

Thus the contraints on the wave vectors are identical to those for the energy normal modes. The solution to the above equation for $q = 0.3\ \pi/a$ were plotted in *Figure 6.1*. The eight branches of the solution lead to:

$$\chi_{J_{vir}}(q,t)=\frac{\sqrt{N}}{4V}\left[\begin{array}{l}
\sum_{q_1}\left(-\frac{\pi}{a}<q_1<\frac{\pi}{a}-q;q_2=q_1+q\right):A(q_1)A(q_2)w(q_1)w(q_2)v_g(q_2)\\
\left(\exp\left(-i\left(w(q_1)-w(q_2)\right)t-\varphi(q_1)+\varphi(q_2)\right)\right)\\
\sum_{q_1}\left(-\frac{\pi}{a}+q<q_1<\frac{\pi}{a};q_2=q_1-q\right):A(q_1)A(q_2)w(q_1)w(q_2)v_g(q_2)\\
\times\left(\exp\left(i\left(w(q_1)-w(q_2)\right)t-\varphi(q_1)+\varphi(q_2)\right)\right)\\
\sum_{q_1}\left(-\frac{\pi}{a}<q_1<\frac{\pi}{a}-q;q_2=-q_1-q\right):A(q_1)A(q_2)w(q_1)w(q_2)v_g(q_2)\\
\times\left(-\exp\left(-i\left(\left(w(q_1)+w(q_2)\right)t-\varphi(q_1)-\varphi(q_2)\right)\right)\right)\\
\sum_{q_1}\left(-\frac{\pi}{a}+q<q_1<\frac{\pi}{a};q_2=-q_1+q\right):A(q_1)A(q_2)w(q_1)w(q_2)v_g(q_2)\\
\times\left(-\exp\left(i\left(\left(w(q_1)+w(q_2)\right)t-\varphi(q_1)-\varphi(q_2)\right)\right)\right)\\
\sum_{q_1}\left(\frac{\pi}{a}-q<q_1<\frac{\pi}{a};q_2=q_1+q-\frac{2\pi}{a}\right):A(q_1)A(q_2)w(q_1)w(q_2)v_g(q_2)\\
\times\left(\exp\left(-i\left(\left(w(q_1)-w(q_2)\right)t-\varphi(q_1)+\varphi(q_2)\right)\right)\right)\\
\sum_{q_1}\left(-\frac{\pi}{a}<q_1<-\frac{\pi}{a}+q;q_2=\frac{2\pi}{a}+q_1-q\right):A(q_1)A(q_2)w(q_1)w(q_2)v_g(q_2)\\
\times\left(\exp\left(i\left(\left(w(q_1)-w(q_2)\right)t-\varphi(q_1)+\varphi(q_2)\right)\right)\right)\\
\sum_{q_1}\left(\frac{\pi}{a}-q<q_1<\frac{\pi}{a};q_2=\frac{2\pi}{a}-q_1-q\right):A(q_1)A(q_2)w(q_1)w(q_2)v_g(q_2)\\
\times\left(-\exp\left(-i\left(\left(w(q_1)+w(q_2)\right)t-\varphi(q_1)-\varphi(q_2)\right)\right)\right)\\
\sum_{q_1}\left(-\frac{\pi}{a}<q_1<-\frac{\pi}{a}+q;q_2=-q_1+q-\frac{2\pi}{a}\right):A(q_1)A(q_2)w(q_1)w(q_2)v_g(q_2)\\
\times\left(-\exp\left(i\left(\left(w(q_1)+w(q_2)\right)t-\varphi(q_1)-\varphi(q_2)\right)\right)\right)
\end{array}\right] \tag{6.52}$$

Rearranging terms:

$$\chi_{J_{vir}}(q,t)=$$

$$\frac{\sqrt{N}}{4V}\left[\begin{array}{l}
\sum_{q_{\eta}}\left(-\frac{\pi}{a}<q_1<\frac{\pi}{a}-q;q_2=q_1+q\right):A(q_1)A(q_2)w(q_1)w(q_2)v_g(q_2)\\
\left(\exp\left(-i\left(w(q_1)-w(q_2)\right)t-\varphi(q_1)+\varphi(q_2)\right)\right)\\
\sum_{q_{\eta}}\left(\frac{\pi}{a}-q<q_1<\frac{\pi}{a};q_2=q_1+q-\frac{2\pi}{a}\right):A(q_1)A(q_2)w(q_1)w(q_2)v_g(q_2)\\
\times\left(\exp\left(-i\left(\left(w(q_1)-w(q_2)\right)t-\varphi(q_1)+\varphi(q_2)\right)\right)\right)\\
\sum_{q_{\eta}}\left(-\frac{\pi}{a}<q_1<-\frac{\pi}{a}+q;q_2=\frac{2\pi}{a}+q_1-q\right):A(q_1)A(q_2)w(q_1)w(q_2)v_g(q_2)\\
\times\left(\exp\left(i\left(\left(w(q_1)-w(q_2)\right)t-\varphi(q_1)+\varphi(q_2)\right)\right)\right)\\
\sum_{q_{\eta}}\left(-\frac{\pi}{a}+q<q_1<\frac{\pi}{a};q_2=q_1-q\right):A(q_1)A(q_2)w(q_1)w(q_2)v_g(q_2)\\
\times\left(\exp\left(i\left(w(q_1)-w(q_2)\right)t-\varphi(q_1)+\varphi(q_2)\right)\right)\\
\sum_{q_{\eta}}\left(-\frac{\pi}{a}<q_1<\frac{\pi}{a}-q;q_2=-q_1-q\right):A(q_1)A(q_2)w(q_1)w(q_2)v_g(q_2)\\
\times\left(-\exp\left(-i\left(\left(w(q_1)+w(q_2)\right)t-\varphi(q_1)-\varphi(q_2)\right)\right)\right)\\
\sum_{q_{\eta}}\left(\frac{\pi}{a}-q<q_1<\frac{\pi}{a};q_2=\frac{2\pi}{a}-q_1-q\right):A(q_1)A(q_2)w(q_1)w(q_2)v_g(q_2)\\
\times\left(-\exp\left(-i\left(\left(w(q_1)+w(q_2)\right)t-\varphi(q_1)-\varphi(q_2)\right)\right)\right)\\
\sum_{q_{\eta}}\left(-\frac{\pi}{a}<q_1<-\frac{\pi}{a}+q;q_2=-q_1+q-\frac{2\pi}{a}\right):A(q_1)A(q_2)w(q_1)w(q_2)v_g(q_2)\\
\times\left(-\exp\left(i\left(\left(w(q_1)+w(q_2)\right)t-\varphi(q_1)-\varphi(q_2)\right)\right)\right)\\
\sum_{q_{\eta}}\left(-\frac{\pi}{a}+q<q_1<\frac{\pi}{a};q_2=-q_1+q\right):A(q_1)A(q_2)w(q_1)w(q_2)v_g(q_2)\\
\times\left(-\exp\left(i\left(\left(w(q_1)+w(q_2)\right)t-\varphi(q_1)-\varphi(q_2)\right)\right)\right)
\end{array}\right] \tag{6.53}$$

Combining common terms:

$$\chi_{J_{vir}}(q,t)=\frac{\sqrt{N}}{4V}\left[\begin{array}{l}\sum_{q_{\eta}}\left(-\frac{\pi}{a}<q_1<\frac{\pi}{a};q_2=q_1+q\right):A(q_1)A(q_2)w(q_1)w(q_2)v_g(q_2)\\ \left(\exp\left(-i\left(w(q_1)-w(q_2)\right)t-\varphi(q_1)+\varphi(q_2)\right)\right)\\ \sum_{q_{\eta}}\left(-\frac{\pi}{a}<q_1<-\frac{\pi}{a};q_2=q_1-q\right):A(q_1)A(q_2)w(q_1)w(q_2)v_g(q_2)\\ \times\left(\exp\left(i\left(\left(w(q_1)-w(q_2)\right)t-\varphi(q_1)+\varphi(q_2)\right)\right)\right)\\ \sum_{q_{\eta}}\left(-\frac{\pi}{a}<q_1<\frac{\pi}{a};q_2=-q_1-q\right):A(q_1)A(q_2)w(q_1)w(q_2)v_g(q_2)\\ \times\left(-\exp\left(-i\left(\left(w(q_1)+w(q_2)\right)t-\varphi(q_1)-\varphi(q_2)\right)\right)\right)\\ \sum_{q_{\eta}}\left(-\frac{\pi}{a}<q_1<-\frac{\pi}{a};q_2=-q_1+q\right):A(q_1)A(q_2)w(q_1)w(q_2)v_g(q_2)\\ \times\left(-\exp\left(i\left(\left(w(q_1)+w(q_2)\right)t-\varphi(q_1)-\varphi(q_2)\right)\right)\right)\end{array}\right] \tag{6.54}$$

Swapping q_1 and q_2 and simplifying:

$$\chi_{J_{vir}}(q,t)=\frac{\sqrt{N}}{4V}\sum_{-\frac{\pi}{a}<q_{\eta}<\frac{\pi}{a}}\left[\begin{array}{l}\left(\begin{array}{l}(q_2=q_1-q):A(q_1)A(q_2)w(q_1)w(q_2)v_g(q_1)\\ \left(\exp\left(i\left(w(q_1)-w(q_2)\right)t-\varphi(q_1)+\varphi(q_2)\right)\right)\end{array}\right)\\ +\left(\begin{array}{l}(q_2=q_1+q):A(q_1)A(q_2)w(q_1)w(q_2)v_g(q_1)\\ \times\left(\exp\left(-i\left(\left(w(q_1)-w(q_2)\right)t-\varphi(q_1)+\varphi(q_2)\right)\right)\right)\end{array}\right)\\ +\left(\begin{array}{l}(q_2=-q_1-q):A(q_1)A(q_2)w(q_1)w(q_2)v_g(q_1)\\ \times\left(-\exp\left(-i\left(\left(w(q_1)+w(q_2)\right)t-\varphi(q_1)-\varphi(q_2)\right)\right)\right)\end{array}\right)\\ +\left(\begin{array}{l}(q_2=-q_1+q):A(q_1)A(q_2)w(q_1)w(q_2)v_g(q_1)\\ \times\left(-\exp\left(i\left(\left(w(q_1)+w(q_2)\right)t-\varphi(q_1)-\varphi(q_2)\right)\right)\right)\end{array}\right)\end{array}\right] \tag{6.55}$$

The heat normal mode projection this can be written as:

$$\chi_{J_{vir}}(q,t)=\sum_{-\frac{\pi}{a}<q_1<\frac{\pi}{a}}\frac{\sqrt{N}A(q_1)w(q_1)v_g(q_1)}{4V}\times\begin{bmatrix}(q_{2A}=q_1-q);(q_{2B}=q_1+q);(q_{2C}=-q_1-q);(q_{2D}=-q_1+q):\\A(q_{2A})w(q_{2A})\exp\left(i\left(w(q_1)-w(q_{2A})\right)t-\varphi(q_1)+\varphi(q_{2A})\right)\\+A(q_{2B})w(q_{2B})\exp\left(-i\left(\left(w(q_1)-w(q_{2B})\right)t-\varphi(q_1)+\varphi(q_{2B})\right)\right)\\-A(q_{2C})w(q_{2C})\exp\left(-i\left(\left(w(q_1)+w(q_{2C})\right)t-\varphi(q_1)-\varphi(q_{2C})\right)\right)\\-A(q_{2D})w(q_{2D})\exp\left(i\left(\left(w(q_1)+w(q_{2D})\right)t-\varphi(q_1)-\varphi(q_{2D})\right)\right)\end{bmatrix} \quad (6.56)$$

Summarizing, the normal mode projection for energy and heat current corresponding to a wave vector q is given by Eqn. (6.57) and Eqn. (6.59) respectively. These are given by:

$$\chi_E(q,t)=\sum_{-\frac{\pi}{a}<q_1<\frac{\pi}{a}}\begin{bmatrix}\left[(q_{2A}=q_1+q);(q_{2B}=q_1-q);(q_{2C}=-q_1-q);(q_{2D}=-q_1+q):\right]\\F(q,q_1,q_{2A})\exp\left(-i\left(\left(w(q_1)-w(q_{2A})\right)t-\varphi(q_1)+\varphi(q_{2A})\right)\right)\\+F(q,q_1,q_{2B})\exp\left(i\left(\left(w(q_1)-w(q_{2B})\right)t-\varphi(q_1)+\varphi(q_{2B})\right)\right)\\-F(q,q_1,q_{2C})\exp\left(-i\left(\left(w(q_1)+w(q_{2C})\right)t-\varphi(q_1)-\varphi(q_{2C})\right)\right)\\-F(q,q_1,q_{2D})\exp\left(i\left(\left(w(q_1)+w(q_{2D})\right)t-\varphi(q_1)-\varphi(q_{2D})\right)\right)\end{bmatrix} \quad (6.57)$$

where:

$$F(q,q_1,q_2)=\frac{1}{4}\sqrt{N}w(q_1)w(q_2)A(q_1)A(q_2)\left(1+\frac{q_1}{|q_1|}\frac{q_2}{|q_2|}\cos\left(\frac{qa}{2}\right)\right) \quad (6.58)$$

$$\chi_{J_{vir}}(q,t)=\sum_{-\frac{\pi}{a}<q_1<\frac{\pi}{a}}\frac{\sqrt{N}A(q_1)w(q_1)v_g(q_1)}{4V}\times\begin{bmatrix}(q_{2A}=q_1-q);(q_{2B}=q_1+q);(q_{2C}=-q_1-q);(q_{2D}=-q_1+q):\\ A(q_{2A})w(q_{2A})\exp\left(i\left(w(q_1)-w(q_{2A})\right)t-\varphi(q_1)+\varphi(q_{2A})\right)\\ +A(q_{2B})w(q_{2B})\exp\left(-i\left(\left(w(q_1)-w(q_{2B})\right)t-\varphi(q_1)+\varphi(q_{2B})\right)\right)\\ -A(q_{2C})w(q_{2C})\exp\left(-i\left(\left(w(q_1)+w(q_{2C})\right)t-\varphi(q_1)-\varphi(q_{2C})\right)\right)\\ -A(q_{2D})w(q_{2D})\exp\left(i\left(\left(w(q_1)+w(q_{2D})\right)t-\varphi(q_1)-\varphi(q_{2D})\right)\right)\end{bmatrix} \tag{6.59}$$

It is fascinating to note that, for both energy and heat current, the normal mode projection corresponding to a wave q admits a non-zero contribution from phonon modes with wavevectors q_1 and q_2 *if and only if* the triplet satisfies the three-phonon scattering condition for wave vectors. Later sections will show that the resultant frequency of the normal mode projection due to a pair contribution (energy/heat current) also corresponds to the frequency combination condition for three-phonon scattering. Thus phonon pairs interfere to form waves of energy and heat current such that their wave vectors and frequencies are same as those corresponding to a phonon mode created by a three-phonon interaction between them (with harmonic interactions).

6.5 Normal mode time correlation

A time correlation of the energy and heat mode projection is required to extract the dispersion relation and decay of the modes. This section evaluates the time correlation corresponding to the normal mode projections derived in the previous section.

6.5.1 Energy normal mode correlation

Substituting the expression for the energy normal mode projection from Eqn. (6.43) into Eqn. (6.15) to evaluate the time correlation of the normal mode projection:

$$
\begin{aligned}
E_{corr}^{NM}(q,t) &= \left\langle \chi_E(q,0)\,\chi_E(-q,t)\right\rangle \\
&\left[(q_{2A}' = q_1' + q);(q_{2B}' = q_1' - q);(q_{2C}' = -q_1' - q);(q_{2D}' = -q_1' + q):\right] \\
&\left[(q_{2A} = q_1 + q);(q_{2B} = q_1 - q);(q_{2C} = -q_1 - q);(q_{2D} = -q_1 + q):\right] \\
&\sum_{-\frac{\pi}{a}<q_1'<\frac{\pi}{a}} \sum_{-\frac{\pi}{a}<q_1<\frac{\pi}{a}} \left[\left\langle \begin{pmatrix} F(q,q_1',q_{2A}')\exp\left(-i\left(-\varphi(q_1')+\varphi(q_{2A}')\right)\right) \\ +F(q,q_1',q_{2B}')\exp\left(i\left(-\varphi(q_1')+\varphi(q_{2B}')\right)\right) \\ -F(q,q_1',q_{2C}')\exp\left(-i\left(-\varphi(q_1')-\varphi(q_{2C}')\right)\right) \\ -F(q,q_1',q_{2D}')\exp\left(i\left(-\varphi(q_1')-\varphi(q_{2D}')\right)\right) \end{pmatrix} \right.\right. \\
&\qquad \left.\left. \begin{pmatrix} F(q,q_1,q_{2A})\exp\left(i\left(\left(w(q_1)-w(q_{2A})\right)t-\varphi(q_1)+\varphi(q_{2A})\right)\right) \\ +F(q,q_1,q_{2B})\exp\left(-i\left(\left(w(q_1)-w(q_{2B})\right)t-\varphi(q_1)+\varphi(q_{2B})\right)\right) \\ -F(q,q_1,q_{2C})\exp\left(i\left(\left(w(q_1)+w(q_{2C})\right)t-\varphi(q_1)-\varphi(q_{2C})\right)\right) \\ -F(q,q_1,q_{2D})\exp\left(-i\left(\left(w(q_1)+w(q_{2D})\right)t-\varphi(q_1)-\varphi(q_{2D})\right)\right) \end{pmatrix} \right\rangle \right]
\end{aligned}
\tag{6.60}
$$

Consider the product of the first term in the lower bracket and with all the terms in the upper bracket:

$$\left[\begin{array}{l}(q_{2A}'=q_1'+q);(q_{2B}'=q_1'-q);(q_{2C}'=-q_1'-q);\\(q_{2D}'=-q_1'+q);(q_{2A}=q_1+q):\end{array}\right]$$

$$= \sum_{-\frac{\pi}{a}<q_1'<\frac{\pi}{a}} \sum_{-\frac{\pi}{a}<q_1<\frac{\pi}{a}} \left[\left\langle \begin{array}{l} F(q,q_1,q_{2A})F(q,q_1',q_{2A}')\times \\ \exp\left(i\left(\left(w(q_1)-w(q_{2A})\right)t-\varphi(q_1)+\varphi(q_{2A})+\varphi(q_1')-\varphi(q_{2A}')\right)\right) \\ +F(q,q_1,q_{2A})F(q,q_1',q_{2B}')\times \\ \exp\left(i\left(\left(w(q_1)-w(q_{2A})\right)t-\varphi(q_1)+\varphi(q_{2A})-\varphi(q_1')+\varphi(q_{2B}')\right)\right) \\ -F(q,q_1,q_{2A})F(q,q_1',q_{2C}')\times \\ \exp\left(i\left(\left(w(q_1)-w(q_{2A})\right)t-\varphi(q_1)+\varphi(q_{2A})+\varphi(q_1')+\varphi(q_{2C}')\right)\right) \\ -F(q,q_1,q_{2A})F(q,q_1',q_{2D}')\times \\ \exp\left(i\left(\left(w(q_1)-w(q_{2A})\right)t-\varphi(q_1)+\varphi(q_{2A})-\varphi(q_1')-\varphi(q_{2D}')\right)\right) \end{array} \right\rangle \right] \quad (6.61)$$

Non-zero correlations are possible only if the phase angles cancel off as the ensemble average of the exponential of any phase angle goes to zero; this results in $q_1 = q_1'$:

$$\left[(q_{2A}=q_1+q);(q_{2B}=q_1-q);(q_{2C}=-q_1-q);(q_{2D}=-q_1+q):\right]$$

$$= \sum_{-\frac{\pi}{a}<q_1<\frac{\pi}{a}} \left[\left\langle \begin{array}{l} F^2(q,q_1,q_{2A})\times\exp\left(i\left(\left(w(q_1)-w(q_{2A})\right)t\right)\right) \\ +F(q,q_1,q_{2A})F(q,q_1,q_{2B})\times \\ \exp\left(i\left(\left(w(q_1)-w(q_{2A})\right)t-2\varphi(q_1)+\varphi(q_{2A})+\varphi(q_{2B})\right)\right) \\ -F(q,q_1,q_{2A})F(q,q_1,q_{2C})\times \\ \exp\left(i\left(\left(w(q_1)-w(q_{2A})\right)t+\varphi(q_{2A})+\varphi(q_{2C})\right)\right) \\ -F(q,q_1,q_{2A})F(q,q_1,q_{2D})\times \\ \exp\left(i\left(\left(w(q_1)-w(q_{2A})\right)t-2\varphi(q_1)+\varphi(q_{2A})-\varphi(q_{2D})\right)\right) \end{array} \right\rangle \right] \quad (6.62)$$

Since the phase angles cannot cancel for the final three terms:

$$= \sum_{-\frac{\pi}{a}<q_1<\frac{\pi}{a}}^{\left[(q_{2A}=q_1+q);(q_{2B}=q_1-q);(q_{2C}=-q_1-q);(q_{2D}=-q_1+q):\right]} \left[\left\langle F^2(q,q_1,q_{2A})\times\exp\left(i\left(\left(w(q_1)-w(q_{2A})\right)t\right)\right)\right\rangle\right] \tag{6.63}$$

A similar argument can be used for the other terms from the product in Eqn. (6.60) to give:

$$E_{corr}^{NM}(q,t) = \sum_{-\frac{\pi}{a}<q_1<\frac{\pi}{a}}^{\left[(q_{2A}=q_1+q);(q_{2B}=q_1-q);(q_{2C}=-q_1-q);(q_{2D}=-q_1+q):\right]} \left[\left\langle \begin{pmatrix} F^2(q,q_1,q_{2A})\exp\left(i\left(\left(w(q_1)-w(q_{2A})\right)t\right)\right) \\ +F^2(q,q_1,q_{2B})\exp\left(-i\left(\left(w(q_1)-w(q_{2B})\right)t\right)\right) \\ +F^2(q,q_1,q_{2C})\exp\left(i\left(\left(w(q_1)+w(q_{2C})\right)t\right)\right) \\ +F^2(q,q_1,q_{2D})\exp\left(-i\left(\left(w(q_1)+w(q_{2D})\right)t\right)\right) \end{pmatrix}\right\rangle\right] \tag{6.64}$$

Splitting the terms:

$$E_{corr}^{NM}(q,t) = \left[\begin{array}{l} \sum_{-\frac{\pi}{a}<q_1<\frac{\pi}{a}}^{(q_{2A}=q_1+q):} \left[\left\langle F^2(q,q_1,q_{2A})\exp\left(i\left(\left(w(q_1)-w(q_{2A})\right)t\right)\right)\right\rangle\right] \\ +\sum_{-\frac{\pi}{a}<q_1<\frac{\pi}{a}}^{(q_{2B}=q_1-q):} \left[\left\langle F^2(q,q_1,q_{2B})\exp\left(-i\left(\left(w(q_1)-w(q_{2B})\right)t\right)\right)\right\rangle\right] \\ +\sum_{-\frac{\pi}{a}<q_1<\frac{\pi}{a}}^{(q_{2C}=-q_1-q):} \left[\left\langle F^2(q,q_1,q_{2C})\exp\left(i\left(\left(w(q_1)+w(q_{2C})\right)t\right)\right)\right\rangle\right] \\ +\sum_{-\frac{\pi}{a}<q_1<\frac{\pi}{a}}^{(q_{2D}=-q_1+q):} \left[\left\langle F^2(q,q_1,q_{2D})\exp\left(-i\left(\left(w(q_1)+w(q_{2D})\right)t\right)\right)\right\rangle\right] \end{array}\right] \tag{6.65}$$

Recombining terms using symmetry:

$$E_{corr}^{NM}(q,t)=\left[\begin{array}{l}(q_{2A}=q_1+q):\\ \sum\limits_{-\frac{\pi}{a}<q_1<\frac{\pi}{a}}\left[\begin{array}{l}\left\langle F^2(q,q_1,q_{2A})\exp\left(i\left(\left(w(q_1)-w(q_{2A})\right)t\right)\right)\right\rangle\\ +\left\langle F^2(q,q_1,-q_{2A})\exp\left(i\left(\left(w(q_1)+w(q_{2C})\right)t\right)\right)\right\rangle\end{array}\right]\\ (q_{2D}=-q_1+q):\\ +\sum\limits_{-\frac{\pi}{a}<q_1<\frac{\pi}{a}}\left[\begin{array}{l}\left\langle F^2(q,q_1,q_{2D})\exp\left(-i\left(\left(w(q_1)+w(q_{2D})\right)t\right)\right)\right\rangle\\ +\left\langle F^2(q,q_1,-q_{2D})\exp\left(-i\left(\left(w(q_1)-w(q_{2B})\right)t\right)\right)\right\rangle\end{array}\right]\end{array}\right] \tag{6.66}$$

Further recombining using symmetry:

$$E_{corr}^{NM}(q,t)=\left[\begin{array}{l}(q_2=q_1+q):\\ \sum\limits_{-\frac{\pi}{a}<q_1<\frac{\pi}{a}}\left[\begin{array}{l}\left\langle F^2(q,q_1,q_2)\exp\left(i\left(\left(w(q_1)-w(q_2)\right)t\right)\right)\right\rangle\\ +\left\langle F^2(q,q_1,-q_2)\exp\left(i\left(\left(w(q_1)+w(q_2)\right)t\right)\right)\right\rangle\\ +\left\langle F^2(q,-q_1,q_2)\exp\left(-i\left(\left(w(q_1)+w(q_2)\right)t\right)\right)\right\rangle\\ +\left\langle F^2(q,-q_1,-q_2)\exp\left(-i\left(\left(w(q_1)-w(q_2)\right)t\right)\right)\right\rangle\end{array}\right]\end{array}\right] \tag{6.67}$$

Since the exponentials are independent of the ensemble average:

$$E_{corr}^{NM}(q,t)=\left[\begin{array}{l}(q_2=q_1+q):\\ \sum\limits_{-\frac{\pi}{a}<q_1<\frac{\pi}{a}}\left[\begin{array}{l}\left\langle F^2(q,q_1,q_2)\right\rangle\exp\left(i\left(\left(w(q_1)-w(q_2)\right)t\right)\right)\\ +\left\langle F^2(q,q_1,-q_2)\right\rangle\exp\left(i\left(\left(w(q_1)+w(q_2)\right)t\right)\right)\\ +\left\langle F^2(q,-q_1,q_2)\right\rangle\exp\left(-i\left(\left(w(q_1)+w(q_2)\right)t\right)\right)\\ +\left\langle F^2(q,-q_1,-q_2)\right\rangle\exp\left(-i\left(\left(w(q_1)-w(q_2)\right)t\right)\right)\end{array}\right]\end{array}\right] \tag{6.68}$$

Recalling that:

$$F\left(q,q_1,q_2,t\right)=\frac{1}{4}\sqrt{N}w\left(q_1\right)w\left(q_2\right)A\left(q_1,t\right)A\left(q_2,t\right)\left(1+\frac{q_1}{\left|q_1\right|}\frac{q_2}{\left|q_2\right|}\cos\left(\frac{qa}{2}\right)\right) \tag{6.69}$$

Thus:

$$\begin{aligned}&\left\langle F\left(q,q_1,q_2,0\right)F\left(q,q_1,q_2,t\right)\right\rangle=\\&\frac{1}{16}Nw^2\left(q_1\right)w^2\left(q_2\right)\left(1+\frac{q_1}{\left|q_1\right|}\frac{q_2}{\left|q_2\right|}\cos\left(\frac{qa}{2}\right)\right)^2\left\langle A\left(q_1,0\right)A\left(q_1,t\right)A\left(q_2,0\right)A\left(q_2,t\right)\right\rangle\end{aligned} \tag{6.70}$$

Hence, it implies that:

$$\left\langle F\left(q,q_1,q_2,0\right)F\left(q,q_1,q_2,t\right)\right\rangle=\left\langle F\left(q,-q_1,-q_2,0\right)F\left(q,-q_1,-q_2,t\right)\right\rangle \tag{6.71}$$

Using the above relation:

$$E_{corr}^{NM}\left(q,t\right)=\left[\begin{array}{l}\left(q_2=q_1+q\right):\\\sum\limits_{-\frac{\pi}{a}<q_1<\frac{\pi}{a}}\left[\begin{array}{l}\left\langle F\left(q,q_1,q_2,0\right)F\left(q,q_1,q_2,t\right)\right\rangle\exp\left(i\left(\left(w\left(q_1\right)-w\left(q_2\right)\right)t\right)\right)\\+\left\langle F\left(q,q_1,-q_2,0\right)F\left(q,q_1,-q_2,t\right)\right\rangle\exp\left(i\left(\left(w\left(q_1\right)+w\left(q_2\right)\right)t\right)\right)\\+\left\langle F\left(q,q_1,-q_2,0\right)F\left(q,q_1,-q_2,t\right)\right\rangle\exp\left(-i\left(\left(w\left(q_1\right)+w\left(q_2\right)\right)t\right)\right)\\+\left\langle F\left(q,q_1,q_2,0\right)F\left(q,q_1,q_2,t\right)\right\rangle\exp\left(-i\left(\left(w\left(q_1\right)-w\left(q_2\right)\right)t\right)\right)\end{array}\right]\end{array}\right] \tag{6.72}$$

Combining terms gives:

$$E_{corr}^{NM}(q,t)=\left[\begin{array}{c}(q_2=q_1+q):\\ 2\sum\limits_{-\frac{\pi}{a}<q_1<\frac{\pi}{a}}\left[\begin{array}{l}\left\langle F(q,q_1,q_2,0)F(q,q_1,q_2,t)\right\rangle\cos\left(\left(w(q_1)-w(q_2)\right)t\right)\\ +\left\langle F(q,q_1,-q_2,0)F(q,q_1,-q_2,t)\right\rangle\cos\left(\left(w(q_1)+w(q_2)\right)t\right)\end{array}\right]\end{array}\right] \tag{6.73}$$

For a harmonic interaction, the mode amplitudes do not interact and are independent of time. Thus:

$$\begin{array}{l}\left\langle F(q,q_1,q_2,0)F(q,q_1,q_2,t)\right\rangle\\ \frac{1}{4N}\left(1+\frac{q_1}{|q_1|}\frac{q_2}{|q_2|}\cos\left(\frac{qa}{2}\right)\right)^2\left(\frac{1}{2}Nw^2(q_1)\left\langle A^2(q_1)\right\rangle\right)\left(\frac{1}{2}Nw^2(q_2)\left\langle A^2(q_2)\right\rangle\right)\end{array} \tag{6.74}$$

Using the relation for energy associated with a mode gives:

$$\left\langle F^2(q,q_1,q_2)\right\rangle=\frac{1}{4N}(k_BT)^2\left(1+\frac{q_1}{|q_1|}\frac{q_2}{|q_2|}\cos\left(\frac{qa}{2}\right)\right)^2 \tag{6.75}$$

Thus the energy normal mode correlation for a perfect 1-D harmonic oscillator chain is given by:

$$E_{corr}^{NM}(q,t)=\frac{(k_BT)^2}{2N}\sum_{-\frac{\pi}{a}<q_1<\frac{\pi}{a}}\left[\begin{array}{c}(q_2=q_1+q):\\ \left(1+\frac{q_1}{|q_1|}\frac{q_2}{|q_2|}\cos\left(\frac{qa}{2}\right)\right)^2\cos\left(\left(w(q_1)-w(q_2)\right)t\right)\\ +\left(1-\frac{q_1}{|q_1|}\frac{q_2}{|q_2|}\cos\left(\frac{qa}{2}\right)\right)^2\cos\left(\left(w(q_1)+w(q_2)\right)t\right)\end{array}\right] \tag{6.76}$$

6.5.2 Heat current normal mode correlation

Substituting the expression for the virial heat current normal mode projection from Eqn. (6.59) into Eqn. (6.16) to evaluate the time correlation of the normal mode projection:

$$
\begin{aligned}
&J_{corr}^{NM}(q,t) = \\
&\frac{N}{16V^2}\times \\
&\qquad (q_{2A}' = q_1' - q);(q_{2B}' = q_1' + q);(q_{2C}' = -q_1' - q);(q_{2D}' = -q_1' + q); \\
&\qquad (q_{2A} = q_1 - q);(q_{2B} = q_1 + q);(q_{2C} = -q_1 - q);(q_{2D} = -q_1 + q): \\
&\qquad w(q_1)w(q_1')v_g(q_1)v_g(q_1')A(q_1,t)A(q_1',0)\times \\
&\sum_{-\frac{\pi}{a}<q_1'<\frac{\pi}{a}}\sum_{-\frac{\pi}{a}<q_1<\frac{\pi}{a}}\left\langle \begin{bmatrix} A(q_{2A}',0)w(q_{2A}')\exp\left(i\left(-\varphi(q_1')+\varphi(q_{2A}')\right)\right) \\ +A(q_{2B}',0)w(q_{2B}')\exp\left(-i\left(-\varphi(q_1')+\varphi(q_{2B}')\right)\right) \\ -A(q_{2C}',0)w(q_{2C}')\exp\left(-i\left(-\varphi(q_1')-\varphi(q_{2C}')\right)\right) \\ -A(q_{2D}',0)w(q_{2D}')\exp\left(i\left(-\varphi(q_1')-\varphi(q_{2D}')\right)\right) \end{bmatrix} \right. \\
&\qquad \left. \times \begin{bmatrix} A(q_{2A},t)w(q_{2A})\exp\left(-i\left(w(q_1)-w(q_{2A})\right)t-\varphi(q_1)+\varphi(q_{2A})\right) \\ +A(q_{2B},t)w(q_{2B})\exp\left(i\left(\left(w(q_1)-w(q_{2B})\right)t-\varphi(q_1)+\varphi(q_{2B})\right)\right) \\ -A(q_{2C},t)w(q_{2C})\exp\left(i\left(\left(w(q_1)+w(q_{2C})\right)t-\varphi(q_1)-\varphi(q_{2C})\right)\right) \\ -A(q_{2D},t)w(q_{2D})\exp\left(-i\left(\left(w(q_1)+w(q_{2D})\right)t-\varphi(q_1)-\varphi(q_{2D})\right)\right) \end{bmatrix} \right\rangle
\end{aligned}
\tag{6.77}
$$

Consider the product of the first term in the lower bracket and with all the terms in the upper bracket:

$$
\begin{aligned}
&(q_{2A}' = q_1' - q);(q_{2B}' = q_1' + q);(q_{2C}' = -q_1' - q);(q_{2D}' = -q_1' + q);\\
&(q_{2A} = q_1 - q);(q_{2B} = q_1 + q);(q_{2C} = -q_1 - q);(q_{2D} = -q_1 + q):\\
&= \sum_{-\frac{\pi}{a}<q_1'<\frac{\pi}{a}} \sum_{-\frac{\pi}{a}<q_1<\frac{\pi}{a}} \left\langle \begin{bmatrix} w(q_1)w(q_1')v_g(q_1)v_g(q_1')A(q_1,t)A(q_1',0)\times \\ \left(\begin{matrix} A(q_{2A}',0)w(q_{2A}')A(q_{2A},t)w(q_{2A})\times \\ \exp\left(-i\left(w(q_1)-w(q_{2A})\right)t-\varphi(q_1)+\varphi(q_{2A})+\varphi(q_1')-\varphi(q_{2A}')\right)\end{matrix}\right) \\ +\left(\begin{matrix} A(q_{2B}',0)w(q_{2B}')A(q_{2A},t)w(q_{2A})\times \\ \exp\left(-i\left(w(q_1)-w(q_{2A})\right)t-\varphi(q_1)+\varphi(q_{2A})-\varphi(q_1')+\varphi(q_{2B}')\right)\end{matrix}\right) \\ -\left(\begin{matrix} A(q_{2C}',0)w(q_{2C}')A(q_{2A},t)w(q_{2A})\times \\ \exp\left(-i\left(w(q_1)-w(q_{2A})\right)t-\varphi(q_1)+\varphi(q_{2A})-\varphi(q_1')-\varphi(q_{2C}')\right)\end{matrix}\right) \\ -\left(\begin{matrix} A(q_{2D}',0)w(q_{2D}')A(q_{2A},t)w(q_{2A})\times \\ \exp\left(-i\left(w(q_1)-w(q_{2A})\right)t-\varphi(q_1)+\varphi(q_{2A})+\varphi(q_1')+\varphi(q_{2D}')\right)\end{matrix}\right) \end{bmatrix} \right\rangle
\end{aligned}
\tag{6.78}
$$

Non-zero correlations are possible only if the phase angles cancel off as the ensemble average of the exponential of any phase angle goes to zero. This gives $q_1 = q_1'$:

$$
\begin{aligned}
&(q_{2A} = q_1 - q);(q_{2B} = q_1 + q);(q_{2C} = -q_1 - q);(q_{2D} = -q_1 + q):\\
&= \sum_{-\frac{\pi}{a}<q_1<\frac{\pi}{a}} \left\langle \begin{bmatrix} w^2(q_1)v_g{}^2(q_1)A(q_1,t)A(q_1,0)\times \\ \left(\begin{matrix} A(q_{2A},0)A(q_{2A},t)w^2(q_{2A})\times \\ \exp\left(-i\left(w(q_1)-w(q_{2A})\right)t\right)\end{matrix}\right) \\ +\left(\begin{matrix} A(q_{2B},0)w(q_{2B})A(q_{2A},t)w(q_{2A})\times \\ \exp\left(-i\left(w(q_1)-w(q_{2A})\right)t-2\varphi(q_1)+\varphi(q_{2A})+\varphi(q_{2B})\right)\end{matrix}\right) \\ -\left(\begin{matrix} A(q_{2C},0)w(q_{2C})A(q_{2A},t)w(q_{2A})\times \\ \exp\left(-i\left(w(q_1)-w(q_{2A})\right)t-2\varphi(q_1)+\varphi(q_{2A})--\varphi(q_{2C})\right)\end{matrix}\right) \\ -\left(\begin{matrix} A(q_{2D},0)w(q_{2D})A(q_{2A},t)w(q_{2A})\times \\ \exp\left(-i\left(w(q_1)-w(q_{2A})\right)t+\varphi(q_{2A})+\varphi(q_{2D})\right)\end{matrix}\right) \end{bmatrix} \right\rangle
\end{aligned}
\tag{6.79}
$$

The phase angles again will not cancel off for the last three terms giving a zero ensemble average for the exponential:

$$\begin{aligned}&\left(q_{2A}=q_1-q\right);\left(q_{2B}=q_1+q\right);\left(q_{2C}=-q_1-q\right);\left(q_{2D}=-q_1+q\right):\\ &=\sum_{-\frac{\pi}{a}<q_1<\frac{\pi}{a}}\left\langle\begin{matrix}w^2\left(q_1\right)v_g{}^2\left(q_1\right)A\left(q_1,t\right)A\left(q_1,0\right)A\left(q_{2A},0\right)A\left(q_{2A},t\right)w^2\left(q_{2A}\right)\\ \times\exp\left(-i\left(w\left(q_1\right)-w\left(q_{2A}\right)\right)t\right)\end{matrix}\right\rangle\end{aligned} \tag{6.80}$$

A similar argument can be used for the other terms from the product in Eqn. (6.77) to give:

$$\begin{aligned}&J_{corr}^{NM}\left(q,t\right)=\frac{N}{16V^2}\times\\ &\left(q_{2A}=q_1-q\right);\left(q_{2B}=q_1+q\right);\left(q_{2C}=-q_1-q\right);\left(q_{2D}=-q_1+q\right):\\ &\sum_{-\frac{\pi}{a}<q_1<\frac{\pi}{a}}\left\langle\begin{matrix}w^2\left(q_1\right)v_g{}^2\left(q_1\right)A\left(q_1,t\right)A\left(q_1,0\right)\times\\ \left[\begin{matrix}A\left(q_{2A},0\right)A\left(q_{2A},t\right)w^2\left(q_{2A}\right)\exp\left(-i\left(\left(w\left(q_1\right)-w\left(q_{2A}\right)\right)t\right)\right)\\ +A\left(q_{2B},0\right)A\left(q_{2B},t\right)w^2\left(q_{2B}\right)\exp\left(i\left(\left(w\left(q_1\right)-w\left(q_{2B}\right)\right)t\right)\right)\\ +A\left(q_{2C},0\right)A\left(q_{2C},t\right)w^2\left(q_{2C}\right)\exp\left(i\left(\left(w\left(q_1\right)+w\left(q_{2C}\right)\right)t\right)\right)\\ +A\left(q_{2D},0\right)A\left(q_{2D},t\right)w^2\left(q_{2D}\right)\exp\left(-i\left(\left(w\left(q_1\right)+w\left(q_{2D}\right)\right)t\right)\right)\end{matrix}\right]\end{matrix}\right\rangle\end{aligned} \tag{6.81}$$

Splitting the terms and removing constants out from the ensemble average:

$$J_{corr}^{NM}(q,t)=\frac{N}{16V^2}\times$$
$$\left[\begin{array}{l}\sum\limits_{-\frac{\pi}{a}<q_1<\frac{\pi}{a}}\left(q_{2A}=q_1-q\right):\left(w(q_1)w(q_{2A})v_g(q_1)\right)^2\times \\ \left\langle A(q_1,t)A(q_1,0)A(q_{2A},0)A(q_{2A},t)\right\rangle\exp\left(i\left(\left(w(q_1)-w(q_{2A})\right)t\right)\right) \\ +\sum\limits_{-\frac{\pi}{a}<q_1<\frac{\pi}{a}}\left(q_{2B}=q_1+q\right):\left(w(q_1)w(q_{2B})v_g(q_1)\right)^2\times \\ \left\langle A(q_1,t)A(q_1,0)A(q_{2B},0)A(q_{2B},t)\right\rangle\exp\left(-i\left(\left(w(q_1)-w(q_{2B})\right)t\right)\right) \\ +\sum\limits_{-\frac{\pi}{a}<q_1<\frac{\pi}{a}}\left(q_{2C}=-q_1-q\right):\left(w(q_1)w(q_{2C})v_g(q_1)\right)^2\times \\ \left\langle A(q_1,t)A(q_1,0)A(q_{2C},0)A(q_{2C},t)\right\rangle\exp\left(-i\left(\left(w(q_1)+w(q_{2C})\right)t\right)\right) \\ +\sum\limits_{-\frac{\pi}{a}<q_1<\frac{\pi}{a}}\left(q_{2D}=-q_1+q\right):\left(w(q_1)w(q_{2D})v_g(q_1)\right)^2\times \\ \left\langle A(q_1,t)A(q_1,0)A(q_{2D},0)A(q_{2D},t)\right\rangle\exp\left(i\left(\left(w(q_1)+w(q_{2D})\right)t\right)\right)\end{array}\right] \tag{6.82}$$

Recombining terms by using symmetry:

$$J_{corr}^{NM}(q,t)=\frac{N}{16V^2}\times$$
$$\left[\begin{array}{l}\left(q_{2A}=q_1-q\right):\left(w(q_1)w(q_{2A})v_g(q_1)\right)^2\times \\ \sum\limits_{-\frac{\pi}{a}<q_1<\frac{\pi}{a}}\left[\begin{array}{l}\left\langle A(q_1,t)A(q_1,0)A(q_{2A},0)A(q_{2A},t)\right\rangle\exp\left(i\left(\left(w(q_1)-w(q_{2A})\right)t\right)\right) \\ +\left\langle A(q_1,t)A(q_1,0)A(-q_{2A},0)A(-q_{2A},t)\right\rangle\exp\left(i\left(\left(w(q_1)+w(q_{2A})\right)t\right)\right)\end{array}\right] \\ \left(q_{2C}=-q_1-q\right):\left(w(q_1)w(q_{2C})v_g(q_1)\right)^2\times \\ +\sum\limits_{-\frac{\pi}{a}<q_1<\frac{\pi}{a}}\left[\begin{array}{l}\left\langle A(q_1,t)A(q_1,0)A(q_{2C},0)A(q_{2C},t)\right\rangle\exp\left(-i\left(\left(w(q_1)+w(q_{2C})\right)t\right)\right) \\ +\left\langle A(q_1,t)A(q_1,0)A(-q_{2C},0)A(-q_{2C},t)\right\rangle\exp\left(-i\left(\left(w(q_1)-w(q_{2C})\right)t\right)\right)\end{array}\right]\end{array}\right] \tag{6.83}$$

Further simplifying using symmetry:

$$J_{corr}^{NM}(q,t)=\frac{N}{16V^2}\times$$
$$\left[\begin{array}{l}(q_2=q_1-q):\left(w(q_1)w(q_2)v_g(q_1)\right)^2\times\\ \sum\limits_{-\frac{\pi}{a}<q_1<\frac{\pi}{a}}\left[\begin{array}{l}\left\langle A(q_1,t)A(q_1,0)A(q_2,0)A(q_2,t)\right\rangle\exp\left(i\left(\left(w(q_1)-w(q_2)\right)t\right)\right)\\ +\left\langle A(q_1,t)A(q_1,0)A(-q_2,0)A(-q_2,t)\right\rangle\exp\left(i\left(\left(w(q_1)+w(q_2)\right)t\right)\right)\\ +\left\langle A(-q_1,t)A(-q_1,0)A(q_2,0)A(q_2,t)\right\rangle\exp\left(-i\left(\left(w(q_1)+w(q_2)\right)t\right)\right)\\ +\left\langle A(-q_1,t)A(-q_1,0)A(-q_2,0)A(-q_2,t)\right\rangle\exp\left(-i\left(\left(w(q_1)-w(q_2)\right)t\right)\right)\end{array}\right]\end{array}\right] \quad (6.84)$$

Symmetry of the wave vector space implies that:

$$\left\langle A(q_1,t)A(q_1,0)A(q_2,0)A(q_2,t)\right\rangle=\left\langle A(-q_1,t)A(-q_1,0)A(-q_2,0)A(-q_2,t)\right\rangle \quad (6.85)$$

Using the above condition gives:

$$J_{corr}^{NM}(q,t)=\frac{N}{16V^2}\times$$
$$\left[\begin{array}{l}(q_2=q_1-q):\left(w(q_1)w(q_2)v_g(q_1)\right)^2\times\\ \sum\limits_{-\frac{\pi}{a}<q_1<\frac{\pi}{a}}\left[\begin{array}{l}\left\langle A(q_1,t)A(q_1,0)A(q_2,0)A(q_2,t)\right\rangle\exp\left(i\left(\left(w(q_1)-w(q_2)\right)t\right)\right)\\ +\left\langle A(q_1,t)A(q_1,0)A(-q_2,0)A(-q_2,t)\right\rangle\exp\left(i\left(\left(w(q_1)+w(q_2)\right)t\right)\right)\\ +\left\langle A(q_1,t)A(q_1,0)A(-q_2,0)A(-q_2,t)\right\rangle\exp\left(-i\left(\left(w(q_1)+w(q_2)\right)t\right)\right)\\ +\left\langle A(q_1,t)A(q_1,0)A(q_2,0)A(q_2,t)\right\rangle\exp\left(-i\left(\left(w(q_1)-w(q_2)\right)t\right)\right)\end{array}\right]\end{array}\right] \quad (6.86)$$

Merging terms:

$$J_{corr}^{NM}(q,t)=$$
$$\frac{N}{8V^2}\left[\sum_{-\frac{\pi}{a}<q_1<\frac{\pi}{a}}\begin{bmatrix}(q_2=q_1-q):\left(w(q_1)w(q_2)v_g(q_1)\right)^2\times\\ \left\langle A(q_1,t)A(q_1,0)A(q_2,0)A(q_2,t)\right\rangle\cos\left(\left(w(q_1)-w(q_2)\right)t\right)\\ +\left\langle A(q_1,t)A(q_1,0)A(-q_2,0)A(-q_2,t)\right\rangle\cos\left(\left(w(q_1)+w(q_2)\right)t\right)\end{bmatrix}\right] \tag{6.87}$$

For a harmonic interaction, the mode amplitudes do not interact and are independent of time. Thus:

$$J_{corr}^{NM}(q,t)=$$
$$\frac{1}{2NV^2}\left[\sum_{-\frac{\pi}{a}<q_1<\frac{\pi}{a}}\begin{bmatrix}(q_2=q_1-q):\left(\frac{N}{2}w^2(q_1)\left\langle A^2(q_1)\right\rangle\right)\left(\frac{N}{2}w^2(q_2)\left\langle A^2(q_2)\right\rangle\right)\\ v_g{}^2(q_1)\left(\cos\left(\left(w(q_1)-w(q_2)\right)t\right)+\cos\left(\left(w(q_1)+w(q_2)\right)t\right)\right)\end{bmatrix}\right] \tag{6.88}$$

Thus, using the relation for energy associated with a mode, the heat current normal mode correlation for a perfect 1-D harmonic oscillator chain is given by:

$$J_{corr}^{NM}(q,t)=$$
$$\frac{(k_BT)^2}{2NV^2}\left[\sum_{-\frac{\pi}{a}<q_1<\frac{\pi}{a}}\begin{bmatrix}(q_2=q_1-q):\\ v_g{}^2(q_1)\left(\cos\left(\left(w(q_1)-w(q_2)\right)t\right)+\cos\left(\left(w(q_1)+w(q_2)\right)t\right)\right)\end{bmatrix}\right] \tag{6.89}$$

6.6 Dispersion

The energy and heat current normal mode correlation in terms of pair contributions from individual phonon modes is derived in the previous section. It is also shown previously that

for a perfect harmonic oscillaotor chain, the correlation depends only on the system temperature as well as the individual phonon frequencies and group velocities; the exact expressions are derived in Chapter 2. On substitution, the dispersion relation for the energy and heat current normal modes can be obtained. The following relations will be used for more compact notation:

$$w(q) = C_w \left| \sin\left(\frac{qa}{2} \right) \right| \tag{6.90}$$

$$v_g(q) = C_v \left| \cos\left(\frac{qa}{2} \right) \right| \frac{q}{|q|} \tag{6.91}$$

where:

$$C_w = \sqrt{\frac{4C}{m}} \tag{6.92}$$

$$C_v = a\sqrt{\frac{C}{m}} \tag{6.93}$$

6.6.1 Energy normal mode dispersion

Substituting the expressions for the frequencies and group velocities for a linear chain into Eqn. (6.76):

$$E_{corr}^{NM}(q,t)=\frac{(k_BT)^2}{2N}\times$$
$$\sum_{-\frac{\pi}{a}<q_1<\frac{\pi}{a}}\left[\begin{array}{l}\left(1+\frac{q_1}{|q_1|}\frac{q_1+q}{|q_1+q|}\cos\left(\frac{qa}{2}\right)\right)^2\cos\left(C_w\left(\left|\sin\left(\frac{q_1a}{2}\right)\right|-\left|\sin\left(\frac{(q_1+q)a}{2}\right)\right|\right)t\right)\\+\left(1-\frac{q_1}{|q_1|}\frac{q_1+q}{|q_1+q|}\cos\left(\frac{qa}{2}\right)\right)^2\cos\left(C_w\left(\left|\sin\left(\frac{q_1a}{2}\right)\right|+\left|\sin\left(\frac{(q_1+q)a}{2}\right)\right|\right)t\right)\end{array}\right] \tag{6.94}$$

Separating terms:

$$E_{corr}^{NM}(q,t)=\frac{(k_BT)^2}{2N}\times$$
$$\left[\begin{array}{l}\sum_{-\frac{\pi}{a}<q_1<-q}\left[\begin{array}{l}\left(1+\frac{q_1}{|q_1|}\frac{q_1+q}{|q_1+q|}\cos\left(\frac{qa}{2}\right)\right)^2\cos\left(C_w\left(\left|\sin\left(\frac{q_1a}{2}\right)\right|-\left|\sin\left(\frac{(q_1+q)a}{2}\right)\right|\right)t\right)\\+\left(1-\frac{q_1}{|q_1|}\frac{q_1+q}{|q_1+q|}\cos\left(\frac{qa}{2}\right)\right)^2\cos\left(C_w\left(\left|\sin\left(\frac{q_1a}{2}\right)\right|+\left|\sin\left(\frac{(q_1+q)a}{2}\right)\right|\right)t\right)\end{array}\right]\\\sum_{-q<q_1<0}\left[\begin{array}{l}\left(1+\frac{q_1}{|q_1|}\frac{q_1+q}{|q_1+q|}\cos\left(\frac{qa}{2}\right)\right)^2\cos\left(C_w\left(\left|\sin\left(\frac{q_1a}{2}\right)\right|-\left|\sin\left(\frac{(q_1+q)a}{2}\right)\right|\right)t\right)\\+\left(1-\frac{q_1}{|q_1|}\frac{q_1+q}{|q_1+q|}\cos\left(\frac{qa}{2}\right)\right)^2\cos\left(C_w\left(\left|\sin\left(\frac{q_1a}{2}\right)\right|+\left|\sin\left(\frac{(q_1+q)a}{2}\right)\right|\right)t\right)\end{array}\right]\\\sum_{0<q_1<\frac{\pi}{a}}\left[\begin{array}{l}\left(1+\frac{q_1}{|q_1|}\frac{q_1+q}{|q_1+q|}\cos\left(\frac{qa}{2}\right)\right)^2\cos\left(C_w\left(\left|\sin\left(\frac{q_1a}{2}\right)\right|-\left|\sin\left(\frac{(q_1+q)a}{2}\right)\right|\right)t\right)\\+\left(1-\frac{q_1}{|q_1|}\frac{q_1+q}{|q_1+q|}\cos\left(\frac{qa}{2}\right)\right)^2\cos\left(C_w\left(\left|\sin\left(\frac{q_1a}{2}\right)\right|+\left|\sin\left(\frac{(q_1+q)a}{2}\right)\right|\right)t\right)\end{array}\right]\end{array}\right] \tag{6.95}$$

Evaluating the modulus operator:

$$E_{corr}^{NM}(q,t)=\frac{(k_BT)^2}{2N}\times$$
$$\left[\begin{array}{l}
\sum\limits_{-\frac{\pi}{a}<q_1<-q}\left[\begin{array}{l}\left(1+\cos\left(\frac{qa}{2}\right)\right)^2\cos\left(C_w\left(-\sin\left(\frac{q_1a}{2}\right)+\sin\left(\frac{(q_1+q)a}{2}\right)\right)t\right)\\ +\left(1-\cos\left(\frac{qa}{2}\right)\right)^2\cos\left(C_w\left(-\sin\left(\frac{q_1a}{2}\right)-\sin\left(\frac{(q_1+q)a}{2}\right)\right)t\right)\end{array}\right]\\
\sum\limits_{-q<q_1<0}\left[\begin{array}{l}\left(1-\cos\left(\frac{qa}{2}\right)\right)^2\cos\left(C_w\left(-\sin\left(\frac{q_1a}{2}\right)-\sin\left(\frac{(q_1+q)a}{2}\right)\right)t\right)\\ +\left(1+\cos\left(\frac{qa}{2}\right)\right)^2\cos\left(C_w\left(-\sin\left(\frac{q_1a}{2}\right)+\sin\left(\frac{(q_1+q)a}{2}\right)\right)t\right)\end{array}\right]\\
\sum\limits_{0<q_1<\frac{\pi}{a}}\left[\begin{array}{l}\left(1+\cos\left(\frac{qa}{2}\right)\right)^2\cos\left(C_w\left(\sin\left(\frac{q_1a}{2}\right)-\sin\left(\frac{(q_1+q)a}{2}\right)\right)t\right)\\ +\left(1-\cos\left(\frac{qa}{2}\right)\right)^2\cos\left(C_w\left(\sin\left(\frac{q_1a}{2}\right)+\sin\left(\frac{(q_1+q)a}{2}\right)\right)t\right)\end{array}\right]
\end{array}\right] \tag{6.96}$$

Merging terms:

$$E_{corr}^{NM}(q,t)=\frac{(k_BT)^2}{2N}\times$$
$$\left[\begin{array}{l}
\sum\limits_{-\frac{\pi}{a}<q_1<0}\left[\begin{array}{l}\left(1+\cos\left(\frac{qa}{2}\right)\right)^2\cos\left(C_w\left(-\sin\left(\frac{q_1a}{2}\right)+\sin\left(\frac{(q_1+q)a}{2}\right)\right)t\right)\\ +\left(1-\cos\left(\frac{qa}{2}\right)\right)^2\cos\left(C_w\left(-\sin\left(\frac{q_1a}{2}\right)-\sin\left(\frac{(q_1+q)a}{2}\right)\right)t\right)\end{array}\right]\\
\sum\limits_{0<q_1<\frac{\pi}{a}}\left[\begin{array}{l}\left(1+\cos\left(\frac{qa}{2}\right)\right)^2\cos\left(C_w\left(\sin\left(\frac{q_1a}{2}\right)-\sin\left(\frac{(q_1+q)a}{2}\right)\right)t\right)\\ +\left(1-\cos\left(\frac{qa}{2}\right)\right)^2\cos\left(C_w\left(\sin\left(\frac{q_1a}{2}\right)+\sin\left(\frac{(q_1+q)a}{2}\right)\right)t\right)\end{array}\right]
\end{array}\right] \tag{6.97}$$

Changing limits of summation:

$$E_{corr}^{NM}(q,t)=\frac{(k_BT)^2}{2N}\times$$
$$\left[\sum_{0<q_1<\frac{\pi}{a}}\left[\begin{array}{l}\left(1+\cos\left(\frac{qa}{2}\right)\right)^2\cos\left(C_w\left(\sin\left(\frac{q_1a}{2}\right)+\sin\left(\frac{(-q_1+q)a}{2}\right)\right)t\right)\\+\left(1-\cos\left(\frac{qa}{2}\right)\right)^2\cos\left(C_w\left(\sin\left(\frac{q_1a}{2}\right)-\sin\left(\frac{(-q_1+q)a}{2}\right)\right)t\right)\end{array}\right]\right.$$
$$\left.\sum_{0<q_1<\frac{\pi}{a}}\left[\begin{array}{l}\left(1+\cos\left(\frac{qa}{2}\right)\right)^2\cos\left(C_w\left(\sin\left(\frac{q_1a}{2}\right)-\sin\left(\frac{(q_1+q)a}{2}\right)\right)t\right)\\+\left(1-\cos\left(\frac{qa}{2}\right)\right)^2\cos\left(C_w\left(\sin\left(\frac{q_1a}{2}\right)+\sin\left(\frac{(q_1+q)a}{2}\right)\right)t\right)\end{array}\right]\right] \tag{6.98}$$

Combining terms:

$$E_{corr}^{NM}(q,t)=\frac{(k_BT)^2}{2N}\times$$
$$\sum_{0<q_1<\frac{\pi}{a}}\left[\begin{array}{l}\left(1+\cos\left(\frac{qa}{2}\right)\right)^2\cos\left(C_w\left(\sin\left(\frac{q_1a}{2}\right)-\sin\left(\frac{(q_1+q)a}{2}\right)\right)t\right)\\+\left(1-\cos\left(\frac{qa}{2}\right)\right)^2\cos\left(C_w\left(\sin\left(\frac{q_1a}{2}\right)+\sin\left(\frac{(q_1+q)a}{2}\right)\right)t\right)\\\left(1+\cos\left(\frac{qa}{2}\right)\right)^2\cos\left(C_w\left(\sin\left(\frac{q_1a}{2}\right)+\sin\left(\frac{(-q_1+q)a}{2}\right)\right)t\right)\\+\left(1-\cos\left(\frac{qa}{2}\right)\right)^2\cos\left(C_w\left(\sin\left(\frac{q_1a}{2}\right)-\sin\left(\frac{(-q_1+q)a}{2}\right)\right)t\right)\end{array}\right] \tag{6.99}$$

Expanding the sine terms:

$$E_{corr}^{NM}(q,t)=\frac{(k_BT)^2}{2N}\times$$
$$\sum_{0<q_1<\frac{\pi}{a}}\left[\begin{array}{l}\left(1+\cos\left(\frac{qa}{2}\right)\right)^2\cos\left(C_w\left(\sin\left(\frac{q_1a}{2}\right)-\sin\left(\frac{q_1a}{2}\right)\cos\left(\frac{qa}{2}\right)-\cos\left(\frac{q_1a}{2}\right)\sin\left(\frac{qa}{2}\right)\right)t\right)\\+\left(1-\cos\left(\frac{qa}{2}\right)\right)^2\cos\left(C_w\left(\sin\left(\frac{q_1a}{2}\right)+\sin\left(\frac{q_1a}{2}\right)\cos\left(\frac{qa}{2}\right)+\cos\left(\frac{q_1a}{2}\right)\sin\left(\frac{qa}{2}\right)\right)t\right)\\\left(1+\cos\left(\frac{qa}{2}\right)\right)^2\cos\left(C_w\left(\sin\left(\frac{q_1a}{2}\right)-\sin\left(\frac{q_1a}{2}\right)\cos\left(\frac{qa}{2}\right)+\cos\left(\frac{q_1a}{2}\right)\sin\left(\frac{qa}{2}\right)\right)t\right)\\+\left(1-\cos\left(\frac{qa}{2}\right)\right)^2\cos\left(C_w\left(\sin\left(\frac{q_1a}{2}\right)+\sin\left(\frac{q_1a}{2}\right)\cos\left(\frac{qa}{2}\right)-\cos\left(\frac{q_1a}{2}\right)\sin\left(\frac{qa}{2}\right)\right)t\right)\end{array}\right] \quad (6.100)$$

Simplifying:

$$E_{corr}^{NM}(q,t)=\frac{(k_BT)^2}{2N}\times$$
$$\sum_{0<q_1<\frac{\pi}{a}}\left[\begin{array}{l}\left(1+\cos\left(\frac{qa}{2}\right)\right)^2\cos\left(C_w\left(\sin\left(\frac{q_1a}{2}\right)\left(1-\cos\left(\frac{qa}{2}\right)\right)-\cos\left(\frac{q_1a}{2}\right)\sin\left(\frac{qa}{2}\right)\right)t\right)\\+\left(1-\cos\left(\frac{qa}{2}\right)\right)^2\cos\left(C_w\left(\sin\left(\frac{q_1a}{2}\right)\left(1+\cos\left(\frac{qa}{2}\right)\right)+\cos\left(\frac{q_1a}{2}\right)\sin\left(\frac{qa}{2}\right)\right)t\right)\\\left(1+\cos\left(\frac{qa}{2}\right)\right)^2\cos\left(C_w\left(\sin\left(\frac{q_1a}{2}\right)\left(1-\cos\left(\frac{qa}{2}\right)\right)+\cos\left(\frac{q_1a}{2}\right)\sin\left(\frac{qa}{2}\right)\right)t\right)\\+\left(1-\cos\left(\frac{qa}{2}\right)\right)^2\cos\left(C_w\left(\sin\left(\frac{q_1a}{2}\right)\left(1+\cos\left(\frac{qa}{2}\right)\right)-\cos\left(\frac{q_1a}{2}\right)\sin\left(\frac{qa}{2}\right)\right)t\right)\end{array}\right] \quad (6.101)$$

Using the relation given in Eqn. (6.90):

$$E_{corr}^{NM}(q,t)=\frac{(k_BT)^2}{2N}\times$$
$$\sum_{0<q_1<\frac{\pi}{a}}\left[\begin{array}{l}\left(1-\cos\left(\frac{qa}{2}\right)\right)^2\cos\left(\left(w(q_1)\left(1+\cos\left(\frac{qa}{2}\right)\right)+w(q)\cos\left(\frac{q_1a}{2}\right)\right)t\right)\\+\left(1+\cos\left(\frac{qa}{2}\right)\right)^2\cos\left(\left(w(q_1)\left(1-\cos\left(\frac{qa}{2}\right)\right)-w(q)\cos\left(\frac{q_1a}{2}\right)\right)t\right)\\+\left(1+\cos\left(\frac{qa}{2}\right)\right)^2\cos\left(\left(w(q_1)\left(1-\cos\left(\frac{qa}{2}\right)\right)+w(q)\cos\left(\frac{q_1a}{2}\right)\right)t\right)\\+\left(1-\cos\left(\frac{qa}{2}\right)\right)^2\cos\left(\left(w(q_1)\left(1+\cos\left(\frac{qa}{2}\right)\right)-w(q)\cos\left(\frac{q_1a}{2}\right)\right)t\right)\end{array}\right] \quad (6.102)$$

Thus the energy normal mode correlation can be simplified as contributions from the four terms as shown in the Eqn. (6.102) above. The frequency of the cosine term due to each of these terms is shown in *Figure 6.2* to *Figure 6.5* as a function of wave vectors q and q_1.

The first term is given by $\cos\left(\left(w(q_1)\left(1+\cos\left(\frac{qa}{2}\right)\right)+w(q)\cos\left(\frac{q_1a}{2}\right)\right)t\right)$

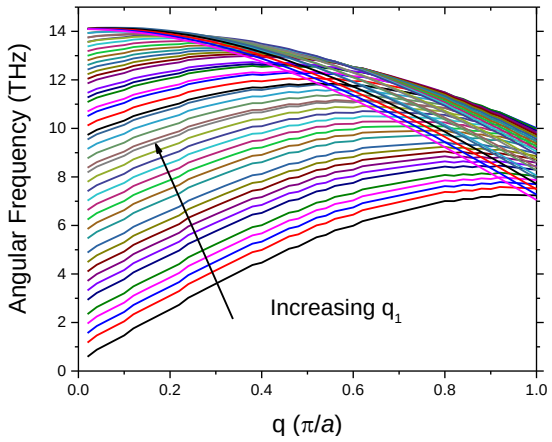

Figure 6.2: Variation of frequency with wave vector q for different values of q_1 from the first term in Eqn. (6.102).

The second term is given by $\cos\left(\left(w(q_1)\left(1-\cos\left(\frac{qa}{2}\right)\right)-w(q)\cos\left(\frac{q_1 a}{2}\right)\right)t\right)$

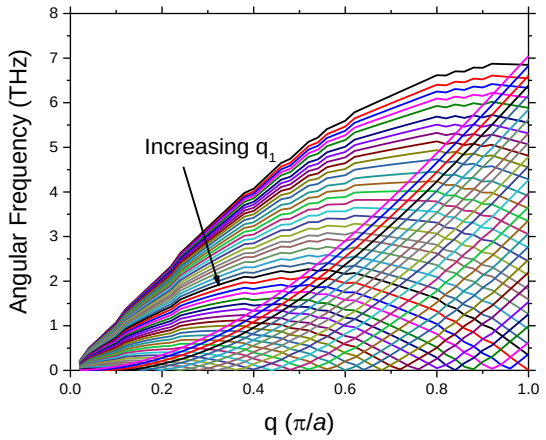

Figure 6.3: Variation of frequency with wave vector q for different values of q_1 from the second term in Eqn. (6.102).

The third term is given by $\cos\left(\left(w(q_1)\left(1-\cos\left(\frac{qa}{2}\right)\right)+w(q)\cos\left(\frac{q_1 a}{2}\right)\right)t\right)$

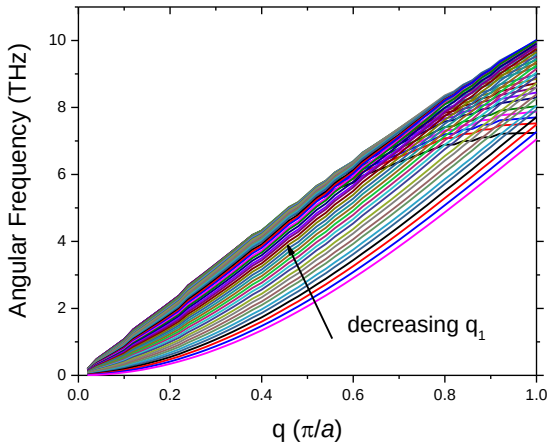

Figure 6.4: Variation of frequency with wave vector q for different values of q_1 from the third term in Eqn. (6.102).

And the fourth term is given by $\cos\left(\left(w(q_1)\left(1+\cos\left(\frac{qa}{2}\right)\right)-w(q)\cos\left(\frac{q_1 a}{2}\right)\right)t\right)$

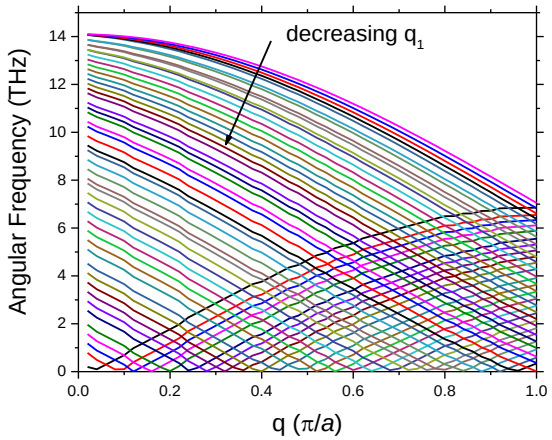

Figure 6.5: Variation of frequency with wave vector q for different values of q_1 from the fourth term in Eqn. (6.102).

Clearly, a wide spread of frequencies is observed. However, the third term from the Eqn. (6.102) contributes a narrow band as shown in *Figure 6.4*. Thus, it is expected that this term would dominate in the dispersion curve. The dispersion due to each of the terms is presented in *Figure 6.6* to *Figure 6.9*. In these figures, the dominance of each frequency for a given wave vector is represented by specific colors – bright red represents the most dominant mode while blue represents the weakest modes.

First term: $\frac{(k_B T)^2}{2N} \sum_{0<q_1<\frac{\pi}{a}} \left(1-\cos\left(\frac{qa}{2}\right)\right)^2 \cos\left(\left(w(q_1)\left(1+\cos\left(\frac{qa}{2}\right)\right)+w(q)\cos\left(\frac{q_1 a}{2}\right)\right)t\right)$

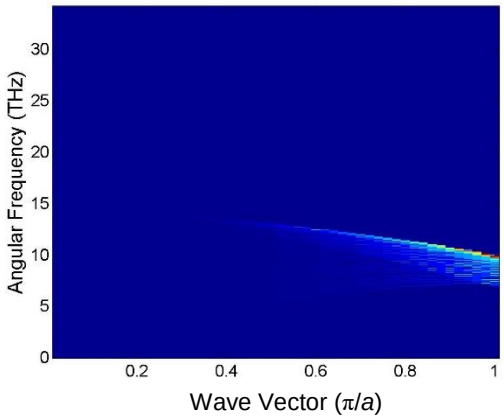

Figure 6.6: Dispersion due to the first term in Eqn. (6.102).

Second term: $\frac{(k_B T)^2}{2N} \sum_{0<q_1<\frac{\pi}{a}} \left(1+\cos\left(\frac{qa}{2}\right)\right)^2 \cos\left(\left(w(q_1)\left(1-\cos\left(\frac{qa}{2}\right)\right)-w(q)\cos\left(\frac{q_1 a}{2}\right)\right)t\right)$

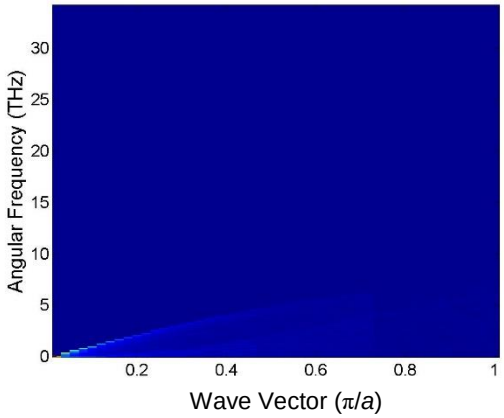

Figure 6.7: Dispersion due to the second term in Eqn. (6.102).

Third term: $\frac{(k_B T)^2}{2N} \sum_{0<q_1<\frac{\pi}{a}} \left(1+\cos\left(\frac{qa}{2}\right)\right)^2 \cos\left(\left(w(q_1)\left(1-\cos\left(\frac{qa}{2}\right)\right)+w(q)\cos\left(\frac{q_1 a}{2}\right)\right)t\right)$

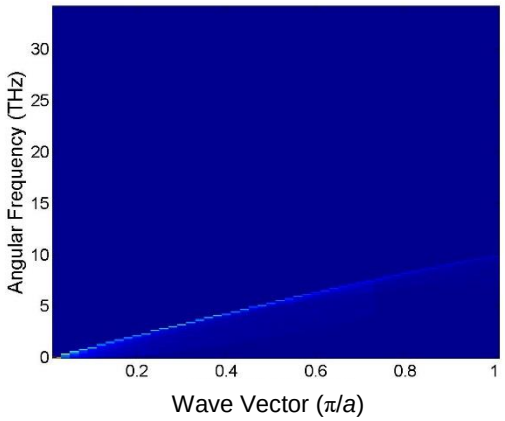

Figure 6.8: Dispersion due to the third term in Eqn. (6.102).

Fourth term: $\frac{(k_B T)^2}{2N} \sum_{0<q_1<\frac{\pi}{a}} \left(1-\cos\left(\frac{qa}{2}\right)\right)^2 \cos\left(\left(w(q_1)\left(1+\cos\left(\frac{qa}{2}\right)\right)-w(q)\cos\left(\frac{q_1 a}{2}\right)\right)t\right)$

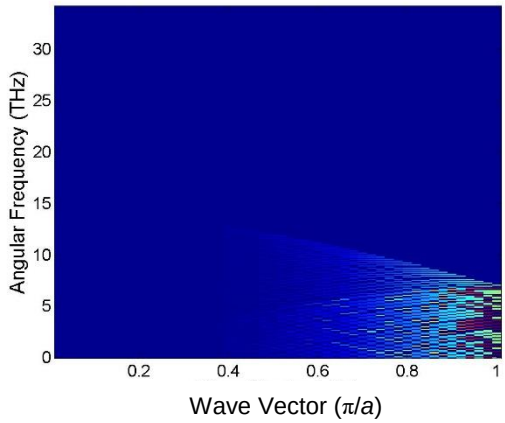

Figure 6.9: Dispersion due to the fourth term in Eqn. (6.102).

Adding the contributions from all the terms of Eqn. (6.102), the net dispersion for the energy normal mode correlation is shown in *Figure 6.10*, with the left panel having the color bar in linear scale while the right panel having the color bar in log scale to highlight the smaller peaks in frequency. As expected, the third term dominates the overall dispersion curve. Also, it is interesting to observe that the most prominent branch in the dispersion of energy normal modes is nearly linear i.e. a dispersion of a form $w = cq$. This is similar to the dispersion of a displacement wave in a continuous medium. Thus, the phase velocity of the energy waves appears to be independent of the wavelength. Another high-frequency branch is also observed which vanishes for larger wavelengths. It may be noted that unlike the phonon dispersion, the Fourier transform of the energy normal modes do not show sharp peaks but a spread around the peak values as it is populated by a contribution from several nearby frequencies.

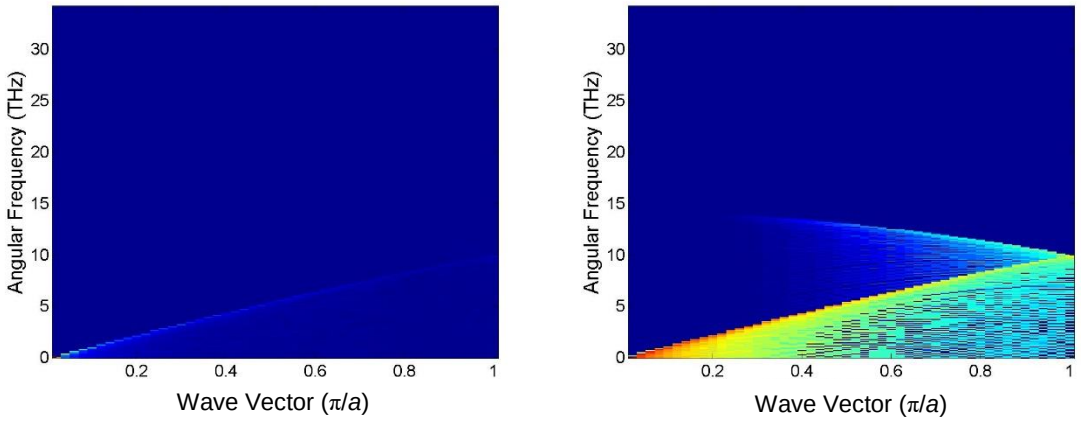

Figure 6.10: Energy normal mode dispersion from Eqn. (6.102) in (left) linear scale and (right) log scale.

6.6.2 Heat current normal mode dispersion

A similar derivation will be performed for the heat current. First define:

$$J_0 = \frac{\left(k_B T\right)^2}{2NV^2} C_v^{\,2} \tag{6.103}$$

Thus the heat current normal mode correlation is given by:

$$J_{corr}^{NM}\left(q,t\right) = \sum_{-\frac{\pi}{a}<q_1<\frac{\pi}{a}} \begin{matrix} \left(q_2 = q_1 - q\right): J_0 \cos^2\left(\frac{q_1 a}{2}\right)\times \\ \left[\left(\cos\left(\left(w\left(q_1\right)-w\left(q_2\right)\right)t\right)+\cos\left(\left(w\left(q_1\right)+w\left(q_2\right)\right)t\right)\right)\right] \end{matrix} \tag{6.104}$$

Substituting the expressions for the frequencies and group velocities for a linear chain into the above relation:

$$J_{corr}^{NM}\left(q,t\right) = \sum_{-\frac{\pi}{a}<q_1<\frac{\pi}{a}} \left[\begin{matrix} J_0 \cos^2\left(\frac{q_1 a}{2}\right)\times \\ \left[\begin{matrix} \cos\left(C_w\left(\left|\sin\left(\frac{q_1 a}{2}\right)\right|-\sin\left(\frac{q_1 a}{2}\right)\cos\left(\frac{qa}{2}\right)+\cos\left(\frac{q_1 a}{2}\right)\sin\left(\frac{qa}{2}\right)\right)t\right)+ \\ \cos\left(C_w\left(\left|\sin\left(\frac{q_1 a}{2}\right)\right|+\sin\left(\frac{q_1 a}{2}\right)\cos\left(\frac{qa}{2}\right)-\cos\left(\frac{q_1 a}{2}\right)\sin\left(\frac{qa}{2}\right)\right)t\right) \end{matrix}\right] \end{matrix}\right] \tag{6.105}$$

Separating terms:

$$J_{corr}^{NM}(q,t)=$$

$$\left(\begin{array}{l}\displaystyle\sum_{-\frac{\pi}{a}<q_1<0}\left[\begin{array}{l}J_0\cos^2\left(\frac{q_1a}{2}\right)\times\\ \left[\begin{array}{l}\cos\left(C_w\left(\left|\sin\left(\frac{q_1a}{2}\right)\right|-\sin\left(\frac{q_1a}{2}\right)\cos\left(\frac{qa}{2}\right)+\cos\left(\frac{q_1a}{2}\right)\sin\left(\frac{qa}{2}\right)\right)t\right)+\\ \cos\left(C_w\left(\left|\sin\left(\frac{q_1a}{2}\right)\right|+\sin\left(\frac{q_1a}{2}\right)\cos\left(\frac{qa}{2}\right)-\cos\left(\frac{q_1a}{2}\right)\sin\left(\frac{qa}{2}\right)\right)t\right)\end{array}\right]\end{array}\right]\\ +\displaystyle\sum_{0<q_1<\frac{\pi}{a}}\left[\begin{array}{l}J\cos^2\left(\frac{q_1a}{2}\right)\times\\ \left[\begin{array}{l}\cos\left(C_w\left(\left|\sin\left(\frac{q_1a}{2}\right)\right|-\sin\left(\frac{q_1a}{2}\right)\cos\left(\frac{qa}{2}\right)+\cos\left(\frac{q_1a}{2}\right)\sin\left(\frac{qa}{2}\right)\right)t\right)+\\ \cos\left(C_w\left(\left|\sin\left(\frac{q_1a}{2}\right)\right|+\sin\left(\frac{q_1a}{2}\right)\cos\left(\frac{qa}{2}\right)-\cos\left(\frac{q_1a}{2}\right)\sin\left(\frac{qa}{2}\right)\right)t\right)\end{array}\right]\end{array}\right]\end{array}\right) \tag{6.106}$$

Changing limits of the summation:

$$J_{corr}^{NM}(q,t)=$$

$$\left(\begin{array}{l}\displaystyle\sum_{0<q_1<\frac{\pi}{a}}\left[\begin{array}{l}J_0\cos^2\left(\frac{-q_1a}{2}\right)\times\\ \left[\begin{array}{l}\cos\left(C_w\left(\left|\sin\left(\frac{-q_1a}{2}\right)\right|-\sin\left(\frac{-q_1a}{2}\right)\cos\left(\frac{qa}{2}\right)+\cos\left(\frac{-q_1a}{2}\right)\sin\left(\frac{qa}{2}\right)\right)t\right)+\\ \cos\left(C_w\left(\left|\sin\left(\frac{-q_1a}{2}\right)\right|+\sin\left(\frac{-q_1a}{2}\right)\cos\left(\frac{qa}{2}\right)-\cos\left(\frac{-q_1a}{2}\right)\sin\left(\frac{qa}{2}\right)\right)t\right)\end{array}\right]\end{array}\right]\\ +\displaystyle\sum_{0<q_1<\frac{\pi}{a}}\left[\begin{array}{l}J\cos^2\left(\frac{q_1a}{2}\right)\times\\ \left[\begin{array}{l}\cos\left(C_w\left(\left|\sin\left(\frac{q_1a}{2}\right)\right|-\sin\left(\frac{q_1a}{2}\right)\cos\left(\frac{qa}{2}\right)+\cos\left(\frac{q_1a}{2}\right)\sin\left(\frac{qa}{2}\right)\right)t\right)+\\ \cos\left(C_w\left(\left|\sin\left(\frac{q_1a}{2}\right)\right|+\sin\left(\frac{q_1a}{2}\right)\cos\left(\frac{qa}{2}\right)-\cos\left(\frac{q_1a}{2}\right)\sin\left(\frac{qa}{2}\right)\right)t\right)\end{array}\right]\end{array}\right]\end{array}\right) \tag{6.107}$$

Evaluating the modulus operator:

$$J_{corr}^{NM}(q,t) =$$

$$\left(\sum_{0<q_1<\frac{\pi}{a}} \left[\begin{array}{l} J_0 \cos^2\left(\frac{q_1 a}{2}\right) \times \\ \left[\begin{array}{l} \cos\left(C_w \left(\sin\left(\frac{q_1 a}{2}\right) + \sin\left(\frac{q_1 a}{2}\right)\cos\left(\frac{qa}{2}\right) + \cos\left(\frac{q_1 a}{2}\right)\sin\left(\frac{qa}{2}\right)\right) t\right) + \\ \cos\left(C_w \left(\sin\left(\frac{q_1 a}{2}\right) - \sin\left(\frac{q_1 a}{2}\right)\cos\left(\frac{qa}{2}\right) - \cos\left(\frac{q_1 a}{2}\right)\sin\left(\frac{qa}{2}\right)\right) t\right) \end{array} \right] \end{array} \right] \right.$$

$$\left. + \sum_{0<q_1<\frac{\pi}{a}} \left[\begin{array}{l} J \cos^2\left(\frac{q_1 a}{2}\right) \times \\ \left[\begin{array}{l} \cos\left(C_w \left(\sin\left(\frac{q_1 a}{2}\right) - \sin\left(\frac{q_1 a}{2}\right)\cos\left(\frac{qa}{2}\right) + \cos\left(\frac{q_1 a}{2}\right)\sin\left(\frac{qa}{2}\right)\right) t\right) + \\ \cos\left(C_w \left(\sin\left(\frac{q_1 a}{2}\right) + \sin\left(\frac{q_1 a}{2}\right)\cos\left(\frac{qa}{2}\right) - \cos\left(\frac{q_1 a}{2}\right)\sin\left(\frac{qa}{2}\right)\right) t\right) \end{array} \right] \end{array} \right] \right) \quad (6.108)$$

Combining terms:

$$J_{corr}^{NM}(q,t) =$$

$$\sum_{0<q_1<\frac{\pi}{a}} \left[\begin{array}{l} J_0 \cos^2\left(\frac{q_{r_1} a}{2}\right) \exp\left(\frac{-t}{\tau_{r_1}}\right) \exp\left(\frac{-t}{\tau_{r_2}}\right) \times \\ \left[\begin{array}{l} \cos\left(C_w \left(\sin\left(\frac{q_{r_1} a}{2}\right) + \sin\left(\frac{q_{r_1} a}{2}\right)\cos\left(\frac{\alpha a}{2}\right) + \cos\left(\frac{q_{r_1} a}{2}\right)\sin\left(\frac{\alpha a}{2}\right)\right) t\right) + \\ \cos\left(C_w \left(\sin\left(\frac{q_{r_1} a}{2}\right) - \sin\left(\frac{q_{r_1} a}{2}\right)\cos\left(\frac{\alpha a}{2}\right) - \cos\left(\frac{q_{r_1} a}{2}\right)\sin\left(\frac{\alpha a}{2}\right)\right) t\right) + \\ \cos\left(C_w \left(\sin\left(\frac{q_{r_1} a}{2}\right) - \sin\left(\frac{q_{r_1} a}{2}\right)\cos\left(\frac{\alpha a}{2}\right) + \cos\left(\frac{q_{r_1} a}{2}\right)\sin\left(\frac{\alpha a}{2}\right)\right) t\right) + \\ \cos\left(C_w \left(\sin\left(\frac{q_{r_1} a}{2}\right) + \sin\left(\frac{q_{r_1} a}{2}\right)\cos\left(\frac{\alpha a}{2}\right) - \cos\left(\frac{q_{r_1} a}{2}\right)\sin\left(\frac{\alpha a}{2}\right)\right) t\right) \end{array} \right] \end{array} \right] \quad (6.109)$$

Using the relation given in Eqn. (6.90):

$$J_{corr}^{NM}(q,t)=\sum_{0<q_1<\frac{\pi}{a}}\left[\begin{array}{l} J_0\cos^2\left(\frac{q_1a}{2}\right)\times \\ \left[\begin{array}{l} \cos\left(\left(w(q_1)\left(1+\cos\left(\frac{qa}{2}\right)\right)+w(q)\cos\left(\frac{q_1a}{2}\right)\right)t\right)+ \\ \cos\left(\left(w(q_1)\left(1-\cos\left(\frac{qa}{2}\right)\right)-w(q)\cos\left(\frac{q_1a}{2}\right)\right)t\right)+ \\ \cos\left(\left(w(q_1)\left(1-\cos\left(\frac{qa}{2}\right)\right)+w(q)\cos\left(\frac{q_1a}{2}\right)\right)t\right)+ \\ \cos\left(\left(w(q_1)\left(1+\cos\left(\frac{qa}{2}\right)\right)-w(q)\cos\left(\frac{q_1a}{2}\right)\right)t\right) \end{array}\right] \end{array}\right] \tag{6.110}$$

Thus the heat current normal mode correlation can also be simplified as contributions from the four terms as shown in the Eqn. (6.110) above. The frequency of the cosine term due to each of these terms is same as that observed in Eqn. (6.102), and have already been shown in *Figure 6.2* to *Figure 6.5* as a function of wavevectors q and q_1. However, the pre-multipliers for these terms are different from those in the energy normal mode correlation, and hence the net dispersion due to these will be different. The dispersion due to each of these terms is shown in *Figure 6.11* to *Figure 6.14*.

First term: $$\sum_{0<q_1<\frac{\pi}{a}}\left[J_0\cos^2\left(\frac{q_1 a}{2}\right)\left[\cos\left(\left(w(q_1)\left(1+\cos\left(\frac{qa}{2}\right)\right)+w(q)\cos\left(\frac{q_1 a}{2}\right)\right)t\right)\right]\right]$$

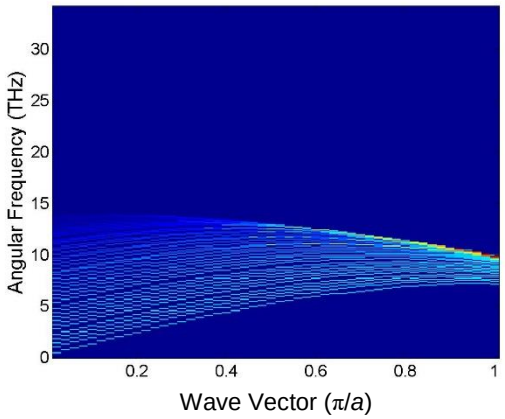

Figure 6.11: Dispersion due to the first term in Eqn. (6.110).

Second term: $$\sum_{0<q_1<\frac{\pi}{a}}\left[J_0\cos^2\left(\frac{q_1 a}{2}\right)\left[\cos\left(\left(w(q_1)\left(1-\cos\left(\frac{qa}{2}\right)\right)-w(q)\cos\left(\frac{q_1 a}{2}\right)\right)t\right)+\right]\right]$$

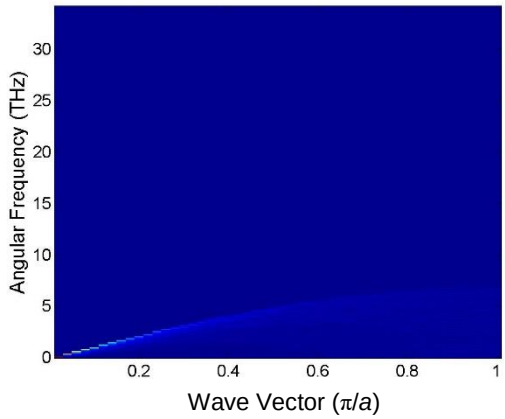

Figure 6.12: Dispersion due to the second term in Eqn. (6.110).

Third term: $$\sum_{0<q_1<\frac{\pi}{a}}\left[J_0\cos^2\left(\frac{q_1 a}{2}\right)\left[\cos\left(\left(w(q_1)\left(1-\cos\left(\frac{qa}{2}\right)\right)+w(q)\cos\left(\frac{q_1 a}{2}\right)\right)t\right)+\right]\right]$$

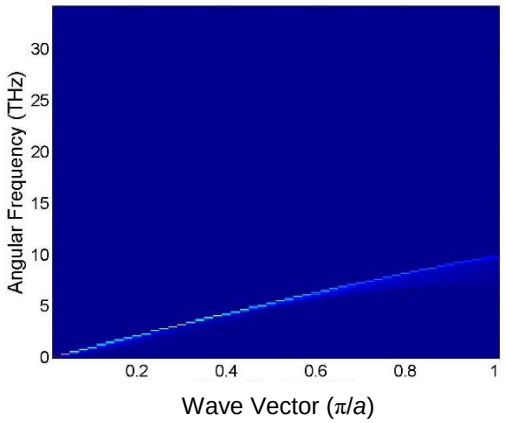

Figure 6.13: Dispersion due to the third term in Eqn. (6.110).

Fourth term: $$\sum_{0<q_1<\frac{\pi}{a}}\left[J_0\cos^2\left(\frac{q_1 a}{2}\right)\left[\cos\left(\left(w(q_1)\left(1+\cos\left(\frac{qa}{2}\right)\right)-w(q)\cos\left(\frac{q_1 a}{2}\right)\right)t\right)\right]\right]$$

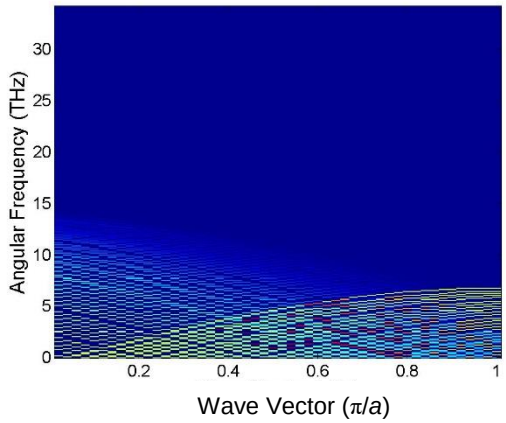

Figure 6.14: Dispersion due to the fourth term in Eqn. (6.110).

Adding the contributions from all the terms of Eqn. (6.110), the net dispersion for the heat current normal mode correlation is shown in *Figure 6.15*, with the left panel having the color bar in linear scale while the right panel having the color bar in log scale to highlight the smaller peaks in frequency. Again, the third term dominates the overall dispersion curve. The dispersion curve is quite similar to that of the energy normal modes with the most prominent branch being nearly linear. However, for this case, the linear branch is sharper with a smaller spread over other frequencies.

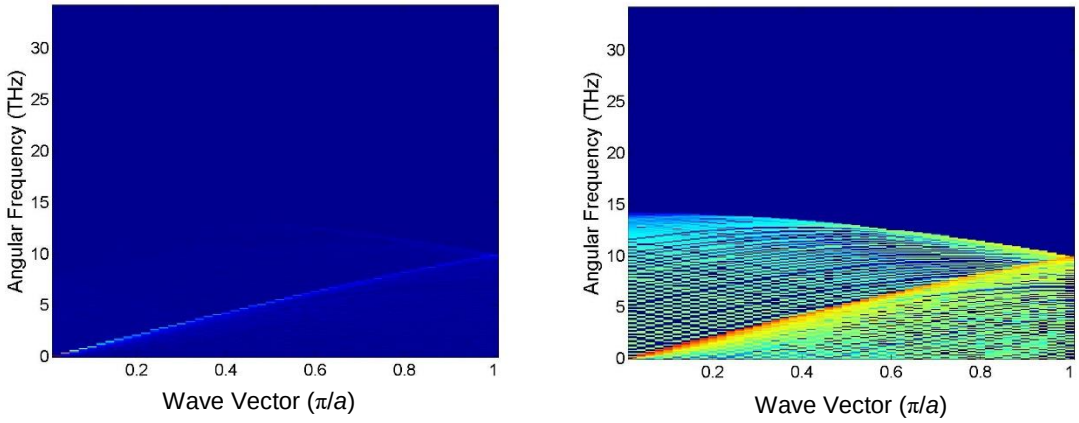

Figure 6.15: Heat current dispersion from Eqn. (6.110) in (left) linear scale and (right) log scale.

6.7 Atomistic Simulations

Atomistic simulations are performed for a linear monoatomic chain to test the theoretical results derived in the previous sections, and to investigate the effect of anharmonicity. The system configuration for these simulations is identical to that used in Chapter 4.

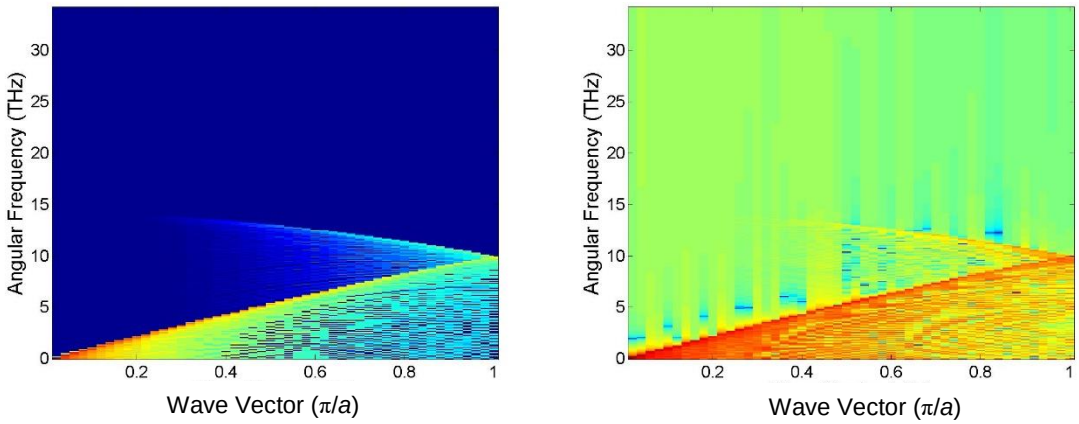

Figure 6.16: Energy dispersion (color bar shown in log scale to amplify the smaller peaks) from (left) theory and (right) from simulation.

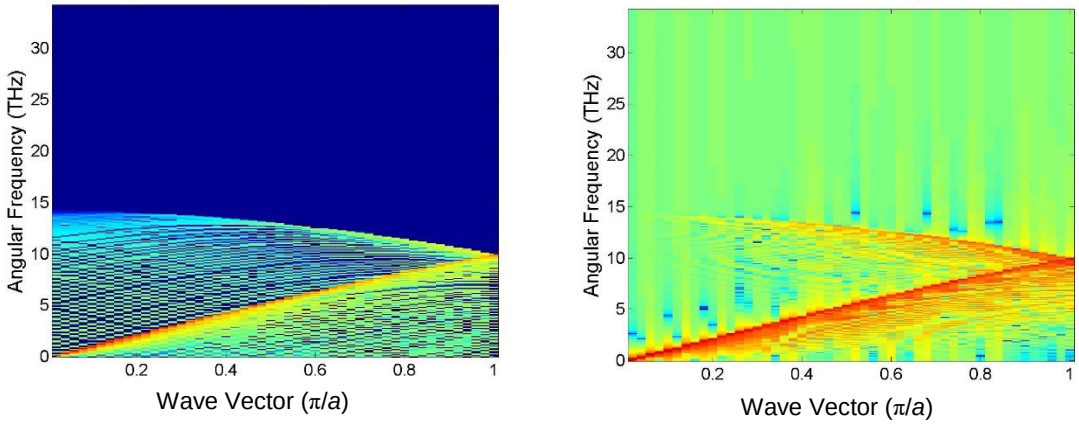

Figure 6.17: Heat current dispersion (color bar is shown in log scale to amplify the smaller peaks) from (left) theory and (right) from simulation.

Figure 6.16 and *Figure 6.17* compare the dispersion curves derived in the previous section to those obtained from the simulation using a harmonic potential at 0.5 K for energy and heat current normal modes respectively. Both the curves show excellent agreement with the theoretical predictions. Now the initial correlation is evaluated as:

$$J_{corr}^{NM}(q,0)=\frac{2(k_BT)^2}{NV^2}\sum_{0<q_1<\frac{\pi}{a}} v_g{}^2(q_1) \tag{6.111}$$

This gives:

$$\frac{J_{corr}^{NM}(q,0)}{J_{corr}^{NM}(0,0)}=1 \tag{6.112}$$

$$\frac{J_{corr}^{NM}(q,0)_{T_1}}{J_{corr}^{NM}(q,0)_{T_2}}=\left(\frac{T_1}{T_2}\right)^2 \tag{6.113}$$

Similarly:

$$E_{corr}^{NM}(q,0)=\frac{(k_BT)^2}{N}\times\sum_{0<q_1<\frac{\pi}{a}}\left[\left(1-\cos\left(\frac{qa}{2}\right)\right)^2+\left(1+\cos\left(\frac{qa}{2}\right)\right)^2\right] \tag{6.114}$$

Thus implying:

$$\frac{E_{corr}^{NM}(q,0)}{E_{corr}^{NM}(0,0)}=\frac{1+\cos^2\left(\frac{qa}{2}\right)}{2} \tag{6.115}$$

$$\frac{E_{corr}^{NM}(q,0)_{T_1}}{E_{corr}^{NM}(q,0)_{T_2}}=\left(\frac{T_1}{T_2}\right)^2 \tag{6.116}$$

Figure 6.18 shows the comparison of the behavior predicted by Eqns. (6.112) and (6.115) to results from the simulations with harmonic interaction. The two sets again show excellent

agreement with the theory. *Figure 6.19* shows a similar comparison for Eqns. (6.113) and (6.116); once again the simulation results agree well with the theoretical predictions.

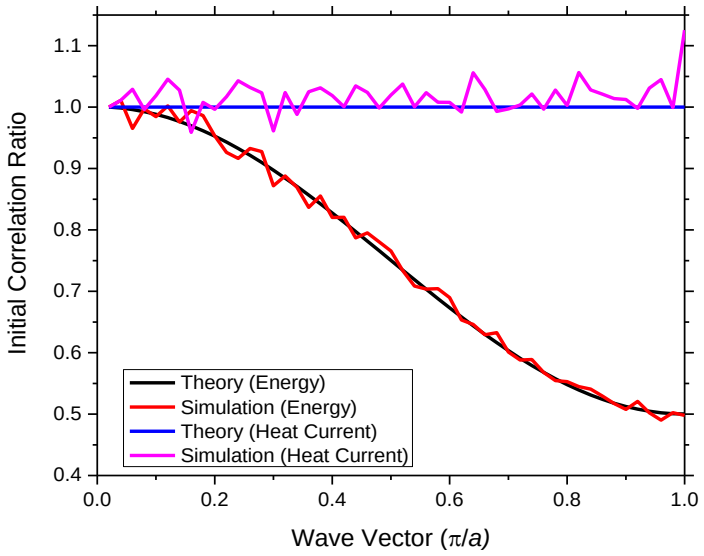

Figure 6.18 Variation of initial correlation with wave vector for both energy and heat current.

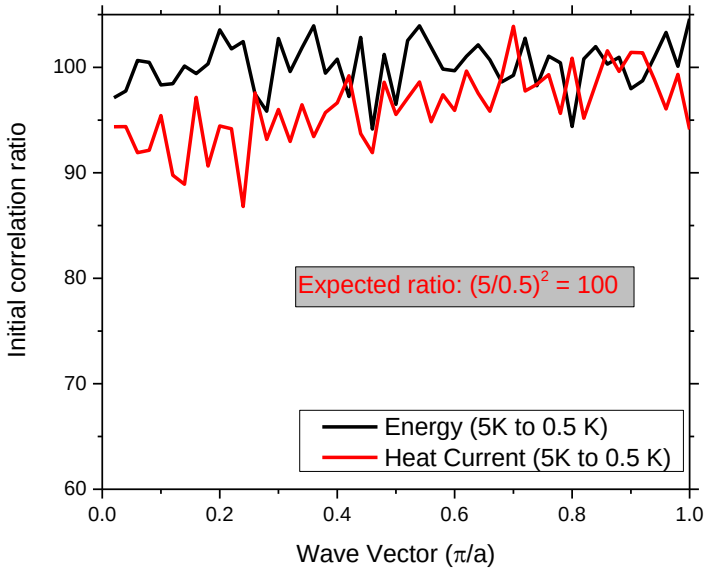

Figure 6.19: Ratio of initial correlation at 5 *K* to that at 0.5 *K* for both energy and heat current. The theoretical expected ratio is 100.

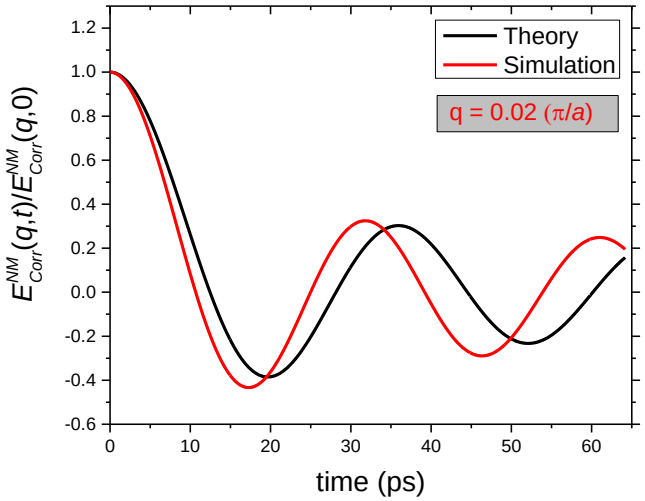

Figure 6.20: Decay of energy correlation for q = 0.02 (π/a) for harmonic interaction.

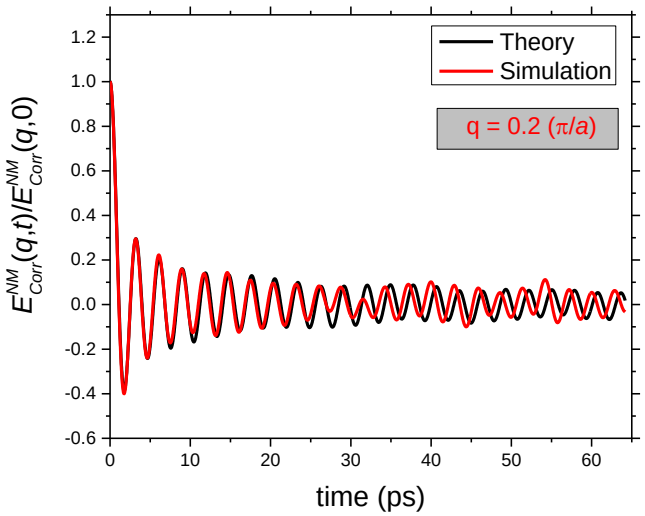

Figure 6.21: Decay of energy correlation for q = 0.2 (π/a) with harmonic interaction.

Figure 6.20 and *Figure 6.21* show the time evolution of the energy normal mode correlation for q = 0.02 (π/a) and q = 0.2 (π/a), respectively. The simulation results reasonable conformance to the theoretical prediction. It is interesting to note that the curves appear to

show an oscillatory decay, which does not arise from the decay of phonon modes, but rather from a superposition of multiple frequencies going out of phase – an effect similar to the formation of a wave packet.

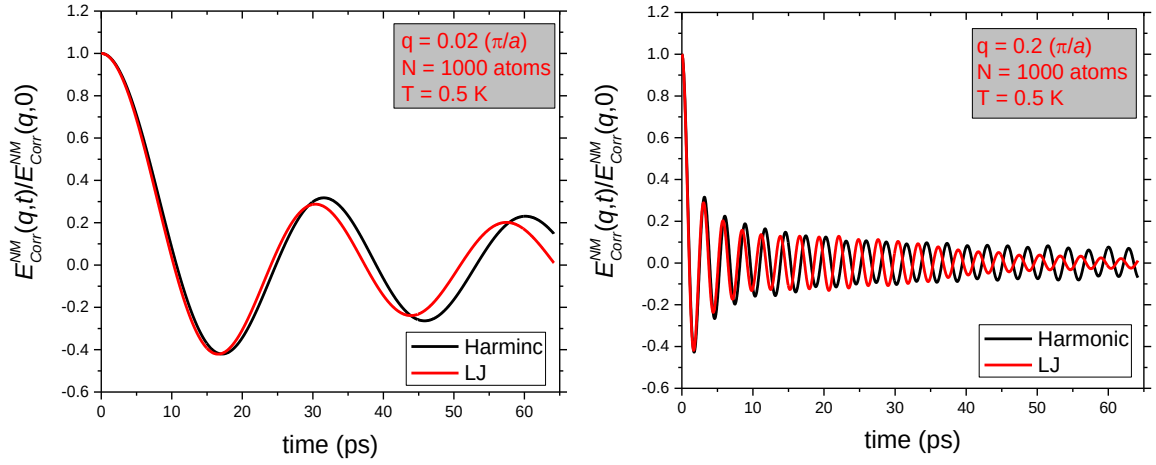

Figure 6.22: Time evolution of energy normal mode correlation for LJ and harmonic potentials with 1000 atoms at 0.5 K for (left) q = 0.02 (π/a) and (right) q = 0.2 (π/a).

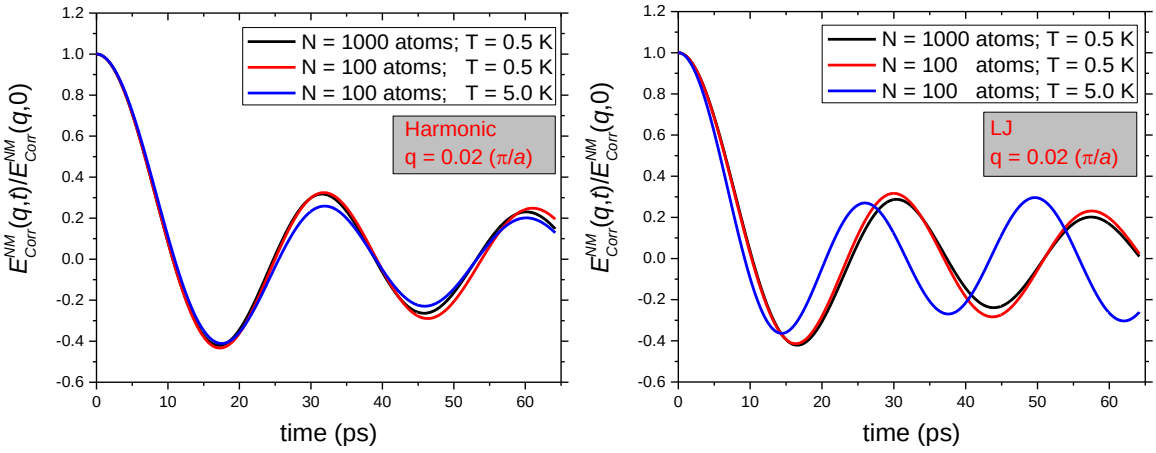

Figure 6.23: Time evolution of energy normal mode correlation for q = 0.02 (π/a) for (left) harmonic and (right) LJ potentials.

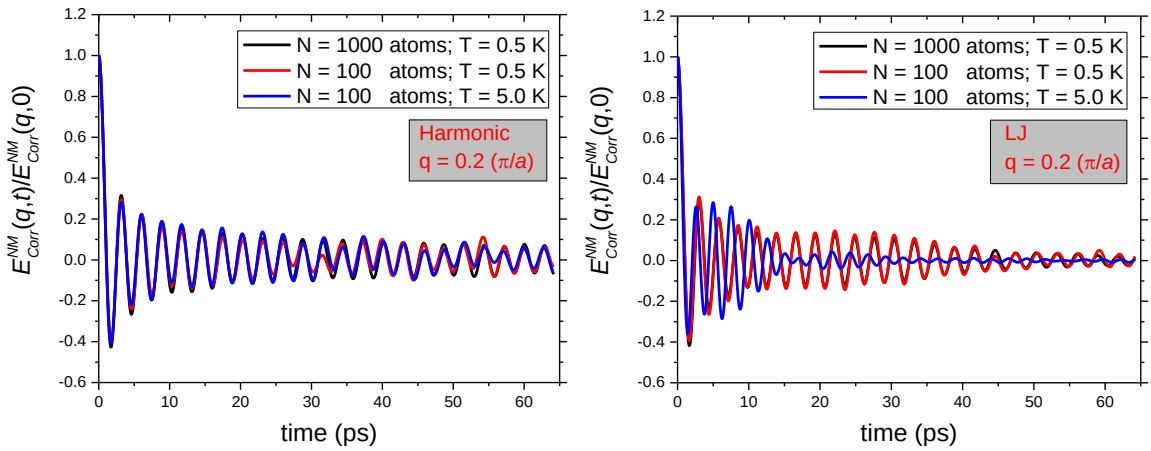

Figure 6.24: Time evolution of energy normal mode correlation for q = 0.2 (π/a) for (left) harmonic and (right) LJ potentials.

The anharmonicity allows the phonon modes to interact with the LJ potential (phonon-phonon scattering), and the phonon correlations will thus decay exponentially. Thus the time evolution of the energy normal modes will also be modified by this decay. A comparison of the behavior of the correlation for harmonic and LJ interactions is shown in *Figure 6.22*. For a smaller wave vector, the difference is very negligible as the decay is slow. For a larger wave vector, however, the difference is more prominent, and a sharper decay of the correlation for the LJ interaction is observed due to the phonon-phonon interactions. It is also interesting to see a slight shift in the frequency with the LJ interaction. This behavior can also be understood in terms of cross-mode interactions. The amplitude corresponding to every pair contribution will decay based on the cross-mode correlation for that mode (see Eqn. (6.73)). Since the amplitude varies across the modes, the net contribution due to each pair will be different. Thus an overall decay in the frequency, which is slightly different from what is expected in the absence of cross-mode interaction, is observed.

Figure 6.23 and *Figure 6.24* shows the effect of temperature and size on the energy correlation for $q = 0.02$ (π/a) and $q = 0.2$ (π/a), respectively. Clearly, for harmonic potential, there is no significant effect of size and temperature on the decay of the energy correlation. For the LJ interaction, it is observed that the decay is not affected by the size of the chain, but the thermal fluctuations is seen to have a significant effect. As expected, the decay is much faster at a higher temperature due to smaller phonon lifetimes, especially for larger wavevectors. Also, there is a shift in the decay frequency with temperature.

Next the theoretical prediction and the simulation results for the heat current normal mode correlations with harmonic interaction is shown in *Figure 6.25* and *Figure 6.26* for $q = 0.02$ (π/a) and $q = 0.2$ (π/a), respectively. For the shorter wave vector, there is noticeable difference between the theory and prediction; the reason for the discrepancy is not evident now. For the longer wave vector the curves show better agreement. *Figure 6.27* compares the behavior of the heat current normal mode correlation for 1000 atoms at 0.5 K for the harmonic and LJ interactions. Again, a sharper decay is observed for the LJ interaction with a small shift in frequency. *Figure 6.28* and *Figure 6.29* delineate the effect of size and temperature on the heat current normal mode correlation decay for $q = 0.02$ (π/a) and $q = 0.2$ (π/a), respectively. As with energy correlations, the harmonic interaction is independent of the system length and temperature, while for the LJ interaction, the decay rate increases with temperature with a small shift in the frequency.

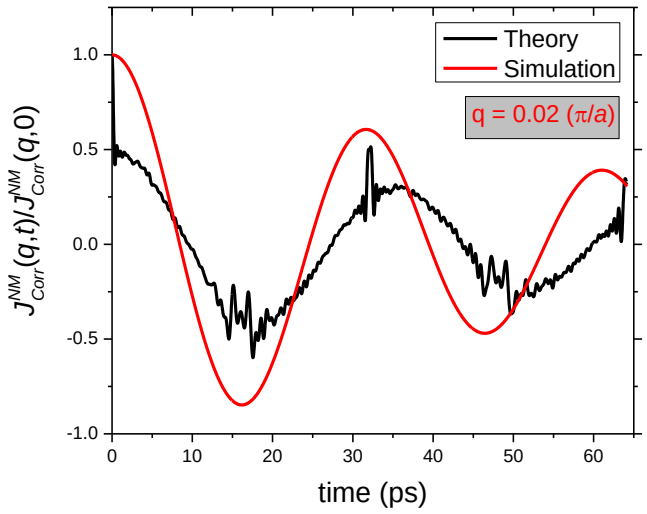

Figure 6.25: Decay of virial heat current normal mode correlation for q = 0.02 (π/a) with the harmonic potential.

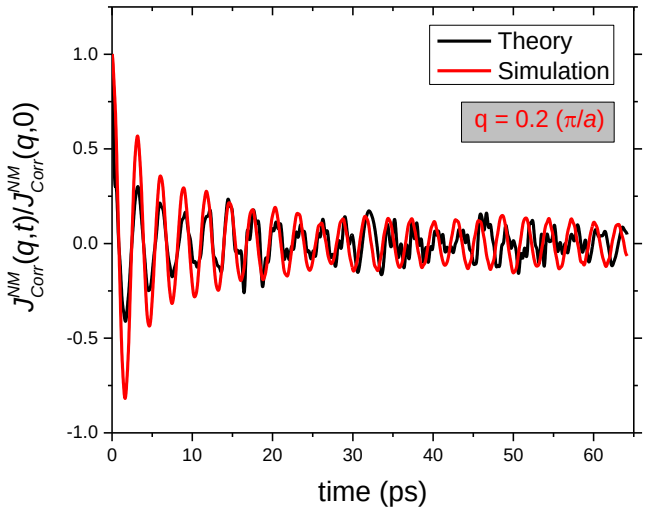

Figure 6.26: Decay of virial heat current normal mode correlation for q = 0.2 (π/a) with the harmonic potential.

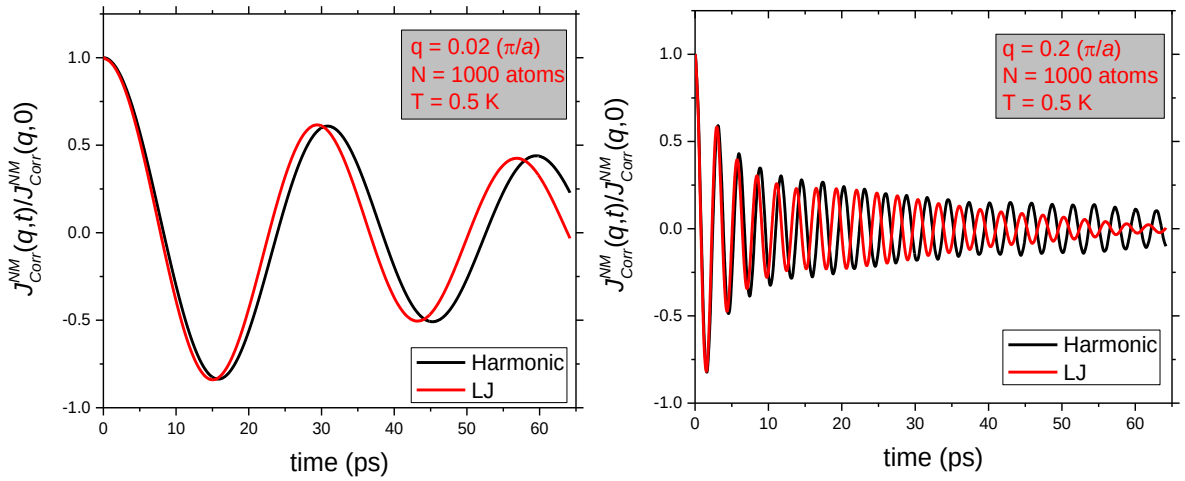

Figure 6.27: Time evolution of virial heat current normal mode correlation for LJ and harmonic potentials for 1000 atoms at 0.5 K for (left) q = 0.02 (π/a) and (right) q = 0.2 (π/a).

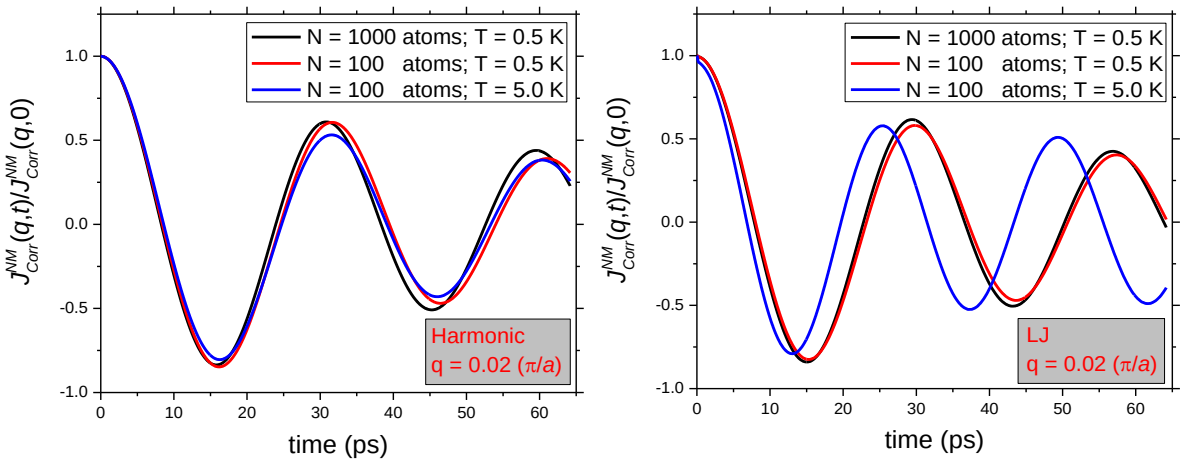

Figure 6.28: Time evolution of virial heat current normal mode correlation for q = 0.02 (π/a) for (left) harmonic and (right) LJ potentials.

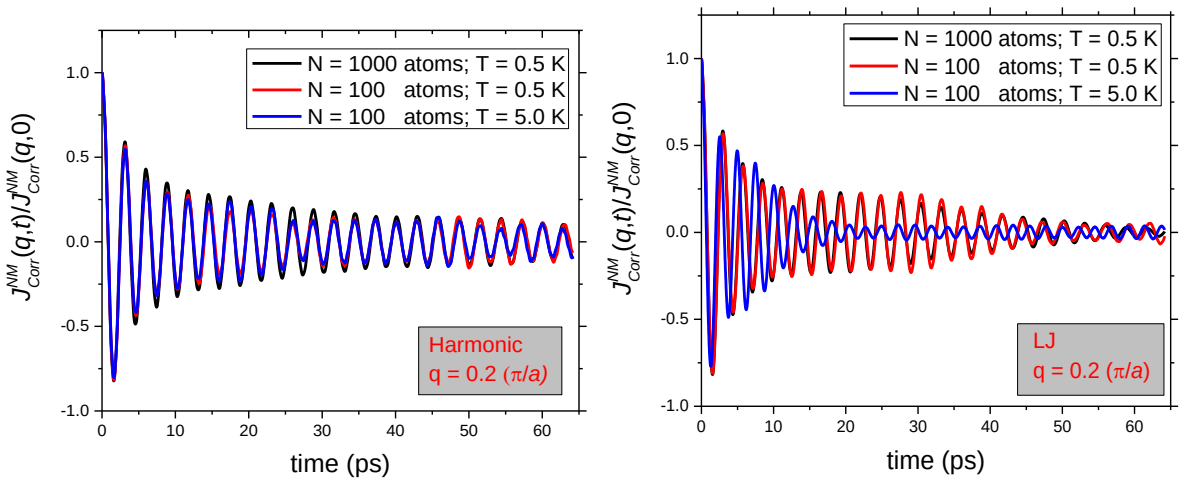

Figure 6.29: Time evolution of virial heat current normal mode correlation for $q = 0.2\ (\pi/a)$ for (left) harmonic and (right) LJ potentials.

The cut-off length for interactions in the simulations has been set to 1.5 in LJ reduced units to ensure that only nearest neighbor interactions take place. To introduce greater anharmonicity in the interactions, the cut-off distance for interactions is increased to 3.0 in LJ reduced units, thereby activating interactions between second nearest neighbors. An increase in anharmonicity causes an increase in the decay rate of the correlation, and the effect is more prominent for larger wavevectors. Anharmonicity also results in the flattening of the Fourier transform of the normal mode correlations. Thus at higher temperatures, the longer wave vectors merely decay and do not show any prominent oscillations.

The prominent region of the linear branch of the dispersion curve for energy and heat current normal modes is shown in *Figure 6.30* and *Figure 6.31*, respectively. The phonon dispersion branch has been overlaid as solid black lines in both figures for reference. A clear increase in the slope of the dispersion curve is observed with increasing anharmonicity. As previously

discussed, collective excitations of phonon modes arise in low dimensional systems due to anharmonic interactions. These collective excitations cause a reduction in the mode decay times and an increase in the excitation frequencies. Thus, the change in the decay time and frequencies can be used as a metric to quantify these collective excitations.

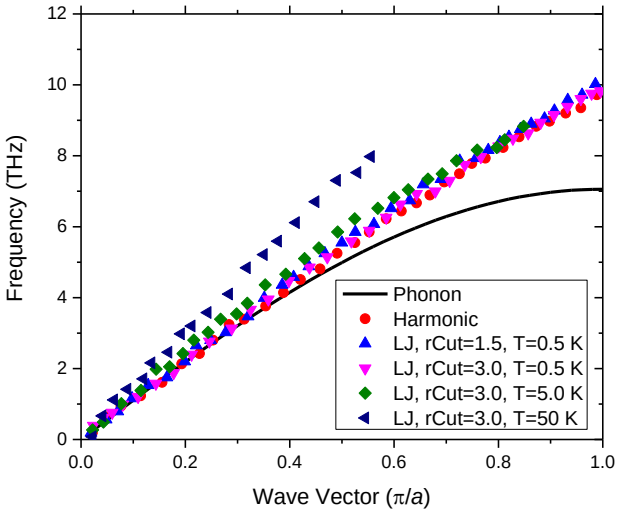

Figure 6.30: Variation of energy normal mode dispersion with increasing anharmonicity.

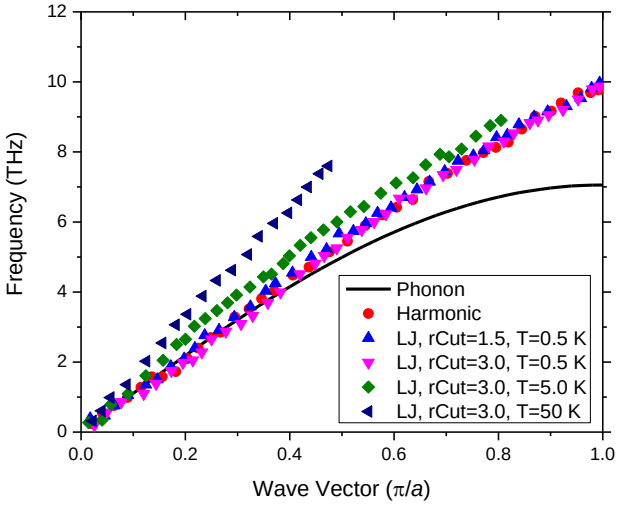

Figure 6.31: Variation of virial heat current normal mode dispersion with increasing anharmonicity.

6.8 Discussion and Conclusion

The projection in wave vector space *i.e.*, the normal mode projection can be obtained for any spatially varying quantity. If the behavior is non-oscillatory, the correlation of the normal mode projection will simply decay with time. However, if the quantity oscillates forming waves, then the amplitude and frequency of the wave are reflected in the normal mode projection. In this chapter, the amplitude of the energy and heat current waves has been extracted by the normal mode projection.

The displacements and velocities of the atoms due to the phonon modes result in the energy and heat current variation in space. The expression for the energy and heat current of any atom due to these displacements indicates that they form traveling waves. It is fascinating to note that these energy and heat current waves are formed even when the phonons are not interacting. The analysis presented in this chapter shows that these waves arise from the interference between phonon pairs. It may be noted that the normal mode projection will not be able to separate the waves moving in positive and negative directions as the normal mode projections for positive and negative wave vectors are simply conjugate of each other. Thus the amplitude of the normal mode projection will depend on the contributions from waves moving in both positive and negative direction.

During the derivation of the normal mode projection, Eqn. (6.117) and Eqn. (6.118) (shown below) are obtained for energy and heat current respectively.

$$\chi_E(q,t)=\sum_{q_1}\sum_{q_2}\sum_{j}\left[\begin{array}{l}\frac{1}{4\sqrt{N}}w(q_1)w(q_2)A(q_1)A(q_2)\times\\ \left(\begin{array}{l}\left(\begin{array}{l}\left(\cos\left((q+q_1-q_2)\,ja\right)+\cos\left((q-q_1+q_2)\,ja\right)\right)\\ \times\cos\left(\left(w(q_1)-w(q_2)\right)t-\varphi(q_1)+\varphi(q_2)\right)+\\ i\left(\cos\left((q-q_1+q_2)\,ja\right)-\cos\left((q+q_1-q_2)\,ja\right)\right)\\ \times\sin\left(\left(w(q_1)-w(q_2)\right)t-\varphi(q_1)+\varphi(q_2)\right)\end{array}\right)\\ \times\left(1+\frac{q_1}{|q_1|}\frac{q_2}{|q_2|}\cos\left((q_1-q_2)\frac{a}{2}\right)\right)-\\ \left(\begin{array}{l}\left(\cos\left((q+q_1+q_2)\,ja\right)+\cos\left((q-q_1-q_2)\,ja\right)\right)\\ \times\cos\left(\left(w(q_1)+w(q_2)\right)t-\varphi(q_1)-\varphi(q_2)\right)+\\ i\left(\cos\left((q-q_1-q_2)\,ja\right)-\cos\left((q+q_1+q_2)\,ja\right)\right)\\ \times\sin\left(\left(w(q_1)+w(q_2)\right)t-\varphi(q_1)-\varphi(q_2)\right)\end{array}\right)\\ \times\left(1+\frac{q_1}{|q_1|}\frac{q_2}{|q_2|}\cos\left((q_1+q_2)\frac{a}{2}\right)\right)\end{array}\right] \tag{6.117}$$

$$\chi_{J_{pot}}(q,t)=\sum_{q_1}\sum_{q_2}\sum_{j}\left[\begin{array}{l}\frac{1}{4V\sqrt{N}}A(q_1)A(q_2)w(q_1)w(q_2)v_g(q_2)\\ \left(\begin{array}{l}\left(\cos\left((q+q_1-q_2)\,ja\right)+\cos\left((q-q_1+q_2)\,ja\right)\right)\\ \times\cos\left(\left(w(q_1)-w(q_2)\right)t-\varphi(q_1)+\varphi(q_2)\right)+\\ i\left(\cos\left((q-q_1+q_2)\,ja\right)-\cos\left((q+q_1-q_2)\,ja\right)\right)\\ \times\sin\left(\left(w(q_1)-w(q_2)\right)t-\varphi(q_1)+\varphi(q_2)\right)-\\ \left(\cos\left((q+q_1+q_2)\,ja\right)+\cos\left((q-q_1-q_2)\,ja\right)\right)\\ \times\cos\left(\left(w(q_1)+w(q_2)\right)t-\varphi(q_1)-\varphi(q_2)\right)-\\ i\left(\cos\left((q-q_1-q_2)\,ja\right)-\cos\left((q+q_1+q_2)\,ja\right)\right)\\ \times\sin\left(\left(w(q_1)+w(q_2)\right)t-\varphi(q_1)-\varphi(q_2)\right)\end{array}\right)\end{array}\right] \tag{6.118}$$

Now, a pair of phonon modes with wavevectors q_1 and q_2 will form wave of energy (or heat current) with wave vector q if and only if one of the following four conditions is satisfied:

$$q - q_1 - q_2 = 0, \pm \frac{2\pi}{a} \tag{6.119}$$

$$q - q_1 + q_2 = 0, \pm \frac{2\pi}{a} \tag{6.120}$$

$$q + q_1 - q_2 = 0, \pm \frac{2\pi}{a} \tag{6.121}$$

$$q + q_1 + q_2 = 0, \pm \frac{2\pi}{a} \tag{6.122}$$

As the amplitude of the normal mode for the positive and negative q are the same, the first condition above is equivalent to the fourth condition. Similarly, the second condition is equivalent to the third condition. Consider the first case:

$$q = q_1 + q_2 + G; G = 0, \pm \frac{2\pi}{a} \tag{6.123}$$

The terms in the Eqn. (6.117) and Eqn. (6.118) which make a non-zero contribution are such that the frequency w follows the relationship:

$$w = w(q_1) + w(q_2) \tag{6.124}$$

Remarkably, these two conditions happen to be the three-phonon scattering condition in which phonons with modes q_1 and q_2 scatter to create a phonon of mode q. This condition arises even when the phonons are not interacting (due to a harmonic interaction) for the linear 1-D chain. Similarly, consider the second case:

$$q_1 = q + q_2 + G; G = 0, \pm \frac{2\pi}{a} \tag{6.125}$$

The terms in the Eqn. (6.117) and Eqn. (6.118) which make a non-zero contribution are such that the frequencies follow the condition:

$$w(q_1) = w + w(q_2) \tag{6.126}$$

Again, the two conditions are identical to that of three-phonon scattering conditions in which phonons with modes q and q_2 scatter to create a phonon of mode q_1. Thus, pairs of phonons with modes q_1 and q_2 interfere to create a wave of energy (or heat current) with wavevector q and frequency w such that a phonon with the same frequency and wave vector can produce a three-phonon interaction with the given pair. Further, every energy (or heat current) normal mode will derive contributions from several such pairs. Thus, the Fourier transform of the energy (or heat current) normal mode correlations do not show sharp peaks, but rather a wide spread over a range of frequencies. Thus, the correlation behaves similar to a wave packet in time and appears to decay even when there is no phonon-phonon interaction (which implies no decay in the phonon mode amplitudes).

The phonon scattering conditions are true even in the absence of phonon-phonon interactions *i.e*. without anharmonicity. *Thus the phonon modes can interfere, even when they cannot scatter*. Phonon interaction has a two-fold effect on this interference. First, the interaction leads to cross-correlation between phonon mode amplitudes. Second, the frequencies due to highly

correlated pairs are likely to become more prominent, which again points towards a collective excitation of phonon modes. The modes with collective excitation are likely to be more correlated and thus have a greater amplitude in the energy (or heat current) normal modes. Further, the interactions can also cause a decay in the energy (or heat current) normal mode correlation.

Now consider an anharmonic interaction arising due to a cubic term in the potential. In the presence of a cubic term, the energy expression will have an additional term involving a product containing three-phonon modes q_1, q_2 and q_3. The energy normal mode amplitude for a wave vector q in this case will have finite contributions such that q, q_1, q_2 and q_3 together satisfy a four-phonon interaction condition. In general, for an n^{th} order phonon-phonon interaction, it is expected that the energy wave will be produced by interference involving n+1 phonon modes. A similar argument holds for the heat current normal modes. While a theoretical derivation for anharmonic interactions has not been attempted in this work, it is expected that the types of phonon interactions will emerge naturally for higher dimensions and for increasing order of anharmonicity. The natural emergence of these modes through energy and heat mode correlations is, perhaps, the most remarkable finding of this dissertation.

Chapter 7: CONCLUSION

With the recent advances in nanotechnology, there is a growing interest in studying the fundamental mechanisms of energy transport, both at micro and nanoscales. The discovery of low-dimensional materials such as graphene and carbon nanotube (CNT) has heightened the necessity for investigating the key mechanisms of energy transport, not just at nanoscales, but also for systems with lower dimensionality. In this dissertation, the fundamental mechanisms of energy and heat transport is investigated using statistical mechanics first principles and atomistic simulations.

Thermal conduction in solid state electrical insulators has long been associated with the normal mode of the vibrating atoms known as phonons. In the quantum framework, phonons are treated as bosons, which can be described by the Boltzmann kinetic theory. While the concept of phonons is critical to explaining several thermal properties, recent developments are challenging the notion of phonons as the true carriers of heat. In an alternate statistical mechanical framework, which is more fundamental, thermal conduction can be described by the linear response, or equivalently, the Green-Kubo (GK) theory. The GK theory, however, does not lend itself naturally to identify the modes of vibrations in a crystalline state. In the past two decades, several attempts have been made to merge these two disparate theories though with limited success. A primary objective of this dissertation is to develop a theoretical framework that can accommodate the GK and phonon theories while maintaining mathematical and physical consistency.

First, a mathematically consistent general solution to the phonon equation of motion is presented. It is shown that the displacements necessarily should include a left moving and a right moving wave train to satisfy all the internal degrees of freedom. The identification of the amplitudes in +**q** and –**q** wavevector directions provides a fundamental breakthrough for describing the correct form of heat current modes expressed in normal mode coordinates.

A numerically efficient method based on the ratio of normal mode coordinates of velocity to those of displacements is presented next for determining the phonon dispersion curve. While the theory is known before, the method has never been employed for computing phonon dispersion using atomistic simulations. Case studies on a monoatomic chain, a diatomic chain, and graphene demonstrate that the ratio method outperforms in accuracy and speed over the conventional method of using a fast Fourier transform (FFT).

The most impactful results of the dissertation are presented in Chapters 5 and 6. It is first shown that a real microscopic heat flux in normal mode coordinates can be consistently defined, and the net phonon population can be expressed as a difference in amplitudes along +**q** and –**q** wave vector directions. It is further demonstarted that phonon-phonon cross-correlations emerge naturally, and can play a dominant role in the thermal transport process, especially for low-dimension systems; the derivation also identifies a correction term for phonon self-correlations. Interestingly, the correction from energy correlations leads to phonon lifetimes that are appreciably lower than those estimated using the existing approaches.

For low dimensional systems, it is more appropriate to investigate the local heat current and energy fluctuations in appropriate normal coordinates than to evaluate an ill-defined thermal conductivity. In Chapter 6, the theoretical framework for analyzing local energy and heat current fluctuations in corresponding (energy/flux) normal coordinates is presented. These energy/current modes are then connected to the phonon normal modes that allows the exciting possibility of analyzing energy/heat modes in the framework of more familiar displacement (phonon) normal modes.

The energy/current modes are next derived exactly for a harmonic one-dimensional monoatomic chain; the theoretical prediction is verified subsequently using atomistic simulations. The theoretical derivation reveals a rather intriguing denouement on the possible combinations of phonon modes. Even with harmonic interaction, pairs of phonon modes combine to produce energy/heat modes if and only if they satisfy the three-phonon scattering law. It is known that three-phonon processes are required for thermal dissipation, and the appearance of the three-phonon scattering condition, from the energy/current modes, indicates the distinct possibility of predicting the phonon interaction types directly from the pertinent microscopic variables (energy/current) – a long sought after goal in recent theoretical studies. The three-phonon synergy has the lowest order of interaction, and this condition arises naturally with the interference of energy/heat waves. It is anticipated that if anharmonicity and higher dimensionality are included, higher order processes will evolve naturally without the need to specify or postulate the nature of phonon interactions in thermal transport.

REFERENCES

[1] E. Pop, "Energy dissipation and transport in nanoscale devices," *Nano Research,* vol. 3, pp. 147-169, 2010.

[2] Z. Gang, *Nanoscale energy transport and harvesting: A computational study*: Pan Stanford Publishing, 2015.

[3] T. S. Fisher, *Thermal energy at the nanoscale*: World Scientific, 2014.

[4] Y. Chalopin and S. Volz, "A microscopic formulation of the phonon transmission at the nanoscale," *Applied Physics Letters,* vol. 103, p. 051602, 2013.

[5] S. Volz, *Microscale and nanoscale heat transfer*: Springer, 2007.

[6] W. Zhang, T. S. Fisher, and N. Mingo, "The atomistic Green's function method: An efficient simulation approach for nanoscale phonon transport," *Numerical Heat Transfer, Part B: Fundamentals,* vol. 51, pp. 333-349, 2007.

[7] G. Chen, *Nanoscale energy transport and conversion: A parallel treatment of electrons, molecules, phonons, and photons*: Oxford University Press, 2005.

[8] G. Romano and J. C. Grossman, "Heat conduction in nanostructured materials predicted by phonon bulk mean free path distribution," *Journal of Heat Transfer,* vol. 137, pp. 071302-071302-7, 2015.

[9] P. Heino, "Lattice-Boltzmann finite-difference model with optical phonons for nanoscale thermal conduction," *Computers & Mathematics with Applications,* vol. 59, pp. 2351-2359, 2010.

[10] J. Zou and A. Balandin, "Phonon heat conduction in a semiconductor nanowire," *Journal of Applied Physics,* vol. 89, pp. 2932-2938, 2001.

[11] D. Baillis and J. Randrianalisoa, "Prediction of thermal conductivity of nanostructures: Influence of phonon dispersion approximation," *International Journal of Heat and Mass Transfer,* vol. 52, pp. 2516-2527, 2009.

[12] H. W. Kim, W. Ko, J. Ku, I. Jeon, D. Kim, H. Kwon, *et al.*, "Nanoscale control of phonon excitations in graphene," *Nature Communications,* vol. 6, p. 7528, 2015.

[13] K. M. Hoogeboom-Pot, J. N. Hernandez-Charpak, X. Gu, T. D. Frazer, E. H. Anderson, W. Chao, *et al.*, "A new regime of nanoscale thermal transport: Collective diffusion

increases dissipation efficiency," *Proceedings of the National Academy of Sciences*, vol. 112, pp. 4846-4851, 2015.

[14] A. K. Geim and K. S. Novoselov, "The rise of graphene," *Nat Mater,* vol. 6, pp. 183-191, 2007.

[15] S. Iijima, "Helical microtubules of graphitic carbon," *Nature,* vol. 354, pp. 56-58, 1991.

[16] H. Aoki and M. S. Dresselhaus, *Physics of Graphene*: Springer Science & Business Media, 2013.

[17] A. S. Mayorov, R. V. Gorbachev, S. V. Morozov, L. Britnell, R. Jalil, L. A. Ponomarenko, *et al.*, "Micrometer-scale ballistic transport in encapsulated graphene at room temperature," *Nano Letters,* vol. 11, pp. 2396-2399, 2011.

[18] A. A. Balandin, "Thermal properties of graphene and nanostructured carbon materials," *Nat Mater,* vol. 10, pp. 569-581, 2011.

[19] S. Berber, Y.-K. Kwon, and D. Tománek, "Unusually high thermal conductivity of carbon nanotubes," *Physical Review Letters,* vol. 84, pp. 4613-4616, 2000.

[20] M. Gill-Comeau and L. J. Lewis, "Heat conductivity in graphene and related materials: A time-domain modal analysis," *Physical Review B,* vol. 92, p. 195404, 2015.

[21] L. Lindsay, D. A. Broido, and N. Mingo, "Flexural phonons and thermal transport in graphene," *Physical Review B,* vol. 82, p. 115427, 2010.

[22] A. A. Balandin, S. Ghosh, W. Bao, I. Calizo, D. Teweldebrhan, F. Miao, *et al.*, "Superior thermal conductivity of single-layer graphene," *Nano Letters,* vol. 8, pp. 902-907, 2008.

[23] S. Ghosh, I. Calizo, D. Teweldebrhan, E. P. Pokatilov, D. L. Nika, A. A. Balandin, *et al.*, "Extremely high thermal conductivity of graphene: Prospects for thermal management applications in nanoelectronic circuits," *Applied Physics Letters,* vol. 92, p. 151911, 2008.

[24] J.-H. Zou, Z.-Q. Ye, and B.-Y. Cao, "Phonon thermal properties of graphene from molecular dynamics using different potentials," *The Journal of Chemical Physics,* vol. 145, p. 134705, 2016.

[25] C. Lee, X. Wei, J. W. Kysar, and J. Hone, "Measurement of the elastic properties and intrinsic strength of monolayer graphene," *Science,* vol. 321, p. 385, 2008.

[26] M. F. Yu, "Strength and breaking mechanism of multiwalled carbon nanotubes under tensile load," *Science,* vol. 287, pp. 637-640, 2000.

[27] F. Liu, P. Ming, and J. Li, "Ab initio calculation of ideal strength and phonon instability of graphene under tension," *Physical Review B*, vol. 76, p. 064120, 2007.

[28] C. Wei, K. Cho, and D. Srivastava, "Tensile strength of carbon nanotubes under realistic temperature and strain rate," *Physical Review B*, vol. 67, p. 115407, 2003.

[29] H. Yang, J. Heo, S. Park, H. J. Song, D. H. Seo, K.-E. Byun, *et al.*, "Graphene barristor, a triode device with a gate-controlled schottky barrier," *Science*, vol. 336, p. 1140, 2012.

[30] K. S. Novoselov, V. I. Falko, L. Colombo, P. R. Gellert, M. G. Schwab, and K. Kim, "A roadmap for graphene," *Nature*, vol. 490, pp. 192-200, 2012.

[31] A. Dhar, "Heat transport in low-dimensional systems," *Advances in Physics*, vol. 57, pp. 457-537, 2008.

[32] A. Lippi and R. Livi, "Heat conduction in two-dimensional nonlinear lattices," *Journal of Statistical Physics*, vol. 100, pp. 1147-1172, 2000.

[33] S. Lepri, R. Livi, and A. Politi, "Thermal conduction in classical low-dimensional lattices," *Physics Reports*, vol. 377, pp. 1-80, 2003.

[34] S. Ghosh, W. Bao, D. L. Nika, S. Subrina, E. P. Pokatilov, C. N. Lau, *et al.*, "Dimensional crossover of thermal transport in few-layer graphene," *Nat Mater*, vol. 9, pp. 555-558, 2010.

[35] L. Yang, P. Grassberger, and B. Hu, "Dimensional crossover of heat conduction in low dimensions," *Physical Review E*, vol. 74, p. 062101, 2006.

[36] Z. Tomofumi, K. Yoshinari, T. Kenji, O. Iwao, and W. Takanobu, "Molecular dynamics simulation on longitudinal optical phonon mode decay and heat transport in a silicon nano-structure covered with oxide films," *Japanese Journal of Applied Physics*, vol. 50, p. 010102, 2011.

[37] J. E. Turney, A. J. H. McGaughey, and C. H. Amon, "In-plane phonon transport in thin films," *Journal of Applied Physics*, vol. 107, p. 024317, 2010.

[38] P. Heino, "Dispersion and thermal resistivity in silicon nanofilms by molecular dynamics," *The European Physical Journal B*, vol. 60, pp. 171-179, 2007.

[39] S. Hamian, T. Yamada, M. Faghri, and K. Park, "Finite element analysis of transient ballistic–diffusive phonon heat transport in two-dimensional domains," *International Journal of Heat and Mass Transfer*, vol. 80, pp. 781-788, 2015.

[40] A. Cepellotti, G. Fugallo, L. Paulatto, M. Lazzeri, F. Mauri, and N. Marzari, "Phonon hydrodynamics in two-dimensional materials," *Nature Communications,* vol. 6, p. 6400, 2015.

[41] G. Backstrom and J. Chaussy, "Determination of thermal conductivity tensor and heat capacity of insulating solids," *Journal of Physics E: Scientific Instruments,* vol. 10, p. 767, 1977.

[42] M. N. Wybourne and J. K. Wigmore, "Phonon spectroscopy," *Reports on Progress in Physics,* vol. 51, p. 923, 1988.

[43] A. Chernatynskiy and S. R. Phillpot, "Phonon-mediated thermal transport: Confronting theory and microscopic simulation with experiment," *Current Opinion in Solid State and Materials Science,* vol. 17, pp. 1-9, 2013.

[44] J. E. Turney, E. S. Landry, A. J. H. McGaughey, and C. H. Amon, "Predicting phonon properties and thermal conductivity from anharmonic lattice dynamics calculations and molecular dynamics simulations," *Physical Review B,* vol. 79, p. 064301, 2009.

[45] P. K. Schelling, S. R. Phillpot, and P. Keblinski, "Comparison of atomic-level simulation methods for computing thermal conductivity," *Physical Review B,* vol. 65, p. 144306, 2002.

[46] O. N. Bedoya-Martínez, J.-L. Barrat, and D. Rodney, "Computation of the thermal conductivity using methods based on classical and quantum molecular dynamics," *Physical Review B,* vol. 89, p. 014303, 2014.

[47] G. P. Srivastava, *The physics of phonons*: Adam Hilger, 1990.

[48] R. E. Peierls, *Quantum theory of solids*: Oxford University Press, 1955.

[49] A. J. H. McGaughey and M. Kaviany, "Quantitative validation of the Boltzmann transport equation phonon thermal conductivity model under the single-mode relaxation time approximation," *Physical Review B,* vol. 69, p. 094303, 2004.

[50] A. Nabovati, D. P. Sellan, and C. H. Amon, "On the lattice Boltzmann method for phonon transport," *Journal of Computational Physics,* vol. 230, pp. 5864-5876, 2011.

[51] A. Cepellotti and N. Marzari, "Thermal transport in crystals as a kinetic theory of relaxons," *Physical Review X,* vol. 6, p. 041013, 2016.

[52] M. Kaviany, *Heat transfer physics*: Cambridge University Press, 2014.

[53] M. S. Green, "Markoff random processes and the statistical mechanics of time-dependent phenomena. II. Irreversible processes in fluids," *The Journal of Chemical Physics,* vol. 22, pp. 398-413, 1954.

[54] R. Kubo, "Statistical-mechanical theory of irreversible processes. I. General theory and simple applications to magnetic and conduction problems," *Journal of the Physical Society of Japan,* vol. 12, p. 570, 1957.

[55] A. J. C. Ladd, B. Moran, and W. G. Hoover, "Lattice thermal conductivity: A comparison of molecular dynamics and anharmonic lattice dynamics," *Physical Review B,* vol. 34, pp. 5058-5064, 1986.

[56] A. Henry and G. Chen, "Anomalous heat conduction in polyethylene chains: Theory and molecular dynamics simulations," *Physical Review B,* vol. 79, p. 144305, 2009.

[57] M. Gill-Comeau and L. J. Lewis, "On the importance of collective excitations for thermal transport in graphene," *Applied Physics Letters,* vol. 106, p. 193104, 2015.

[58] M. Gill-Comeau and L. J. Lewis, "Cross-correlations between phonon modes in anharmonic oscillator chains: Role in heat transport," *Physical Review E,* vol. 89, p. 042114, 2014.

[59] A. J. H. McGaughey and M. Kaviany, "Thermal conductivity decomposition and analysis using molecular dynamics simulations: Part II. Complex silica structures," *International Journal of Heat and Mass Transfer,* vol. 47, pp. 1799-1816, 2004.

[60] A. J. H. McGaughey and M. Kaviany, "Thermal conductivity decomposition and analysis using molecular dynamics simulations. Part I. Lennard-Jones argon," *International Journal of Heat and Mass Transfer,* vol. 47, pp. 1783-1798, 2004.

[61] J. A. Thomas, J. E. Turney, R. M. Iutzi, C. H. Amon, and A. J. H. McGaughey, "Predicting phonon dispersion relations and lifetimes from the spectral energy density," *Physical Review B,* vol. 81, p. 081411, 2010.

[62] A. J. H. McGaughey and M. Kaviany, "Observation and description of phonon interactions in molecular dynamics simulations," *Physical Review B,* vol. 71, p. 184305, 2005.

[63] S. Lepri, R. Livi, and A. Politi, "Heat conduction in chains of nonlinear oscillators," *Physical Review Letters,* vol. 78, pp. 1896-1899, 1997.

[64] G. P. Berman and F. M. Izrailev, "The Fermi–Pasta–Ulam problem: Fifty years of progress," *Chaos: An Interdisciplinary Journal of Nonlinear Science,* vol. 15, p. 015104, 2005.

[65] S. Liu, P. Hänggi, N. Li, J. Ren, and B. Li, "Anomalous heat diffusion," *Physical Review Letters*, vol. 112, p. 040601, 2014.

[66] T. Meier, F. Menges, P. Nirmalraj, H. Hölscher, H. Riel, and B. Gotsmann, "Length-dependent thermal transport along molecular chains," *Physical Review Letters*, vol. 113, p. 060801, 2014.

[67] X. Xu, L. F. C. Pereira, Y. Wang, J. Wu, K. Zhang, X. Zhao, *et al.*, "Length-dependent thermal conductivity in suspended single-layer graphene," *Nature Communications*, vol. 5, p. 3689, 2014.

[68] Y. Shen, G. Xie, X. Wei, K. Zhang, M. Tang, J. Zhong, *et al.*, "Size and boundary scattering controlled contribution of spectral phonons to the thermal conductivity in graphene ribbons," *Journal of Applied Physics*, vol. 115, p. 063507, 2014.

[69] J. C. Ward and J. Wilks, "III. Second sound and the thermo-mechanical effect at very low temperatures," *The London, Edinburgh, and Dublin Philosophical Magazine and Journal of Science*, vol. 43, pp. 48-50, 1952.

[70] S. Lee, D. Broido, K. Esfarjani, and G. Chen, "Hydrodynamic phonon transport in suspended graphene," *Nature Communications*, vol. 6, p. 6290, 2015.

[71] H. B. G. Casimir, "Note on the conduction of heat in crystals," *Physica*, vol. 5, pp. 495-500, 1938.

[72] G. Fugallo, A. Cepellotti, L. Paulatto, M. Lazzeri, N. Marzari, and F. Mauri, "Thermal conductivity of graphene and graphite: Collective excitations and mean free paths," *Nano Letters*, vol. 14, pp. 6109-6114, 2014.

[73] M. T. Dove, *Introduction to lattice dynamics* vol. 4: Cambridge university press, 1993.

[74] N. I. Papanicolaou, I. E. Lagaris, and G. A. Evangelakis, "Modification of phonon spectral densities of the (001) copper surface due to copper adatoms by molecular dynamics simulation," *Surface Science*, vol. 337, pp. L819-L824, 1995.

[75] P. D. Ditlevsen, P. Stoltze, and J. K. No/rskov, "Anharmonicity and disorder on the Cu(110) surface," *Physical Review B*, vol. 44, pp. 13002-13009, 1991.

[76] J. M. Dickey and A. Paskin, "Computer simulation of the lattice dynamics of solids," *Physical Review*, vol. 188, pp. 1407-1418, 1969.

[77] R. Berman, *Thermal conduction in solids*: Clarendon Press, 1976.

[78] J. M. Ziman, *Electrons and phonons: the theory of transport phenomena in solids*: Oxford University Press, 1960.

[79] C. Kittel, *Quantum theory of solids*, Second ed. USA: John Wiley & Sons, Inc, 1987.

[80] L.F. Lou, *Introduction to phonons and electrons*: World Scientific, 2003.

[81] M. Born and K. Huang, *Dynamical theory of crystal lattices*: Clarendon Press, 1998.

[82] Z. Fan, L. F. C. Pereira, H.-Q. Wang, J.-C. Zheng, D. Donadio, and A. Harju, "Force and heat current formulas for many-body potentials in molecular dynamics simulations with applications to thermal conductivity calculations," *Physical Review B*, vol. 92, p. 094301, 2015.

[83] A. Kinaci, J. B. Haskins, and T. Çağın, "On calculation of thermal conductivity from Einstein relation in equilibrium molecular dynamics," *The Journal of Chemical Physics*, vol. 137, 2012.

[84] R. Vogelsang, C. Hoheisel, and G. Ciccotti, "Thermal conductivity of the Lennard-Jones liquid by molecular dynamics calculations," *The Journal of Chemical Physics*, vol. 86, pp. 6371-6375, 1987.

[85] G. Kresse, J. Furthmüller, and J. Hafner, "Ab initio force constant approach to phonon dispersion relations of diamond and graphite," *EPL (Europhysics Letters)*, vol. 32, p. 729, 1995.

[86] L. T. Kong, "Phonon dispersion measured directly from molecular dynamics simulations," *Computer Physics Communications*, vol. 182, pp. 2201-2207, 2011.

[87] C. Z. Wang, C. T. Chan, and K. M. Ho, "Tight-binding molecular-dynamics study of phonon anharmonic effects in silicon and diamond," *Physical Review B*, vol. 42, pp. 11276-11283, 1990.

[88] N. de Koker, "Thermal conductivity of MgO periclase from equilibrium first principles molecular dynamics," *Physical Review Letters*, vol. 103, p. 125902, 2009.

[89] A. Strachan, "Normal modes and frequencies from covariances in molecular dynamics or Monte Carlo simulations," *The Journal of Chemical Physics*, vol. 120, pp. 1-4, 2004.

[90] N. Rega, "Vibrational analysis beyond the harmonic regime from ab-initio molecular dynamics," *Theoretical Chemistry Accounts*, vol. 116, pp. 347-354, 2006.

[91] M. Schmitz and P. Tavan, "Vibrational spectra from atomic fluctuations in dynamics simulations. I. Theory, limitations, and a sample application," *The Journal of Chemical Physics*, vol. 121, pp. 12233-12246, 2004.

[92] D. C. Rapaport, *The art of molecular dynamics simulation*: Cambridge university press, 2004.

[93] D. Gray, A. McCaughan, and B. Mookerji, "Crystal structure of graphite, graphene and silicon," *Physics for solid state applications. WVU, Boston,* 2009.

[94] H. Ghasemi and A. Rajabpour, "Thermal expansion coefficient of graphene using molecular dynamics simulation: A comparative study on potential functions," in *Journal of Physics: Conference Series*, vol. 785, p. 012006, 2017.

[95] H. J. Berendsen, J. v. Postma, W. F. van Gunsteren, A. DiNola, and J. Haak, "Molecular dynamics with coupling to an external bath," *The Journal of Chemical Physics,* vol. 81, pp. 3684-3690, 1984.

[96] J. Tersoff, "New empirical approach for the structure and energy of covalent systems," *Physical Review B,* vol. 37, pp. 6991-7000, 1988.

[97] L. Lindsay and D. A. Broido, "Optimized Tersoff and Brenner empirical potential parameters for lattice dynamics and phonon thermal transport in carbon nanotubes and graphene," *Physical Review B,* vol. 81, p. 205441, 2010.

[98] E. N. Koukaras, G. Kalosakas, C. Galiotis, and K. Papagelis, "Phonon properties of graphene derived from molecular dynamics simulations," *Scientific Reports,* vol. 5, p. 12923, 2015.

[99] A. V. Evteev, L. Momenzadeh, E. V. Levchenko, I. V. Belova, and G. E. Murch, "Decomposition model for phonon thermal conductivity of a monatomic lattice," *Philosophical Magazine,* vol. 94, pp. 3992-4014, 2014.

[100] T. Hori, T. Shiga, and J. Shiomi, "Phonon transport analysis of silicon germanium alloys using molecular dynamics simulations," *Journal of Applied Physics,* vol. 113, p. 203514, 2013.

[101] B. Qiu, H. Bao, G. Zhang, Y. Wu, and X. Ruan, "Molecular dynamics simulations of lattice thermal conductivity and spectral phonon mean free path of PbTe: Bulk and nanostructures," *Computational Materials Science,* vol. 53, pp. 278-285, 2012.

[102] Z. Wei, J. Yang, K. Bi, and Y. Chen, "Mode dependent lattice thermal conductivity of single layer graphene," *Journal of Applied Physics,* vol. 116, p. 153503, 2014.

[103] K. Sääskilahti, J. Oksanen, S. Volz, and J. Tulkki, "Frequency-dependent phonon mean free path in carbon nanotubes from nonequilibrium molecular dynamics," *Physical Review B,* vol. 91, p. 115426, 2015.

[104] K. Sääskilahti, J. Oksanen, S. Volz, and J. Tulkki, "Nonequilibrium phonon mean free paths in anharmonic chains," *Physical Review B,* vol. 92, p. 245411, 2015.

[105] K. Sääskilahti, J. Oksanen, J. Tulkki, and S. Volz, "Role of anharmonic phonon scattering in the spectrally decomposed thermal conductance at planar interfaces," *Physical Review B,* vol. 90, p. 134312, 2014.

[106] T. Feng and X. Ruan, "Prediction of spectral phonon mean free path and thermal conductivity with applications to thermoelectrics and thermal management: A review," *Journal of Nanomaterials,* vol. 2014, p. 25, 2014.

[107] L. F. C. Pereira and D. Donadio, "Divergence of the thermal conductivity in uniaxially strained graphene," *Physical Review B,* vol. 87, p. 125424, 2013.

[108] W. J. Evans, L. Hu, and P. Keblinski, "Thermal conductivity of graphene ribbons from equilibrium molecular dynamics: Effect of ribbon width, edge roughness, and hydrogen termination," *Applied Physics Letters,* vol. 96, p. 203112, 2010.

[109] H. Zhang, G. Lee, A. F. Fonseca, T. L. Borders, and K. Cho, "Isotope effect on the thermal conductivity of graphene," *Journal of Nanomaterials,* vol. 2010, p. 7, 2010.

[110] Z. Wang and X. Ruan, "On the domain size effect of thermal conductivities from equilibrium and nonequilibrium molecular dynamics simulations," *Journal of Applied Physics,* vol. 121, p. 044301, 2017.

[111] H. Zhang, G. Lee, and K. Cho, "Thermal transport in graphene and effects of vacancy defects," *Physical Review B,* vol. 84, p. 115460, 2011.

[112] Z.-Y. Ong and E. Pop, "Effect of substrate modes on thermal transport in supported graphene," *Physical Review B,* vol. 84, p. 075471, 2011.

[113] L. Chen and S. Kumar, "Thermal transport in graphene supported on copper," *Journal of Applied Physics,* vol. 112, p. 043502, 2012.

[114] C. Faugeras, B. Faugeras, M. Orlita, M. Potemski, R. R. Nair, and A. Geim, "Thermal conductivity of graphene in corbino membrane geometry," *ACS Nano,* vol. 4, pp. 1889-1892, 2010.

[115] W. Cai, A. L. Moore, Y. Zhu, X. Li, S. Chen, L. Shi, *et al.*, "Thermal transport in suspended and supported monolayer graphene grown by chemical vapor deposition," *Nano Letters,* vol. 10, pp. 1645-1651, 2010.

[116] S. Chen, A. L. Moore, W. Cai, J. W. Suk, J. An, C. Mishra, *et al.*, "Raman measurements of thermal transport in suspended monolayer graphene of variable sizes in vacuum and gaseous environments," *ACS Nano,* vol. 5, pp. 321-328, 2010.

[117] B. Qiu and X. Ruan, "Reduction of spectral phonon relaxation times from suspended to supported graphene," *Applied Physics Letters,* vol. 100, p. 193101, 2012.

APPENDICES

Appendix A: Properties derived from normal modes for a linear monoatomic chain

Consider a linear chain of N atoms with a two-body harmonic potential and only nearest neighbor interaction. The potential due to interaction between a pair of atoms l and k is given by Eqn. (A1) while the equation of motion for an atom l is given by Eqn. (A2):

$$U_{lk}(t) = \frac{1}{2} C \left(u(l,t) - u(k,t) \right)^2 \tag{A1}$$

$$F(l,t) = m \frac{\partial^2 u(l,t)}{\partial t^2} = C \left(u(l-1,t) - 2u(l,t) + u(l+1,t) \right) \tag{A2}$$

The general solution for the equation of motion is given by:

$$u(j,t) = \sum_q \frac{1}{\sqrt{m}} A(q) \cos\left(q.r_j - w(q)t + \phi(q) \right) \tag{A3}$$

The allowed wave vectors and the corresponding frequencies are given by:

$$q = r \frac{2\pi}{Na}; r = 0, \pm 1, \pm 2..... \tag{A4}$$

$$-\frac{\pi}{a} < q \leq \frac{\pi}{a} \tag{A5}$$

$$w(q) = \sqrt{\frac{4C}{m}} \left| \sin\left(\frac{qa}{2} \right) \right| \tag{A6}$$

The phase and group velocities are given by:

$$v_p(q) = \frac{w(q)}{q} = \frac{1}{q}\sqrt{\frac{4C}{m}}\left|\sin\left(\frac{qa}{2}\right)\right| \tag{A7}$$

$$v_g(q) = \frac{\partial w(q)}{\partial q} = a\sqrt{\frac{C}{m}}\cos\left(\frac{qa}{2}\right)\frac{q}{|q|} \tag{A8}$$

The net kinetic energy of an atom *l* at time *t* due to contribution from each mode is given by:

$$K(l,t) = \frac{1}{2}mv(l,t)^2 \tag{A9}$$

Substituting the general solution from Eqn. (A3) into the above expression:

$$K(l,t) = \frac{1}{2}m\left(\sum_q \frac{1}{\sqrt{m}} w(q)A(q)\sin\left(qla - w(q)t + \varphi(q)\right)\right)^2 \tag{A10}$$

Expanding:

$$K(l,t) = \frac{1}{2}\sum_{q_1}\sum_{q_2}\left[\begin{array}{l} w(q_1)w(q_2)A(q_1)A(q_2)\times \\ \sin\left(q_1la - w(q_1)t + \varphi(q_1)\right)\sin\left(q_2la - w(q_2)t + \varphi(q_2)\right)\end{array}\right] \tag{A11}$$

Thus:

$$K^{q_1q_2}(l,t)=\left[\begin{array}{l}\frac{1}{2}w(q_1)w(q_2)A(q_1)A(q_2)\times\\ \sin\left(q_1la-w(q_1)t+\varphi(q_1)\right)\sin\left(q_2la-w(q_2)t+\varphi(q_2)\right)\end{array}\right] \tag{A12}$$

$$K(l,t)=\sum_{q_1}\sum_{q_2}K^{q_1q_2}(l,t) \tag{A13}$$

Splitting the sine terms as a difference of cosines:

$$K^{q_1q_2}(l,t)=\left[\begin{array}{l}\frac{1}{4}w(q_1)w(q_2)A(q_1)A(q_2)\times\\ \left(\cos\left((q_1-q_2)la-\left(w(q_1)-w(q_2)\right)t+\left(\varphi(q_1)-\varphi(q_2)\right)\right)-\right.\\ \left.\cos\left((q_1+q_2)la-\left(w(q_1)+w(q_2)\right)t+\left(\varphi(q_1)+\varphi(q_2)\right)\right)\end{array}\right] \tag{A14}$$

Thus the instantaneous kinetic energy of an atom is the sum of the kinetic energies due to the pair contributions from individual modes.

Similarly, the potential energy of an atom *j* at time *t* due to contribution from each mode is given by:

$$U(l,t)=\frac{1}{4}C\left[\left(u(l,t)-u(l-1,t)\right)^2+\left(u(l,t)-u(l+1,t)\right)^2\right] \tag{A15}$$

Expanding in terms of normal modes:

$$U(l,t)=\frac{1}{4}C\left[\begin{array}{l}\sum_{r_1}\sum_{r_2}\left(u^{q_1}(l,t)-u^{q_1}(l-1,t)\right)\left(u^{q_2}(l,t)-u^{q_2}(l-1,t)\right)\\ +\sum_{r_1}\sum_{r_2}\left(u^{q_1}(l,t)-u^{q_1}(l+1,t)\right)\left(u_j^{r_2}(l,t)-u^{q_2}(l+1,t)\right)\end{array}\right] \tag{A16}$$

$$U(l,t)=\sum_{r_1}\sum_{r_2}U^{q_1q_2}(l,t) \tag{A17}$$

Splitting the pair contribution:

$$U^{q_1q_2}(l,t)=\frac{1}{4}C\begin{bmatrix}\left(u^{q_1}(l,t)-u^{q_1}(l-1,t)\right)\left(u^{q_2}(l,t)-u^{q_2}(l-1,t)\right)\\+\left(u^{q_1}(l,t)-u^{q_1}(l+1,t)\right)\left(u^{q_2}(l,t)-u^{q_2}(l+1,t)\right)\end{bmatrix} \tag{A18}$$

Substituting the general solution from Eqn. (A3) into the above expression:

$$U^{q_1q_2}(l,t)=$$
$$\frac{C}{4m}\begin{bmatrix}A(q_1)\left(\cos\left(q_1la-w(q_1)t+\varphi(q_1)\right)-\cos\left(q_1(l-1)a-w(q_1)t+\varphi(q_1)\right)\right)\times\\A(q_2)\left(\cos\left(q_2la-w(q_2)t+\varphi(q_2)\right)-\cos\left(q_2(l-1)a-w(q_2)t+\varphi(q_2)\right)\right)+\\A(q_1)\left(\cos\left(q_1la-w(q_1)t+\varphi(q_1)\right)-\cos\left(q_1(l+1)a-w(q_1)t+\varphi(q_1)\right)\right)\times\\A(q_2)\left(\cos\left(q_2la-w(q_2)t+\varphi(q_2)\right)-\cos\left(q_2(l+1)a-w(q_2)t+\varphi(q_2)\right)\right)+\end{bmatrix} \tag{A19}$$

Expanding:

$$U^{q_1q_2}(l,t)=\frac{C}{m}A(q_1)A(q_2)\begin{bmatrix}\sin\left(-\frac{q_1a}{2}\right)\sin\left(q_1(l-0.5)a-w(q_1)t+\varphi(q_1)\right)\times\\\sin\left(-\frac{q_2a}{2}\right)\sin\left(q_2(l-0.5)a-w(q_2)t+\varphi(q_2)\right)+\\\sin\left(\frac{q_1a}{2}\right)\sin\left(q_1(l+0.5)a-w(q_1)t+\varphi(q_1)\right)\times\\\sin\left(\frac{q_2a}{2}\right)\sin\left(q_2(l+0.5)a-w(q_2)t+\varphi(q_2)\right)\end{bmatrix} \tag{A20}$$

Simplifying:

$$U^{q_1q_2}(l,t)=\frac{C}{m}A(q_1)A(q_2)\sin\left(\frac{q_1a}{2}\right)\sin\left(\frac{q_2a}{2}\right)\begin{bmatrix}\sin\left(q_1(l-0.5)a-w(q_1)t+\varphi(q_1)\right)\times\\ \sin\left(q_2(l-0.5)a-w(q_2)t+\varphi(q_2)\right)+\\ \sin\left(q_1(l+0.5)a-w(q_1)t+\varphi(q_1)\right)\times\\ \sin\left(q_2(l+0.5)a-w(q_2)t+\varphi(q_2)\right)\end{bmatrix} \quad \text{(A21)}$$

Splitting the sine terms as a difference of cosines:

$$U^{q_1q_2}(l,t)=\left(\begin{array}{l}\frac{CA(q_1)A(q_2)}{2m}\sin\left(\frac{q_1a}{2}\right)\sin\left(\frac{q_2a}{2}\right)\times\\ \left[\begin{array}{l}\cos\left((q_1-q_2)(l-0.5)a-\left(w(q_1)-w(q_2)\right)t+\varphi(q_1)-\varphi(q_2)\right)\\ -\cos\left((q_1+q_2)(l-0.5)a-\left(w(q_1)+w(q_2)\right)t+\varphi(q_1)+\varphi(q_2)\right)\\ \cos\left((q_1-q_2)(l+0.5)a-\left(w(q_1)-w(q_2)\right)t+\varphi(q_1)-\varphi(q_2)\right)\\ -\cos\left((q_1+q_2)(l+0.5)a-\left(w(q_1)+w(q_2)\right)t+\varphi(q_1)+\varphi(q_2)\right)\end{array}\right]\end{array}\right) \quad \text{(A22)}$$

Simplifying:

$$U^{q_1q_2}(l,t)=\left(\begin{array}{l}\frac{C}{m}A(q_1)A(q_2)\sin\left(\frac{q_1a}{2}\right)\sin\left(\frac{q_2a}{2}\right)\times\\ \left[\begin{array}{l}\cos\left((q_1-q_2)\,ja-\left(w(q_1)-w(q_2)\right)t+\varphi(q_1)-\varphi(q_2)\right)\cos\left((q_1-q_2)\frac{a}{2}\right)\\ -\cos\left((q_1+q_2)\,ja-\left(w(q_1)+w(q_2)\right)t+\varphi(q_1)+\varphi(q_2)\right)\cos\left((q_1+q_2)\frac{a}{2}\right)\end{array}\right]\end{array}\right) \quad \text{(A23)}$$

Substituting the expression for mode frequency from Eqn. (A6) into the above expression:

$$U^{q_1q_2}(l,t)=$$
$$\left(\begin{array}{l}\frac{1}{4}A(q_1)A(q_2)w(q_1)w(q_2)\frac{q_1}{|q_1|}\frac{q_2}{|q_2|}\times \\ \left[\begin{array}{l}\cos\left((q_1-q_2)\,ja-\left(w(q_1)-w(q_2)\right)t+\varphi(q_1)-\varphi(q_2)\right)\cos\left((q_1-q_2)\frac{a}{2}\right) \\ -\cos\left((q_1+q_2)\,ja-\left(w(q_1)+w(q_2)\right)t+\varphi(q_1)+\varphi(q_2)\right)\cos\left((q_1+q_2)\frac{a}{2}\right)\end{array}\right]\end{array}\right) \tag{A24}$$

Thus the instantaneous potential energy of an atom is also the sum of the potential energies due to the pair contributions from individual modes.

The total energy is simply the sum of the kinetic and potential energies. Thus:

$$E(l,t)=\sum_{q_1}\sum_{q_2}E^{q_1q_2}(l,t)=\sum_{q_1}\sum_{q_2}\left(U^{q_1q_2}(l,t)+K^{q_1q_2}(l,t)\right) \tag{A25}$$

Substituting the expressions for potential and kinetic energies from Eqn. (A24) and Eqn. (A14) , respectively, into the above expression:

$$E^{q_1q_2}(l,t)=$$
$$\left(\begin{array}{l}\frac{1}{4}w(q_1)w(q_2)A(q_1)A(q_2)\times \\ \left[\begin{array}{l}\left(\begin{array}{l}\cos\left((q_1-q_2)\,ja-\left(w(q_1)-w(q_2)\right)t+\left(\varphi(q_1)-\varphi(q_2)\right)\right)- \\ \cos\left((q_1+q_2)\,ja-\left(w(q_1)+w(q_2)\right)t+\left(\varphi(q_1)+\varphi(q_2)\right)\right)\end{array}\right)+\frac{q_1}{|q_1|}\frac{q_2}{|q_2|}\times \\ \left[\begin{array}{l}\cos\left((q_1-q_2)\,ja-\left(w(q_1)-w(q_2)\right)t+\varphi(q_1)-\varphi(q_2)\right)\cos\left((q_1-q_2)\frac{a}{2}\right) \\ -\cos\left((q_1+q_2)\,ja-\left(w(q_1)+w(q_2)\right)t+\varphi(q_1)+\varphi(q_2)\right)\cos\left((q_1+q_2)\frac{a}{2}\right)\end{array}\right]\end{array}\right]\end{array}\right) \tag{A26}$$

Simplifying:

$$E^{q_1 q_2}(l,t) = \left(\begin{array}{l} \frac{1}{4} w(q_1) w(q_2) A(q_1) A(q_2) \times \\ \left(\begin{array}{l} \cos\left((q_1 - q_2)\, ja - \left(w(q_1) - w(q_2) \right) t + \left(\varphi(q_1) - \varphi(q_2) \right) \right) \\ \times \left(1 + \frac{q_1}{|q_1|} \frac{q_2}{|q_2|} \cos\left((q_1 - q_2) \frac{a}{2} \right) \right) - \\ \cos\left((q_1 + q_2)\, ja - \left(w(q_1) + w(q_2) \right) t + \left(\varphi(q_1) + \varphi(q_2) \right) \right) \\ \times \left(1 + \frac{q_1}{|q_1|} \frac{q_2}{|q_2|} \cos\left((q_1 + q_2) \frac{a}{2} \right) \right) \end{array} \right) \end{array} \right) \tag{A27}$$

As expected, the instantaneous total energy of an atom is the sum of the total energies due to the pair contributions from individual modes.

The net heat current at an atom *l* is given by:

$$J(l,t) = \frac{1}{V} \left[E(l,t) v(l,t) + \frac{1}{2} \sum_{k=1, \neq l}^{N} \left[F_{lk}(t) . v(l,t) \right] r_{lk} \right] \tag{A28}$$

The first term is associated with the total energy current (flux), while the second term represents the current (flux) corresponding to the virial interaction. As discussed in Chapter 3, only the virial part of the heat current is significant for thermal transport in a non-diffusive system.

$$J_{kin}(l,t)=\frac{1}{V}E(l,t)v(l,t) \tag{A29}$$

$$J_{vir}(l,t)=\frac{1}{2V}\sum_{k=1,\neq l}^{N}\left[F_{lk}(t).v(l,t)\right]r_{lk} \tag{A30}$$

For a two-body harmonic potential with only 1st neighbor interaction, the virial part is given by:

$$J_{vir}(l,t)=\frac{1}{2V}\begin{bmatrix}\left(-C\left(u(l,t)-u(l-1,t)\right)v(l,t)\right)\left(u(l,t)-u(l-1,t)+a\right)\\ \left(-C\left(u(l,t)-u(l+1,t)\right)v(l,t)\right)\left(u(l,t)-u(l+1,t)-a\right)\end{bmatrix} \tag{A31}$$

For small displacements about the equilibrium position, this can be approximated as:

$$J_{vir}(l,t)\approx-\frac{a}{2V}\left[C\left(u(l+1,t)-u(l-1,t)\right)v(l,t)\right] \tag{A32}$$

Substituting the general solution from Eqn. (A3) into the above expression:

$$J_{vir}(l,t)\approx\sum_{q_1}\sum_{q_2}-\frac{a}{2V}\left[C\left(u^{q_2}(l+1,t)-u^{q_2}(l-1,t)\right)v^{q_1}(l,t)\right] \tag{A33}$$

$$J_{vir}(l,t)\approx\sum_{q_1,q_2}J_{vir}^{q_1,q_2}(l,t) \tag{A34}$$

$$J_{vir}^{q_1,q_2}(l,t)\approx -\frac{aC}{2Vm}\begin{bmatrix}A(q_1)A(q_2)w(q_1)\sin\left(q_1ja-w(q_1)t+\varphi(q_1)\right)\times\\ \left(\cos\left(q_2(l+1)a-w(q_2)t+\varphi(q_2)\right)-\cos\left(q_2(l-1)a-w(q_2)t+\varphi(q_2)\right)\right)\end{bmatrix} \tag{A35}$$

Simplifying:

$$J_{vir}^{q_1,q_2}(l,t) \approx \frac{aC}{Vm}\left[\begin{array}{l} A(q_1)A(q_2)w(q_1)\sin\left(\frac{q_2 a}{2}\right)\cos\left(\frac{q_2 a}{2}\right)\times \\ \sin\left(q_1 la - w(q_1)t + \varphi(q_1)\right)\sin\left(q_2 la - w(q_2)t + \varphi(q_2)\right)\end{array}\right] \quad \text{(A36)}$$

Substituting the expressions for mode frequency and group velocity (see Eqn. (A6) and Eqn. (A8)):

$$J_{vir}^{q_1,q_2}(l,t) \approx \frac{1}{2V}\left[\begin{array}{l} A(q_1)A(q_2)w(q_1)w(q_2)v_g(q_2)\times \\ \left[\begin{array}{l}\cos\left((q_1-q_2)la-\left(w(q_1)-w(q_2)\right)t+\varphi(q_1)-\varphi(q_2)\right)- \\ \cos\left((q_1+q_2)la-\left(w(q_1)+w(q_2)\right)t+\varphi(q_1)+\varphi(q_2)\right)\end{array}\right]\end{array}\right] \quad \text{(A37)}$$

Thus the instantaneous heat current at an atom is also the sum of the heat currents due to the pair contributions from individual modes.

Next, the total contribution due to all atoms is computed. While computing the total contributions, the following result will be used:

$$\sum_{l=1}^{N}\cos(qla+\alpha) = 0 \forall q = r\frac{2\pi}{Na}; r = \pm 1, \pm 2.....; \alpha \equiv \text{constant} \quad \text{(A38)}$$

Starting with the expression for the net kinetic energy:

$$K(t)=\sum_{q_1,q_2}\sum_{l=1}^{N}K^{q_1q_2}(l,t) \tag{A39}$$

$$K(t)=\sum_{q_1,q_2}\sum_{l=1}^{N}\left[\begin{array}{l}\frac{1}{4}w(q_1)w(q_2)A(q_1)A(q_2)\times\\ \left(\begin{array}{l}\cos\left((q_1-q_2)la-\left(w(q_1)-w(q_2)\right)t+\left(\varphi(q_1)-\varphi(q_2)\right)\right)-\\ \cos\left((q_1+q_2)la-\left(w(q_1)+w(q_2)\right)t+\left(\varphi(q_1)+\varphi(q_2)\right)\right)\end{array}\right)\end{array}\right] \tag{A40}$$

Rearranging:

$$K(t)=\sum_{q_1,q_2}\left[\begin{array}{l}\frac{1}{4}w(q_1)w(q_2)A(q_1)A(q_2)\times\\ \sum_{l=1}^{N}\left(\begin{array}{l}\cos\left((q_1-q_2)la-\left(w(q_1)-w(q_2)\right)t+\left(\varphi(q_1)-\varphi(q_2)\right)\right)-\\ \cos\left((q_1+q_2)la-\left(w(q_1)+w(q_2)\right)t+\left(\varphi(q_1)+\varphi(q_2)\right)\right)\end{array}\right)\end{array}\right] \tag{A41}$$

Using the relation given by Eqn. (A38), for wave vectors given by Eqn. (A4), the summation over the cosine term above goes to zero unless $q_1 = q_2$ or $q_1 = -q_2$. This gives:

$$K(t)=\frac{N}{4}\sum_{q}w^2(q)A^2(q)-\frac{N}{4}\sum_{q}w^2(q)A(q)A(-q)\cos\left(-2w(q)t+\varphi(q)+\varphi(-q)\right) \tag{A42}$$

Similarly, computing the total potential energy due to all atoms:

$$U(t)=\sum_{q_1,q_2}\sum_{l=1}^{N}U^{q_1q_2}(l,t) \tag{A43}$$

$$U(t)=$$
$$\sum_{q_1,q_2}\sum_{l=1}^{N}\left(\begin{array}{l}\frac{1}{4}A(q_1)A(q_2)w(q_1)w(q_2)\frac{q_1}{|q_1|}\frac{q_2}{|q_2|}\times \\ \left[\begin{array}{l}\cos\left((q_1-q_2)\,ja-\left(w(q_1)-w(q_2)\right)t+\varphi(q_1)-\varphi(q_2)\right)\cos\left((q_1-q_2)\frac{a}{2}\right) \\ -\cos\left((q_1+q_2)\,ja-\left(w(q_1)+w(q_2)\right)t+\varphi(q_1)+\varphi(q_2)\right)\cos\left((q_1+q_2)\frac{a}{2}\right)\end{array}\right]\end{array}\right) \quad \text{(A44)}$$

Rearranging:

$$U(t)=$$
$$\sum_{q_1,q_2}\left(\begin{array}{l}\frac{1}{4}A(q_1)A(q_2)w(q_1)w(q_2)\frac{q_1}{|q_1|}\frac{q_2}{|q_2|}\times \\ \sum_{l=1}^{N}\left(\left[\begin{array}{l}\cos\left((q_1-q_2)\,ja-\left(w(q_1)-w(q_2)\right)t+\varphi(q_1)-\varphi(q_2)\right)\cos\left((q_1-q_2)\frac{a}{2}\right) \\ -\cos\left((q_1+q_2)\,ja-\left(w(q_1)+w(q_2)\right)t+\varphi(q_1)+\varphi(q_2)\right)\cos\left((q_1+q_2)\frac{a}{2}\right)\end{array}\right]\right)\end{array}\right) \quad \text{(A45)}$$

Again, the summation over the cosine term above goes to zero unless $q_1 = q_2$ or $q_1 = -q_2$, which gives:

$$U(t)=\frac{N}{4}\sum_q A^2(q)w^2(q)+\frac{N}{4}\sum_q A(q)A(-q)w^2(q)\cos\left(-2w(q)t+\varphi(q)+\varphi(-q)\right) \quad \text{(A46)}$$

The total energy of the system is given by:

$$E(t)=K(t)+U(t)=\sum_q\frac{N}{2}w^2(q)A^2(q)=\sum_q E(q,t) \quad \text{(A47)}$$

Thus the total energy associated with any mode is constant and keeps oscillating between the kinetic and potential energy. Next, computing the virial part of the net heat current:

$$J_{vir}(t) = \sum_{q_1,q_2} \sum_{l=1}^{N} J_{vir}^{q_1 q_2}(l,t) \tag{A48}$$

$$J_{vir}(t) \approx \sum_{q_1,q_2} \sum_{l=1}^{N} \frac{1}{2V} \left[\begin{array}{l} A(q_1) A(q_2) w(q_1) w(q_2) v_g(q_2) \times \\ \left[\cos\left((q_1 - q_2) la - \left(w(q_1) - w(q_2) \right) t + \varphi(q_1) - \varphi(q_2) \right) - \right. \\ \left. \cos\left((q_1 + q_2) la - \left(w(q_1) + w(q_2) \right) t + \varphi(q_1) + \varphi(q_2) \right) \right] \end{array} \right] \tag{A49}$$

Again, the summation over the cosine term above goes to zero unless $q_1 = q_2$ or $q_1 = -q_2$:

$$J_{vir}(t) \approx \frac{N}{2V} \left[\begin{array}{l} \sum_q A^2(q,t) w^2(q) v_g(q) + \\ \sum_q A(q,t) A(-q,t) w^2(q) v_g(q) \cos\left(2w(q)t - \varphi(q) - \varphi(-q) \right) \end{array} \right] \tag{A50}$$

As the group velocities for the positive and negative modes are opposite to each other, the second term in the above summation will cancel off. Thus:

$$J_{vir}(t) \approx \frac{N}{2V} \sum_q A^2(q,t) w^2(q) v_g(q) \tag{A51}$$

Substituting the expression for the energy due to each mode (Eqn. (A47)):

$$J_{vir}(t) \approx \frac{1}{V} \sum_q E(q,t) v_g(q) \tag{A52}$$

Finally, the VACF is expressed as:

$$VACF(t) = \frac{\langle v(0)v(t)\rangle}{\langle v(0)v(0)\rangle} \tag{A53}$$

For an *N*-particle system, it is computed as:

$$VACF(t) = \frac{\frac{1}{N}\sum_{l=1}^{N}\langle v(l,0)v(l,t)\rangle}{\frac{1}{N}\sum_{l=1}^{N}\langle v(l,0)v(l,0)\rangle} \tag{A54}$$

Expanding in terms of normal modes:

$$\sum_{l}\frac{\langle v(l,0)v(l,t)\rangle}{N} = \frac{1}{N}\sum_{l}\left\langle \sum_{q_1 q_2}\begin{bmatrix}\frac{w(q_1)}{\sqrt{m}}A(q_1)\sin\left(q_1.r_l+\phi(q_1)\right)\\ \frac{w(q_2)}{\sqrt{m}}A(q_2)\sin\left(q_2.r_l-w(q_2)t+\phi(q_2)\right)\end{bmatrix}\right\rangle \tag{A55}$$

Splitting the sine terms as a difference of cosines:

$$\sum_{l}\frac{\langle v(l,0)v(l,t)\rangle}{N} = \sum_{q_1 q_2}\left\langle \begin{matrix}\frac{1}{2mN}w(q_1)w(q_2)A(q_1)A(q_2)\\ \sum_{l=1}^{N}\cos\left((q_1-q_2)la+w(q_2)t+\varphi(q_1)-\varphi(q_2)\right)\\ -\cos\left((q_1+q_2)la-w(q_2)t+\varphi(q_1)+\varphi(q_2)\right)\end{matrix}\right\rangle \tag{A56}$$

Again, the summation over the cosine term above goes to zero unless $q_1 = q_2$ or $q_1 = -q_2$:

$$\sum_l \frac{\langle v(l,0)v(l,t)\rangle}{N} = \left[\sum_q \left\langle \frac{1}{2m} w^2(q) A^2(q) \cos\left(w(q)t\right) \right\rangle - \left\langle \frac{1}{2m} w^2(q) A(q) A(-q) \cos\left(-w(q)t + \varphi(q) + \varphi(-q)\right) \right\rangle \right] \tag{A57}$$

The ensemble average of the cosine with remnant phases in the second term goes to zero. Thus:

$$\sum_l \frac{\langle v(l,0)v(l,t)\rangle}{N} = \left[\sum_q \frac{\langle A^2(q)\rangle w^2(q)}{2m} \cos\left(w(q)t\right) \right] \tag{A58}$$

Substituting the expression for total energy of a normal mode from Eqn. (A47):

$$\sum_l \frac{\langle v(l,0)v(l,t)\rangle}{N} = \left[\sum_q \frac{\langle E(q,t)\rangle}{mN} \cos\left(w(q)t\right) \right] \tag{A59}$$

Equipartition of energy requires that the total energy associated with any mode is equal to $k_B T$:

$$\sum_l \frac{\langle v(l,0)v(l,t)\rangle_T}{N} = \left[\frac{k_B T}{mN} \sum_q \cos\left(w(q)t\right) \right] \tag{A60}$$

Substituting back in Eqn. (A54):

$$VACF(t) = \frac{1}{N} \sum_q \cos\left(w(q)t\right) \tag{A61}$$

Thus the Fourier transform of the VACF gives the density of states. It may be noted that for a system with anharmonicity, the mode amplitude correlation would decay leading to:

$$\sum_{l} \frac{\langle v(l,0)v(l,t)\rangle}{N} = \sum_{q} \left\langle \frac{w^2(q)A(q,0)A(q,t)}{2m} \cos\left(w(q)t\right) \right\rangle \tag{A62}$$

Assuming an exponential decay for the correlation gives:

$$VACF(t) = \frac{1}{N} \sum_{q} \exp\left(-\frac{t}{\tau_q}\right) \cos\left(w(q)t\right) \tag{A63}$$

Appendix B: Heat current expression for Tersoff potential

Consider an N atom system with the energy and position of an atom i at time t denoted by $\varepsilon_i(t)$ and $\mathbf{r}_i(t)$ respectively. The net heat current of the system is equal to the rate of change of the first moment of energy as given below:

$$\mathbf{J}(t) = \frac{\partial}{\partial t}\sum_{i=1}^{N}\varepsilon_i(t)\mathbf{r}_i(t) \tag{B1}$$

Expanding:

$$\mathbf{J}(t) = \sum_{i=1}^{N}\varepsilon_i(t)\mathbf{v}_i(t) + \sum_{i=1}^{N}\mathbf{r}_i(t)\frac{\partial}{\partial t}\varepsilon_i(t) \tag{B2}$$

The second term above, can be expressed as:

$$\sum_{i=1}^{N}\mathbf{r}_i(t)\frac{\partial}{\partial t}\varepsilon_i(t) = \sum_{i=1}^{N}\mathbf{r}_i(t)\frac{\partial}{\partial t}\left(\frac{1}{2}m\mathbf{v}_i(t).\mathbf{v}_i(t)\right) + \sum_{i=1}^{N}\sum_{j=1;i\neq j}^{N}\mathbf{r}_i(t)\frac{\partial}{\partial t}\left(\frac{U_{ij}(t)+U_{ji}(t)}{4}\right) \tag{B3}$$

The force on atom i from an atom j due to interaction of atom k with atom l is defined as:

$$\mathbf{F}_{ij}^{kl}(t) = \nabla_{\mathbf{r}_{ij}}U_{kl}(t) \tag{B4}$$

For Tersoff potential, only four of the all possible permutations described by Eqn. (B4) are non-zero, namely, $\mathbf{F}_{ij}^{ij}(t)$, $\mathbf{F}_{ij}^{ji}(t)$, $\mathbf{F}_{ij}^{ik}(t)$ and $\mathbf{F}_{ij}^{jk}(t)$.

Expanding Eqn. (B3) using Eqn. (B4) and dropping *t* for a more compact notation; however, it should be noted that all of the variables in the equations that follow are a function of time:

$$= \begin{pmatrix} \sum_{i=1}^{N}\sum_{j=1;j\neq i}^{N} \mathbf{r}_i \left[\left(\mathbf{F}_{ij}^{ij} + \mathbf{F}_{ij}^{ji} \right).\mathbf{v}_i \right] + \sum_{i=1}^{N}\sum_{j=1;j\neq i}^{N}\sum_{k=1;k\neq i,j}^{N} \mathbf{r}_i \left[\left(\mathbf{F}_{ij}^{ik} + \mathbf{F}_{ij}^{jk} \right).\mathbf{v}_i \right] + \\ \sum_{i=1}^{N}\sum_{j=1;i\neq j}^{N} \mathbf{r}_i \left[\begin{array}{l} \left\{ \left(\frac{\partial}{\partial \mathbf{r}_i} \left(\frac{U_{ij} + U_{ji}}{4} \right) \right).\mathbf{v}_i \right\} + \left\{ \left(\frac{\partial}{\partial \mathbf{r}_j} \left(\frac{U_{ij} + U_{ji}}{4} \right) \right).\mathbf{v}_j \right\} \\ + \sum_{k=1;k\neq i,\mathrm{j}}^{N} \left\{ \left(\frac{\partial}{\partial \mathbf{r}_k} \left(\frac{U_{ij} + U_{ji}}{4} \right) \right).\mathbf{v}_k \right\} \end{array} \right] \end{pmatrix} \quad \text{(B5)}$$

Simplifying:

$$= \begin{pmatrix} \sum_{i=1}^{N}\sum_{j=1;j\neq i}^{N} \mathbf{r}_i \left[\left(\mathbf{F}_{ij}^{ij} + \mathbf{F}_{ij}^{ji} \right).\mathbf{v}_i \right] + \sum_{i=1}^{N}\sum_{j=1;j\neq i}^{N}\sum_{k=1;k\neq i,j}^{N} \mathbf{r}_i \left[\left(\mathbf{F}_{ij}^{ik} + \mathbf{F}_{ij}^{jk} \right).\mathbf{v}_i \right] - \\ \sum_{i=1}^{N}\sum_{j=1;i\neq j}^{N} \frac{\mathbf{r}_i}{2} \left[\begin{array}{l} \left\{ \left(\mathbf{F}_{ij}^{ij} + \mathbf{F}_{ij}^{ji} \right).\mathbf{v}_i \right\} + \left\{ \left(\mathbf{F}_{ji}^{ij} + \mathbf{F}_{ij}^{ji} \right).\mathbf{v}_j \right\} + \\ \sum_{k=1;k\neq i,\mathrm{j}}^{N} \left\{ \mathbf{F}_{ik}^{ij}.\mathbf{v}_i \right\} + \left\{ \mathbf{F}_{jk}^{ji}.\mathbf{v}_j \right\} + \left\{ \left(\mathbf{F}_{ki}^{ij} + \mathbf{F}_{kj}^{ji} \right).\mathbf{v}_k \right\} \end{array} \right] \end{pmatrix} \quad \text{(B6)}$$

Combining terms:

$$= \begin{pmatrix} \sum_{i=1}^{N}\sum_{j=1;j\neq i}^{N} \frac{\mathbf{r}_i}{2} \left[\left(\mathbf{F}_{ij}^{ij} + \mathbf{F}_{ij}^{ji} \right).\left(\mathbf{v}_i + \mathbf{v}_j \right) \right] + \sum_{i=1}^{N}\sum_{j=1;j\neq i}^{N}\sum_{k=1;k\neq i,j}^{N} \mathbf{r}_i \left[\left(\mathbf{F}_{ij}^{ik} + \mathbf{F}_{ij}^{jk} \right).\mathbf{v}_i \right] \\ -\sum_{i=1}^{N}\sum_{j=1;i\neq j}^{N}\sum_{k=1;k\neq i,\mathrm{j}}^{N} \frac{\mathbf{r}_i}{2} \left[\left\{ \mathbf{F}_{ik}^{ij}.\mathbf{v}_i \right\} + \left\{ \mathbf{F}_{jk}^{ji}.\mathbf{v}_j \right\} + \left\{ \left(\mathbf{F}_{ki}^{ij} + \mathbf{F}_{kj}^{ji} \right).\mathbf{v}_k \right\} \right] \end{pmatrix} \quad \text{(B7)}$$

Consider first term in Eqn. (B7):

$$\sum_{i=1}^{N}\sum_{j=1;j\neq i}^{N}\frac{\mathbf{r}_i}{2}\left[\left(\mathbf{F}_{ij}^{ij}+\mathbf{F}_{ij}^{ji}\right).\left(\mathbf{v}_i+\mathbf{v}_j\right)\right] \tag{B8}$$

Interchanging *i* and *j* and adding:

$$=\frac{1}{2}\left(\sum_{i=1}^{N}\sum_{j=1;j\neq i}^{N}\frac{\mathbf{r}_i}{2}\left[\left(\mathbf{F}_{ij}^{ij}+\mathbf{F}_{ij}^{ji}\right).\left(\mathbf{v}_i+\mathbf{v}_j\right)\right]+\sum_{j=1}^{N}\sum_{i=1;j\neq i}^{N}\frac{\mathbf{r}_j}{2}\left[\left(\mathbf{F}_{ji}^{ji}+\mathbf{F}_{ji}^{ij}\right).\left(\mathbf{v}_j+\mathbf{v}_i\right)\right]\right) \tag{B9}$$

Combining terms:

$$=\frac{1}{4}\left(\sum_{i=1}^{N}\sum_{j=1;j\neq i}^{N}\mathbf{r}_{ij}\left[\left(\mathbf{F}_{ij}^{ij}+\mathbf{F}_{ij}^{ji}\right).\left(\mathbf{v}_i+\mathbf{v}_j\right)\right]\right) \tag{B10}$$

Splitting into two summations:

$$=\frac{1}{4}\left(\sum_{i=1}^{N}\sum_{j=1;j\neq i}^{N}\mathbf{r}_{ij}\left[\left(\mathbf{F}_{ij}^{ij}+\mathbf{F}_{ij}^{ji}\right).\mathbf{v}_i\right]+\sum_{i=1}^{N}\sum_{j=1;j\neq i}^{N}\mathbf{r}_{ij}\left[\left(\mathbf{F}_{ij}^{ij}+\mathbf{F}_{ij}^{ji}\right).\mathbf{v}_j\right]\right) \tag{B11}$$

Merging by symmetry:

$$=\frac{1}{2}\sum_{i=1}^{N}\sum_{j=1;j\neq i}^{N}\mathbf{r}_{ij}\left[\left(\mathbf{F}_{ij}^{ij}+\mathbf{F}_{ij}^{ji}\right).\mathbf{v}_i\right] \tag{B12}$$

Evaluating the 2nd and 3rd terms in Eqn. (B7):

$$\left(\begin{array}{l}\sum_{i=1}^{N}\sum_{j=1;j\neq i}^{N}\sum_{k=1;k\neq i,j}^{N}\mathbf{r}_i\left[\left(\mathbf{F}_{ij}^{ik}+\mathbf{F}_{ij}^{jk}\right).\mathbf{v}_i\right]- \\ \sum_{i=1}^{N}\sum_{j=1;i\neq j}^{N}\sum_{k=1;k\neq i,\mathrm{j}}^{N}\frac{\mathbf{r}_i}{2}\left[\left\{\mathbf{F}_{ik}^{ij}.\mathbf{v}_i\right\}+\left\{\mathbf{F}_{jk}^{ji}.\mathbf{v}_j\right\}+\left\{\left(\mathbf{F}_{ki}^{ij}+\mathbf{F}_{kj}^{ji}\right).\mathbf{v}_k\right\}\right]\end{array}\right) \quad \text{(B13)}$$

Interchanging *i*, *j*, *k* to all six permutations and adding:

$$=\frac{1}{6}\times$$

$$\left(\begin{array}{l}\sum_{i=1}^{N}\sum_{j=1;j\neq i}^{N}\sum_{k=1;k\neq i,j}^{N}\mathbf{r}_i\left[\left(\mathbf{F}_{ij}^{ik}+\mathbf{F}_{ij}^{jk}\right).\mathbf{v}_i\right]-\sum_{i=1}^{N}\sum_{j=1;i\neq j}^{N}\sum_{k=1;k\neq i,\mathrm{j}}^{N}\frac{\mathbf{r}_i}{2}\left[\left\{\mathbf{F}_{ik}^{ij}.\mathbf{v}_i\right\}+\left\{\mathbf{F}_{jk}^{ji}.\mathbf{v}_j\right\}+\left\{\left(\mathbf{F}_{ki}^{ij}+\mathbf{F}_{kj}^{ji}\right).\mathbf{v}_k\right\}\right] \\ +\sum_{i=1}^{N}\sum_{j=1;j\neq i}^{N}\sum_{k=1;k\neq i,j}^{N}\mathbf{r}_i\left[\left(\mathbf{F}_{ik}^{ij}+\mathbf{F}_{ik}^{kj}\right).\mathbf{v}_i\right]-\sum_{i=1}^{N}\sum_{j=1;i\neq j}^{N}\sum_{k=1;k\neq i,\mathrm{j}}^{N}\frac{\mathbf{r}_i}{2}\left[\left\{\mathbf{F}_{ij}^{ik}.\mathbf{v}_i\right\}+\left\{\mathbf{F}_{kj}^{ki}.\mathbf{v}_k\right\}+\left\{\left(\mathbf{F}_{ji}^{ik}+\mathbf{F}_{jk}^{ki}\right).\mathbf{v}_j\right\}\right] \\ +\sum_{i=1}^{N}\sum_{j=1;j\neq i}^{N}\sum_{k=1;k\neq i,j}^{N}\mathbf{r}_j\left[\left(\mathbf{F}_{ji}^{jk}+\mathbf{F}_{ji}^{ik}\right).\mathbf{v}_j\right]-\sum_{i=1}^{N}\sum_{j=1;i\neq j}^{N}\sum_{k=1;k\neq i,\mathrm{j}}^{N}\frac{\mathbf{r}_j}{2}\left[\left\{\mathbf{F}_{jk}^{ji}.\mathbf{v}_j\right\}+\left\{\mathbf{F}_{ik}^{ij}.\mathbf{v}_i\right\}+\left\{\left(\mathbf{F}_{kj}^{ji}+\mathbf{F}_{ki}^{ij}\right).\mathbf{v}_k\right\}\right] \\ +\sum_{i=1}^{N}\sum_{j=1;j\neq i}^{N}\sum_{k=1;k\neq i,j}^{N}\mathbf{r}_j\left[\left(\mathbf{F}_{jk}^{ji}+\mathbf{F}_{jk}^{ki}\right).\mathbf{v}_j\right]-\sum_{i=1}^{N}\sum_{j=1;i\neq j}^{N}\sum_{k=1;k\neq i,\mathrm{j}}^{N}\frac{\mathbf{r}_j}{2}\left[\left\{\mathbf{F}_{ji}^{jk}.\mathbf{v}_j\right\}+\left\{\mathbf{F}_{ki}^{kj}.\mathbf{v}_k\right\}+\left\{\left(\mathbf{F}_{ij}^{jk}+\mathbf{F}_{ik}^{kj}\right).\mathbf{v}_i\right\}\right] \\ +\sum_{i=1}^{N}\sum_{j=1;j\neq i}^{N}\sum_{k=1;k\neq i,j}^{N}\mathbf{r}_k\left[\left(\mathbf{F}_{ki}^{kj}+\mathbf{F}_{ki}^{ij}\right).\mathbf{v}_k\right]-\sum_{i=1}^{N}\sum_{j=1;i\neq j}^{N}\sum_{k=1;k\neq i,\mathrm{j}}^{N}\frac{\mathbf{r}_k}{2}\left[\left\{\mathbf{F}_{kj}^{ki}.\mathbf{v}_k\right\}+\left\{\mathbf{F}_{ij}^{ik}.\mathbf{v}_i\right\}+\left\{\left(\mathbf{F}_{jk}^{ki}+\mathbf{F}_{ji}^{ik}\right).\mathbf{v}_j\right\}\right] \\ +\sum_{i=1}^{N}\sum_{j=1;j\neq i}^{N}\sum_{k=1;k\neq i,j}^{N}\mathbf{r}_k\left[\left(\mathbf{F}_{kj}^{ki}+\mathbf{F}_{kj}^{ji}\right).\mathbf{v}_k\right]-\sum_{i=1}^{N}\sum_{j=1;i\neq j}^{N}\sum_{k=1;k\neq i,\mathrm{j}}^{N}\frac{\mathbf{r}_k}{2}\left[\left\{\mathbf{F}_{ki}^{kj}.\mathbf{v}_k\right\}+\left\{\mathbf{F}_{ji}^{jk}.\mathbf{v}_j\right\}+\left\{\left(\mathbf{F}_{ik}^{kj}+\mathbf{F}_{ij}^{jk}\right).\mathbf{v}_i\right\}\right]\end{array}\right) \quad \text{(B14)}$$

Rearranging:

$$
= \frac{1}{6}\left(\begin{array}{l}
\sum_{i=1}^{N}\sum_{j=1;j\neq i}^{N}\sum_{k=1;k\neq i,j}^{N}\mathbf{r}_i\left[\left\{\frac{\mathbf{F}_{ij}^{ik}.\left(\mathbf{v}_i+\mathbf{v}_j\right)}{2}\right\}+\mathbf{F}_{ij}^{jk}.\mathbf{v}_i\right]-\sum_{i=1}^{N}\sum_{j=1;i\neq j}^{N}\sum_{k=1;k\neq i,j}^{N}\frac{\mathbf{r}_i}{2}\left[\left\{\mathbf{F}_{jk}^{ji}.\mathbf{v}_j\right\}+\left\{\mathbf{F}_{kj}^{ji}.\mathbf{v}_k\right\}\right] \\
+\sum_{i=1}^{N}\sum_{j=1;j\neq i}^{N}\sum_{k=1;k\neq i,j}^{N}\mathbf{r}_i\left[\left\{\frac{\mathbf{F}_{ik}^{ij}.\left(\mathbf{v}_i+\mathbf{v}_k\right)}{2}\right\}+\mathbf{F}_{ik}^{kj}.\mathbf{v}_i\right]-\sum_{i=1}^{N}\sum_{j=1;i\neq j}^{N}\sum_{k=1;k\neq i,j}^{N}\frac{\mathbf{r}_i}{2}\left[\left\{\mathbf{F}_{kj}^{ki}.\mathbf{v}_k\right\}+\left\{\mathbf{F}_{jk}^{ki}.\mathbf{v}_j\right\}\right] \\
+\sum_{i=1}^{N}\sum_{j=1;j\neq i}^{N}\sum_{k=1;k\neq i,j}^{N}\mathbf{r}_j\left[\left\{\frac{\mathbf{F}_{ji}^{jk}.\left(\mathbf{v}_j+\mathbf{v}_i\right)}{2}\right\}+\mathbf{F}_{ji}^{ik}.\mathbf{v}_j\right]-\sum_{i=1}^{N}\sum_{j=1;i\neq j}^{N}\sum_{k=1;k\neq i,j}^{N}\frac{\mathbf{r}_j}{2}\left[\left\{\mathbf{F}_{ik}^{ij}.\mathbf{v}_i\right\}+\left\{\mathbf{F}_{ki}^{ij}.\mathbf{v}_k\right\}\right] \\
+\sum_{i=1}^{N}\sum_{j=1;j\neq i}^{N}\sum_{k=1;k\neq i,j}^{N}\mathbf{r}_j\left[\left\{\frac{\mathbf{F}_{jk}^{ji}.\left(\mathbf{v}_j+\mathbf{v}_k\right)}{2}\right\}+\mathbf{F}_{jk}^{ki}.\mathbf{v}_j\right]-\sum_{i=1}^{N}\sum_{j=1;i\neq j}^{N}\sum_{k=1;k\neq i,j}^{N}\frac{\mathbf{r}_j}{2}\left[\left\{\mathbf{F}_{ki}^{kj}.\mathbf{v}_k\right\}+\left\{\mathbf{F}_{ik}^{kj}.\mathbf{v}_i\right\}\right] \\
+\sum_{i=1}^{N}\sum_{j=1;j\neq i}^{N}\sum_{k=1;k\neq i,j}^{N}\mathbf{r}_k\left[\left\{\frac{\mathbf{F}_{ki}^{kj}.\left(\mathbf{v}_k+\mathbf{v}_i\right)}{2}\right\}+\mathbf{F}_{ki}^{ij}.\mathbf{v}_k\right]-\sum_{i=1}^{N}\sum_{j=1;i\neq j}^{N}\sum_{k=1;k\neq i,j}^{N}\frac{\mathbf{r}_k}{2}\left[\left\{\mathbf{F}_{ij}^{ik}.\mathbf{v}_i\right\}+\left\{\mathbf{F}_{ji}^{ik}.\mathbf{v}_j\right\}\right] \\
+\sum_{i=1}^{N}\sum_{j=1;j\neq i}^{N}\sum_{k=1;k\neq i,j}^{N}\mathbf{r}_k\left[\left\{\frac{\mathbf{F}_{kj}^{ki}.\left(\mathbf{v}_k+\mathbf{v}_j\right)}{2}\right\}+\mathbf{F}_{kj}^{ji}.\mathbf{v}_k\right]-\sum_{i=1}^{N}\sum_{j=1;i\neq j}^{N}\sum_{k=1;k\neq i,j}^{N}\frac{\mathbf{r}_k}{2}\left[\left\{\mathbf{F}_{ji}^{jk}.\mathbf{v}_j\right\}+\left\{\mathbf{F}_{ij}^{jk}.\mathbf{v}_i\right\}\right]
\end{array}\right) \qquad \text{(B15)}
$$

Collecting terms:

$$
= \frac{1}{6}\left(\begin{array}{l}
\sum_{i=1}^{N}\sum_{j=1;j\neq i}^{N}\sum_{k=1;k\neq i,j}^{N}\mathbf{r}_i\left[\left\{\frac{\mathbf{F}_{ij}^{ik}.\left(\mathbf{v}_i+\mathbf{v}_j\right)}{2}\right\}\right]-\frac{\mathbf{r}_k}{2}\left[\left\{\mathbf{F}_{ij}^{ik}.\mathbf{v}_i\right\}+\left\{\mathbf{F}_{ji}^{ik}.\mathbf{v}_j\right\}\right]+\mathbf{r}_j\left[\mathbf{F}_{ji}^{ik}.\mathbf{v}_j\right] \\
+\sum_{i=1}^{N}\sum_{j=1;j\neq i}^{N}\sum_{k=1;k\neq i,j}^{N}\mathbf{r}_i\left[\left\{\frac{\mathbf{F}_{ik}^{ij}.\left(\mathbf{v}_i+\mathbf{v}_k\right)}{2}\right\}\right]-\frac{\mathbf{r}_j}{2}\left[\left\{\mathbf{F}_{ik}^{ij}.\mathbf{v}_i\right\}+\left\{\mathbf{F}_{ki}^{ij}.\mathbf{v}_k\right\}\right]+\mathbf{r}_k\left[\mathbf{F}_{ki}^{ij}.\mathbf{v}_k\right] \\
+\sum_{i=1}^{N}\sum_{j=1;j\neq i}^{N}\sum_{k=1;k\neq i,j}^{N}\mathbf{r}_j\left[\left\{\frac{\mathbf{F}_{ji}^{jk}.\left(\mathbf{v}_j+\mathbf{v}_i\right)}{2}\right\}\right]-\frac{\mathbf{r}_k}{2}\left[\left\{\mathbf{F}_{ji}^{jk}.\mathbf{v}_j\right\}+\left\{\mathbf{F}_{ij}^{jk}.\mathbf{v}_i\right\}\right]+\mathbf{r}_i\left[\mathbf{F}_{ij}^{jk}.\mathbf{v}_i\right] \\
+\sum_{i=1}^{N}\sum_{j=1;j\neq i}^{N}\sum_{k=1;k\neq i,j}^{N}\mathbf{r}_j\left[\left\{\frac{\mathbf{F}_{jk}^{ji}.\left(\mathbf{v}_j+\mathbf{v}_k\right)}{2}\right\}+\right]-\frac{\mathbf{r}_i}{2}\left[\left\{\mathbf{F}_{jk}^{ji}.\mathbf{v}_j\right\}+\left\{\mathbf{F}_{kj}^{ji}.\mathbf{v}_k\right\}\right]+\mathbf{r}_k\left[\mathbf{F}_{kj}^{ji}.\mathbf{v}_k\right] \\
+\sum_{i=1}^{N}\sum_{j=1;j\neq i}^{N}\sum_{k=1;k\neq i,j}^{N}\mathbf{r}_k\left[\left\{\frac{\mathbf{F}_{ki}^{kj}.\left(\mathbf{v}_k+\mathbf{v}_i\right)}{2}\right\}\right]-\frac{\mathbf{r}_j}{2}\left[\left\{\mathbf{F}_{ki}^{kj}.\mathbf{v}_k\right\}+\left\{\mathbf{F}_{ik}^{kj}.\mathbf{v}_i\right\}\right]+\mathbf{r}_i\left[\mathbf{F}_{ik}^{kj}.\mathbf{v}_i\right] \\
+\sum_{i=1}^{N}\sum_{j=1;j\neq i}^{N}\sum_{k=1;k\neq i,j}^{N}\mathbf{r}_k\left[\left\{\frac{\mathbf{F}_{kj}^{ki}.\left(\mathbf{v}_k+\mathbf{v}_j\right)}{2}\right\}\right]-\frac{\mathbf{r}_i}{2}\left[\left\{\mathbf{F}_{kj}^{ki}.\mathbf{v}_k\right\}+\left\{\mathbf{F}_{jk}^{ki}.\mathbf{v}_j\right\}\right]+\mathbf{r}_j\left[\mathbf{F}_{jk}^{ki}.\mathbf{v}_j\right]
\end{array}\right) \qquad \text{(B16)}
$$

Simplifying:

$$= \frac{1}{6}\left(\begin{array}{l} \sum_{i=1}^{N}\sum_{j=1;j\neq i}^{N}\sum_{k=1;k\neq i,j}^{N} \frac{\mathbf{r}_{ik}}{2}\left\{\mathbf{F}_{ij}^{ik}.\mathbf{v}_i\right\} + \frac{\mathbf{r}_{ji}+\mathbf{r}_{jk}}{2}\left\{\mathbf{F}_{ji}^{ik}.\mathbf{v}_j\right\} \\ +\sum_{i=1}^{N}\sum_{j=1;j\neq i}^{N}\sum_{k=1;k\neq i,j}^{N} \frac{\mathbf{r}_{ij}}{2}\left\{\mathbf{F}_{ik}^{ij}.\mathbf{v}_i\right\} + \frac{\mathbf{r}_{ki}+\mathbf{r}_{kj}}{2}\left\{\mathbf{F}_{ki}^{ij}.\mathbf{v}_k\right\} \\ +\sum_{i=1}^{N}\sum_{j=1;j\neq i}^{N}\sum_{k=1;k\neq i,j}^{N} \frac{\mathbf{r}_{jk}}{2}\left\{\mathbf{F}_{ji}^{jk}.\mathbf{v}_j\right\} + \frac{\mathbf{r}_{ij}+\mathbf{r}_{ik}}{2}\left\{\mathbf{F}_{ij}^{jk}.\mathbf{v}_i\right\} \\ +\sum_{i=1}^{N}\sum_{j=1;j\neq i}^{N}\sum_{k=1;k\neq i,j}^{N} \frac{\mathbf{r}_{ji}}{2}\left\{\mathbf{F}_{jk}^{ji}.\mathbf{v}_j\right\} + \frac{\mathbf{r}_{kj}+\mathbf{r}_{ki}}{2}\left\{\mathbf{F}_{kj}^{ji}.\mathbf{v}_k\right\} \\ +\sum_{i=1}^{N}\sum_{j=1;j\neq i}^{N}\sum_{k=1;k\neq i,j}^{N} \frac{\mathbf{r}_{ki}}{2}\left\{\mathbf{F}_{kj}^{ki}.\mathbf{v}_k\right\} + \frac{\mathbf{r}_{jk}+\mathbf{r}_{ji}}{2}\left\{\mathbf{F}_{jk}^{ki}.\mathbf{v}_j\right\} \\ +\sum_{i=1}^{N}\sum_{j=1;j\neq i}^{N}\sum_{k=1;k\neq i,j}^{N} \frac{\mathbf{r}_{kj}}{2}\left\{\mathbf{F}_{ki}^{kj}.\mathbf{v}_k\right\} + \frac{\mathbf{r}_{ik}+\mathbf{r}_{ij}}{2}\left\{\mathbf{F}_{ik}^{kj}.\mathbf{v}_i\right\} \end{array} \right) \tag{B17}$$

Combining terms:

$$= \sum_{i=1}^{N}\sum_{j=1;j\neq i}^{N}\sum_{k=1;k\neq i,j}^{N} \frac{\mathbf{r}_{ik}}{2}\left[\mathbf{F}_{ij}^{ik}.\mathbf{v}_i\right] + \frac{\mathbf{r}_{ij}+\mathbf{r}_{ik}}{2}\left[\mathbf{F}_{ij}^{jk}.\mathbf{v}_i\right] \tag{B18}$$

Substituting Eqn. (B12) and Eqn. (B18) back into Eqn. (B2) gives:

$$\mathbf{J}(t) = \left(\begin{array}{l} \sum_{i=1}^{N}\varepsilon_i(t)\mathbf{v}_i(t) + \sum_{i=1}^{N}\sum_{j=1;j\neq i}^{N}\left[\frac{\mathbf{r}_{ij}(t)}{2}\left[\left(\mathbf{F}_{ij}^{ij}(t)+\mathbf{F}_{ij}^{ji}(t)\right).\mathbf{v}_i(t)\right]\right] + \\ \sum_{i=1}^{N}\sum_{j=1;j\neq i}^{N}\sum_{k=1;k\neq i,j}^{N}\left[\frac{\mathbf{r}_{ik}(t)}{2}\left[\mathbf{F}_{ij}^{ik}(t).\mathbf{v}_i(t)\right] + \frac{\mathbf{r}_{ij}(t)+\mathbf{r}_{ik}(t)}{2}\left[\mathbf{F}_{ij}^{jk}(t).\mathbf{v}_i(t)\right]\right] \end{array} \right) \tag{B19}$$

Eqn. (B19) is expression for heat current due to Tersoff potential.